ÉCOLE POLYTECHNIQUE
FÉDÉRALE DE LAUSANNE

Centre de Recherches en Physique des Plasmas (CRPP)

Faculté des sciences de base
Section de physique

Association EURATOM
Confédération Suisse

Plasma Physics II

Kinetic theory of plasmas

lecture notes

academic year 2010

Prof. Ambrogio FASOLI

PPB 318, station 13
CH-1015 Lausanne
Switzerland

document revised on Monday 19th September, 2011

Made with pdfLaTeX

Contents

Chapter 1 Definition of Plasma

1. Ensemble of free charged particles
2. Globally neutral(*)
3. Exhibiting collective behavior

We will discuss condition (1) and its implications later. Let's first review (2) and (3).

1.1 Static properties of plasmas

1.1.1 Plasmas are globally neutral

How easy is it for a plasma to stay neutral? The strength of the restoring force that would result from a deviation from neutrality is enormous, compared to other forces as gravity and pressure force.
Let's consider a simple model: a one-dimensional (*slab*) plasma composed by protons and electrons. Suppose that the ion density is slightly higher than the electron density, say $(n_i - n_e)/n_e \simeq 1\%$ everywhere:

$$\text{Charge density} \qquad \rho = e(n_i - n_e) \simeq 10^{-2} e n_e \tag{1.1}$$

$$\text{Inside the slab} \qquad \nabla \cdot \mathbf{E} = \frac{\rho}{\varepsilon_0} \tag{1.2}$$

$$\text{1–D along } x \qquad \frac{dE}{dx} = \frac{10^{-2} e n_e}{\varepsilon_0} \Longrightarrow E(x) = \frac{10^{-2} e n_e}{\varepsilon_0} x \tag{1.3}$$

Note that $E(x) \lessgtr 0$ for $x \lessgtr 0$: ions are pushed away and electrons are pulled in (see figure 1.1).

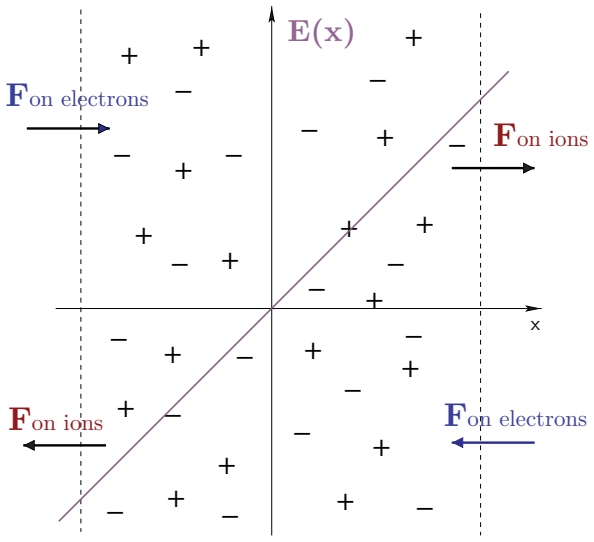

Figure 1.1: The force due to the electric field (resulting from a deviation from neutrality) pushes ions out and drags electrons inside the plasma.

(*) Sometimes are called 'plasmas' also non-neutral collections of particles of the same species (e.g. electrons), confined by means of electrostatic external fields. Here and in the following we will only consider globally neutral plasmas.

The resulting force tries to remove the excess of positive charge. Let us estimate the strength of the force density and compare it to that due to the gravity(†) and that due to the pressure. Assume $x \simeq 1$ m, $T = 1$ keV, $n_e = 10^{19}$ m^{-3}:

$$\frac{\text{e.s. force}}{\text{volume}} = \rho E = \frac{(10^{-2} e n_e)^2}{\varepsilon_0} x \simeq 3 \cdot 10^7 \ \frac{\text{N}}{\text{m}^3} \tag{1.4}$$

$$\frac{\text{gravity force}}{\text{volume}} \simeq n m_i g \simeq 10^{-7} \ \frac{\text{N}}{\text{m}^3} \ll \text{e.s. force} \tag{1.5}$$

$$\frac{\text{pressure force}}{\text{volume}} = \frac{p}{x} = \frac{n_e T}{x} \simeq \frac{10^{19} \times 1.6 \cdot 10^{-19} \times 10^3}{1} = 1.6 \cdot 10^3 \ \frac{\text{N}}{\text{m}^3} \ll \text{e.s. force} \tag{1.6}$$

As we can see from the examples reported above, the e.s. force that brings the plasma back to a condition of global neutrality is dominant, and thus the plasma remains globally neutral.
This is an example of the fact that plasma dynamics is governed by long–range electrostatic (electromagnetic) interactions.

1.1.2 Collective behavior (Debye shielding)

The neutrality condition $n_i q_i - n_e e = 0$ (or $n_e = \sum_{j=1}^{M} Z_j n_j$ with M = number of ion species) is only an average property. If we go *close enough* to a single particle, obviously, neutrality breaks. Question is: *How close is 'close enough'?*
This is something you have learnt in Plasma I course. Let's review the main results (the formal derivation is reported in appendix A).

In plasmas the main quantities as particle density (velocity), charge density (currents) and e.s. fields (e.m. fields) are intrinsically coupled. To break the closed self-consistent loop existing between these quantities (figure 1.2.a) one has to choose a *model* for the plasma.

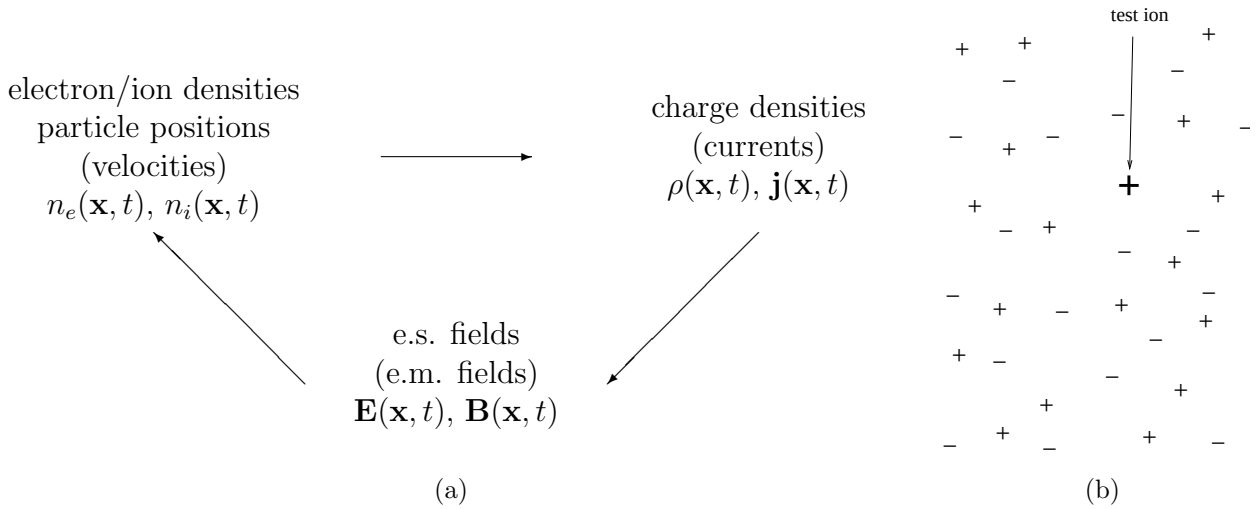

Figure 1.2: (a) Particle, current and field distributions form a self–consistent loop characterising the plasma. (b) What happens to a test particle (a single ion) inside a plasma?

(†) We consider here the gravity force acting on ions. For electrons the same type of force is even smaller, by a factor m_e/m_i.

Take a single ion and place it in the plasma (figure 1.2.b). What do we expect? It will be surrounded by a cloud of electrons feeling its potential. You have already calculated the distribution of the potential and the electron density around the ion. In Plasma I you have assumed $T_i = 0$, and electrons described by Maxwell-Boltzmann distribution: $f(v) = A\exp(\frac{-\text{energy}}{T}) = A\exp\left\{-\frac{\frac{1}{2}mv^2 - e\phi}{T}\right\}$, ($\phi$ is the potential), which integrated over v gives $n_e = n_0\exp(\frac{e\phi}{T})$. You have also assumed $\frac{e\phi}{T} \ll 1$, so that $n_e \approx n_0(1 + \frac{e\phi}{T})$.

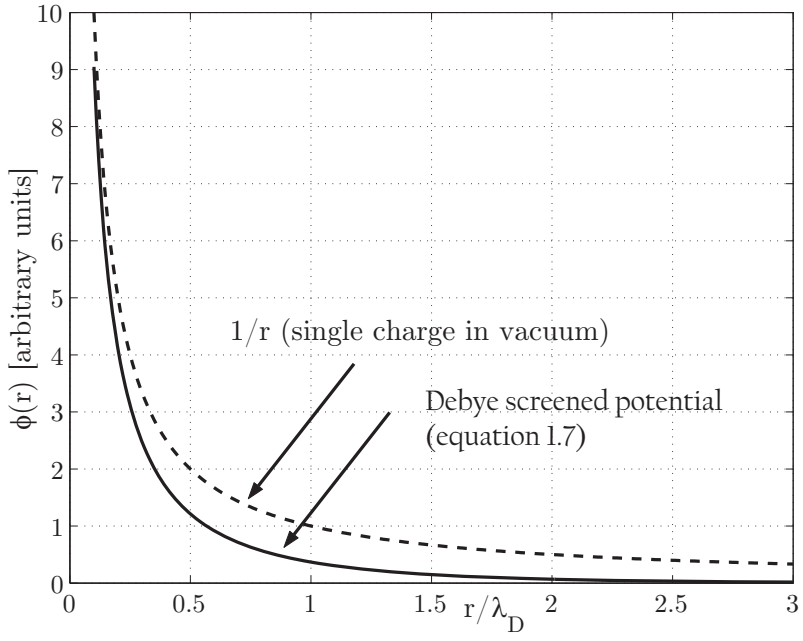

Figure 1.3: Debye screened potential (straight line): The correction of the vacuum potential (dotted line) is small, but essential.

The solution for the potential in a spherically symmetric case is (figure 1.3):

$$\phi(r) = \underbrace{\frac{e}{4\pi\varepsilon_0}\frac{1}{r}}_{\substack{\text{singe charge}\\ \text{in vacuum}}} \times \underbrace{\exp\left\{-\frac{r}{\lambda_D}\right\}}_{\substack{\text{term due to plasma}\\ \text{collective interactions}}} \tag{1.7}$$

$$n_e(r) \simeq n_{e0}\left\{1 + \frac{e\phi}{T}\right\} = n_{e0}\left(1 + \frac{e^2}{4\pi\varepsilon_0 T}\frac{1}{r}\exp\left\{-\frac{r}{\lambda_D}\right\}\right)$$
$$= n_{e0} + \underbrace{\frac{n_{e0}}{3}g_p\frac{\lambda_D}{r}\exp\left\{-\frac{r}{\lambda_D}\right\}}_{\delta n_e > 0} \tag{1.8}$$

where $\lambda_D := \sqrt{\varepsilon_0 T/n_{e,0}e^2}$ is the Debye length, $g_p := N_D^{-1} \ll 1$ is the *plasma parameter*, and $N_D = \frac{4}{3}\pi\lambda_D^3 n_{e,0}$ is the number of particles inside a Debye sphere.

Note that in the expression

$$\lambda_D = \sqrt{\frac{\varepsilon_0 T}{n_{e,0}e^2}} \quad : \quad \frac{\text{thermal effect}}{\text{space charge effect}} \tag{1.9}$$

T is related to the thermal motion trying to violate neutrality and $n_0 e^2/\varepsilon_0$ to the space–charge force trying to restore neutrality. The Debye shielding is invisible for $r \gg \lambda_D$ – as if a single charge was placed in the vacuum.

The term δn_e represents a positive, but small perturbation: as expected the electrons tend to 'accumulate' around the positive charge.
Plasma can exhibit a static collective behavior if:

- Enough particles are in a Debye sphere so that they can give the 'screening'

$$N_D = \frac{4}{3}\pi\lambda_D^3 n_0 \gg 1 \tag{1.10}$$

  or equivalently the plasma parameter g_p is such that $g_p = N_D^{-1} \ll 1$

- Plasma dimensions are larger than the Debye length λ_D

$$\lambda_D \ll L_{\text{plasma}} \tag{1.11}$$

In the table below we'll compare ideal gases and plasmas in terms of some statistical quantities, the range of interaction, the average distance between particles and the ratio between kinetic and potential energy.

	Ideal Gas	Plasma
Average inter–particle distance	$n^{-\frac{1}{3}}$	$n^{-\frac{1}{3}}$
Range of interaction	$\ll n^{-\frac{1}{3}}$	$\sim \lambda_D \gg n^{-\frac{1}{3}}$ (a)
$\dfrac{E_{\text{kinetic}}}{E_{\text{potential}}}$	$\gg 1$	$= \dfrac{T}{\frac{1}{4\pi\varepsilon_0}\frac{e^2}{r}} = \dfrac{T}{e^2/4\pi\varepsilon_0 n^{-\frac{1}{3}}}$ (b) $= 4\pi\lambda_D^2 n^{\frac{2}{3}}$ (c) $= 4\pi\left(\frac{3}{4\pi}\right)^{\frac{2}{3}} N_D^{\frac{2}{3}} \gg 1$ (d)

(a) Does this mean that plasmas are completely different from ideal gas in terms of their statistical mechanics?
(b) solve (1.9) for T
(c) solve (1.10) for λ_D
(d) As in ideal gases, despite the long range of interactions! This means that the concepts and methods of thermodynamics are valid and applicable in the plasma state.

Table 1: Comparison between Ideal Gas and Plasma

We have seen a characteristic length for screening of electrostatic perturbation in plasmas, λ_D, as the first and most fundamental evidence of collective behavior. But we have dealt with *static* perturbations only. What about the *dynamical* response of the plasma, i.e. the characteristic time associated with a local displacement from quasi–neutrality?

1.2 Dynamic properties of plasmas

Heuristic Approach

Thermal motion of electrons	$v_{the} \sim \sqrt{\dfrac{T}{m_e}}$	(1.12)
Characteristic length	$\lambda_D = \sqrt{\dfrac{\varepsilon_0 T}{e^2 n}}$	(1.13)
Characteristic time	$\tau = \dfrac{\lambda_D}{v_{\rm th}} = \dfrac{\sqrt{\varepsilon_0 T/e^2 n}}{\sqrt{T/m}} = \sqrt{\dfrac{\varepsilon_0 m}{e^2 n}}$	(1.14)
Characteristic frequency	$\omega_p = \dfrac{1}{\tau} = \sqrt{\dfrac{e^2 n}{\varepsilon_0 m}}$ "plasma frequency"	(1.15)

You have completed the formal calculation[‡] in Plasma I. From

$$\nabla \cdot \mathbf{E} = \frac{\rho}{\varepsilon_0}, \quad m\frac{d\mathbf{u}}{dt} = -e\mathbf{E}, \quad \frac{\partial n}{\partial t} = -\nabla \cdot (n\mathbf{u}) \tag{1.16}$$

you have obtained for the perturbed density

$$\frac{\partial^2 \tilde{n}}{\partial t^2} + \omega_p^2 \tilde{n} = 0, \tag{1.17}$$

the equation of a harmonic oscillator of angular frequency ω_p. Numerically

$$f_p[\mathrm{Hz}] = \frac{\omega_p}{2\pi} \simeq 9\sqrt{n[\mathrm{m}^{-3}]} \tag{1.18}$$

For example one finds the following values:

Aurora	$f_p \sim 9\sqrt{10^{12}} = 9$ MHz.
Tokamak	$f_p \sim 9\sqrt{10^{20}} = 90$ GHz.

Note that for a wave to be able to propagate in a cold unmagnetized plasma, its angular frequency must be $\omega \gg \omega_p$. Otherwise the plasma electrons have enough time to respond and cancel the external excitation (i.e. the wave electric field).
Also note that, for dynamical collective effects to manifest, the oscillations at the frequency ω_p should not be prevented by collision processes. Stated otherwise, it should be $\omega_p > \nu_{collisions}$.

[‡] see notes on http://crpp.epfl.ch/physplas1/program.html

Chapter 2 Production of plasmas

2.1 Ionisation and Recombination

Ionisation of the neutral atoms is a "necessary condition" to have a plasma. This is an example of inelastic collisions. Figure 2.1 shows the most important ionisation and recombination mechanisms.

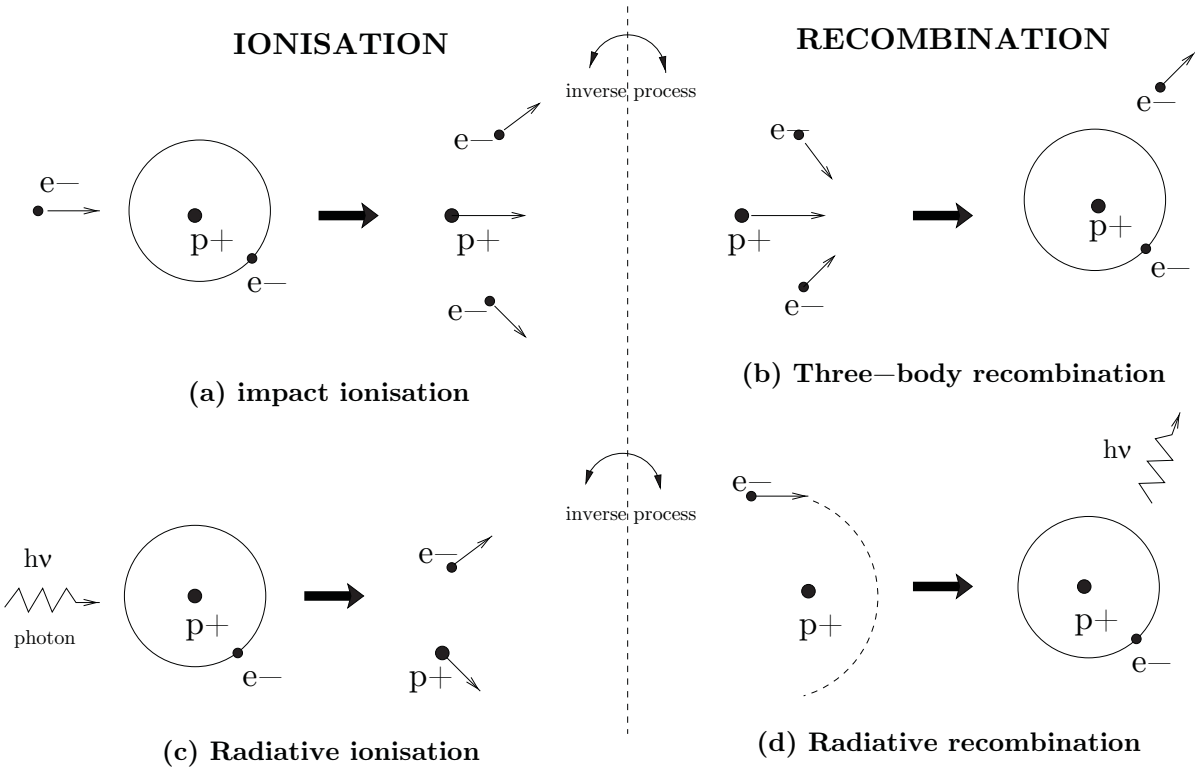

Figure 2.1: Main ionisation and recombination processes. For radiative ionisation to take place, the photon energy $E_{\text{photon}} = h\nu$ is required to exceed the ionisation energy E_i.

Both mechanisms of ionisation shown in figure 2.1 are present in nature, e.g.

- **Aurora (strong magnetic field):** Impact ionisation dominates (a)
- **Nebula (no magnetic field):** Radiative ionisation dominates (c)

High energy photons are required for the radiative ionisation. $E_i = 13.6$ eV for hydrogen, $\lambda = \frac{hc}{E_i} \simeq 50$ nm (ultraviolet range). In the absence of strong UV fluxes, impact ionisation is the dominant mechanism for plasma production. This is the case for common laboratory plasmas, where strong UV sources are unavailable.
For typical densities of plasmas in the laboratory and in space, three–body recombination is very unlikely and can in general be neglected. Other types of ionisation/recombination processes are also possible(§), but they are usually negligible compared to the processes shown in figure 2.1.
The equilibrium of impact ionisation and radiative recombination can be used to characterise many plasmas. Such equilibrium is called 'coronal' , as it is believed to regulate the solar corona parameters.

(§) Examples:
Charge–exchange recombination : $H^+ + H^- \rightarrow 2H$
Dissociative recombination (only for molecules): $e + (AB)^+ \rightarrow A + B$

2.1.1 Single Particle Cross–Sections

Impact ionisation and radiative recombination are collisional phenomena and as such they can be described by a cross–section, σ (figure 2.2).

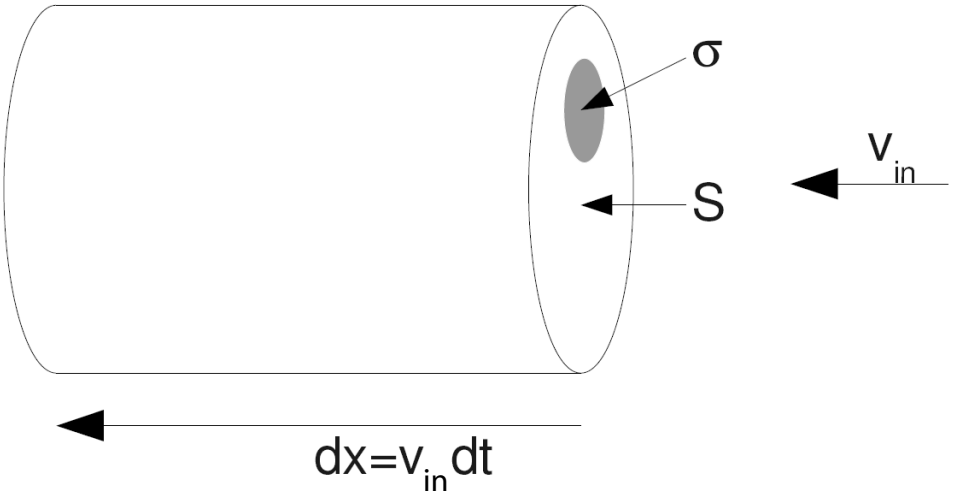

Figure 2.2: The collision probability of an electron beam incident on a homogenous distribution of neutral particles is equal to the ratio of the cross–section σ of this process and the section S of the beam.

Basic Notions

- For a single electron:

$$\#\text{ of collisions} = \underbrace{\underbrace{S\, v_{in}\, dt}_{\text{volume } V}\, n_{\text{targets}}}_{\#\text{ of targets}} \underbrace{\frac{\sigma}{S}}_{\substack{\text{probability of collisions} \\ \text{in volume V}}}$$

$$\frac{\#\text{ of collisions}}{\text{unit time}} = n_{\text{targets}}\sigma v_{\text{in}}, \quad \text{where} \quad n_{targets} = \frac{\#\text{ of targets}}{\text{unit volume}} \tag{2.1}$$

  and v_{in} is the relative velocity between incoming particles and targets. The density of the targets n_{targets} is assumed to be constant and uniform.

- For ionisation:

$$\frac{\#\text{ of ionisations}}{\text{unit time}} = n_n \sigma_{ion} v_{\text{el}}, \tag{2.2}$$

  where n_n is the neutral particle density and v_{el} the electron velocity[(¶)]

- Mean–free path:

$$\lambda_{\text{ion}}^{\text{mfp}} := \frac{1}{n_n \sigma_{\text{ion}}} \tag{2.3}$$

(¶) We assume $v_{\text{el}} \gg v_n$, since $m_e \ll m_n$.

Properties

Figure 2.3 shows the ionisation/recombination cross–sections for one single electron as a function of electron energy.

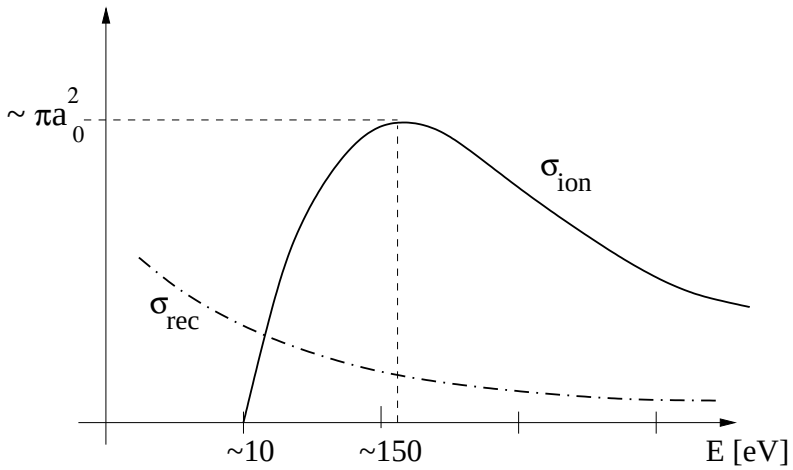

Figure 2.3: Cross–sections ω for ionisation and recombination processes. Note that no ionisation occurs below the ionisation energy ($E_i \sim 10$ eV).

Note that

- σ_{ion} depends on the electron velocity (energy)
- $\sigma_{\text{ion}} \equiv 0$ for $E < E_i$, where E_i is the ionisation threshold energy(‖)
- σ_{ion} increases with energy, but not indefinitely.
- σ_{rec} (recombination cross–section) decreases with energy

The third point can be intuitively justified by means of the duality established by the quantum mechanics between particles and waves with a convenient wavelength. If we associate to an electron its *de Broglie* wavelength $\lambda_{\text{el}} = \frac{h}{m_e v_e}$ (h is the Planck constant), the maximum interaction between the electron and the neutral is expected for $\lambda_{\text{el}} \sim 2a_0$, see figure 2.4. For example, $\sigma_{\text{ion}} = \sigma_{\text{ion}}^{\max}$ for H–atom at $\lambda \sim 2a_0 \rightarrow E \sim 100$–$200$ eV.

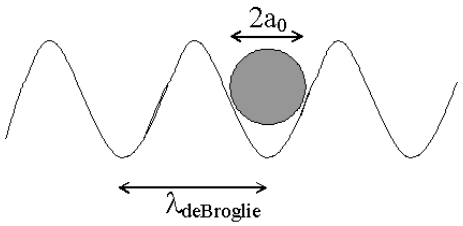

Figure 2.4: Qualitative explanation based on quantum mechanics of the dependence of σ_{ion} upon the energy of the colliding electron. The interaction is expected to be maximum at $\lambda \sim 2a_0$

(‖) e.g. H–atom:

$$E_i \simeq \frac{1}{2}\frac{e^2}{4\pi\varepsilon_0 a_0} \simeq 13.6 \text{ eV}, \qquad \text{where} \qquad a_0 = \frac{4\pi\varepsilon_0\hbar^2}{m_e e^2} \simeq 5 \cdot 10^{-11} \text{ m} \tag{2.4}$$

is the Bohr radius of the H–atom.

The decreased efficiency of the recombination process results from the reduced interaction time between particles as the relative velocity increases.

You have seen in Plasma I that in practice we produce ionisation by injecting a known pressure of gas in a vacuum chamber, which was previously brought to very low base pressures. The pressure of the injected gas is in general much lower than atmospheric so that enough energy can be given to electrons between collisions by an applied voltage:

$$E = \frac{e\Delta V}{d}\lambda_{\text{mfp}} \tag{2.5}$$

where d is the distance between the electrodes across which a potential difference ΔV is applied (figure 2.5).

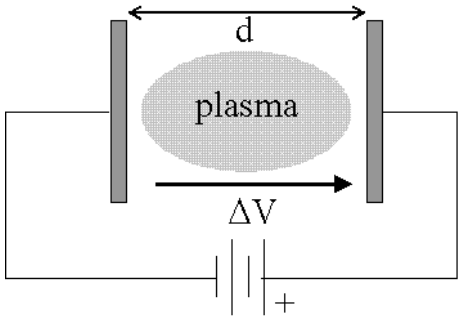

Figure 2.5: A voltage ΔV is applied between two electrodes (distance d in between) to accelerate the electrons and sustain a plasma discharge.

Examples : Which is the voltage to ionize the gas?

a.) Spark plug: electrode gap $d \simeq 1$ mm, $\Delta V \simeq 1$ kV.

b.) Lightning: discharge height $d \simeq 1$ km, $\Delta V \simeq 1$ GV.

c.) Plasma monitor: noble gaz at very low pressure (high λ_{mfp}) in tiny cells, sandwiched between electrodes.

2.1.2 Average Cross–Sections

Up to now we dealt with a single electron. Let us now consider a distribution, for example a Maxwellian characterised by a temperature T.
To calculate the ionisation rate for a distribution we need to average over such distribution the expression that gives the number of ionising collisions per unit time, which in general depends on energy.

$$\text{Ionisation rate} = \left\langle \frac{\#\text{ of ionisations}}{\text{unit time}} \right\rangle = n_n \langle \sigma_{\text{ion}} v_e \rangle \tag{2.6}$$

where n_n is the density of neutrals playing the role of 'targets'. Thus

$$\langle \sigma_{\text{ion}} v_e \rangle = \frac{\int dv_e f_e(v_e) \sigma_{\text{ion}}(v_e) v_e}{\int dv_e f_e(v_e)}, \tag{2.7}$$

where v_e is the velocity of electrons. Figure 2.6 shows the result as a function of the temperature.

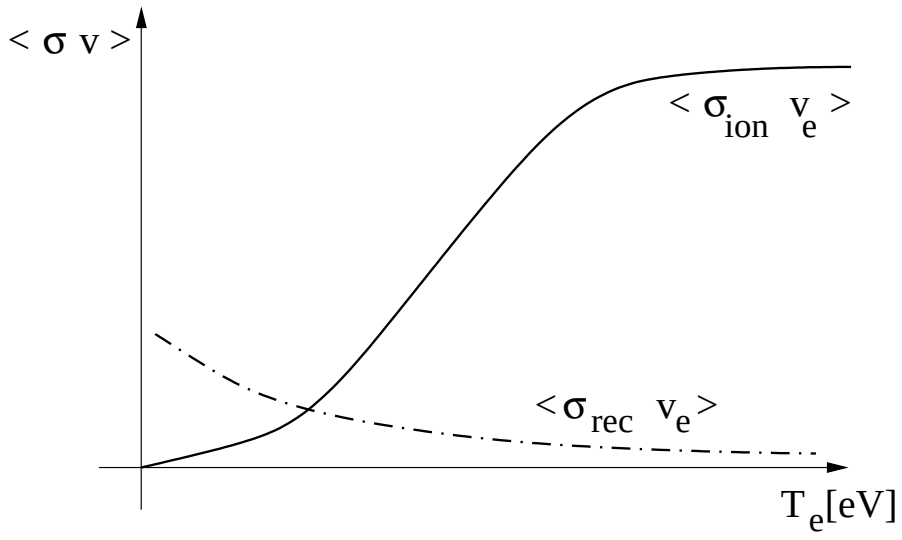

Figure 2.6: $\langle \sigma_{\rm ion} v_e \rangle$ as a function of T. Note that $\langle \sigma_{\rm ion} v_e \rangle \neq 0$ for $T < E_i$, as even then there will be some particles with energy greater than E_i, i.e. able to ionise

2.1.3 Equilibrium between impact ionisation and recombination

The equilibrium condition between impact ionisation and radiative recombination can be expressed as:

$$n_n \langle \sigma_{\rm ion} v_e \rangle = n_e \langle \sigma_{\rm rec} v_e \rangle, \qquad \text{or} \qquad \frac{n_e}{n_n} = \frac{\langle \sigma_{\rm ion} v_e \rangle}{\langle \sigma_{\rm rec} v_e \rangle}. \tag{2.8}$$

The ratio n_e/n_n [(**)] is called *degree of ionisation*. Clearly it increases with the temperature of the plasma.
The exact expression for n_e/n_n depends on the assumptions taken for the equilibrium. Consider the simplest model for hydrogen: a global thermodynamical equilibrium (G.T.E.), where all species are characterised by the same temperature T: $T_e = T_i = T_n \equiv T$. Note that this condition is rarely satisfied in plasmas. Under such assumptions and with $n_e \approx n_i$ one finds the so–called *Saha equation*

$$\frac{n_e}{n_n} \simeq 3 \cdot 10^{27} \frac{T^{3/2}[\mathrm{eV}]}{n_i[\mathrm{m}^{-3}]} \exp\left\{ -\frac{E_i}{T} \right\}. \tag{2.9}$$

A good representation of the transition to plasma state is given by the quantity

$$\alpha = n_e/(n_e + n_n) \tag{2.10}$$

called the *relative degree of ionisation* (see figure 2.7).

(**) Note that $n_e \approx n_i$ in plasmas.

The transition is made sharp by the exponential term in Saha equation. We can consider this as a *phase transition*. For $T > E_i$ ionisation is practically 100%.
Note that 'life' ($T \ll 1$ eV, $n \gg 10^{20}$ m^{-3}) is incompatible with plasma state, although, as we know, most of the energy that is necessary for life comes from fusion reactions that occur in the Sun. However, it is possible to have a plasma at very low T, if the density is *very* low, e.g. interstellar plasma, $n_e \sim 10^6$ m^{-3}.
Ordinary matter lies in a very small corner of the T, n diagram (see figure 2.8). We will consider plasmas over a wide range, but below energies at which relativistic effects become important ($T \ll 500$ keV).

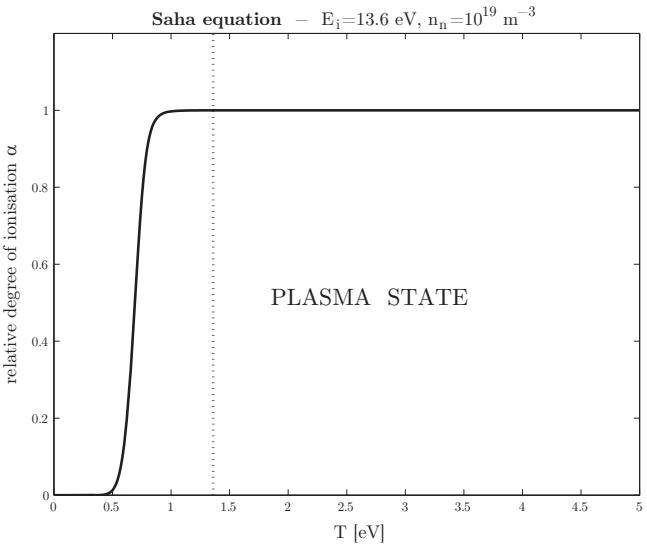

Figure 2.7: Relative degree of ionisation α for a hydrogen plasma of density $n_n = 10^{19}$ m^{-3}. The dotted line indicates $T = E_i/10$.

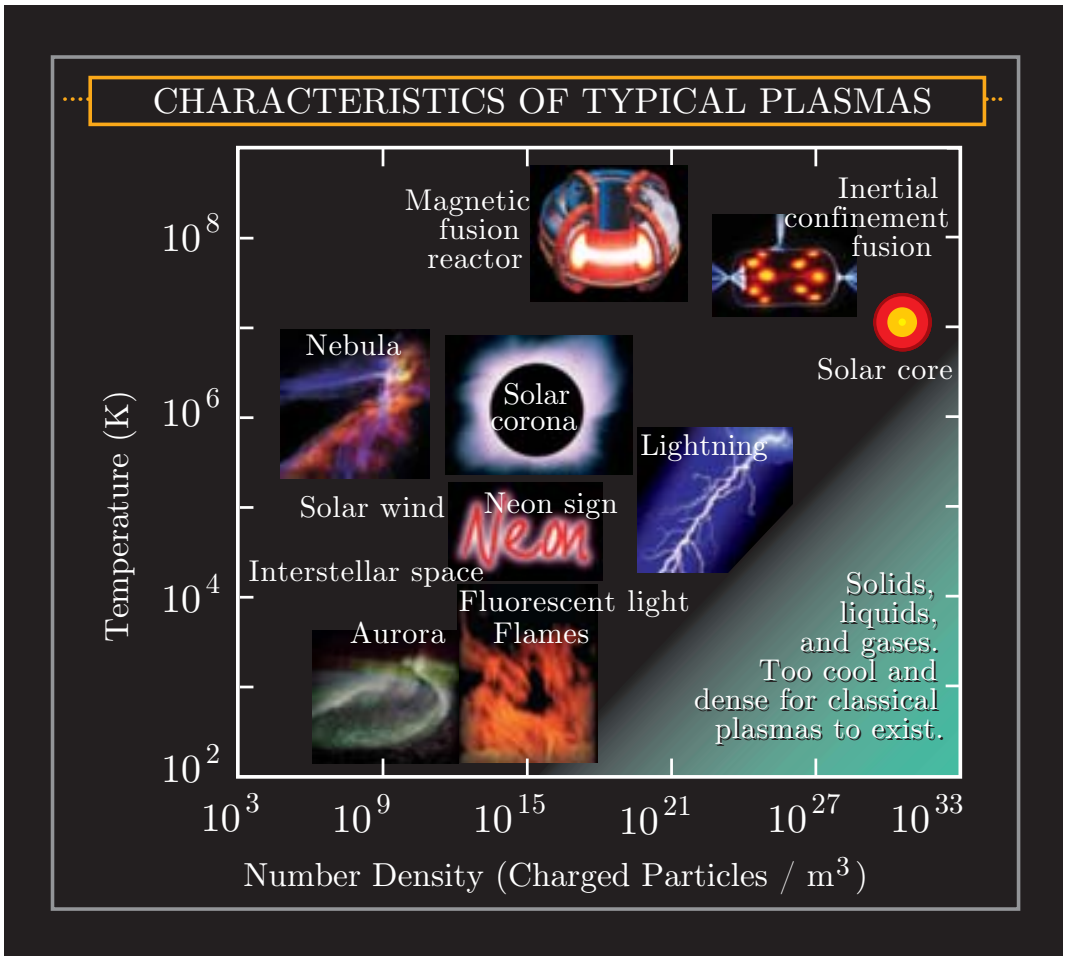

Figure 2.8: Characterisation of typical plasmas. (††)

(††) Image courtesy of Contemporary Physics Education Project (CPEP), http://FusEdWeb.llnl.gov/CPEP/

Example 1

Air at room temperature and pressure. Consider N_2:

$$E_i \sim 14.5 \text{ eV}, \quad T \sim \frac{1}{40} \text{ eV}, \quad n_n \sim 10^{25} \text{ m}^{-3} \implies \frac{n_e}{n_n} \approx \alpha < 10^{-100} \tag{2.11}$$

→ Thermal ionisation in air is negligible (of course, ionisation by non-thermal particles, such as from cosmic rays, is possible).

→ The exponential factor in Saha equation becomes non–negligibly small for T approaching E_i (but, again, we can have $T < E_i$).

Example 2

Solar corona

$$T \sim 500 \text{ eV}, \quad n_e \sim 10^{13} \text{ m}^{-3} \qquad \implies \frac{n_e}{n_n} \sim 3 \cdot 10^{18} \quad \text{or} \quad \frac{n_e}{n_e + n_n} \simeq 1 \tag{2.12}$$

→ The plasma is completely ionised.

2.1.4 Weak vs. Strong Ionisation

Definition: Weakly ionised plasma
charged particles ↔ neutral collisions dominate

Definition: Strongly ionised plasma
charged particles ↔ charged particles collisions dominate

The quantities to compare are the respective mean free paths. For a strongly ionised plasma we have

$$n_i \sigma_{\text{Coulomb}} > n_n \sigma_{\text{ion}}, \qquad \lambda_{\text{mfp}}^{\text{Coulomb}} < \lambda_{\text{mfp}}^{\text{ion}}, \tag{2.13}$$

where σ_{Coulomb} is the cross–section for Coulomb (electrostatic force) collisions. We will calculate σ_{Coulomb} later in the course, but we can have a first, rough estimate by considering

$$\sigma_{\text{Coulomb}} \simeq \pi b^2, \tag{2.14}$$

where $b := e^2/4\pi\varepsilon_0 T$ ("**Landau length**") is the distance at which the electrostatic energy is equal to the thermal energy. Note that we should expect an effective length for collective e.s. interactions larger than b, hence a larger cross–section, as particles will 'keep interacting' at distances larger than b since we are still within the Debye sphere (for most plasmas of interest $b << \lambda_D$).
Taking $\sigma_{\text{ion}} \simeq \pi a_0^2$ for hydrogen we can evaluate the degree of ionisation above which we have a *strongly* ionised plasma

$$\frac{n_e}{n_n} > \frac{\sigma_{ion}}{\sigma_{Coulomb}} \sim \frac{\pi a_0^2}{\pi b^2} = a_0^2 \left(\frac{4\pi\varepsilon_0}{e^2}\right)^2 T^2 = 1.2 \times 10^{-3} T^2 [\text{eV}]. \tag{2.15}$$

Example

A neon tube has an electron temperature of about 10 eV (see figure 2.8). Equation (2.15) yields $n_e/n_n > 12\%$. For example, if $n_e/n_n \cong 20\%$, and there are more neutrals than electrons, the tube contains a strongly ionized plasma where collisions among charged particles dominate. The reason for this is the long range of interaction of the Coulomb force.

Chapter 3 Charged particle collisions

We have seen that collisions between electrons and atoms can produce ionisation, with $\sigma_{\text{ion}}^{\max} \sim \pi a_0^2$ ($a_0 \equiv$ Bohr radius). For these collisions the range of interaction is very short, namely about a_0.

In Plasma I you have seen that at high enough energies ($E \gtrsim 10$ keV) nuclei can collide and produce nuclear fusion reactions. Also, in this case the range of interaction is very short, of the order of the size of the nuclei, namely about 10^{-15} m.

Both of these are examples of *inelastic collisions*. We now focus on collisions between charged particles, occurring once the plasma is formed. Collisions of charged particles are the result of the *long–range* Coulomb force and can be considered as *elastic*(*).

We define as '**collision**' the binary interaction between *two* charged particles.

This approach of considering the trajectory of a particle affected by a number of binary interactions (collisions) is only an approximation. In reality, the trajectory of a particle is affected by many other particles (those within the Debye sphere) at once. We will need to find a way to account for this effect, and we will do it by considering the combined effect of many binary collisions.

We have seen that a plasma with much less ions/electrons than neutral atoms can still be *strongly ionised* in the sense that Coulomb collisions can dominate over collisions with neutrals. This is due to the long range of Coulomb collisions. Based on a very simple model we took the Landau length b, such that

$$\frac{e^2}{4\pi\varepsilon_0 b} \sim T \;\Rightarrow\; b \sim \frac{e^2}{4\pi\varepsilon_0 T} \quad \text{and} \quad \sigma_{\text{ Coulomb}} \sim \pi b^2 \sim \frac{10^{-17}}{T_{[\text{eV}]}^2}\ [\text{m}^2]$$

Now we need to calculate σ_{Coulomb} properly, in particular considering multiple small–angle collisions. We will find that

$$\sigma_{\text{Coulomb}} \gg \pi b^2$$

and we will be in a position to evaluate the effective collision cross-section or frequency for the different processes of interest. We will evaluate:

- Energy transfer rates (thermalisation, equilibrium, heating)
- Momentum transfer rates (isotropisation, "pitch angle" scattering)
- Plasma resistivity (drag)
- Diffusion rates (transport of particles across and along the magnetic field $\mathbf{B}$)

This analysis will occupy this section of the course.

(*) Charged particles, if accelerated, emit radiation, so they loose energy. For example, electrons deflected by collisions with ions in fusion plasmas emit radiation (*Bremsstrahlung*) in the form of X-rays. $\frac{\text{Radiated energy}}{\frac{1}{2}m_e v^2} \sim \left(\frac{v}{c}\right)^3 \ll 1$. Here we neglect the power loss by radiation and consider Coulomb collisions as elastic.

3.1 Two particles interacting via Coulomb potential

We just review the lines of the calculation, as you have seen it in lecture 3 of Plasma Physics I.

initial		final
$\mathbf{v}_1; \mathbf{v}_2$	$\Longrightarrow$	$\mathbf{v}_1'; \mathbf{v}_2'$
$m_1, q_1; m_2, q_2$	$\Longrightarrow$	$m_1, q_1; m_2, q_2$

Note that the mass and the charge are conserved. In elastic collisions the energy and the momentum are also conserved:

$$m_1 v_1^2 + m_2 v_2^2 = m_1 {v_1'}^2 + m_2 {v_2'}^2 \tag{3.1}$$
$$m_1 \mathbf{v}_1 + m_2 \mathbf{v}_2 = m_1 \mathbf{v}_1' + m_2 \mathbf{v}_2' \tag{3.2}$$

Definition 1: velocity of center–of–mass

$$\mathbf{u} := \frac{m_1 \mathbf{v}_1 + m_2 \mathbf{v}_2}{m_1 + m_2} = \text{const} \tag{3.3}$$

Definition 2: relative velocity

$$\mathbf{v} := \mathbf{v}_1 - \mathbf{v}_2 \tag{3.4}$$

Definition 3: reduced mass(†)

$$\mu := \frac{m_1 m_2}{m_1 + m_2} \tag{3.5}$$

3.1.1 Going to the Center–of–Mass reference frame

$$\mathbf{v}_1 - \mathbf{u} = \frac{m_2}{m_1 + m_2}\mathbf{v} \tag{3.6}$$
$$\mathbf{v}_2 - \mathbf{u} = -\frac{m_1}{m_1 + m_2}\mathbf{v} \tag{3.7}$$

The force in this frame(‡) is

$$\mathbf{F}_{12} = m_1 \frac{d}{dt}(\mathbf{v}_1 - \mathbf{u}) = \frac{m_1 m_2}{m_1 + m_2}\dot{\mathbf{v}} = \mu\dot{\mathbf{v}} \tag{3.8}$$
$$\mathbf{F}_{21} = m_2 \frac{d}{dt}(\mathbf{v}_2 - \mathbf{u}) = -\frac{m_1 m_2}{m_1 + m_2}\dot{\mathbf{v}} = -\mu\dot{\mathbf{v}} \tag{3.9}$$

and the equation of motion

$$\mu\dot{\mathbf{v}} = \mathbf{F}(\mathbf{r}) \tag{3.10}$$

where $\mathbf{r} = \mathbf{x}_1 - \mathbf{x}_2$ and $\mathbf{v} = \dot{\mathbf{r}}$. The Coulomb force $\mathbf{F}$ is a central force

$$\mathbf{F}(\mathbf{r}) = \frac{q_1 q_2}{4\pi\varepsilon_0}\frac{\mathbf{r}}{r^3} \tag{3.11}$$

(†) if $m_2 \gg m_1$ then $\mu \sim m_1$
(‡) $\mathbf{F}_{12} = -\mathbf{F}_{21}$

From conservation of energy and momentum we know that

$$|\mathbf{v}| = |\mathbf{v}'|$$

and

$$|\mathbf{v}_1 - \mathbf{u}| = |(\mathbf{v}_1 - \mathbf{u})'|$$
$$|\mathbf{v}_2 - \mathbf{u}| = |(\mathbf{v}_2 - \mathbf{u})'|$$

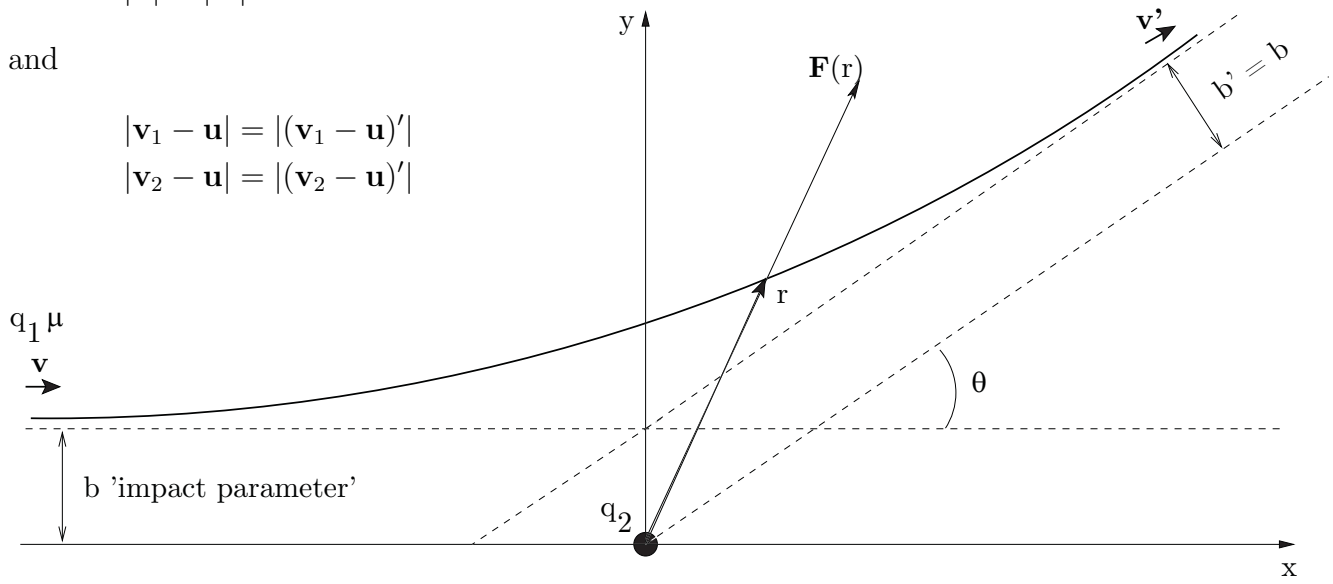

Figure 3.1: Geometry of the Coulomb collision in the center–of–mass frame. As $|\mathbf{v}| = |\mathbf{v}'|$ we know that $b' = b$. At $t \to -\infty$ the particle m_1, q_1 has velocity $(v) = v(e)_x$ and impact parameter b.

i.e. velocities change *direction* but *not* absolute value. We also know that for a central force the motion is in a plane and angular momentum is conserved. The problem is solved in the center–of–mass frame (figure 3.1). Note that the process is entirely described by ϑ, v and the impact parameter b. Using conservation laws in the relevant geometry (see lecture notes in Plasma I), we find:

$$\tan\frac{\theta}{2} = \frac{b_{90}}{b} \quad \text{with}^{(\S)} \quad b_{90} \equiv b_{90}(v) = \frac{q_1 q_2}{4\pi\varepsilon_0 \mu v^2} \tag{3.12}$$

b_{90} is the impact parameter corresponding to a deflection by 90°.[(¶)] In general the deflections will be smaller with $b > b_{90}$, but we expect they will also be more frequent.

3.1.2 From Center–of–Mass to laboratory frame

In different frames the deflection angles will be different (figure 3.2).

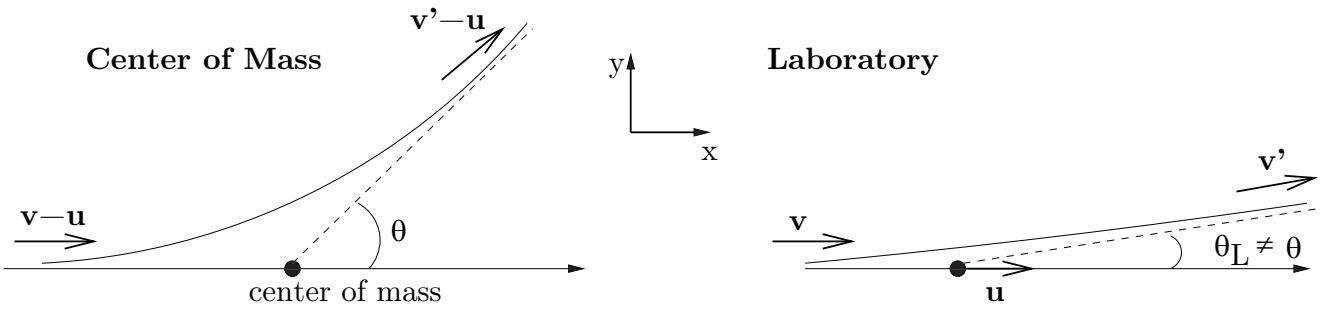

Figure 3.2: Deflection angle in center–of–mass frame (left) and in the frame of the laboratory (right). Note that the angles of deflection are very different in the two frames.

(¶) for $\theta = \pi/2 = 90°$, $\tan\pi/2 = 1$ and $b = b_{90}$

After some trigonometry one finds for the deflection angle in the laboratory frame:

$$\tan\theta_L = \frac{\frac{m_2}{m_1+m_2} v\sin\theta}{u + \frac{m_2}{m_1+m_2} v\cos\theta}. \tag{3.13}$$

For *small angles* and $v_1 \gg v_2$ we have $\theta_L \simeq \frac{m_2}{m_1+m_2}\theta$[(‖)]. Furthermore, if $m_2 \gg m_1$ – as in the case of electrons colliding with ions – then $\theta_L \simeq \theta$.

3.2 Effect of multiple collisions

To account for the overall effect of collisions we need to look at different deflection angles and impact parameters.

3.2.1 Rutherford differential cross–section

Particles with impact parameter in $(b,\ b-db)$ are scattered into angles $(\theta,\ \theta+d\theta)$, corresponding to $d\Omega$ (figure 3.3).

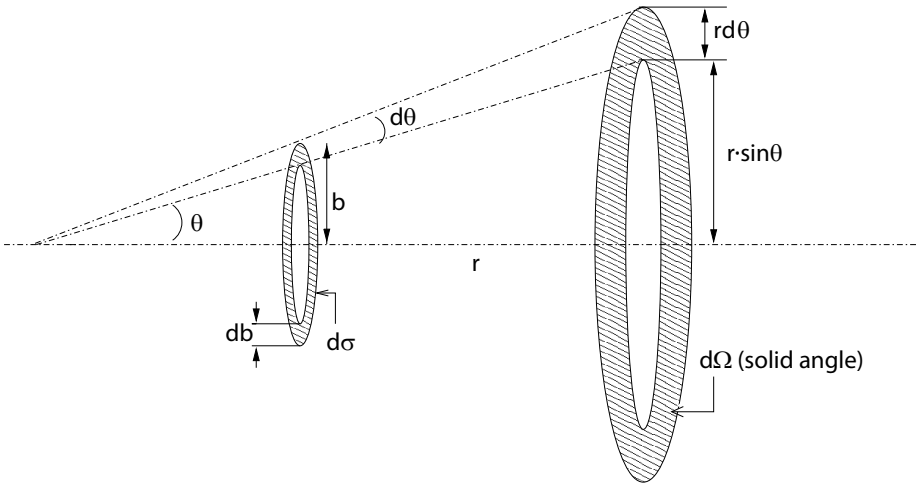

Figure 3.3: Concept of the differential cross–section

We have

$$d\Omega = \frac{2\pi r\sin\theta\cdot r|d\theta|}{r^2} = 2\pi\sin\theta|d\theta| \tag{3.14}$$

$$d\sigma = 2\pi b|db| \tag{3.15}$$

Definition: Differential cross–section $d\sigma/d\Omega$

$$n_{targets}\left(\frac{d\sigma}{d\Omega}\right)d\Omega \quad\Leftrightarrow\quad \begin{array}{l}\#\text{ of particles per unit path length which}\\ \text{are scattered into the solid angle } d\Omega\end{array}$$

Alternatively, $d\sigma/d\Omega$ can be defined in terms of the number of particles dN_{sc} scattered in $d\Omega$ per unit time dt divided by the total flux of particles. The incoming flux Φ_{in} is $\Phi_{in} = n_{in}v = \frac{N_{in}}{Avdt}v$ thus for one electron ($N_{in}=1$) we find

$$\frac{dN_{sc}/dt}{\text{incoming flux}} = N_{targets}\left(\frac{d\sigma}{d\Omega}\right)d\Omega \quad\Longrightarrow\quad \frac{dN_{sc}}{dt} = \frac{N_{targets}}{Adt}\left(\frac{d\sigma}{d\Omega}\right)d\Omega$$

Since the unit length dl is equal to vdt and the volume is $V = Adl \equiv Avdt$ we obtain again

$$\frac{dN_{sc}}{dl} = \frac{N_{targets}}{A\,vdt}\left(\frac{d\sigma}{d\Omega}\right)d\Omega = \frac{N_{targets}}{V}\left(\frac{d\sigma}{d\Omega}\right)d\Omega = n_{targets}\left(\frac{d\sigma}{d\Omega}\right)d\Omega$$

(‖) This approximation is valid only if $v_1 \gg v_2$

Using the relation between b and σ and the definitions of $d\sigma$, eq.(3.15), and $d\Omega$, eq.(3.14), we find (in the center–of–mass frame) the **Rutherford cross–section**:

$$\frac{d\sigma}{d\Omega} = \frac{2\pi b|\mathrm{d}b|}{2\pi \sin\theta|\mathrm{d}\theta|} = \frac{b}{\sin\theta}\frac{d}{d\theta}(b) = \frac{b}{\sin\theta}\frac{\mathrm{d}}{\mathrm{d}\theta}\left(b_{90}\ \mathrm{cotg}\frac{\theta}{2}\right) = \frac{b_{90}^2}{4\sin^4\frac{\theta}{2}} = \frac{q_1^2 q_2^2}{(4\pi\varepsilon_0)^2\mu^2 v^4}\frac{1}{4\sin^4\frac{\theta}{2}} \tag{3.16}$$

It describes the scattering of charged particles by Coulomb forces. To get the effective cross-section for collisions giving deflections in a range $\theta \in (\theta_1, \theta_2)$, we need to integrate(**)

$$\int_{\theta_1}^{\theta_2} \frac{d\sigma}{d\Omega} d\Omega(\theta)$$

For example, for collisions giving $\theta \geq 90°$:

$$\sigma(\theta \geq 90°) = \int_{\theta=\pi/2}^{\theta=\pi} \frac{d\sigma}{d\Omega} d\Omega(\theta) = \frac{b_{90}^2}{4}\int_{\pi/2}^{\pi} \frac{2\pi \sin\theta\, d\theta}{\sin^4\frac{\theta}{2}} = \pi b_{90}^2 \tag{3.17}$$

Note that in this case the same result could have been found intuitively: from the definition of b_{90}, follows that the "target surface" σ for which $\theta \geq 90°$ is πb_{90}^2. The expression of the Rutherford cross-section was used for the scattering of α–particles through metal foils:

- The dependence $\propto \sin^{-4}\frac{\theta}{2}$ gave a proof of the nuclear model of atoms, and detailed measurements gave estimates of the radius of the nucleons and of Z.
- Departure from $\propto \sin^{-4}\frac{\theta}{2}$ at high energies indicated the presence of short range nuclear forces.

Observations

1. $d\sigma/d\Omega \propto v^{-4}$: as the number of collisions goes as $v\, d\sigma/d\Omega$, collisional effects will scale as $T^{-3/2}$: the *hotter* the plasma, the *less* collisional.
2. For fixed v, $d\sigma/d\Omega$ increases for decreasing θ. For small θ: $d\sigma/d\Omega \propto \theta^{-4}$: small angle collisions are much more frequent.

In the following we will consider, unless explicitly stated otherwise, only small angle collisions.

3.2.2 Integration over possible impact parameters and Coulomb logarithm

To consider the cumulative effect of many small angle collisions let's analyse the *energy transfer rate* as an example. This is the mechanism responsible for thermalisation. In this case we are interested in how much energy is lost in each collision, and in summing over all possible collisions, for example considering all possible impact parameters.
The energy lost by particle '1' in one collision is(††)

$$\Delta E_k \cong \frac{1}{2} m_1 v^2 \frac{m_1 m_2}{(m_1+m_2)^2}\theta^2 \tag{3.18}$$

(**) the cross-section, derived here, corresponds to the effective cross-section for momentum transfer, which will be defined in sec.(3.3).

(††) the derivation of ΔE_k is given in the appendix B.

Considering that for small angles $\theta \simeq 2b_{90}/b$, this can be re–written as[(‡‡)]

$$\Delta E_k \cong \frac{1}{2} m_1 v^2 \frac{m_1 m_2}{(m_1+m_2)^2} \left(\frac{2b_{90}}{b}\right)^2 \tag{3.19}$$

This is the energy lost in a *single*, small angle collision on a stationary target. Let's calculate the loss of energy per unit length for impact parameter interval db:

$$\left.\frac{dE_k}{dl}\right|_{\text{over } db} = \Delta E_k \, d\sigma \, n \tag{3.20}$$

Remember that $d\sigma\, n$ is the number of collisions per unit length with impact parameter $b \in (b, b+db)$. The total loss of energy per unit length is obtained by integrating over all relevant impact parameters

$$\begin{aligned}
\left.\frac{dE_k}{dl}\right|_{\text{all } b} &= \int_{b_{\min}}^{b_{\max}} \left.\frac{dE_k}{dl}\right|_{\text{over } db} = \int_{b_{\min}}^{b_{\max}} \Delta E_k \, n \, 2\pi b \, db = \\
&= \int_{b_{\min}}^{b_{\max}} \frac{1}{2} m_1 v^2 \frac{m_1 m_2}{(m_1+m_2)^2} \left(\frac{2b_{90}}{b}\right)^2 n \, 2\pi b \, db = \\
&= E_k \, n \, 8\pi b_{90}^2 \frac{m_1 m_2}{(m_1+m_2)^2} \int_{b_{\min}}^{b_{\max}} \frac{db}{b}
\end{aligned} \tag{3.21}$$

What are $b_{\min}$ and $b_{\max}$? If we simply take $b_{\min} = 0$, $b_{\max} = \infty$ we have a logarithmic divergence, and not much physical meaning.

$b_{\min}$: We are considering only small angles. For $b < b_{90}$ the assumption of small angles would be violated.

$$\Longrightarrow \qquad b_{\min} \simeq b_{90}. \tag{3.22}$$

Note that at very high T_e, b_{90} becomes so small that quantum mechanical corrections must be included. In such cases one can take $b_{\min} \simeq \lambda_{\text{DeBroglie}} = h/mv$.

$b_{\max}$: Remember the Debye screening effect. Outside the Debye sphere, the potential is screened, so the 'collision' does not 'occur'

$$\Longrightarrow \qquad b_{\max} \simeq \lambda_D. \tag{3.23}$$

Thus

$$\frac{dE_k}{dl} = E_k \, n \, 8\pi b_{90}^2 \frac{m_1 m_2}{(m_1+m_2)^2} \ln\Lambda, \tag{3.24}$$

where $\ln\Lambda$ is the so called *Coulomb logarithm* and

$$\Lambda = \frac{\lambda_D}{b_{90}} = \frac{\sqrt{\varepsilon_0 T_e / e^2 n}}{q_1 q_2 / 4\pi\varepsilon_0 \mu v^2}. \tag{3.25}$$

Note that because of the very weak logarithmic dependence, the *exact* choice of $b_{\min}$, $b_{\max}$ is irrelevant. Typically, for most plasmas treated in this course, one can take $\ln\Lambda \sim 10$–20.

(‡‡) if $m_1 \ll m_2$, then

$$\frac{\Delta E_k}{E_k} \simeq \frac{m_1}{m_2} \left(\frac{2b_{90}}{b}\right)^2$$

It will take a long time to loose all the initial energy.

3.3 Effective collision frequencies for relaxation processes

We have to transform the loss per unit length to a loss per unit time.

3.3.1 Energy loss/transfer rate

$$\frac{dE_k}{dt} = v_1 \frac{dE_k}{dl} = v \frac{dE_k}{dl}, \tag{3.26}$$

if we identify v_1 with v (i.e. $v_2 = 0$).

Definition: Effective collision frequency for energy loss

$$\nu_{E_k} := \frac{1}{E_k} \frac{dE_k}{dt} \tag{3.27}$$

Note that by 'collision frequency' we don't simply mean the rate at which collisions take place, but *the rate at which collisions produce a certain effect* (in this case the loss of energy).
From the definition of ν_{E_k}:

$$\nu_{E_k} = v \frac{1}{E_k} \frac{dE_k}{dl} = 8\pi n \frac{q_1^2 q_2^2}{(4\pi\varepsilon_0)^2} \frac{\ln \Lambda}{m_1 m_2 v^3}, \tag{3.28}$$

or with the general relation between collision frequency and cross–section

$$\nu = n\sigma v \tag{3.29}$$

we have

$$\sigma_{E_k} = \frac{\nu_{E_k}}{nv} = \frac{q_1^2 q_2^2}{2\pi\varepsilon_0^2} \frac{\ln \Lambda}{m_1 m_2 v^4}. \tag{3.30}$$

3.3.2 Momentum loss/transfer rate

Again, we consider only small angles[(§§)]

$$\Delta p_x = m_1(v_1 - v_{1x}') \simeq \frac{m_2}{m_1 + m_2} \frac{\theta^2}{2} p_x, \qquad \text{or} \qquad \frac{\Delta p_x}{p_x} \simeq \frac{m_2}{m_1 + m_2} \frac{\theta^2}{2}. \tag{3.31}$$

With eq.(3.18) we find

$$\frac{\Delta p_x}{p_x} = \frac{1}{2} \frac{m_1 + m_2}{m_1} \frac{\Delta E_k}{E_k}. \tag{3.32}$$

If, for example, $m_1 \ll m_2$, then

$$\frac{\Delta p_x}{p_x} \simeq \frac{m_2}{2m_1} \frac{\Delta E_k}{E_k} \gg \frac{\Delta E_k}{E_k}. \tag{3.33}$$

We can apply the same concepts of effective collision frequency and cross–section as discussed for E_k:

$$\sigma_p = \sigma_{E_k} \frac{m_1 + m_2}{2m_1} = \frac{1}{2}\sigma_{E_k}\left(1 + \frac{m_2}{m_1}\right) = \sigma_{E_k} \times \begin{cases} \frac{1}{2}, & m_2 \ll m_1 \\ 1, & m_2 = m_1 \\ \gg 1, & m_2 \gg m_1 \end{cases}. \tag{3.34}$$

The third case corresponds to electrons scattered by ions, for which the transfer of momentum (and related change in the direction of the "pitch angle scattering") is dominant over the transfer of energy.

(§§) the formal derivation of Δp_x is given in the appendix B.

Chapter 4 Relaxation process and plasma resistivity

4.1 Summary of the velocity–dependent collision frequencies

In a plasma we have 4 kinds of collisions between charged particles:

	Energy	Momentum	
$e \to i$	$\nu_{E_k}^{e/i} = n_i \dfrac{Z^2 e^4}{2\pi\varepsilon_0^2} \dfrac{\ln\Lambda}{m_i m_e v_e^3}$	$\nu_p^{e/i} = \nu_{E_k}^{e/i} \dfrac{m_i}{2m_e}$	(4.1a)
$i \to e$	$\nu_{E_k}^{i/e} = n_e \dfrac{Z^2 e^4}{2\pi\varepsilon_0^2} \dfrac{\ln\Lambda}{m_i m_e v_i^3}$	$\nu_p^{i/e} = \dfrac{1}{2}\nu_{E_k}^{i/e}$	(4.1b)
$i \to i$	$\nu_{E_k}^{i/i} = n_i \dfrac{Z^4 e^4}{2\pi\varepsilon_0^2} \dfrac{\ln\Lambda}{m_i^2 v_i^3}$	$\nu_p^{i/i} = \nu_{E_k}^{i/i}$	(4.1c)
$e \to e$	$\nu_{E_k}^{e/e} = n_e \dfrac{e^4}{2\pi\varepsilon_0^2} \dfrac{\ln\Lambda}{m_e^2 v_e^3}$	$\nu_p^{e/e} = \nu_{E_k}^{e/e}$	(4.1d)

where Z is the charge number of the ions. In principle $\ln\Lambda_e \neq \ln\Lambda_i$, but – due to the weak logarithmic dependence – the difference can usually be neglected.

In summary, the general form of ν_{E_k} for collisions of particles of the species j (projectiles) upon particles of the species k (targets) is

$$\nu_{E_k}^{j/k} \sim n_k \frac{Z_j^2\, Z_k^2 e^4}{2\pi\varepsilon_0^2} \frac{\ln\Lambda_k}{m_j\, m_k v_j^3} \tag{4.2}$$

and for most cases we can take $\ln\Lambda_k \approx$ const.

4.2 Average collision frequencies

Until now we have considered the case of a particle with a given velocity v colliding with a fixed target. We have averaged over the impact parameters and summed all the contributions from the continuous distribution of scatterers.

In a plasma we usually deal with many particles of the same species with different velocities – what we call a 'population'. Of course, the full description of the dynamics of each particle is impossible. Thus we might be interested in the *average* behaviour of this population in terms of energy and momentum transfer, instead of considering the behaviour of single particles.

The common way to describe a population is through its distribution function $f(\mathbf{x}, \mathbf{v}, t)$. For the time being let's forget the dependence of f upon the spatial and temporal coordinates, and retain only the information on the distribution of velocities: $f = f(\mathbf{v})$. To get information on the average behaviour of a population, we need to average our previous results for the collision frequencies over the velocity distribution.

'Philosophical' problem: we do not know yet what kind of distribution we can consider (e.g. Maxwellian?), as we do not know yet the averaged value of collisional cross–sections. As we must assume one form for the distribution in order to perform the average, we choose a Maxwellian; then we will check whether in the plasmas of interest there is enough time for collisions to *thermalise* the particles and force their distributions to relax into Maxwellians.

To get out of this logical trap one can look for experimental evidence (see appendix C) for methods to measure distribution functions). It is found experimentally that $f_{e,i}(\mathbf{v})$ is in general well approximated by a Maxwellian even before collisions have the time to act on the particles, especially in the case of electrons.(*)

In the next sections we will derive the expressions for the average collision frequencies for exchange of energy and momentum.

A Maxwellian can be characterised by only two parameters, its width and the shift. Physically, these correspond to a temperature and a drift, and we will try to express our results in terms of these quantities.

The average rate of change for the generic quantity A (energy or momentum) can be expressed as a frequency $\bar{\nu}_A$ or by a characteristic time $\tau_A \equiv 1/\bar{\nu}_A$, with

$$\bar{\nu}_A = \frac{1}{\langle |A| \rangle} \left\langle \frac{d|A|}{dt} \right\rangle \tag{4.3}$$

and the average $\langle \cdot \rangle$ is performed over the distribution function $f(\mathbf{v})$. Eq.(4.3) tells us that if we start at $t = 0$ with a value $A = A_0$, after a time τ_A the change of $A = A(t)$ will be *of the same order as* A_0 (figure 4.1).

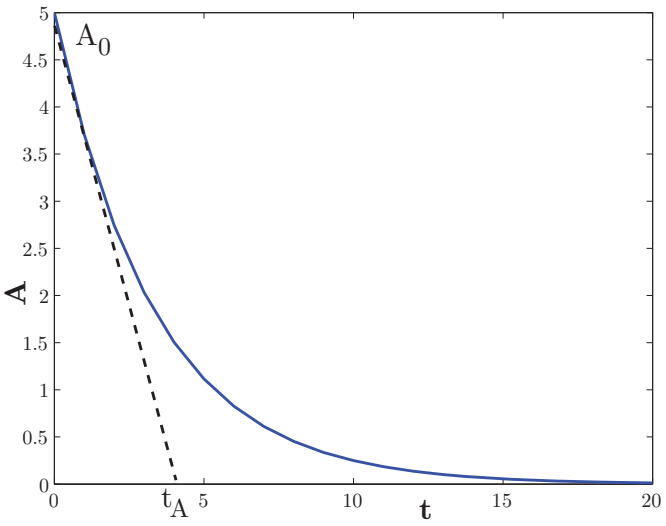

Figure 4.1: Concept of 'average collision frequency' and associated characteristic time: after τ_A the change of A with respect to its initial value A_0 is of the order of the initial value A_0.

4.3 Momentum loss of thermal plasma

4.3.1 $e \to i$

Ignore the ion thermal motion: $v_i \ll v_e$. The electrons are described by a Maxwellian distribution shifted by a drift velocity $\mathbf{v}_\mathrm{d}$

$$f_e(\mathbf{v}_e) = n_e \left(\frac{m_e}{2\pi\, T_e} \right)^{3/2} \exp\left\{ -\frac{m_e(\mathbf{v}_e - \mathbf{v}_\mathrm{d})^2}{2\, T_e} \right\}. \tag{4.4}$$

The rate at which an electron of velocity v_e loses momentum has been given in eq.(4.1a)

$$\nu_p^{e/i}(v_e) = n_i \frac{Z^2 e^4}{4\pi\varepsilon_0^2} \frac{\ln\Lambda}{m_e^2 v_e^3}. \tag{4.5}$$

The total loss of momentum per unit volume per unit time defines the average collision frequency

$$\bar{\nu}_p^{e/i} := \frac{1}{|\mathbf{p}|} \left\langle \left| \frac{d\mathbf{p}}{dt} \right| \right\rangle, \tag{4.6}$$

(*) This is called the *Langmuir paradox*, and it is still unsolved. Turbulent electric fields are thought to be the key–issue.

with

$$\left\langle \frac{d\mathbf{p}}{dt} \right\rangle = \frac{1}{n_e} \int f_e(\mathbf{v}) \underbrace{m_e \mathbf{v}\, \nu_p(v)}_{d\mathbf{p}/dt} d^3v, \tag{4.7}$$

where $\nu_p \equiv \nu_p^{e/i}$ and $v \equiv v_e$ have been introduced to simplify the notation. An intuitive guess is

$$\bar{\nu}_p^{e/i} \sim \nu_p^{e/i}(v_{\mathrm{the}}) \tag{4.8}$$

where $v_{\mathrm{the}} = \sqrt{T_e/m_e}$. A more accurate calculation(†), assuming $\mathbf{v}_{\mathrm{d}} = v_{\mathrm{d}}\hat{\mathbf{x}}$, $v_{\mathrm{d}} \ll v_{\mathrm{the}}$ and $\ln\Lambda \simeq$ const, independent of v, yields

$$\bar{\nu}_p^{e/i} = \frac{1}{3}\sqrt{\frac{2}{\pi}}\nu_p^{e/i}(v_{\mathrm{the}}) \simeq 0.26\, \nu_p^{e/i}(v_{\mathrm{the}}) \tag{4.9}$$

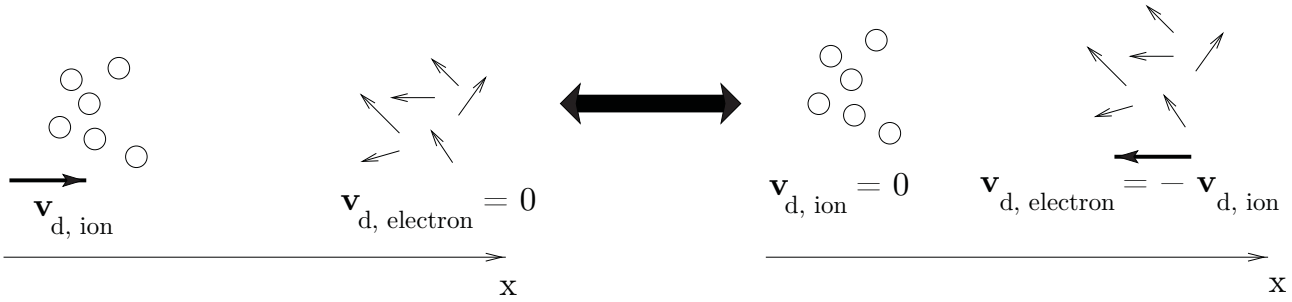

Figure 4.2: Galileian transformation of the collision $e \to i$ (left) into $i \leftarrow e$ (right).

4.3.2 $i \to e$

As it is still the *electron* thermal motion which is dominating the relative motion, the result can be obtained from the case $e \to i$ by a simple Galileian transformation (figure 4.2). Since the total momentum of the plasma is conserved, the momentum lost by the electrons must be equal to that acquired by the ions, then the rate of momentum transfer is the same

$$\left|\frac{dp_e}{dt}\right| = \left|\frac{dp_i}{dt}\right| \quad \Rightarrow \quad \left|p_e \nu_p^{e/i}\right| = \left|p_i \nu_p^{i/e}\right| \quad \Rightarrow \quad |p_e|\, \bar{\nu}_p^{e/i} = |p_i|\, \bar{\nu}_p^{i/e}$$

and

$$\begin{aligned}
\bar{\nu}_p^{i/e} &= \frac{1}{n_i m_i v_d} \int d\underline{v} f_e(\underline{v}) \underbrace{p_{i,x}\nu_p^{i/e}}_{p_{e,x}\nu_p^{e/i}} \\
&= \frac{1}{n_i m_i v_d} \frac{m_e}{m_e} \int d\underline{v} f_e(\underline{v}) p_{e,x} \nu_p^{e/i} \\
&= \frac{m_e}{m_i} \underbrace{\frac{1}{n_i m_e v_d} \int d\underline{v} f_e(\underline{v}) p_{e,x} \nu_p^{e/i}}_{\bar{\nu}_p^{e/i}} \\
\bar{\nu}_p^{i/e} &= \frac{m_e}{m_i} \bar{\nu}_p^{e/i}
\end{aligned} \tag{4.10}$$

Note that $\bar{\nu}_p^{i/e} \ll \bar{\nu}_p^{e/i}$ since $\frac{m_e}{m_i} \ll 1$. This makes sense, since for the light electrons it is much more difficult to scatter (e.g. isotropize) the heavy ions.

(†) See exercise no.2, given on Thursday, 30th of September, 2010.

4.3.3 $i \to i$

We can consider the same formalism as above, with one caveat: both classes of particles move, and we need to consider *two* drifting Maxwellian distributions. Using the center–of–mass frame one finds:

- The two ion masses are equal[‡] (same ion species)

$$\bar{\nu}_p^{i/i} \simeq \frac{1}{\sqrt{2}} \left(\frac{m_e}{m_i}\right)^{1/2} \left(\frac{T_e}{T_i}\right)^{3/2} Z^2 \bar{\nu}_p^{e/i}, \tag{4.11}$$

- The ion species are different

$$\bar{\nu}_p^{i/i'} = \frac{1}{3}\sqrt{\frac{2}{\pi}} n_{i'} \frac{q_i^2 q_{i'}^2}{4\pi\varepsilon_0^2} \frac{\ln\Lambda_{i'}}{m_i^{1/2} T_i^{3/2}} \left(\frac{m_{i'}}{m_i + m_{i'}}\right)^{1/2}, \tag{4.12}$$

4.3.4 $e \to e$

Again, this is similar to $i \to i$ and $e \to i$. The result is

$$\bar{\nu}_p^{e/e} \simeq \frac{1}{\sqrt{2}} \bar{\nu}_p^{e/i}. \tag{4.13}$$

4.4 Summary of average collision frequencies

4.4.1 Momentum loss

$$\bar{\nu}_p^{e/i} = \frac{1}{3}\sqrt{\frac{2}{\pi}} \nu_p^{e/i}(v_{\text{the}}) = \frac{1}{3}\sqrt{\frac{2}{\pi}} n_i \frac{Z^2 e^4}{4\pi\varepsilon_0^2} \frac{\ln\Lambda}{m_e^2 v_{\text{the}}^3} = \frac{1}{3}\sqrt{\frac{2}{\pi}} n_i \frac{Z^2 e^4 \ln\Lambda}{4\pi\varepsilon_0^2 m_e^{1/2}} \frac{1}{T_e^{3/2}} \tag{4.14a}$$

$$\bar{\nu}_p^{e/e} \simeq \frac{1}{\sqrt{2}} \bar{\nu}_p^{e/i} \tag{4.14b}$$

$$\bar{\nu}_p^{i/e} \simeq \frac{n_e m_e}{n_i m_i} \bar{\nu}_p^{e/i} \tag{4.14c}$$

$$\bar{\nu}_p^{i/i} \simeq \frac{1}{\sqrt{2}} \sqrt{\frac{m_e}{m_i}} \left(\frac{T_e}{T_i}\right)^{3/2} \bar{\nu}_p^{e/i} \tag{4.14d}$$

4.4.2 Energy loss

Based on $\nu_{E_k} \simeq \frac{2m_1}{m_1+m_2}\nu_p$ we find

$$\bar{\nu}_{E_k}^{e/i} = 2\frac{m_e}{m_i} \bar{\nu}_p^{e/i} \tag{4.15a}$$

$$\bar{\nu}_{E_k}^{i/e} = 2\bar{\nu}_p^{i/e} \simeq \bar{\nu}_{E_k}^{e/i} \tag{4.15b}$$

$$\bar{\nu}_{E_k}^{i/i} = \bar{\nu}_p^{i/i} \tag{4.15c}$$

$$\bar{\nu}_{E_k}^{e/e} = \bar{\nu}_p^{e/e} \tag{4.15d}$$

i.e. the same relations as for the NOT averaged collision frequencies.

Note: We only treated the cases $e \to i$ and $i \to e$ rigorously, as we assumed $v_2 = 0$.

[‡] Hint: Eq.(4.11) is just $\bar{\nu}_p^{e/i}/\sqrt{2}$ calculated for parameters for ions instead of electrons

4.5 Hierarchy of characteristic time scales

Let's have a look at the hierarchy of characteristic time scales $\tau \equiv \bar{\nu}^{-1}$. The shortest time scale corresponds to the largest $\bar{\nu}$, *i.e.* $1/\bar{\nu}_p^{e/i}$. Note that

$$\frac{\tau_p^{i/i}}{\tau_p^{e/e}} = \left(\frac{\bar{\nu}_p^{i/i}}{\bar{\nu}_p^{e/i}}\right)^{-1} \simeq \left(\frac{m_i}{m_e}\right)^{1/2} \left(\frac{T_i}{T_e}\right)^{3/2} \frac{1}{Z^2}.$$

We can identify three typical time–scales, as shown in figure 4.3:

a.) – electrons lose momentum on ions
– electrons lose momentum on other electrons
– electrons lose energy to other electrons(§)

b.) – ions lose momentum on other ions
– ions lose energy to other ions(¶)

c.) – electrons *and* ions reach the thermal equilibrium

$$\frac{dT_e}{dt} = -\frac{dT_i}{dt} = -\bar{\nu}_{E_k}^{e/i}(T_e - T_i) \to 0 \tag{4.16}$$

– ions lose momentum on electrons

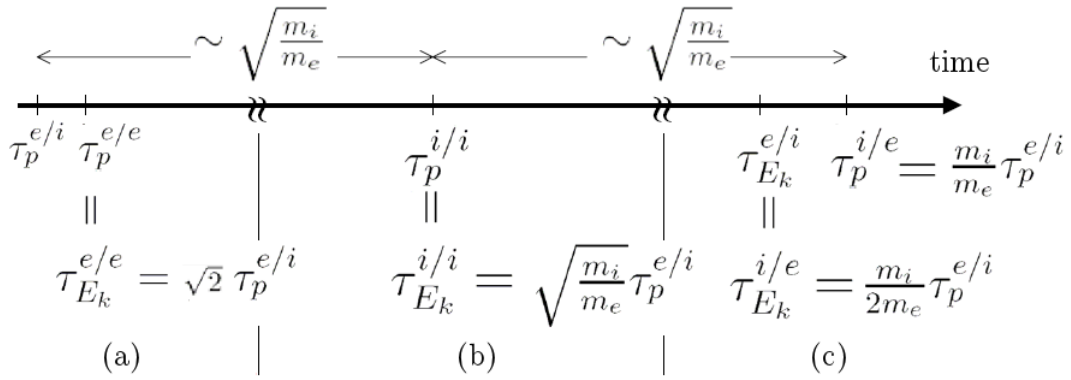

Figure 4.3: Characteristic time scales $\tau = 1/\nu$. All these time scales can be expressed as a function of the fastest one ($\tau_p^{e/i}$).

4.5.1 Quantitative estimates

We introduce the following definitions to simplify the notation:

$$\nu_e \equiv \bar{\nu}_p^{e/i} \qquad (\sim \bar{\nu}_p^{e/e}) \qquad \equiv \text{electron collision frequency} \tag{4.17}$$

$$\nu_i \equiv \bar{\nu}_p^{i/i} \qquad (= \bar{\nu}_{E_k}^{i/i}) \qquad \equiv \text{ion collision frequency} \tag{4.18}$$

Thus

$$\frac{\nu_e}{\nu_i} \simeq \sqrt{\frac{m_i}{m_e}} \qquad \text{for} \qquad T_e = T_i,\ Z = 1. \tag{4.19}$$

(§) e/e has both types of 'exchanges': isotropisation and thermalisation
(¶) i/i has both types of 'exchanges': isotropisation and thermalisation

For example, for a hydrogen plasma:

$$\nu_e\ [\mathrm{s}^{-1}] \sim 5 \cdot 10^{-11} \times \frac{n\,[\mathrm{m}^{-3}]}{T_e^{3/2}[\mathrm{eV}]} \quad \text{and} \quad \nu_i[\mathrm{s}^{-1}] \sim 10^{-12} \times \frac{n\,[\mathrm{m}^{-3}]}{T_i^{3/2}[\mathrm{eV}]}\ . \tag{4.20}$$

Take $T_e = T_i = 10$ keV; $n \simeq 10^{20}$ m^{-3}. The time–scales after which we can speak of electron and ion 'temperatures' (i.e. the population is at the thermal equilibrium) are

$$\nu_e \sim 5 \cdot 10^3\ \mathrm{s}^{-1} \to \tau_e \sim 0.2\ \mathrm{ms} \qquad \text{and} \qquad \nu_i \sim 100\ \mathrm{s}^{-1} \to \tau_i \sim 10\ \mathrm{ms} \tag{4.21}$$

$$\text{but} \qquad \tau_{T_i \to T_e} \sim \frac{m_i}{m_e}\tau_e \sim 1840 \cdot 0.2\ \mathrm{ms} \simeq 0.4\ \mathrm{s}. \tag{4.22}$$

This means that on short time–scales $\tau < \tau_{T_i \to T_e}$ we could have reached the thermal equilibrium between particles of the same species at two different temperatures T_e and T_i. But this does not necessarily imply that the two populations are in thermal equilibrium with each other, i.e. $T_e = T_i = T$. In fact, in most laboratory and fusion plasmas it is found that $T_e \neq T_i$. For example, remember the Lawson criterion(‖). For the same values as above we have $\tau_E \sim 1$ s. Over this time we should have thermalised electrons and ions (i.e. have well defined T_e, T_i) but not quite $T_e = T_i$.

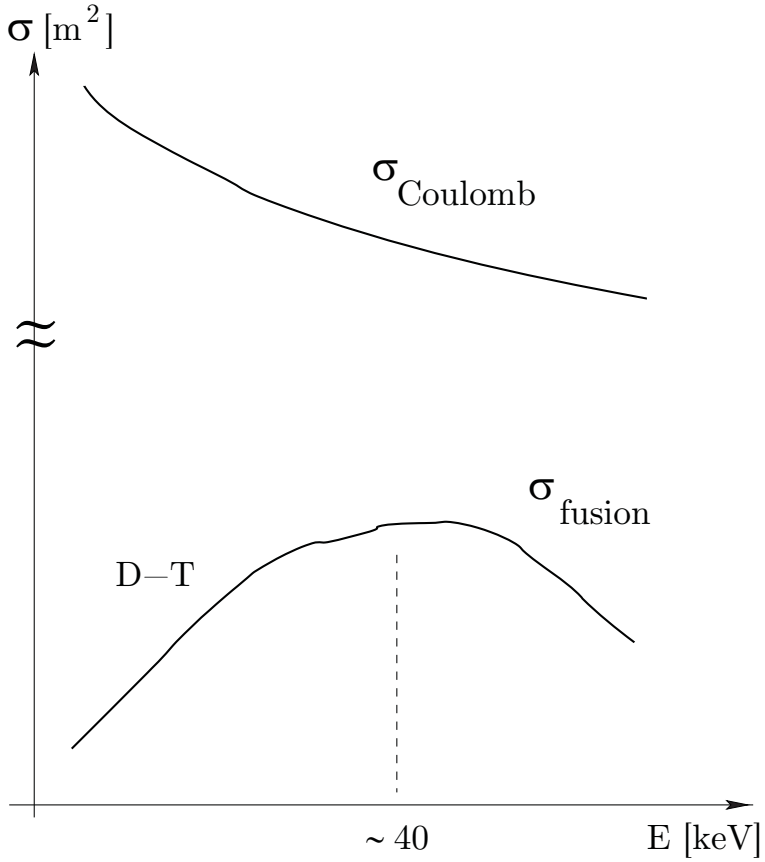

Figure 4.4: Fusion and Coulomb–scattering cross–sections

Note that compared to ion and electron gyrofrequencies, ν_e and ν_i are very small: the Larmor motion is essentially unperturbed by collisions. 'Larmor' physics is still valid (e.g. plasma diamagnetism).

Note also that for $T \sim 10$ keV we have $\sigma^{\alpha/\alpha}_{\mathrm{Coul},Q} \gg \sigma_{\mathrm{fusion}}$ where $\alpha = e$ or $\alpha = i$ and Q is the energy or the momentum (see figure 4.4), so the ions must be confined for many collision times before they can give rise to fusion reactions. In general it does make sense to consider Maxwellian distributions (in particular for evaluating the fusion reactivity).

(‖) This criterion gives the ignition condition in fusion devices. It can be written as follows: $n\tau_E T_i > 3 \times 10^{21}$ m$^{-3}\cdot$keV$\cdot$s where n is the ion density, τ_E is the energy confinement time and T_i is the ion temperature, refer to lecture 4 of Plasma Physics I or Chapter 9 in F.F. Chen's textbook (vol.2).

4.6 Plasma resistivity

Take a fully ionised plasma to which we apply an external electric field **E**. Electrons and ions will be accelerated in opposite directions, but will also be subject to a *friction force* due to Coulomb collisions. This friction force is responsible for the finite *resistivity* of the plasma. In order to calculate it, we assume

- Only electrons carry currents(**)
- Only $e \to i$ collisions occur (ignore $e \to e$)
- Distribution of electrons remains Maxwellian with a drift v_d

The momentum equation(††) along **E** (along **B** or with $\mathbf{B}=0$) is

$$m_e \frac{d\mathbf{v}_\mathrm{de}}{dt} = \underbrace{-e\mathbf{E}}_{acceleration} \underbrace{- m(\mathbf{v}_\mathrm{de} - \mathbf{v}_\mathrm{di})\nu_p^{e/i}}_{deceleration} \tag{4.23}$$

or, in its scalar form

$$m_e \frac{dv_\mathrm{d}}{dt} = -eE - \frac{m_e v_\mathrm{d}}{\tau_p^{e/i}(v)} \tag{4.24}$$

Note that for electrons the directions of $\mathbf{v}_\mathrm{d}$ and **E** are opposite. To solve eq.(4.24) we need to evaluate $\tau_p^{e/i}$; but for which velocity? Two cases can be distinguished:

1. $v_\mathrm{d} \ll v_\mathrm{the}$
2. $v_\mathrm{d} \geq v_\mathrm{the}$

4.6.1 $v_\mathrm{d} \ll v_{the}$

In this case, the velocity that dominates corresponds to the electron thermal motion and does not depend on v_d, as calculated in 4.3.1. We have a steady–state solution ($\frac{d}{dt}=0$) in which the acceleration due to the electric field is balanced by the collisional drag exerted by the ions:

$$\bar{\tau}_p^{e/i} eE = -m_e v_\mathrm{d} \quad \Rightarrow \quad v_\mathrm{d}^\mathrm{terminal} = -\frac{\bar{\tau}_p^{e/i} eE}{m_e}. \tag{4.25}$$

As $j = -en_e v_\mathrm{d}$ the previous equation can be recast as

$$\bar{\tau}_p^{e/i} eE = \frac{m_e j}{e n_e} \quad \text{or} \quad j = \frac{e^2 n_e}{m_e\, \bar{\nu}_p^{e/i}} E. \tag{4.26}$$

With the definition of the resistivity η, $j = \eta^{-1} E$, we find

$$\eta = \frac{m_e \bar{\nu}_p^{e/i}}{e^2 n_e} = \frac{m_e}{e^2 n_e} \frac{1}{3} \sqrt{\frac{2}{\pi}} \frac{(n_i Z) Z e^4 \ln\Lambda}{4\pi\varepsilon_0^2 m_e^{1/2} T_e^{3/2}} = \frac{\sqrt{2}}{\pi^{3/2}} \frac{m_e^{1/2} Z e^2 \ln\Lambda}{12 \varepsilon_0^2 T_e^{3/2}}. \tag{4.27}$$

(**) $m_e \ll m_i$; for similar energies $\longrightarrow |v_i| \ll |v_e|$

(††) Note that we need to consider *momentum* exchange collisions, as we have to do with directed velocity.

We observe that

- There is no dependence on the plasma density. In fact, the effect of density is to increase both the number of carriers and the number of collisions, so the two effects balance out.
- $\eta \propto T_e^{-3/2}$. For a metal, $\eta \propto T_e^{\alpha},\ \alpha > 0$: very different!
- Our simple calculation *over*–estimates η by a factor of 2 because we did not account for the acceleration of electrons by **E**: faster electrons are less subject to collisions and carry more current.
- From more complete calculations:

$$\eta \quad [\Omega\mathrm{m}] = \frac{Ze^2\sqrt{m_e}\ln\Lambda}{4\pi\epsilon_0^2 3\sqrt{2\pi}T_e^{3/2}} = 5.1\cdot 10^{-5}\times\frac{Z\ln\Lambda}{(T_e[\mathrm{eV}])^{3/2}} \qquad \text{“Spitzer resistivity”} \tag{4.28}$$

  This value agrees reasonably well with the experiments.

Examples:

1. Plasma at 100 eV: $\eta \sim 6\cdot 10^{-7}$ Ωm [$\sim \eta$ of stainless steel]
2. Plasma at 1 keV: $\eta \sim 2\cdot 10^{-8}$ Ωm [$\sim \eta$ of copper][(‡‡)]
3. For $T \gg 1$ keV plasma becomes almost superconducting

The decrease of the resistivity with the temperature has two consequences:

1. Magnetic flux is ‘frozen’ within plasma – a general property of supraconductors[(§§)]
2. Heating by current (‘ohmic heating’) becomes less and less effective at high T_e. The increase in energy per unit volume is

$$\frac{\text{Power}}{\text{Volume}} = \text{force}\times\text{velocity}\times\text{density} = e|E|\times v_\mathrm{d}\times n = \eta j^2 \propto T_e^{-3/2}. \tag{4.29}$$

Note that in the presence of **B** (with **B**$\|$**E**), we would have $\eta_\| \approx \eta$ and $\eta_\perp > \eta$: particles move preferentially along the magnetic field lines, therefore the resistivity in this direction is smaller than in the direction perpendicular to **B**.

(‡‡) e.g. solar flares: gigantic eruptions with $I \sim$ MA sustained by a small $\Delta V \leq 1$ Volt
(§§) e.g. solar wind carrying B–field with it.

4.6.2 $v_\mathrm{d} \gtrsim v_\mathrm{the}$

If E is sufficiently high that the relative speed is not much smaller than the electron thermal speed, $\bar{\tau}_p^{e/i}$ cannot be considered independent of v_d and we do not have necessarily a steady–state solution. In this case we cannot take the value of $\nu_p^{e/i}$ averaged over a Maxwellian distribution, but we need to retain the velocity dependent expression of $\nu_p^{e/i}(v_\mathrm{d})$ *and* the time derivative d/dt.

Thus

$$m_e \frac{dv_\mathrm{d}}{dt} = -eE - \nu_p^{e/i}(v_\mathrm{d}) m_e v_\mathrm{d}. \tag{4.30}$$

The key question is the sign of the term on the right hand side. For

$$e|E| > \nu_p^{e/i} m_e v_\mathrm{d} \tag{4.31}$$

we have acceleration, otherwise deceleration. If we have *acceleration*, an increase in v_d leads to a decrease in $\nu_p^{e/i}$. Then there is even more acceleration and so on. This is called the *run-away* regime: electrons with sufficiently high velocity are more and more accelerated by E as the collisional drag due to the friction force is insufficient to balance the acceleration given by the electric field (figure 4.5).

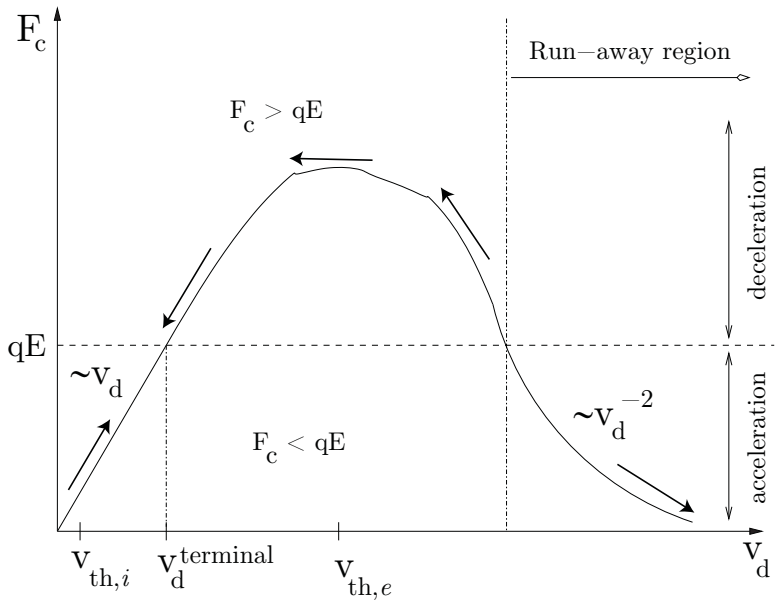

Figure 4.5: Sketch of the collisional drag F_c acting on electrons as a function of their velocity v_d for $E > E_D$. The black arrows indicate the overall acceleration or deceleration.

By expressing $\nu_p^{e/i}$ in terms of v_d, $\nu_p^{e/i} = \nu_p^{e/i}(v_\mathrm{d})$, see eq.4.5, we have

$$e|E| > \frac{(n_i Z) Z e^4}{4\pi\epsilon_0^2} \frac{\ln\Lambda}{m_e^2 v_\mathrm{d}^3} m_e v_\mathrm{d}$$

$$|E| > \frac{n_e Z e^3 \ln\Lambda}{4\pi\varepsilon_0^2 m_e v_\mathrm{d}^2} \qquad \text{or} \qquad \frac{1}{2} m_e v_\mathrm{d}^2 > \frac{n_e Z e^3 \ln\Lambda}{8\pi\varepsilon_0^2 |E|} \tag{4.32}$$

Let's divide by T_e:

$$\frac{1}{2} \frac{m_e v_d^2}{T_e} > \frac{E_D}{|E|} \tag{4.33}$$

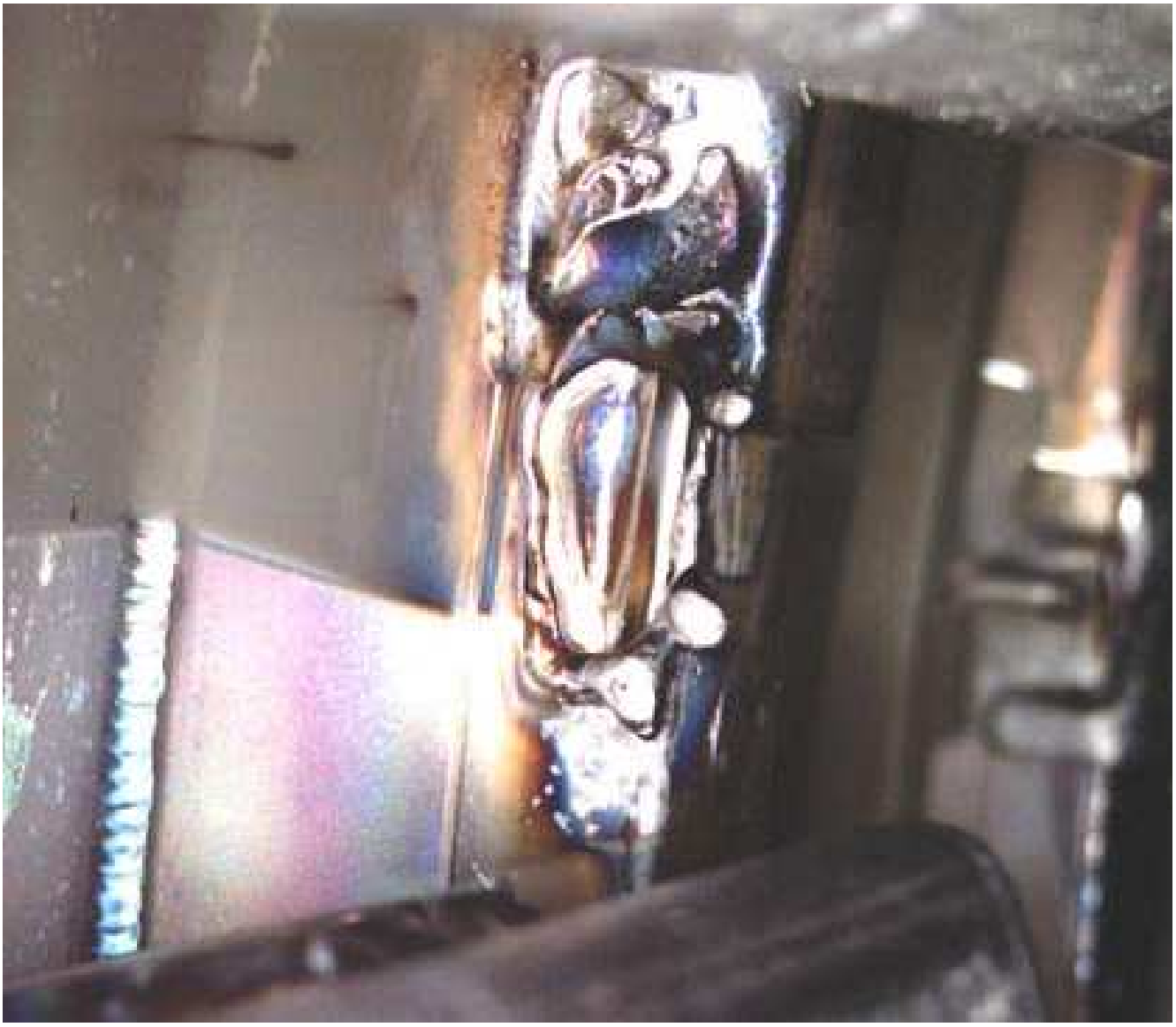

Figure 4.6: Melting damage to the upper inner wall of JET, thought to be caused by run-away electrons.

where we have introduced the Dreicer electric field $E_D := \frac{n_e Z e^3 \ln\Lambda}{8\pi\varepsilon_0^2 T_e}$. The meaning of this form is that for $|E| = E_D$ the run-away regime is reached at $E_{\text{drift}} = \frac{1}{2} m_e v_{\text{d}}^2 = T_e$.

The production of run-away electrons is a serious problem in tokamaks. For typical parameters of fusion plasmas the Dreicer field can be as low as 1 V/m. The probability of generating run-away electrons is then quite high, and these electrons can reach energies of the order of a few MeV. If their number is sufficiently high they give rise to 'electron beams' that are no more confined inside the plasma. In fact, they are thought to be responsible for damages to the vacuum vessel walls and to other components installed inside the vessel (figure 4.6).

Once an electron exceeds the critical velocity, eq.(4.33), it is continuously accelerated and can reach energies of several tens of MeV. Because of the toroidal acceleration, electrons emit synchrotron radiation. A relativistic limit to the maximum energy an electron can reach is given by a balance between the amount of power that is absorbed from the accelerating electric field and the amount of power lost by electromagnetic radiation.

So far we have studied the physics of collisions in *uniform* plasmas. The effect of collisions in *non–uniform* plasmas is to provide *transport* of both particles and energy. The transport in velocity space will be discussed later on in the course. Now we deal with transport in *real space*.

Chapter 5 Diffusion and transport

Let us review some general results of statistical mechanisms for a *random walk* in one dimension (figure 5.1). A particle undergoing N statistically independent steps of size $\xi = |\xi_i|$ will arrive at position

$$x = \sum_{i=1}^{N} \xi_i \tag{5.1}$$

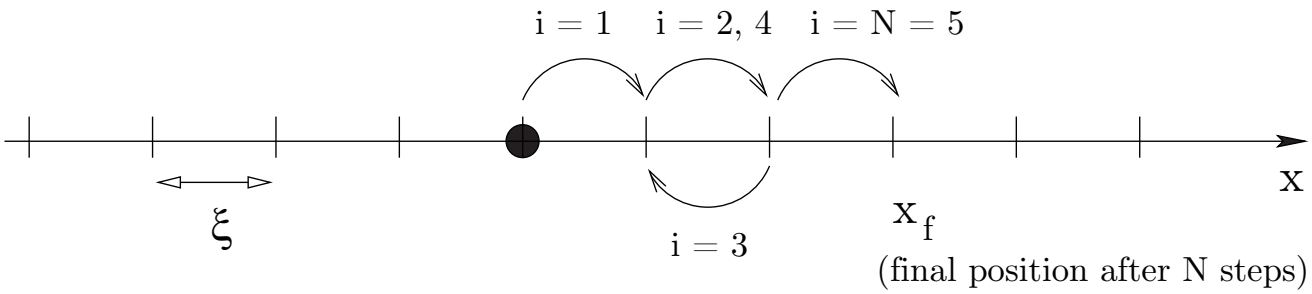

Figure 5.1: Random walk

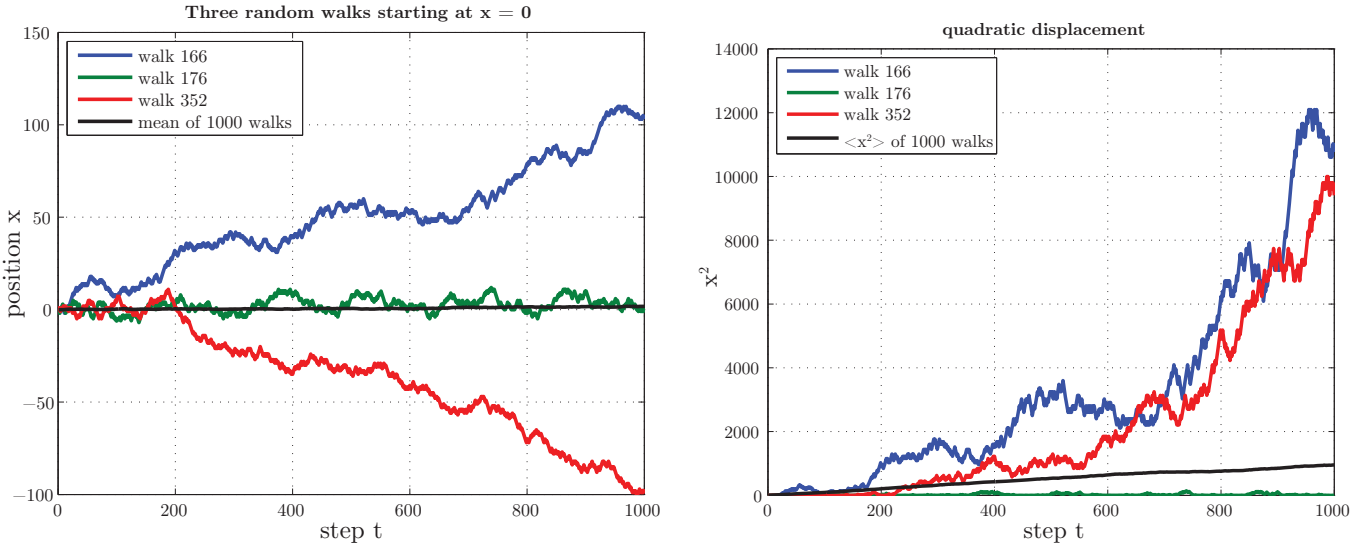

(a) (b)

Figure 5.2: (a) Deviation from origin as a function of time for three random walks. The black line indicates the average deviation as a function of time calculated for 1000 random walks.
(b) Squared deviation for the three random walks. The black line indicates the average square deviation as a function of time calculated for 1000 random walks. Note that the diffusion coefficient D is given by the slope of $\overline{x^2}$.

As each displacement is in a random direction the average displacement(*)

$$\overline{x} = 0. \tag{5.2}$$

(*) Here 'average' means: averaged over many random walks, *not* averaged over time for one random walk

(figure 5.2a). However, the mean *quadratic* displacement (figure 5.2b)

$$\overline{x^2} = \sum_i \overline{\xi_i^2} + \sum_i \sum_{j\neq i} \overline{\xi_i \xi_j} = N\xi^2 + \sum_i \sum_{j\neq i} \overline{\xi_i \xi_j} = N\xi^2 \neq 0, \tag{5.3}$$

where we could set $\overline{\xi_i \xi_j} = \overline{\xi_i} \cdot \overline{\xi_j} = 0$ by virtue of the statistical independence of the ξ_i. Introducing the inter–collision time τ and replacing

$$\xi^2 \cong \langle v^2 \rangle \tau^2 \qquad \text{and} \qquad N = \frac{t}{\tau} \tag{5.4}$$

we finally obtain

$$\overline{x^2} \cong \frac{\xi^2}{\tau} t = \langle v^2 \rangle \tau \, t \equiv Dt, \tag{5.5}$$

where D is the diffusion coefficient. In general

$$D \cong (\text{step size})^2 \times \text{frequency}. \tag{5.6}$$

where the step size is the distance particles travel in one direction in between and as a consequence of a collision and the frequency corresponds to the inverse of the characteristic time between collisions.

5.1 Transport of particles

5.1.1 Weakly ionised plasmas with B = 0

We consider here the case of a weakly ionised plasma, but the same formalism can be applied also to strongly ionized plasmas.

For electrons we have

$$\text{step size} = \lambda_{\text{mfp}} = \frac{1}{n\sigma} = \frac{v_{\text{the}}}{\nu^{e/n}} \tag{5.7}$$

$$\text{frequency} = \nu^{e/n} \tag{5.8}$$

where $\nu^{e/n} = n_{\text{neutrals}} \sigma_e v_{\text{the}}$ is the frequency of electron/neutral collisions. The choice of the collision frequency depends on the degree of ionisation: in strongly ionised plasmas one should use ν_e instead.

Thus

$$D_e \cong \lambda_{\text{mfp}}^2 \nu^{e/n} = \frac{v_{\text{the}}^2}{\nu^{e/n}}, \tag{5.9}$$

$$D_i \cong \frac{v_{\text{th}i}^2}{\nu^{i/n}}. \tag{5.10}$$

Note that

$$\frac{D_e}{D_i} = \frac{v_{\text{the}}^2}{v_{\text{th}i}^2} \frac{\nu^{i/n}}{\nu^{e/n}} \sim \frac{v_{\text{the}}}{v_{\text{th}i}} \gg 1 \qquad \text{as} \qquad \frac{\nu^{e/n}}{\nu^{i/n}} \sim \frac{v_{\text{the}}}{v_{\text{th}i}} \tag{5.11}$$

because the atomic cross–section for elastic collisions is similar for electrons and ions. We see that *collisions reduce transport.*

In the following we want to answer the following questions:

1. Is diffusion really the important transport mechanism?
2. Can ions and electrons diffuse at (very) different rates in real plasmas?

To answer these questions we need a model. The equation of motion in non-magnetised plasmas ($\mathbf{B} = 0$) is sufficiently simple that we can use it and compare the result with the simple random walk model.

$$m\frac{d\mathbf{v}}{dt} = q\mathbf{E} - \frac{\nabla p}{n} - \underbrace{m\mathbf{v}\nu^{q/n}}_{\text{drag term}} \tag{5.12}$$

We are interested in small v relative to v_{the} and steady–state ($d/dt = 0$). Thus

$$\mathbf{v} = \left(\frac{q}{m\nu}\right)\mathbf{E} - \left(\frac{1}{m\nu}\right)\frac{\nabla p}{n} \tag{5.13}$$

The plasma pressure is defined as $p = nT$ and if we assume an uniform temperature T, the pressure gradient becomes

$$\nabla p = \nabla(nT) = T\nabla n \tag{5.14}$$

and

$$\mathbf{v} = \underbrace{\left(\frac{q}{m\nu}\right)}_{\mu \equiv \frac{|q|}{m\nu}}\mathbf{E} - \underbrace{\left(\frac{T}{m\nu}\right)}_{D \equiv \frac{T}{m\nu}}\frac{\nabla n}{n}, \tag{5.15}$$

where μ is called "mobility" and $D = T/m\nu = v_{\text{th}}^2/\nu$ is the diffusion coefficient as defined before in our heuristic model. The relation

$$\frac{\mu}{D} = \frac{|q|}{T} \tag{5.16}$$

is called *Einstein relation*. Let's calculate the particle flux for the species j:

$$\mathbf{\Gamma}_j = n_j\mathbf{v}_j = \frac{q_j}{|q_j|}n_j\mu_j\mathbf{E} - D_j\nabla n_j. \tag{5.17}$$

If $\mathbf{E} = 0$

$$\mathbf{\Gamma}_j = -D_j\nabla n_j \qquad \text{"Fick's law"} \tag{5.18}$$

saying that particles diffuse down along the density gradient. With the continuity equation

$$\frac{\partial n_j}{\partial t} + \nabla\cdot\mathbf{\Gamma}_j = 0 \tag{5.19}$$

assuming $D_j = \text{const}$, we get the *diffusion equation*(†)

$$\frac{\partial n_j}{\partial t} + \nabla\cdot(-D_j\nabla n_j) = \frac{\partial n_j}{\partial t} - D_j\nabla^2 n_j = 0, \tag{5.21}$$

(†) The diffusion equation is a consequence of the continuity equation. If there are sources and sinks, these will appear in the right-hand side of the diffusion equation. For example consider an ionisation term S (source, sign "+") and a recombination term $-\alpha n^2$ (sink, sign "−"). Then the diffusion equation becomes

$$\frac{\partial n}{\partial t} - D\nabla^2 n = S - \alpha n^2. \tag{5.20}$$

Remember our second question: can ions and electrons diffuse at different rates? The answer is *no*; to maintain quasi–neutrality we need $\mathbf{\Gamma}_e \approx \mathbf{\Gamma}_i$. As $D_e \neq D_i$, this means that an electric field must be created in the plasma. This field will try to slow down the electrons and accelerate the ions. Assuming $n_e = n_i = n$, we have

$$\mathbf{\Gamma}_i = \mu_i n\mathbf{E} - D_i\nabla n = \mathbf{\Gamma}_e = -\mu_e n\mathbf{E} - D_e\nabla_n. \tag{5.22}$$

Solving for $\mathbf{E}$ yields

$$\mathbf{E} = \Big(\frac{D_i - D_e}{\mu_i + \mu_e}\Big)\frac{\nabla n}{n} \qquad \text{“ambipolar field”} \tag{5.23}$$

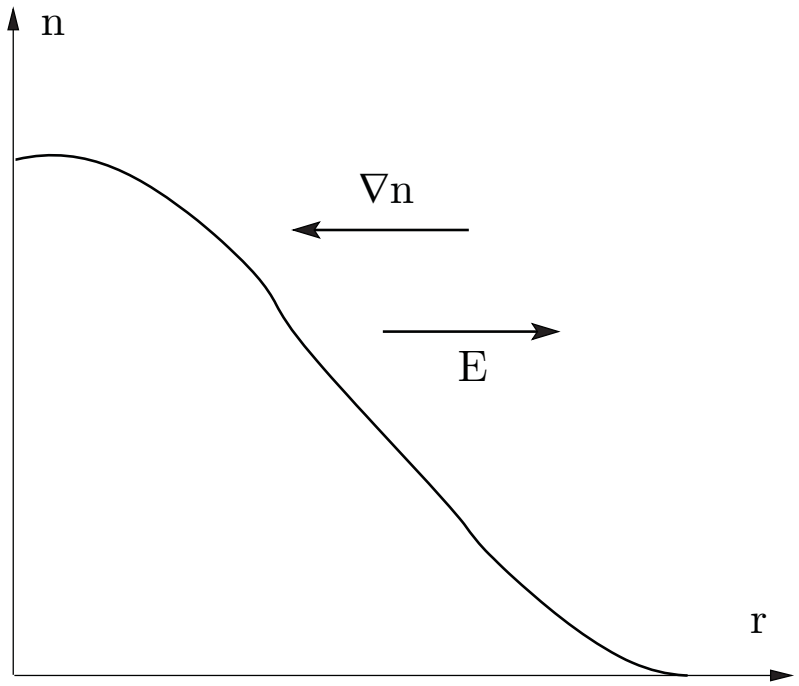

Figure 5.3: Direction of ambipolar field

(figure 5.3). Note that if $D_e = D_i$ then $\mathbf{E} = 0$ even for $\mu_e \neq \mu_i$. Now we can calculate the flux of *both* species.

$$\mathbf{\Gamma} = \mathbf{\Gamma}_e = \mathbf{\Gamma}_i = -\Big(\underbrace{\frac{\mu_i D_e + \mu_e D_i}{\mu_i + \mu_e}}_{D_a}\Big)\nabla n. \tag{5.24}$$

This is the form we found for the Fick's law, with the *ambipolar diffusion coefficient* D_a.
To estimate the order of magnitude we have ($\mu_e \gg \mu_i$)

$$D_a \sim D_i + \frac{\mu_i}{\mu_e}D_e = D_i + \frac{D_i}{T_i}\frac{T_e}{D_e}D_e = D_i + \frac{T_e}{T_i}D_i \overset{T_e=T_i}{=} 2D_i, \tag{5.25}$$

where we have used the Einstein relation between μ, D and T. Thus we find that

$$D_i < D_a \ll D_e; \tag{5.26}$$

the ambipolar field slows down electrons and increases ion diffusion (by a significant amount, in this example a factor of 2).

5.1.2 Plasmas with $\mathbf{B} \neq 0$

Dynamics along B This case is of particular importance for fusion, as we try to confine plasmas by magnetic fields. The dynamics *along* B will be very similar to the case $\mathbf{B} = 0$, with one difference: ambipolarity is more complicated as there is now a privileged direction in the plasma. The quasi–neutrality condition is 3–D. Such condition will depend on the specific configuration. For example, in a closed configuration the ambipolar field could be short–circuited by electron motion along $\mathbf{B}$, and/or across conducting end plates, if the configuration is linear.

Dynamics across B The equations of motion and continuity are much more complicated, but we can use our general concepts of diffusion and the simple random walk model.

Observation:

Without collisions:
there would be no diffusion across $\mathbf{B}$ (over distances greater than ρ_L)

With collisions:
particles can *jump* across $\mathbf{B}$ (figure 5.4). After each collision the *guiding center* is displaced by approximately ρ_L (this is our step size)[‡]

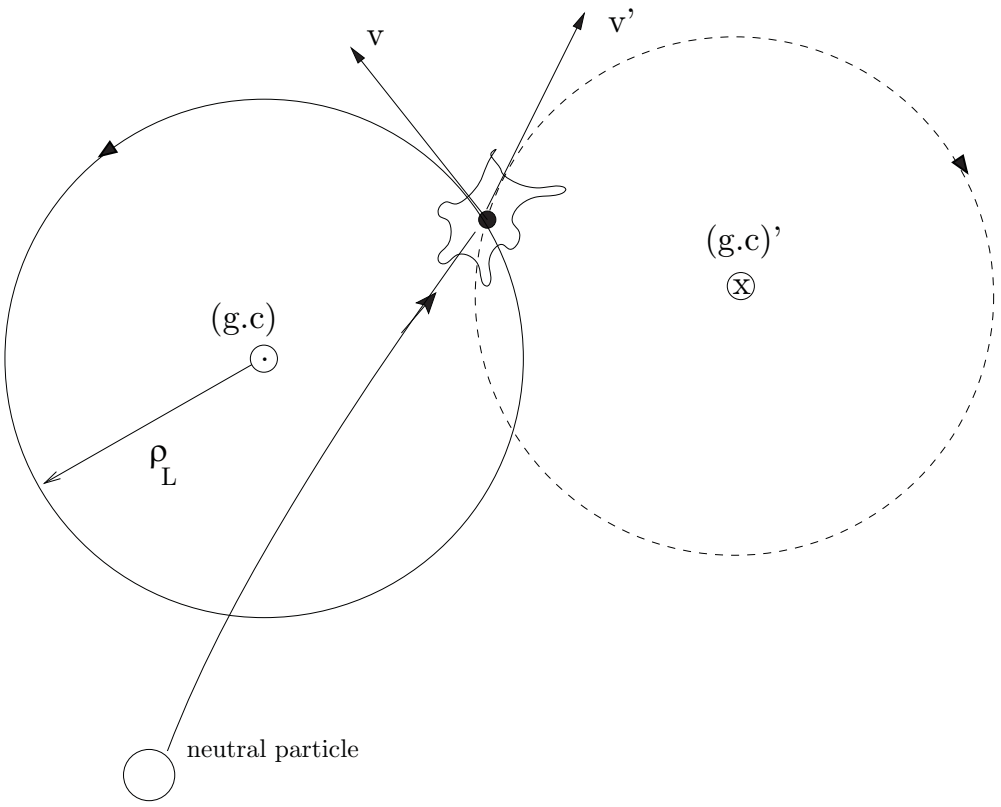

Figure 5.4: Step size for perpendicular diffusion

Weakly ionised plasmas In this case the diffusion coefficient depends on the neutral density

$$D_{\perp e,i} \sim \rho^2_{L\,e,i}\, \nu^{e,i/n}, \tag{5.27}$$

with $D_{\perp i} \gg D_{\perp e}$.

[‡] We need to have a gyro–motion that is not *too* perturbed by collisions, i.e. $\Omega \gg \nu$

Strongly ionised plasmas Which collision frequency to use? To answer this question we state first that only collisions between *un–like* particles give rise to a *net* diffusion and particle transport. Like particles' collisions only produce a 'swapping' of the guiding center positions. Stated otherwise, for identical particles $\Delta\mathbf{v}$ is equal and opposite due to conservation of momentum. Thus[§]

$$D_{\perp e} \simeq \rho_{L\,e}^2 \bar{\nu}_p^{e/i}, \tag{5.29}$$

$$D_{\perp i} \simeq \rho_{L\,i}^2 \bar{\nu}_p^{i/e}. \tag{5.30}$$

Note that

$$\frac{D_{\perp e}}{D_{\perp i}} \simeq 1 \qquad (\text{if} \quad T_e \sim T_i), \tag{5.31}$$

i.e. that cross–field diffusion is automatically ambipolar. No need for **E**–field to maintain neutrality.

5.2 Transport of energy

Let's study now the transport of energy due to heat conduction, i.e. the flux of heat due to temperature gradient. It follows the same diffusion equation as for particles (we will not prove it)

$$\frac{3}{2}\frac{\partial T}{\partial t} - \chi \nabla^2 T = 0, \tag{5.32}$$

where we assumed that the *thermal diffusivity* $\chi = \text{const}$. The main difference is that for χ *all* collisions contribute, including those between like–particles. Also, the relevant collision frequency is ν_{E_k}.

5.2.1 Across B

$$\chi_{\perp e} \simeq \rho_{Le}^2 \left[\bar{\nu}_{E_k}^{e/i} + \bar{\nu}_{E_k}^{e/e}\right] \simeq \frac{1}{\sqrt{2}}\,\rho_{Le}^2 \bar{\nu}_p^{e/i}, \tag{5.33}$$

$$\chi_{\perp i} \simeq \rho_{Li}^2 \left[\bar{\nu}_{E_k}^{i/e} + \bar{\nu}_{E_k}^{i/i}\right] \simeq \rho_{Li}^2 \bar{\nu}_{E_k}^{i/i} = \rho_{Li}^2 \bar{\nu}_p^{i/i}, \tag{5.34}$$

where $\bar{\nu}_{E_k}^{e/i} \ll \bar{\nu}_{E_k}^{e/e}$, $\bar{\nu}_{E_k}^{e/e} \simeq \sqrt{2}\,\bar{\nu}_p^{e/i}$ and $\bar{\nu}_p^{i/i} = \bar{\nu}_{E_k}^{i/i} \gg \bar{\nu}_{E_k}^{i/e}$ was used. Assuming $T_e = T_i$ we get the ratio

$$\frac{\chi_{\perp e}}{\chi_{\perp i}} \simeq \frac{\rho_{Le}^2}{\rho_{L_i}^2}\frac{\sqrt{2}\,\bar{\nu}_p^{e/i}}{\bar{\nu}_p^{i/i}} \simeq \sqrt{2}\frac{m_e}{m_i}\sqrt{\frac{m_i}{m_e}} = \sqrt{\frac{2m_e}{m_i}} \ll 1 \tag{5.35}$$

$\Longrightarrow$ Ions 'transport' heat *across* **B** much more efficiently than electrons.

[§] In this "classical" diffusion picture ("minimum diffusion" state) the diffusion coefficients behave as

$$D_\perp \propto \frac{1}{B^2} n. \tag{5.28}$$

5.2.2 Along B

$$\chi_{\parallel e} \simeq \lambda_{\rm mfp}^2 \left[\bar{\nu}_{E_k}^{e/i} + \bar{\nu}_{E_k}^{e/e}\right] \simeq \frac{v_{{\rm th}e}^2}{\left[\bar{\nu}_{E_k}^{e/i} + \bar{\nu}_{E_k}^{e/e}\right]} \simeq \frac{v_{{\rm th}e}^2}{\sqrt{2}\,\bar{\nu}_p^{e/i}}, \tag{5.36}$$

$$\chi_{\parallel i} \simeq \frac{v_{{\rm th}i}^2}{\left[\bar{\nu}_{E_k}^{i/i} + \bar{\nu}_{E_k}^{i/e}\right]} \simeq \frac{v_{{\rm th}i}^2}{\bar{\nu}_p^{i/i}}, \tag{5.37}$$

the ratio is

$$\frac{\chi_{\parallel e}}{\chi_{\parallel i}} \simeq \frac{1}{\sqrt{2}}\frac{m_i}{m_e}\sqrt{\frac{m_e}{m_i}} = \sqrt{\frac{m_i}{2m_e}} \gg 1 \tag{5.38}$$

$\Longrightarrow$ Electrons 'transport' heat *along* **B** much more efficiently than ions.

5.2.3 Compare $\parallel$ and $\perp$ Transport

$$\frac{\max(\chi_{\parallel e}, \chi_{\parallel i})}{\max(\chi_{\perp e}, \chi_{\perp i})} \cong \frac{\chi_{\parallel e}}{\chi_{\perp i}} = \frac{v_{{\rm th}e}^2}{\sqrt{2}\,\bar{\nu}_p^{e/i}} \frac{1}{\rho_{L_i}^2 \bar{\nu}_p^{i/i}} = \left(\frac{\rho_{Le}}{\rho_{Li}}\right)^2 \frac{\Omega_e^2}{\sqrt{2}\,\bar{\nu}_p^{e/i}\bar{\nu}_p^{i/i}} \gg 1, \tag{5.39}$$

e.g. $\sim 10^{13}$ for JET tokamak plasma. In general

$$\chi_{\parallel e} \gg \chi_{\parallel i} \ggg \chi_{\perp i} \gg \chi_{\perp e}, \tag{5.40}$$

$$D_{\parallel a} \gg D_{\perp i} = D_{\perp e}. \tag{5.41}$$

Thus the different types of transport are dominated by

Parallel heat	$\longrightarrow$	electrons
Parallel particle	$\longrightarrow$	electrons (ambipolar **E**)
Perpendicular heat	$\longrightarrow$	ions
Perpendicular particle	$\longrightarrow$	neither

Note that

$$D_\parallel \propto \frac{1}{\nu}, \qquad\qquad D_\perp \propto \nu. \tag{5.42}$$

Thus parallel transport is *slowed down* by collisions whereas perpendicular transport *needs* collisions.

5.3 Qualitative survey on the limits of this "classical" model

Let us concentrate on $\perp$ transport of particles ($D_\perp$)

$$D_\perp \simeq \rho_{L_e}^2 \bar{\nu}_p^{e/i} \propto \begin{cases} B^{-2} \\ T^{-1/2} \end{cases} ; \tag{5.43}$$

by increasing B (magnets) and by heating the plasma we should be able to make it as small as we need it to be to achieve fusion! To find out whether this optimistic conclusion is valid in practice we need an *experimental verification*. This means we need a way to measure directly the motion of test–particles and verify that

1. It follows the diffusion equation
2. D is consistent with our "classical" theory

For the simplest plasma (a linear long column with magnetic field along its axis, and very quiescent), *yes*, diffusion *can* be classical and follow our (approximate) calculation (details on this experimental verification are given in Appendix A).

But, how often is plasma behaving 'classically'? Take the JET tokamak for example: $R = 1$ m; $\tau = 0.5$ s; $B = 3$ T; $T_e \simeq 10$ keV; $n = 10^{20}$ m^{-3}. Experimentally one finds[¶]

$$D_\perp^{\text{exp}} \simeq 1 \text{ m}^2/\text{s}. \tag{5.44}$$

Compare it to classical prediction:

$$D_{\perp e}^{\text{cl}} \sim \rho_{Le}^2 \bar{\nu}_p^{e/i} \simeq (10^{-4})^2 \times 5 \cdot 10^3 \text{ m}^2/\text{s} \simeq 5 \cdot 10^{-5} \text{ m}^2/\text{s}, \tag{5.45}$$

thus

$$D_\perp^{\text{exp}} \gg D_{\perp e}^{\text{cl}}. \tag{5.46}$$

This is probably the most critical physics problem for fusion. Is there something wrong in our 'classical' estimate for tokamaks? Is the Larmor radius really the step size to use? The answer is *no*, we need to modify our estimate of diffusion due to Coulomb collisions somewhat, that leads to *"neo–classical" diffusion*.

A tokamak is not a cylinder, but a torus with twisted field lines: particles follow more complicated orbits than just gyro–orbits. It is the size of these orbits that needs to be considered for diffusion. This size is $5 \div 10$ times larger than the Larmor radius, so the resulting diffusion is $25 \div 100$ times larger, *but still much smaller in most cases that measured experimentally.*

[¶] Note that one cannot have a direct measure of D in fusion plasmas, but macroscopic analysis can give a relation between D and measurable quantities: $D \sim \frac{a^2}{\tau_E}$

5.3.1 Qualitative explanation for 'neo–classical' diffusion

1. Particles move along helical B–field:

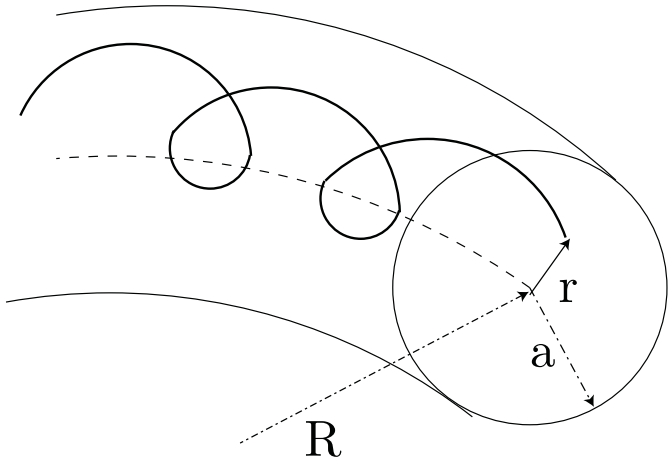

2. As $B \propto 1/R$, particles experience along their motion minima (outside) and maxima (inside) of B

3. Particles can be trapped in the effective magnetic mirror they see. The fraction of trapped particles depends on the ratio a/R (aspect ratio), see figure (a) below.

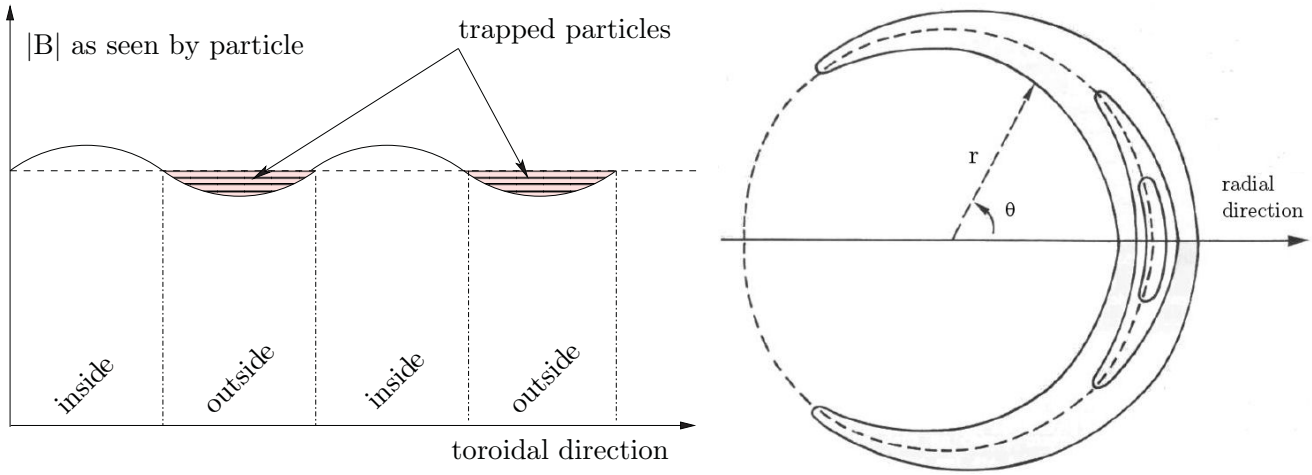

(a) (b)

4. Projected on the poloidal plane (i.e. a section of the torus), this trapped orbit has the shape of a *banana*, so it is called the *banana orbit*, see figure (b) above.

Thus particles move quickly around the *banana*, then, when they collide, they jump to a different banana orbit, so the width of this orbit is the size of the jump to be used for $D^{\perp}_{\text{neo–cl.}}$. Example for JET:

$$D_{\perp}^{\text{neo–cl.}} \sim 60\ D_{\perp}^{\text{cl.}} \ll D_{\perp}^{\text{exp}}. \tag{5.47}$$

So the 'neo–classical' model is still far off the experimental behavior. This behavior is called *"anomalous" transport* and is still not entirely understood, although it is unanimously attributed to the effect of plasma turbulence, originating from unstable waves in the plasma.

Chapter 6 Waves in plasmas

All plasma particles are "sources" for Maxwell's equations. Therefore most dynamical processes in plasmas are related to electromagnetic waves and oscillations. Waves are used to heat plasmas, and to drive current non–inductively. Another example of the importance of waves is the role that microscopic electromagnetic waves and instabilities play in producing transport of particles and energy in plasmas well above the levels due to collisional effects.

6.1 Mathematical technique

a.) We will use normal mode (or plane wave) analysis. This corresponds to considering all quantities in Fourier space, using the Fourier transform defined for any quantity $\mathbf{g}$ as

$$\widetilde{\mathbf{g}}(\mathbf{k},\omega) = \frac{1}{(2\pi)^4}\int d^3x \int dt\, \mathbf{g}(\mathbf{x},t) e^{-i(\mathbf{k}\cdot\mathbf{x}-\omega t)}, \tag{6.1}$$

with the inverse transform given by

$$\mathbf{g}(\mathbf{x},t) = \int d^3k \int d\omega\, \widetilde{\mathbf{g}}(\mathbf{k},\omega) e^{i(\mathbf{k}\cdot\mathbf{x}-\omega t)}. \tag{6.2}$$

This will lead to complex quantities. Naturally, all physical quantities are real, and we will need to consider the real part at the end of all calculations.

The Fourier transformation is a *linear* operation. Its use comes from the fact that by using it we can split a complicated problem into small pieces, solve it for these small pieces, and combine the pieces together to form the complete solution. This implies that the system of equations to be solved is *linear*.

b.) What we do is to *linearise* the systems of equations, considering small perturbations to an existing equilibrium. Take for example the continuity equation (a differential equation) for the mass density ρ and the fluid velocity $\mathbf{u}$:

$$\frac{\partial \rho}{\partial t} + \nabla\cdot(\rho\mathbf{u}) = 0, \tag{6.3}$$

where $\rho \equiv \rho(\mathbf{x},t)$ and $\mathbf{u} \equiv \mathbf{u}(\mathbf{x},t)$.

1. Chose an equilibrium → no time dependence → steady state:

$$\rho_0(\mathbf{x}) = \rho_0 \quad \text{(uniform equilibrium)}, \qquad \mathbf{u}_0(\mathbf{x}) = 0 \quad \text{(static equilibrium)} \tag{6.4}$$

2. Consider small perturbations to this equilibrium

$$\rho = \rho_0 + \rho_1(\mathbf{x},t), \qquad \left|\frac{\rho_1}{\rho_0}\right| \ll 1 \quad \text{(expansion parameter)} \tag{6.5}$$

3. Linearise by retaining first order terms only to get the linearised continuity equation

$$\frac{\partial(\rho_0+\rho_1)}{\partial t} + \nabla\cdot\left((\rho_0+\rho_1)(\underbrace{\mathbf{u}_0}_{=0}+\mathbf{u}_1)\right) = 0$$

$$\underbrace{\frac{\partial \rho_0}{\partial t}}_{\text{Order 0; = 0 by definition}} + \underbrace{\frac{\partial \rho_1}{\partial t}}_{\text{Order 1}} + \underbrace{\nabla\cdot(\rho_0\mathbf{u}_1)}_{\text{Order 1 and } \rho_0=\text{cte}} + \underbrace{\nabla\cdot(\rho_1\mathbf{u}_1)}_{\text{Order 2; neglected}} = 0$$

$$\frac{\partial \rho_1}{\partial t} + \rho_0\nabla\cdot\mathbf{u}_1 = 0. \tag{6.6}$$

4. Now we consider normal modes, i.e. we consider the perturbed quantities as Fourier transforms:

$$\rho_1(\mathbf{x},t) = \int d^3k \int d\omega\, \widetilde{\rho}_1(\mathbf{k},\omega) e^{i(\mathbf{k}\cdot\mathbf{x}-\omega t)} \tag{6.7}$$

and the same for $\mathbf{u}_1$. Thus

$$\begin{aligned} & \frac{\partial}{\partial t}\left\{\int d^3k \int d\omega\ \widetilde{\rho}_1(\mathbf{k},\omega) e^{i(\mathbf{k}\cdot\mathbf{x}-\omega t)}\right\} \\ + \quad & \rho_0 \nabla\cdot\left\{\int d^3k \int d\omega\ \widetilde{\mathbf{u}}_1(\mathbf{k},\omega) e^{i(\mathbf{k}\cdot\mathbf{x}-\omega t)}\right\} = 0 \\ \Rightarrow \quad & \int d^3k \int d\omega \Big[-i\omega\widetilde{\rho}_1(\mathbf{k},\omega)\Big] e^{i(\mathbf{k}\cdot\mathbf{x}-\omega t)} \\ + \quad & \rho_0 \int d^3k \int d\omega \Big[i\mathbf{k}\cdot\widetilde{\mathbf{u}}_1(\mathbf{k},\omega)\Big] e^{i(\mathbf{k}\cdot\mathbf{x}-\omega t)} = 0. \end{aligned} \tag{6.8}$$

Where we have used the following formal substitutions:

$$\nabla \to i\mathbf{k} \qquad \text{and} \qquad \frac{\partial}{\partial t} \to -i\omega. \tag{6.9}$$

So in our example the linearised continuity equation becomes in Fourier space an algebraic equation:

$$-i\omega\widetilde{\rho}_1 + i\rho_0 \mathbf{k}\cdot\widetilde{\mathbf{u}}_1 = 0. \tag{6.10}$$

In the following we will drop the tilde symbol to simplify the notation.
Note that it is important to refer to the equilibrium, in respect to which the linearisation was done.

6.2 Phase and group velocities

6.2.1 Phase velocity

$$\mathbf{v}_{\rm ph} = \frac{\omega}{k}\frac{\mathbf{k}}{k}. \tag{6.11}$$

It *can* be $|\mathbf{v}_{\rm ph}| > c$, as $\mathbf{v}_{\rm ph}$ does not carry information.

6.2.2 Group velocity

$$\mathbf{v}_{\rm g} = \frac{\partial\omega}{\partial\mathbf{k}}. \tag{6.12}$$

It *cannot* be $|\mathbf{v}_{\rm g}| > c$, as $\mathbf{v}_{\rm g}$ does carry information. Proof in 1–D:

$$E_1 = E_0 e^{i(k+\Delta k)x - i(\omega+\Delta\omega)t}, \tag{6.13}$$

$$E_2 = E_0 e^{i(k-\Delta k)x - i(\omega-\Delta\omega)t}. \tag{6.14}$$

The modulated wave packet resulting from the superposition of E_1 and E_2 is

$$E_{\rm tot} = E_1 + E_2 = E_0 e^{i(kx-\omega t)}\left\{e^{i(\Delta k\, x - \Delta\omega\, t)} + e^{-i(\Delta k\, x - \Delta\omega\, t)}\right\}. \tag{6.15}$$

As $e^{ia} + e^{-ia} = 2\cos a$ we have

$$E_{tot} = 2E_0 e^{i(kx-\omega t)} \cos(\Delta k\, x - \Delta\omega\, t). \tag{6.16}$$

The envelope of the wave, given by $\cos(\Delta k\, x - \Delta\omega\, t)$, is what carries the information, and propagates at the group velocity

$$v_{\rm g} = \frac{\Delta\omega}{\Delta k} \cong \frac{\partial\omega}{\partial k}. \tag{6.17}$$

6.3 Reminder of the MHD plasma model

The first plasma model we consider to analyse plasma waves is the simplest, the Magneto-hydrodynamics model (MHD). Let's review very briefly its basis and some of its properties (already covered in Plasma I). The system of equations for the MHD plasma model is:

$$\frac{\partial\rho}{\partial t} + \nabla\cdot(\rho\mathbf{u}) = 0; \qquad \nabla\cdot\mathbf{J} = 0; \tag{6.18}$$

$$\rho\frac{\mathrm{d}\mathbf{u}}{\mathrm{d}t} = \mathbf{J}\times\mathbf{B} - \nabla p; \qquad \mathbf{E} + \mathbf{u}\times\mathbf{B} = \begin{cases} 0 & \text{“ideal” MHD} \\ \eta\mathbf{J} & \text{“resistive” MHD} \end{cases} \tag{6.19}$$

$$\frac{\mathrm{d}}{\mathrm{d}t}(p\rho^{-\gamma}) = 0; \qquad \nabla\times\mathbf{B} = \mu_0\mathbf{J}; \tag{6.20}$$

$$\nabla\times\mathbf{E} = -\frac{\partial\mathbf{B}}{\partial t}; \qquad \nabla\cdot\mathbf{B} = 0; \tag{6.21}$$

Here

$$\frac{\mathrm{d}}{\mathrm{d}t} \equiv \frac{\partial}{\partial t} + \mathbf{u}\cdot\nabla \tag{6.22}$$

is the **convective derivative**. Variables are ρ (*mass* density)(*), $\mathbf{u}$ (fluid velocity), $\mathbf{J}$, p, $\mathbf{E}$, $\mathbf{B}$. We have 16 equations, of which 14 are independent, and 14 unknowns. The MHD approximation describes phenomena that are

- Macroscopic (taking place on length-scales $L \gg \rho_L$)
- Relatively slow (with time-scales $\tau \gg \Omega_{ci}^{-1}$, Ω_{ci} the ion-cyclotron frequency)
- But fast enough that $u \gtrsim v_{{\rm th}i}$

Note that the charge density does not appear, as we consider quasi–neutrality, and that the electric field in the Lorentz force and in the displacement current (in Ampère law) has been neglected.

6.3.1 Flux freezing and diffusion of B–fields through plasma

In hot plasmas the resistivity is so small that usually we can take $\eta \to 0$. An important consequence is that the magnetic flux is 'frozen' into the plasma. The field lines and the flux tubes associated with them acquire an important physical meaning as if they were real objects. To estimate over how much time the flux can be considered as frozen in the plasma, let us consider Ohm's law with

(*) the exponent γ in the equation of state is the adiabatic index, $\gamma = \frac{c_p}{c_v}$, where c_v and $c_p = c_v + R$ represent the specific heat evaluated by keeping constant the volume or the pressure, respectively. For a mono-atomic gas $\gamma = 5/3$, for polyatomic gases, $\gamma = \frac{5+f}{3+f}$, where f denotes the number of internal degrees of freedom.

$\eta \neq 0$ (resistive MHD)[†]. We are interested in the typical time-scale associated with variations of $\mathbf{B}$ in the plasma

$$\frac{\partial \mathbf{B}}{\partial t} \overset{\text{Faraday}}{=} -\nabla \times \mathbf{E} \overset{\text{Ohm}}{=} -\nabla \times \big\{ -\mathbf{u} \times \mathbf{B} + \eta \mathbf{J} \big\}. \tag{6.23}$$

Assume $\eta \cong$ constant and consider Ampère law $\mathbf{J} = \frac{1}{\mu_0} \nabla \times \mathbf{B}$

$$\begin{aligned} \frac{\partial \mathbf{B}}{\partial t} &= \nabla \times (\mathbf{u} \times \mathbf{B}) - \frac{\eta}{\mu_0} \nabla \times (\nabla \times \mathbf{B}) \\ &= \nabla \times (\mathbf{u} \times \mathbf{B}) - \frac{\eta}{\mu_0} \big(\nabla (\nabla \cdot \mathbf{B}) - \nabla^2 \mathbf{B} \big) \\ &= \underbrace{\nabla \times (\mathbf{u} \times \mathbf{B})}_{\text{convection}} + \underbrace{\frac{\eta}{\mu_0} \nabla^2 \mathbf{B}}_{\text{diffusion}}. \end{aligned} \tag{6.24}$$

So $\mathbf{B}$ varies in a plasma because it is transported by it (convective term) or because it diffuses through it (diffusion term). To estimate the relative importance of the two terms, consider the scale length $L \sim |\nabla|^{-1}$. Thus

$$\frac{\text{diffusion}}{\text{convection}} = \frac{\left| \frac{\eta}{\mu_0} \nabla^2 \mathbf{B} \right|}{|\nabla \times (\mathbf{u} \times \mathbf{B})|} \sim \frac{\frac{\eta}{\mu_0} \frac{B}{L^2}}{\frac{uB}{L}} = \frac{\eta}{\mu_0 u L} \equiv R_{\text{m}}^{-1}, \tag{6.25}$$

where $R_{\text{m}} = \mu_0 u L / \eta$ is the magnetic Reynolds number[‡]. In most plasmas of interest $R_{\text{m}} \gg 1$.

The characteristic time for the diffusion of $\mathbf{B}$ in plasmas is

$$\tau = \left(\frac{\eta}{\mu_0 L^2} \right)^{-1} = \frac{R_{\text{m}} L}{u} \tag{6.27}$$

and in general is macroscopic, e.g. in the JET tokamak ($L \cong 1$ m, $T_e = 10$ keV, $\eta = 5 \times 10^{-5} \times T_{e\,[\text{eV}]}^{-3/2} \ln \Lambda \sim 7.5 \times 10^{-10}$ Ωm)

$$\tau \sim 1700 \text{ s}. \tag{6.28}$$

In space plasmas this is even larger, due to the enormous values of L. An example demonstrating the long time that it takes to decouple plasma and magnetic field comes from solar flares and solar wind.

The solar wind is generated by a plasma that 'erupts' from the sun and is ejected out radially. Each 'blob' of plasma forming the solar wind carries with it the magnetic field that it had inside the sun, practically unchanged until it reaches the earth magnetosphere. The interaction with the magnetosphere and the earth magnetic field depends on the orientation of $\mathbf{B}$ in the solar wind. This is difficult to predict, as the field inside the sun is turbulent and changes orientation.

(†) Note that this has been discussed in the Plasma I lecture (see relevant notes). It is summarized here for completeness. One can also refer to the second problem of problemset #5.

(‡) in ordinary fluids, described by the Navier–Stokes equation, we define

$$R \equiv \frac{\text{inertial force}}{\text{viscous force}} = \frac{|\rho \mathbf{u} \cdot \nabla \mathbf{u}|}{|\mu \nabla^2 \mathbf{u}|} \sim \frac{\rho u L}{\mu}, \tag{6.26}$$

where μ is the viscosity.

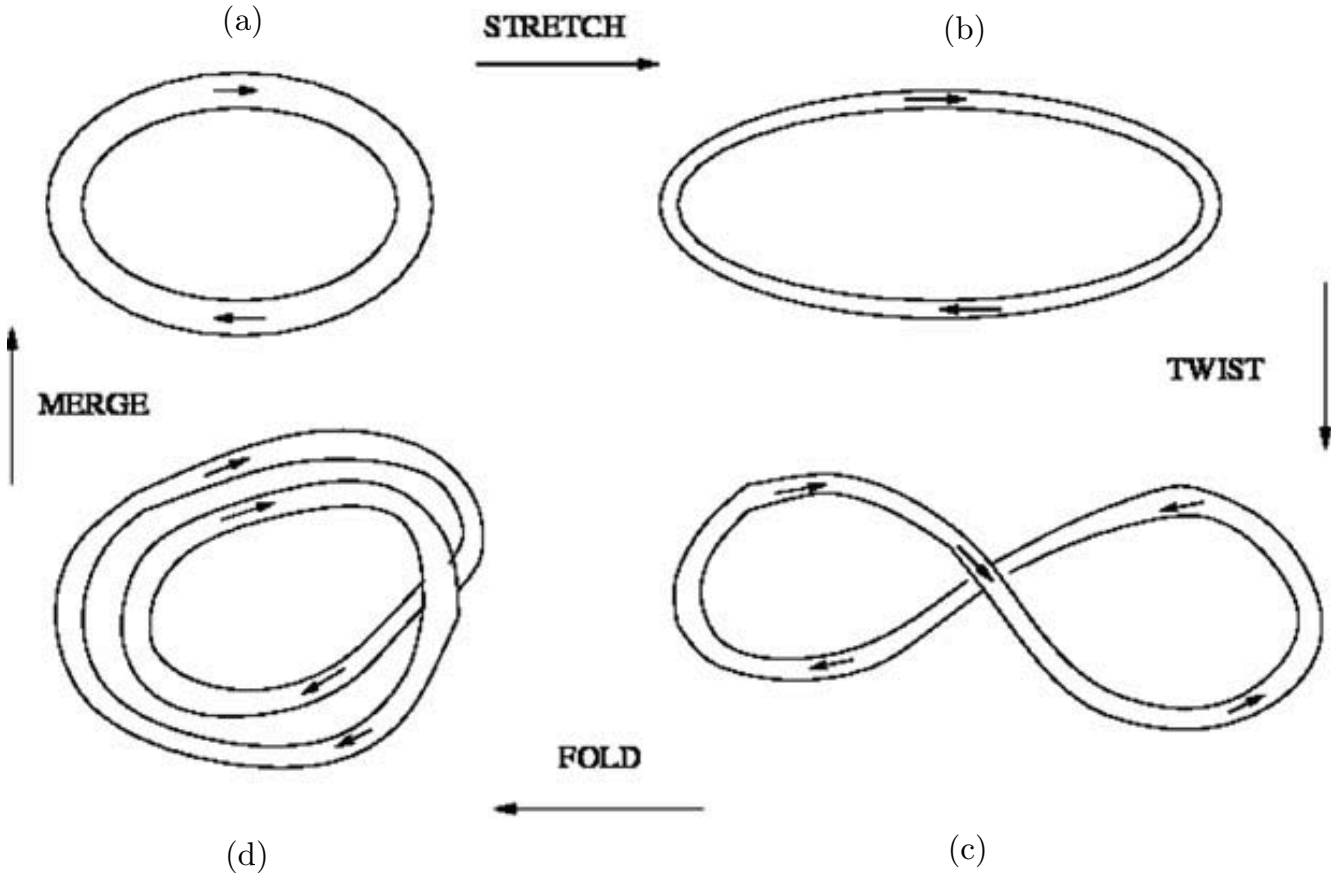

Figure 6.1: The stretch-twist-fold scheme for fast dynamo effect. *Courtesy of A. Brandenburg, K. Subramanian, Physics Reports 417 (2005) 1–209.*

The freezing of **B** in a plasma is also believed to be at the origin of the magnetic field in the universe and in the (melted) metallic core of planets such as the earth through "dynamo effect", illustrated in figure 6.1.

The dynamo algorithm starts with first stretching a closed flux rope of cross–section S_0 to twice its length preserving its volume, as in an incompressible flow, see (a) $\rightarrow$ (b) in figure 6.1. The rope's cross-section then decreases by a factor of two ($S_1 = S_0/2$), and because of flux freezing the magnetic field doubles ($B_1 = 2B_0$). In the next step, the rope is twisted into a figure eight, (b) $\rightarrow$ (c), and then folded, (c) $\rightarrow$ (d), so that now there are two loops, whose fields now point in the same direction and together occupy the same volume as the original flux loop. The flux through this volume has now doubled. The last important step consists of merging the two loops into one, (d) $\rightarrow$ (a), through small diffusive effects. This is important in order that the new arrangement doesn't easily undo itself and the whole process becomes irreversible. The newly merged loops now become topologically the same as the original single loop, but with the field strength scaled up by a factor of 2.

It is believed that complex fluid motion can lead to effective stretching and folding of flux tubes, therefore to amplification (or creation from thermal noise) of magnetic fields ("dynamo effect").

6.4 Ideal MHD waves

The ideal MHD can be reduced by combining its equations, obtaining

$$\frac{\partial \rho}{\partial t} + \nabla \cdot (\rho \mathbf{u}) = 0 \qquad \rho \frac{\mathrm{d}\mathbf{u}}{\mathrm{d}t} = -\nabla p + \frac{1}{\mu_0}(\nabla \times \mathbf{B}) \times \mathbf{B} \tag{6.29}$$

$$\frac{\partial \mathbf{B}}{\partial t} = \nabla \times (\mathbf{u} \times \mathbf{B}) \qquad \frac{\mathrm{d}}{\mathrm{d}t}(p\rho^{-\gamma}) = 0^{(\S)} \tag{6.30}$$

This is a system of 8 equations with 8 unknowns: ρ, p, $\mathbf{u}$, $\mathbf{B}$. We now consider small perturbations to a uniform and static (no flow) equilibrium

$$\mathbf{B}(\mathbf{x},t) = \mathbf{B}_0 + \mathbf{B}_1(\mathbf{x},t) \qquad \mathbf{u}(\mathbf{x},t) = \mathbf{u}_1(\mathbf{x},t) \tag{6.31}$$

$$\rho(\mathbf{x},t) = \rho_0 + \rho_1(\mathbf{x},t) \qquad p(\mathbf{x},t) = p_0 + p_1(\mathbf{x},t) \tag{6.32}$$

and linearise the original system of equations in respect to the equilibrium

$$\frac{\partial \rho_1}{\partial t} + \rho_0 \nabla \cdot \mathbf{u}_1 = 0 \qquad \rho_0 \frac{\partial \mathbf{u}_1}{\partial t} = -\nabla p_1 + \frac{1}{\mu_0}(\nabla \times \mathbf{B}_1) \times \mathbf{B}_0 \tag{6.33}$$

$$\frac{\partial \mathbf{B}_1}{\partial t} = \nabla \times (\mathbf{u}_1 \times \mathbf{B}_0) \qquad p_1 = \frac{\gamma p_0}{\rho_0}\rho_1 \equiv c_s^2 \rho_1^{(\P)} \tag{6.34}$$

Here $c_s \equiv \sqrt{\gamma p_0/\rho_0}$ is the *sound speed*. After elimination of p_1 and Fourier transformation (refer to section 6.1) this becomes

$$-\omega\rho_1 + \rho_0 \mathbf{k} \cdot \mathbf{u}_1 = 0 \tag{6.35}$$

$$-\omega\rho_0\mathbf{u}_1 = -\mathbf{k}\rho_1 c_s^2 + \frac{1}{\mu_0}(\mathbf{k} \times \mathbf{B}_1) \times \mathbf{B}_0 \tag{6.36}$$

$$-\omega\mathbf{B}_1 = \mathbf{k} \times (\mathbf{u}_1 \times \mathbf{B}_0) \tag{6.37}$$

6.4.1 The shear Alfvén wave

Without loss of generality we can choose $\mathbf{B}_0 = B_0\hat{\mathbf{z}}$ and $k_y = 0$ (see figure 6.5). Let us now consider the particular case of a transverse wave $u_{1x} = u_{1z} = 0$, i.e.

$$\mathbf{k} = (k_x, 0, k_z) \tag{6.38}$$

$$\mathbf{u}_1 = (0, u_{1y}, 0) \tag{6.39}$$

We will treat the case $u_{1x} \neq 0 \neq u_{1z}$ later.

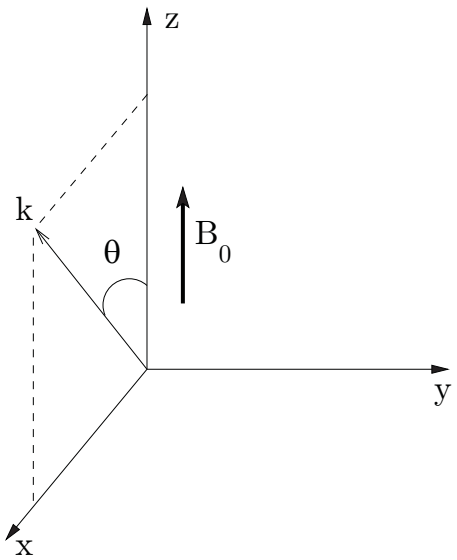

Figure 6.2: Notation for the study of MHD waves.

(§) Rewriting the continuity equation as $\frac{\mathrm{d}\rho}{\mathrm{d}t} = -\rho\nabla \cdot \mathbf{u}$, we have $\frac{\mathrm{d}p}{\mathrm{d}t} + \gamma p \nabla \cdot \mathbf{u} = 0$.

(¶) From eq.(6.30) and eq.(6.32) we have $(p_0 + p_1)(\rho_0 + \rho_1)^{-\gamma} = p_0\rho_0^{-\gamma} \Rightarrow (p_0 + p_1)(1 - \gamma\frac{\rho_1}{\rho_0}) = p_0$. At the 'zero' order (i.e. neglecting all the perturbation terms labelled as $'1'$) we simply have $p_0 \equiv p_0$, while at the first order we obtain $p_1 = \gamma p_0 \frac{\rho_1}{\rho_0}$.

We have $\mathbf{k}\cdot\mathbf{u}_1 = \begin{pmatrix} k_x \\ 0 \\ k_z \end{pmatrix} \cdot \begin{pmatrix} 0 \\ u_{1y} \\ 0 \end{pmatrix} = 0$ and therefore from Eq.(6.35), we find $\rho_1 = 0$, i.e. there is no variation of the mass density and we can conclude that the wave is of non–compressional type.

The component along the y-axis of eq.(6.36) becomes

$$\begin{aligned}
\omega\rho_0 u_y &= -\frac{1}{\mu_0}\Big[(\mathbf{k}\times\mathbf{B}_1)\times\mathbf{B}_0\Big]_y = \\
&= -\frac{1}{\mu_0}\begin{vmatrix} \hat{x} & \hat{y} & \hat{z} \\ (\mathbf{k}\times\mathbf{B}_1)_x & (\mathbf{k}\times\mathbf{B}_1)_y & (\mathbf{k}\times\mathbf{B}_1)_z \\ 0 & 0 & B_0 \end{vmatrix}_y = \\
&= \frac{B_0}{\mu_0}(\mathbf{k}\times\mathbf{B}_1)_x = \frac{B_0}{\mu_0}\begin{vmatrix} \hat{x} & \hat{y} & \hat{z} \\ k_x & 0 & k_z \\ B_{1x} & B_{1y} & B_{1z} \end{vmatrix}_x = -\frac{B_0}{\mu_0}\,k_z B_{1y}
\end{aligned}$$

Eq.(6.37) gives

$$-\omega B_{1y} = \Big[\mathbf{k}\times(\mathbf{u}_1\times\mathbf{B}_0)\Big]_y = \Big[\mathbf{k}\times\hat{x}B_o u_{1y}\Big]_y = B_0 k_z u_{1y} \tag{6.40}$$

Then the system of eq.(6.35), eq.(6.36) and eq.(6.37) can be written as:

$$\rho_1 = 0, \tag{6.41}$$

$$\omega\rho_0 u_{1y} + \frac{k_z B_0}{\mu_0} B_{1y} = 0, \tag{6.42}$$

$$k_z B_0 u_{1y} + \omega B_{1y} = 0, \tag{6.43}$$

where eq.(6.42) and eq.(6.43) can be written as a homogenous linear system

$$\mathbf{A}\cdot\begin{pmatrix} u_{1y} \\ B_{1y} \end{pmatrix} = 0, \qquad \text{where} \qquad \mathbf{A} = \begin{pmatrix} \omega\rho_0 & \frac{k_z B_0}{\mu_0} \\ k_z B_0 & \omega \end{pmatrix}. \tag{6.44}$$

To have a non–trivial solution ($u_{1y} \neq 0 \neq B_{1y}$), we must have $\det\mathbf{A} = 0$. Thus, we obtain the following dispersion relation

$$\omega^2 = \frac{B_0^2}{\rho_0\mu_0}k_z^2 \equiv c_A^2 k_z^2 = c_A^2 k^2\cos^2\theta, \tag{6.45}$$

where $c_A \equiv B_0/\sqrt{\mu_0\rho_0}$ is the *Alfvén speed*. Typical values are

Magnetosphere:

$$\left.\begin{aligned} B &\sim 5\times10^{-8}\ \text{T} \\ n &\sim 10^6\ \text{m}^{-3} \end{aligned}\right\} \Rightarrow c_A \sim \frac{5\times10^{-8}}{\sqrt{1.7\times10^{-27}\cdot10^6\cdot4\pi\cdot10^{-7}}} \sim 10^6\ \text{m/s}.$$

Tokamak:

$$\left.\begin{aligned} B &\sim 3\ \text{T} \\ n &\sim 10^{20}\ \text{m}^{-3} \end{aligned}\right\} \Rightarrow c_A \sim \frac{3}{\sqrt{1.7\times10^{-27}\cdot10^{20}\cdot4\pi\cdot10^{-7}}} \sim 6\times10^6\ \text{m/s}.$$

The solution given by eq.(6.45) is called *shear Alfvén wave* or *non–compressional Alfvén wave*, as there is no density perturbation:

$$\rho_1 = \frac{\mathbf{k}\cdot\mathbf{u}_1}{\omega} = 0, \tag{6.46}$$

This is different from sound waves, for example. Note that

- The velocity of α particles born with energies 3.5 MeV is $> c_A$, so the α's become *resonant*(‖) with Alfvén waves during slowing down in a fusion reactor.
- Alfvén waves were observed in space first, then in mercury plasma (large $\rho_0 \rightarrow$ smaller λ: easier to measure in a bounded laboratory plasma).
- Alfvén waves are equivalent to waves on a string with tension S and mass per unit length M

$$M\frac{\partial^2 y}{\partial t^2} = S\frac{\partial^2 y}{\partial z^2} \qquad \Longrightarrow \qquad \omega^2 = \frac{S}{M}k_z^2 \tag{6.47}$$

  See problem #1 of problemset #5 where you can show the analogy between a wave travelling along a magnetic field line and a chord.

6.4.2 The compressional Alfvén waves and the magneto–sonic waves

Now we consider the other case $u_{1x} \neq 0$, $u_{1y} = 0$, $u_{1z} \neq 0$, where the perturbation has a longitudinal component. Choosing $B_{1y} = 0$ we get with our previous choices $\mathbf{B}_0 = B_0\mathbf{e}_z$ and $k_y = 0$ from eq.(6.37)

$$\mathbf{B}_1 = \frac{u_{1x}B_0}{\omega}(\mathbf{k}\times\hat{\mathbf{y}}). \tag{6.48}$$

Inserting ρ_1 from eq.(6.35) and $\mathbf{B}_1$ from eq.(6.48) in eq.(6.36) we get a linear system for u_{1x} and u_{1z}, which again has only a non–trivial solution if the determinant of the coefficient matrix vanishes. After some algebra one finds the dispersion relation

$$\omega^4 - \omega^2k^2(c_A^2 + c_s^2) + k_z^2k^2c_A^2c_s^2 = 0, \tag{6.49}$$

which has the solutions

$$\omega^2 = \frac{1}{2}(c_A^2 + c_s^2)k^2 \pm \sqrt{\frac{1}{4}(c_A^2 + c_s^2)^2k^4 - c_A^2c_s^2k^2k_z^2}. \tag{6.50}$$

Note that

$$\left(\frac{c_s}{c_A}\right)^2 = \frac{\gamma p_0}{\rho_0}\frac{\mu_0\rho_0}{B_0^2} = \frac{\gamma}{2}\frac{p_0}{\frac{B_0^2}{2\mu_0}} = \frac{\gamma}{2}\beta, \tag{6.51}$$

The pressure ratio β is an important parameter to characterize a plasma(**). For many plasmas of interest we have $\beta \ll 1$, so $c_s \ll c_A$. In this limit the "+" branch of eq.(6.50) becomes

$$\omega^2 \simeq k^2c_A^2. \tag{6.52}$$

(‖) As we will see later in the kinetic model, the condition $v_{\text{particle}} \sim v_{\text{ph}}$ makes it possible that a strong interaction between waves and particles with exchange of energy may occur. This may lead to instabilities, and the particle motion may be affected by the wave.

(**) $B_0^2/2\mu_0$ is often referred to as "magnetic pressure".

This solution is called *fast wave* or *compressional Alfvén wave*[††]. For the "−" branch we find the so–called *slow wave* or *magneto–sonic wave*

$$\omega^2 \simeq c_s^2 k_z^2 = k^2 c_s^2 \cos^2\theta. \tag{6.53}$$

A useful way to represent the solutions is the surface described by the vector of phase velocity $\omega\mathbf{k}/k^2$ (figure 6.3).
These are *all* possible modes of oscillation that an (unbounded) "MHD plasma" can sustain. As we relax the assumptions that lead to the MHD model many other modes appear, for example separating ions and electrons in their oscillatory motion. To describe these modes we need a more detailed plasma model, such as the multi–fluid or the kinetic models.

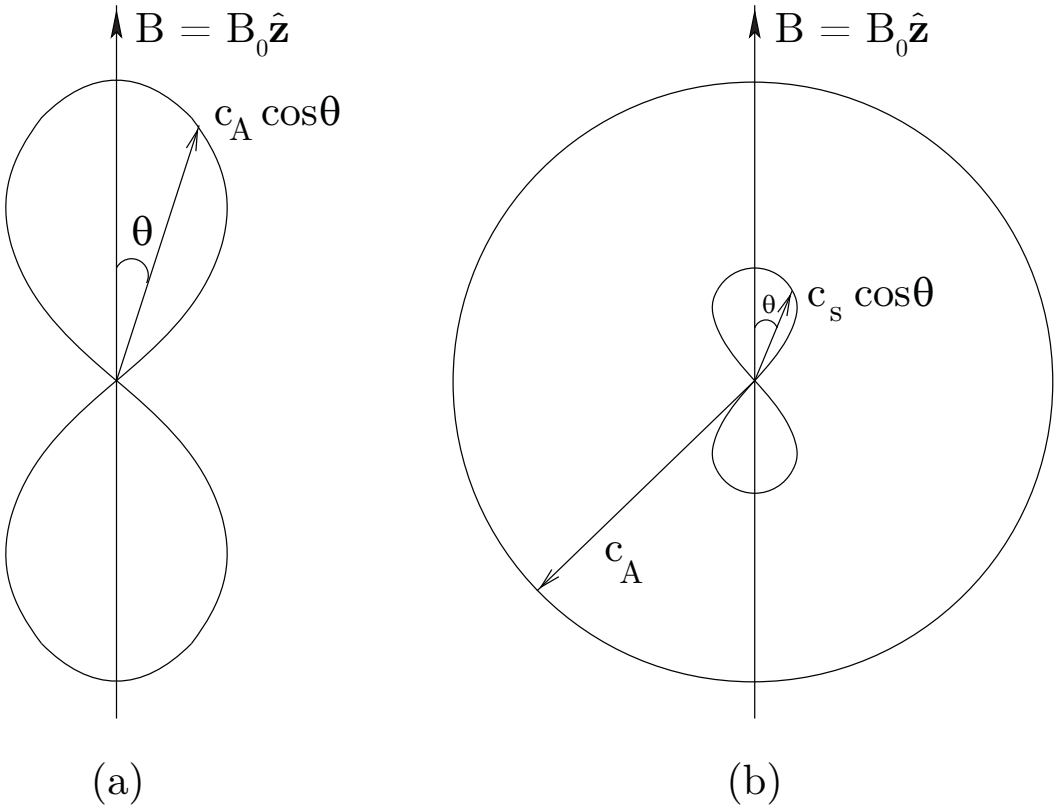

Figure 6.3: Alfvén waves
(a) non-compressional transverse shear Alfvén wave, dispersion relation eq.(6.45).
(b) outer circle: compressional fast Alfvén wave, dispersion relation eq.(6.52), inner curve: slow magneto-sonic wave, dispersion relation eq.(6.53).

[††] $\rho_1 \neq 0 \longleftrightarrow \nabla \cdot \mathbf{u}_1 \neq 0$

6.5 General Description of Plasma Waves

We start from Maxwell equations, with the plasma, present through ρ and $\mathbf{j}$ as "source", for the fields

$$\nabla \times \mathbf{E} = -\frac{\partial \mathbf{B}}{\partial t} \qquad \nabla \times \mathbf{B} = \mu_0 \mathbf{j} + \frac{1}{c^2}\frac{\partial \mathbf{E}}{\partial t} \tag{6.54}$$

$$\nabla \cdot \mathbf{E} = \frac{\rho}{\varepsilon_0} \qquad \nabla \cdot \mathbf{B} = 0 \tag{6.55}$$

and take the curl of the first equation to obtain the *wave equation*

$$\nabla \times (\nabla \times \mathbf{E}) = -\mu_0 \frac{\partial \mathbf{j}}{\partial t} - \frac{1}{c^2}\frac{\partial^2 \mathbf{E}}{\partial t^2} \tag{6.56}$$

We need to assume a constitutive relation between $\mathbf{j}$ and $\mathbf{E}$ totally general,

$$\mathbf{j}(\mathbf{x}, t) = \int \mathrm{d}t' \int \mathrm{d}^3x' \underline{\boldsymbol{\sigma}}(t, t', \mathbf{x}, \mathbf{x}') \cdot \mathbf{E}(\mathbf{x}', t') \tag{6.57}$$

where $\underline{\boldsymbol{\sigma}}$ is the conductivity tensor which contains the model for the plasma dynamics. Note that in general this is a non–local relation. However, if the unperturbed system is *uniform* and *stationary*, then, as a consequence of translation invariance,

$$\underline{\boldsymbol{\sigma}}(t, t'; \mathbf{x}, \mathbf{x}') = \underline{\boldsymbol{\sigma}}(t - t'; \mathbf{x} - \mathbf{x}') \tag{6.58}$$

and we can use Fourier decomposition

$$\mathbf{j}_{\omega,\mathbf{k}} = \underline{\boldsymbol{\sigma}}_{\omega,\mathbf{k}} \cdot \mathbf{E}_{\omega,\mathbf{k}} \tag{6.59}$$

From the Fourier transform of eq.(6.56), i.e. for plane waves, we have

$$-\mathbf{k} \times (\mathbf{k} \times \mathbf{E}_{\omega,\mathbf{k}}) = \mathrm{i}\omega\mu_0 \underline{\boldsymbol{\sigma}} \cdot \mathbf{E}_{\omega,\mathbf{k}} + \frac{\omega^2}{c^2}\mathbf{E}_{\omega,\mathbf{k}} \tag{6.60}$$

Multiplying by c^2/ω^2 we find(*)

$$-\frac{c^2}{\omega^2}\mathbf{k} \times (\mathbf{k} \times \mathbf{E}) = \mathrm{i}\frac{c^2\mu_0}{\omega}\underline{\boldsymbol{\sigma}} \cdot \mathbf{E} + \mathbf{E} = \left(\frac{\mathrm{i}\underline{\boldsymbol{\sigma}}}{\varepsilon_0\omega} + \mathbb{1}\right) \cdot \mathbf{E} \equiv \underline{\boldsymbol{\varepsilon}} \cdot \mathbf{E} \tag{6.61}$$

where

$$\mathbb{1} = \begin{pmatrix} 1 & 0 & 0 \\ 0 & 1 & 0 \\ 0 & 0 & 1 \end{pmatrix} = \delta_{ij} \tag{6.62}$$

is the identity dyad, $\varepsilon_0\mu_0 = 1/c^2$ and

$$\underline{\boldsymbol{\varepsilon}} \equiv \frac{\mathrm{i}\underline{\boldsymbol{\sigma}}}{\varepsilon_0\omega} + \mathbb{1} \tag{6.63}$$

is the *dielectric tensor*. Finally the wave equation becomes

$$\left\{ N^2 \left[\frac{\mathbf{kk}}{k^2} - \mathbb{1} \right] + \underline{\boldsymbol{\varepsilon}} \right\} \cdot \mathbf{E} = 0 \tag{6.64}$$

(*) Again the heavy notation has been dropped, e.g. $\mathbf{E}_{\omega,\mathbf{k}} \to \mathbf{E}$

where the *index of refraction*

$$N^2 \equiv \frac{k^2 c^2}{\omega^2} = \frac{c^2}{v_{\rm ph}^2} \tag{6.65}$$

has been defined and

$$\mathbf{k} \times (\mathbf{k} \times \mathbf{E}) = k^2 \left[\frac{\mathbf{kk}}{k^2} - \mathbb{1}\right] \cdot \mathbf{E} \tag{6.66}$$

was given in dyadic notation.(†) Note that, as we are in Fourier space, all quantities are complex. Eq.(6.64) only has a non–trivial solution $\mathbf{E} \neq 0$ (i.e. a condition for waves to propagate) if

$$\det \left\{ N^2 \left[\frac{\mathbf{kk}}{k^2} - \mathbb{1}\right] + \underline{\varepsilon} \right\} = 0 \tag{6.68}$$

that leads to the *dispersion relation*

$$D(\omega, \mathbf{k}) = 0 \tag{6.69}$$

which may be solved to obtain $\omega = \omega(\mathbf{k})$ or $\mathbf{k} = \mathbf{k}(\omega)$. Frequency and wavelength are thus related in a way that depends on plasma dynamics.

6.6 Dispersion Relations

6.6.1 Summary of Two–Fluid Model for $\mathbf{B}_0 = 0$, $T \neq 0$ [see in Plasmas I]

In the following we assume that the wave propagates along the z–direction. Note that the fluid model is expected to break down for $k^2 \lambda_D^2 > 1$.

- **Transverse waves ("T"):** $E_x, E_y \neq 0$, $E_z = 0$

$$\omega^2 = \omega_{\rm pe}^2 + k^2 c^2 \tag{6.70}$$

- **Longitudinal waves, ("L"):** $E_x, E_y = 0$, $E_z \neq 0$

$$\omega^2 = \omega_{\rm pe}^2 + 3\, k^2 v_{{\rm th},e}^2 \qquad \text{"Langmuir waves"} \tag{6.71}$$

$$\omega^2 = k^2 c_s^2 \tag{6.72}$$

$$\omega^2 \simeq \omega_{{\rm p}i}^2 \qquad \text{"Ion acoustic waves"} \tag{6.73}$$

$$\omega^2 \simeq \omega_{{\rm p}i}^2 + k^2 v_{{\rm th},i}^2 \gamma \tag{6.74}$$

Note that ion acoustic waves can propagate only in plasmas with $T_e \gg T_i$, otherwise we have resonant interaction and damping (as we will show in the study of wave-particle interactions using the kinetic model). If $T_e \gtrsim T_i$ waves with $\omega < \omega_{{\rm p}i}$ do not propagate.

(†) The explicit expression for $\mathbf{kk}$ is

$$\mathbf{kk} = [k_i k_j] = \begin{pmatrix} k_x^2 & k_x k_y & k_x k_z \\ k_y k_x & k_y^2 & k_y k_z \\ k_z k_x & k_z k_y & k_z^2 \end{pmatrix} \tag{6.67}$$

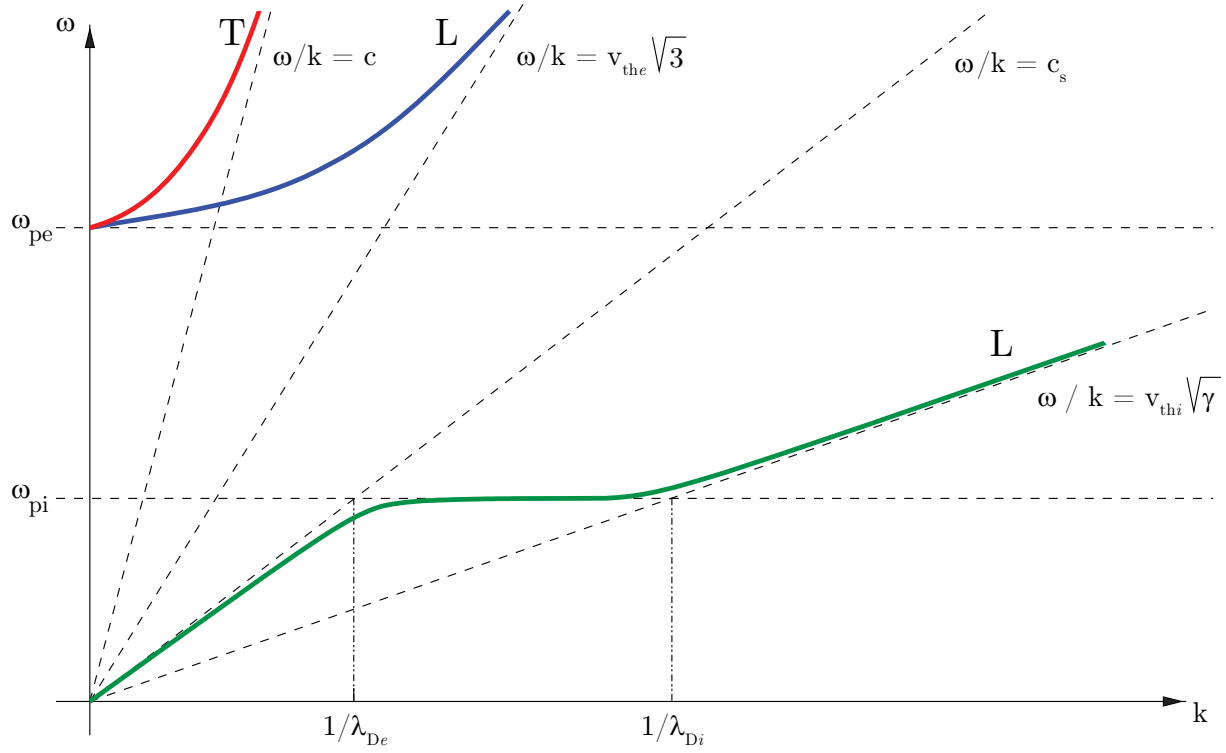

Figure 6.4: Summary of the dispersion relations derived for an warm ($T \neq 0$) unmagnetised plasma ($B_0 = 0$) in the frame of the two–fluid model. γ is the adiabatic index. ´´T" stands for transverse, ´´L" for longitudinal waves.

The solutions of the dispersion relation are shown in figure 6.4.

6.6.2 Two–Fluid Model for $\mathbf{B}_0 \neq 0$, $T = 0$

We will now consider plasma waves and oscillations with $\mathbf{B}_0 \neq 0$[(‡)] in the cold plasma model, $T = 0$. We expect that $\mathbf{B}_0$, by introducing a "privileged" direction, will bring a much wider variety of plasma modes of oscillation.

Langmuir waves and ion acoustic waves (for the case $T \neq 0$) are expected to be the same in magnetised plasma if $\mathbf{E}_1 \parallel \mathbf{B}_0$, as in such geometry the Lorentz force will have no effect.

Let's take a two–fluid model with $T = 0$, and therefore $p = 0$, with an equilibrium

$$\mathbf{u}_{\alpha 0} = 0 \qquad\qquad \mathbf{B}_0 = B_0 \mathbf{e}_z \tag{6.75}$$

where $\alpha = e, i$ denotes the plasma species and B_0, $n_{\alpha 0} \equiv n_0$ and ρ_0 are uniform. The linearisation of the equation of motion

$$m_\alpha \left\{ \frac{\partial \mathbf{u}_\alpha}{\partial t} + (\mathbf{u}_\alpha \cdot \nabla)\mathbf{u}_\alpha \right\} = q_\alpha \left\{ \mathbf{E} + \mathbf{u}_\alpha \times \mathbf{B} \right\} \tag{6.76}$$

yields

$$m_\alpha \frac{\partial \mathbf{u}_\alpha}{\partial t} = q_\alpha \mathbf{E}_1 + q_\alpha \mathbf{u}_{\alpha 1} \times \mathbf{B}_0 \tag{6.77}$$

(‡) Most plasmas of interest, also because of flux freezing, have $\mathbf{B}_0 \neq 0$ somewhere

and after Fourier transformation

$$-\mathrm{i}\omega m_\alpha \mathbf{u}_{\alpha 1} = q_\alpha \mathbf{E}_1 + q_\alpha \mathbf{u}_{\alpha 1} \times \mathbf{B}_0. \tag{6.78}$$

With

$$q_\alpha \mathbf{u}_{\alpha 1} \times \mathbf{B}_0 = q_\alpha B_0 \begin{vmatrix} \hat{x} & \hat{y} & \hat{z} \\ u_{\alpha 1x} & u_{\alpha 1y} & u_{\alpha 1z} \\ 0 & 0 & 1 \end{vmatrix} = q_\alpha B_0 (u_{\alpha 1y}\hat{x} - u_{\alpha 1x}\hat{y}) \tag{6.79}$$

Eq. (6.78) becomes

$$\begin{pmatrix} -i\omega & -\Omega_\alpha & 0 \\ \Omega_\alpha & -i\omega & 0 \\ 0 & 0 & -i\omega \end{pmatrix} \cdot \mathbf{u}_{\alpha 1} = \frac{q_\alpha}{m_\alpha} \mathbf{E}_1 \tag{6.80}$$

and finally

$$\mathbf{u}_{\alpha 1} = \frac{q_\alpha}{m_\alpha} \begin{pmatrix} -i\omega & -\Omega_\alpha & 0 \\ \Omega_\alpha & -i\omega & 0 \\ 0 & 0 & -i\omega \end{pmatrix}^{-1} \cdot \mathbf{E}_1 = \underline{\boldsymbol{\mu}}_\alpha \cdot \mathbf{E}_1 \tag{6.81}$$

where we have introduced the *mobility tensor* $\underline{\boldsymbol{\mu}}_\alpha$. Note that due to the $\mathbf{u}_\alpha \times \mathbf{B}_0$ term, $\underline{\boldsymbol{\mu}}_\alpha$ (hence $\underline{\boldsymbol{\sigma}}$ and $\underline{\boldsymbol{\varepsilon}}$) will not be diagonal. From Eq. (6.81), we find

$$\underline{\boldsymbol{\mu}}_\alpha = \frac{q_\alpha}{m_\alpha} \begin{pmatrix} \frac{-\mathrm{i}\omega}{\Omega_\alpha^2 - \omega^2} & \frac{\Omega_\alpha}{\Omega_\alpha^2 - \omega^2} & 0 \\ -\frac{\Omega_\alpha}{\Omega_\alpha^2 - \omega^2} & \frac{-\mathrm{i}\omega}{\Omega_\alpha^2 - \omega^2} & 0 \\ 0 & 0 & \frac{\mathrm{i}}{\omega} \end{pmatrix} \tag{6.82}$$

Note that, as mentioned before, the x and y–directions are coupled. As

$$\mathbf{j} = \sum_\alpha q_\alpha n_{\alpha 0} \mathbf{u}_{\alpha 1} = \sum_\alpha q_\alpha n_{\alpha 0} \underline{\boldsymbol{\mu}}_\alpha \cdot \mathbf{E}_1 \equiv \underline{\boldsymbol{\sigma}} \cdot \mathbf{E}_1 \tag{6.83}$$

we get for the conductivity tensor

$$\underline{\boldsymbol{\sigma}} = \sum_\alpha q_\alpha n_{\alpha 0} \underline{\boldsymbol{\mu}}_\alpha = \sum_\alpha \frac{q_\alpha^2}{m_\alpha} n_{\alpha 0} \begin{pmatrix} \frac{-\mathrm{i}\omega}{\Omega_\alpha^2 - \omega^2} & \frac{\Omega_\alpha}{\Omega_\alpha^2 - \omega^2} & 0 \\ -\frac{\Omega_\alpha}{\Omega_\alpha^2 - \omega^2} & \frac{-\mathrm{i}\omega}{\Omega_\alpha^2 - \omega^2} & 0 \\ 0 & 0 & \frac{\mathrm{i}}{\omega} \end{pmatrix}. \tag{6.84}$$

Finally we obtain from the definition Eq. (6.63) for the dielectric tensor

$$\underline{\boldsymbol{\varepsilon}} = \begin{pmatrix} \epsilon_1 & -\mathrm{i}\epsilon_2 & 0 \\ \mathrm{i}\epsilon_2 & \epsilon_1 & 0 \\ 0 & 0 & \epsilon_3 \end{pmatrix} \tag{6.85}$$

where

$$\epsilon_1 = 1 + \sum_\alpha \frac{\omega_{\mathrm{p}\alpha}^2}{\Omega_\alpha^2 - \omega^2} \text{ (§)} \tag{6.86}$$

$$\epsilon_2 = -\sum_\alpha \frac{\Omega_\alpha}{\omega} \frac{\omega_{\mathrm{p}\alpha}^2}{\Omega_\alpha^2 - \omega^2} \tag{6.87}$$

$$\epsilon_3 = 1 - \sum_\alpha \frac{\omega_{\mathrm{p}\alpha}^2}{\omega^2} \tag{6.88}$$

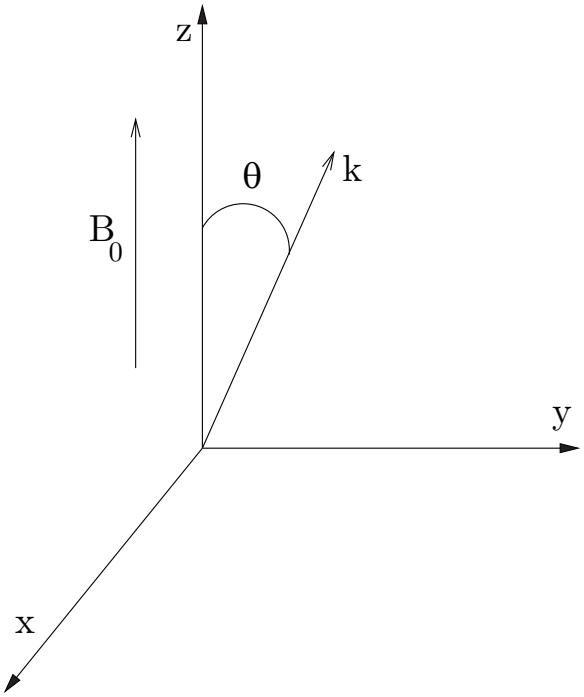

Figure 6.5: Notation: Geometry of magnetic field and wave.

Note that, for a cold plasma, $\underline{\varepsilon}$ does *not* depend on $\mathbf{k}$, but only on ω. For $\mathbf{B} \to 0$ we have $\epsilon_2 \to 0$ and $\epsilon_1 \to \epsilon_3$, thus $\underline{\varepsilon}$ becomes a diagonal matrix with all elements equal to ϵ_3. As we have expected, there is no privileged direction anymore.
Let's use these results to discuss the wave equation eq.(6.64) and its solutions given by eq.(6.68). Choosing $\mathbf{k}$ in the yz–plane and defining the angle θ with respect to the z–axis as shown in figure 6.5, we find

$$\begin{aligned} N^2\left[\frac{\mathbf{kk}}{k^2} - \mathbb{1}\right] + \underline{\varepsilon} &= \begin{pmatrix} -N^2 & 0 & 0 \\ 0 & -N^2\cos^2\theta & N^2\sin\theta\cos\theta \\ 0 & N^2\sin\theta\cos\theta & -N^2\sin^2\theta \end{pmatrix} + \begin{pmatrix} \epsilon_1 & -\mathrm{i}\epsilon_2 & 0 \\ \mathrm{i}\epsilon_2 & \epsilon_1 & 0 \\ 0 & 0 & \epsilon_3 \end{pmatrix} \\ &= \begin{pmatrix} -N^2+\epsilon_1 & -\mathrm{i}\epsilon_2 & 0 \\ \mathrm{i}\epsilon_2 & -N^2\cos^2\theta+\epsilon_1 & N^2\sin\theta\cos\theta \\ 0 & N^2\sin\theta\cos\theta & -N^2\sin^2\theta+\epsilon_3 \end{pmatrix} \end{aligned}$$

and we impose the condition

$$\det\begin{pmatrix} -N^2+\epsilon_1 & -\mathrm{i}\epsilon_2 & 0 \\ \mathrm{i}\epsilon_2 & -N^2\cos^2\theta+\epsilon_1 & N^2\sin\theta\cos\theta \\ 0 & N^2\sin\theta\cos\theta & -N^2\sin^2\theta+\epsilon_3 \end{pmatrix} = 0 \tag{6.89}$$

to have a non–trivial solution for $\mathbf{E}_1$. This leads to a dispersion relation of the type

$$AN^4 + BN^2 + C = 0 \tag{6.90}$$

where A, B and C depend on the *angle* θ between $\mathbf{k}$ and $\mathbf{B}_0$, but not on $|\mathbf{k}|$, and on ω. Explicitly

(§) calculation: $\epsilon_1 = 1 + \frac{i}{\epsilon_0\omega}\sum_\alpha \frac{q_\alpha^2 n_{\alpha 0}}{m_\alpha}\left(\frac{-i\omega}{\Omega_\alpha^2-\omega^2}\right) = 1 + \sum_\alpha \frac{\omega_{\mathrm{p}\alpha}^2}{\Omega_\alpha^2-\omega^2}$

$$A = \varepsilon_1 \sin^2\theta + \varepsilon_3 \cos^2\theta \tag{6.91}$$
$$B = -\left(\varepsilon_1 - \varepsilon_2\right)^2 \sin^2\theta + \varepsilon_1\varepsilon_3\left(1 + \cos^2\theta\right) \tag{6.92}$$
$$C = \varepsilon_3\left(\varepsilon_1 + \varepsilon_2\right)\left(\varepsilon_1 - \varepsilon_2\right) \tag{6.93}$$

Some important points are

- **"cut–off"** – where the wave is *reflected*

$$N = 0,\, C = 0 \qquad \Longrightarrow \qquad \frac{\omega}{k} \to \infty \qquad (k \to 0,\, \omega \neq 0) \tag{6.94}$$

- **"resonance"** – where the wave is *absorbed*

$$N \to \infty,\, A \to 0 \qquad \Longrightarrow \qquad \frac{\omega}{k} \to 0 \tag{6.95}$$

6.6.3 Cut-offs

Introducing

$$\epsilon_R \equiv \epsilon_1 + \epsilon_2 \tag{6.96}$$
$$\epsilon_L \equiv \epsilon_1 - \epsilon_2 \tag{6.97}$$

we can write

$$C = \epsilon_R \epsilon_L \epsilon_3 \tag{6.98}$$

Note that C is independent of θ. In the cold plasma model, the cut–offs do not depend on the propagation angle. In general there are three cut–offs

$$\epsilon_R = 0 \qquad \Longrightarrow \qquad \omega = \omega_R \tag{6.99}$$
$$\epsilon_L = 0 \qquad \Longrightarrow \qquad \omega = \omega_L \tag{6.100}$$
$$\epsilon_3 = 0 \qquad \Longrightarrow \qquad \omega^2 \simeq \omega_{\mathrm{pe}}^2 \tag{6.101}$$

where in the limit $\Omega_e \gg \Omega_i$,

$$\omega_{R,L} \cong \frac{1}{2}\left\{\sqrt{\Omega_e^2 + 4\omega_{\mathrm{pe}}^2} \pm \Omega_e\right\} \tag{6.102}$$

thus $\omega_L \leq \omega_{\mathrm{pe}} \leq \omega_R$.

In the limit $\mathbf{B} \to 0$ we find that $\omega_{R,L} = \omega_{\mathrm{pe}}$, consistently with our previous model. A useful form is

$$\epsilon_{R,L} = \frac{(\omega \mp \omega_R)(\omega \pm \omega_L)}{(\omega \mp \Omega_e)(\omega \pm \Omega_i)} \tag{6.103}$$

6.6.4 Resonances

As the condition

$$A = A(\omega, \theta) = \epsilon_1 \sin^2\theta + \epsilon_3 \cos^2\theta = 0 \qquad (\text{if } \epsilon_1 \neq 0) \tag{6.104}$$

depends on the angle θ, for given values of ϵ_1, ϵ_3 (*i.e.* of plasma parameters and frequency), there will be one angle for which the wave will encounter a resonance. Let's consider the "principal" directions $\theta = 0$ and $\theta = \pi/2$.

For $\theta = 0$ ($\mathbf{k} \parallel \mathbf{B}_0$), eq.(6.104) becomes

$$\tan^2\theta = -\frac{\epsilon_3}{\epsilon_1} = 0 \tag{6.105}$$

Thus there are resonances for

$$\epsilon_3 = 0 \qquad \Longrightarrow \qquad \omega^2 = \omega_{\mathrm{p}}^2 \text{(¶)} \tag{6.106}$$

$$\epsilon_1 \to \infty \qquad \Longrightarrow \qquad \omega^2 = \Omega_{e,i}^2 \qquad \textbf{"cyclotron resonances"} \tag{6.107}$$

A useful expression for the index of refraction in parallel propagation is:

$$N^2 = \frac{k^2c^2}{\omega^2} = \frac{(\omega \mp \omega_R)(\omega \pm \omega_L)}{(\omega_\pm \Omega_i)(\omega \mp \Omega_e)} \simeq 1 - \frac{\omega_{\mathrm{p}e}^2/\omega^2}{1 \mp \Omega_e/\omega}$$

$$\frac{\omega_{\mathrm{p}e}^2/\omega^2}{1 \mp \Omega_e/\omega} \ll 1$$

(¶) ω_{p} seems to be both a cut–off and a resonance. In reality, as we have seen for $T \neq 0$ and $\mathbf{B}_0 = 0$, ω_{p} is only a cut–off.

In the previous lecture, we have seen that the general expression of the dispersion relation is $AN^4 + BN^2 + C = 0$. The cut-off frequencies are given by $N \to 0 \Rightarrow C = 0$ and in the cold plasma model, they don't depend on the propagation angle θ. The resonance frequencies are given by $N \to \infty \Rightarrow A = 0$ and they depend on the propagation angle θ. Let's consider the "principal" directions, i.e. parallel and perpendicular propagation.

6.6.5 Propagation parallel to $\mathbf{B}_0$: $\theta = 0$

In that case, the expression for the coefficient A, found in the previous lecture, becomes

$$A(\omega, 0) = 0 \qquad \to \qquad \tan^2\theta = 0 = -\frac{\epsilon_3}{\epsilon_1} \tag{6.108}$$

Thus there are resonances for

$$\epsilon_3 = 0 \qquad \longrightarrow \qquad \omega^2 = \omega_{\mathrm{p}}^{2\,(*)} \tag{6.109}$$

$$\epsilon_1 \to \infty \qquad \longrightarrow \qquad \omega^2 = \Omega_{e,i}^2 \qquad \textbf{"cyclotron resonances"} \tag{6.110}$$

Let's analyse the meaning of the cyclotron resonances by looking at the dispersion relation and wave equation for waves propagating *parallel* to $\mathbf{B}_0$:

$$\begin{pmatrix} -N^2+\epsilon_1 & -\mathrm{i}\epsilon_2 & 0 \\ \mathrm{i}\epsilon_2 & -N^2+\epsilon_1 & 0 \\ 0 & 0 & \epsilon_3 \end{pmatrix} \cdot \mathbf{E}_1 = 0 \tag{6.111}$$

One can note that $\epsilon_3 = 0$ gives the usual longitudinal ($\mathbf{E} = (0, 0, E_z)$) dispersion relation $\omega = \omega_{\mathrm{p}}$, as in the case $\mathbf{B}_0 = 0$, as $E_z\mathbf{e}_z \parallel \mathbf{B}_0 \parallel k_z\mathbf{e}_z$. Let us now concentrate on transverse waves ($\mathbf{E} = (E_x, E_y, 0)$), dropping the subscript for $\mathbf{E}_1$

$$\begin{cases} (-N^2+\epsilon_1)\,E_x - \mathrm{i}\epsilon_2 E_y &= 0 \\ \mathrm{i}\epsilon_2 E_x + (-N^2+\epsilon_1)\,E_y &= 0 \end{cases} \tag{6.112}$$

therefore $(-N^2+\epsilon_1)^2 - \epsilon_2^2 = 0 \qquad \to \qquad -N^2+\epsilon_1 = \pm\epsilon_2$ and

$$N^2 = \begin{cases} \epsilon_1 + \epsilon_2 = \epsilon_R \\ \epsilon_1 - \epsilon_2 = \epsilon_L \end{cases} \tag{6.113}$$

by introducing the "**rotating vectors**" $E_{R,L} \equiv E_x \mp \mathrm{i}E_y$ we can separate the two components and give a physical interpretation to the two solutions. As

$$\begin{pmatrix} E_R \\ E_L \end{pmatrix} = \begin{pmatrix} 1 & -\mathrm{i} \\ 1 & +\mathrm{i} \end{pmatrix} \begin{pmatrix} E_x \\ E_y \end{pmatrix} \quad \text{and} \quad \begin{pmatrix} E_x \\ E_y \end{pmatrix} = \begin{pmatrix} 1 & -\mathrm{i} \\ 1 & +\mathrm{i} \end{pmatrix}^{-1} \begin{pmatrix} E_R \\ E_L \end{pmatrix} = \frac{1}{2}\begin{pmatrix} 1 & 1 \\ \mathrm{i} & -\mathrm{i} \end{pmatrix} \begin{pmatrix} E_R \\ E_L \end{pmatrix}$$

the wave equation becomes

$$\frac{1}{2}\begin{pmatrix} -N^2+\epsilon_1 & -\mathrm{i}\epsilon_2 \\ \mathrm{i}\epsilon_2 & -N^2+\epsilon_1 \end{pmatrix} \begin{pmatrix} 1 & 1 \\ \mathrm{i} & -\mathrm{i} \end{pmatrix} \begin{pmatrix} E_R \\ E_L \end{pmatrix} = \begin{pmatrix} -N^2+\epsilon_R & -N^2+\epsilon_L \\ \mathrm{i}\,(-N^2+\epsilon_R) & -\mathrm{i}\,(-N^2+\epsilon_L) \end{pmatrix} \begin{pmatrix} E_R \\ E_L \end{pmatrix} = 0 \tag{6.114}$$

(*) ω_{p} seems to be both a cut–off and a resonance. In reality, as we have seen for $T \neq 0$ and $\mathbf{B}_0 = 0$, ω_{p} is only a cut–off.

and for

$$N^2 = \epsilon_R \quad \rightarrow \quad \begin{cases} E_R \neq 0 \\ E_L = 0 \end{cases} \tag{6.115}$$

$$N^2 = \epsilon_L \quad \rightarrow \quad \begin{cases} E_R = 0 \\ E_L \neq 0 \end{cases} \tag{6.116}$$

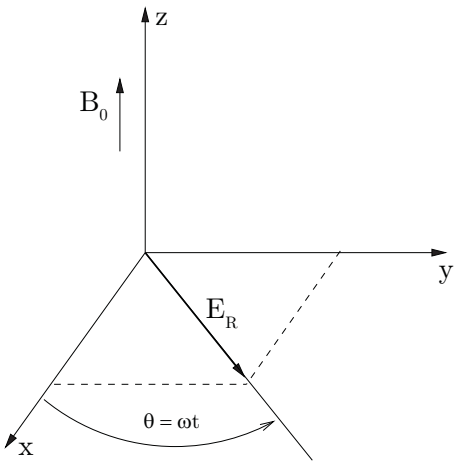

Figure 6.6: A wave field E_R rotating with the electrons.

Right–handed wave (R)

$$N^2 = \epsilon_R \quad E_R \neq 0 \quad E_L = 0 \;\rightarrow\; E_y = \mathrm{i}E_x$$

To understand whether the electric field of the wave rotates with or against the direction of the cyclotron rotation of ions and electrons, let's look at the normal mode in real space on a plane (x, y)

$$\mathbf{E}_r = \Re\left\{ \begin{pmatrix} E_r \\ iE_r \\ 0 \end{pmatrix} e^{i(\mathbf{k}\cdot\mathbf{x}-\omega t)} \right\}\Bigg|_{\mathbf{x}=0} = E_r \begin{pmatrix} \cos\omega t \\ \sin\omega t \\ 0 \end{pmatrix} \tag{6.117}$$

Thus, for $\omega > 0$, the field rotates with the *electrons*.(†)

Left–handed wave (L)

$$N^2 = \epsilon_L \quad E_L \neq 0 \quad E_R = 0 \;\rightarrow\; E_x = \mathrm{i}E_y$$

In this case the electric field rotates with the *ions*.

We expect (R) and (L) to resonate with electrons and ions, respectively:

$$N^2 = \frac{k^2c^2}{\omega^2} = \frac{(\omega \mp \omega_R)(\omega \pm \omega_L)}{(\omega \mp \mid \Omega_e \mid)(\omega \pm \Omega_i)} \tag{6.118}$$

where the upper sign is for the R-wave, the lower for the L-wave. As expected, the resonances $(N^2 \rightarrow \infty)$ are given by the denominator of eq.(6.118):

$$(R) \qquad \omega \rightarrow \mid \Omega_e \mid \qquad\qquad (L) \qquad \omega \rightarrow \Omega_i \tag{6.119}$$

We find again the cut–off frequencies given by the numerator:

$$\omega = \omega_R \qquad\qquad \omega = \omega_L \tag{6.120}$$

For these frequencies $k \rightarrow 0$ but ω remains finite.

(†) Consider the diamagnetic nature of particle orbits, i.e. the magnetic field of a rotating particle will always try to *decrease* the magnetic field which makes it rotate. This argument yields a positive rotation for electrons and a negative for ions.
In general polarization can be defined as $P = \mathrm{i}\frac{E_x}{E_y}$, where $P > 0$ means clockwise rotation and $P < 0$ counter-clock rotation. If $|E_x| = |E_y|$ the polarization is circular, and $P = \pm 1$, where $P = +1$ is for the R-wave and $P = -1$ is for the L-wave.

If we let $\omega \to 0$ and $\mathbf{k} \to 0$ (the limit of "slow" and "large" processes described by MHD), both branches behave in the same way

$$\frac{k^2c^2}{\omega^2} \simeq \frac{\omega_R\,\omega_L}{\Omega_i \mid \Omega_e \mid} = \frac{\omega_{\rm p}^2}{\Omega_i \mid \Omega_e \mid} = \frac{e^2\,n}{\varepsilon_0\,m_e}\frac{1}{\frac{e^2\,B^2}{m_e\,m_i}} = \frac{m_i\,n}{\varepsilon_0 B^2} \overset{\varepsilon_0\mu_0=1/c^2}{=} \frac{c^2\mu_0\,m_i\,n}{B^2} = \frac{c^2}{\frac{B^2}{\rho\mu_0}} = \frac{c^2}{c_A^2}$$
$$\longrightarrow \qquad \omega^2 \simeq c_A^2 k^2$$

As expected, we find the shear (incompressional) Alfvén waves, as found in the MHD model, in the low frequency/long wavelength limit.

The phase velocities of R- and L-waves are different: if we send a wave propagating parallel to $\mathbf{B}_0$ polarised in the perpendicular plane, its polarisation will rotate as it propagates through the plasma (i.e. the plasma is a birefringent medium). This phenomenon is called *Faraday rotation* (figure 6.7) and is used to get information on the $\mathbf{B}$–field or the density inside the plasma. It is useful in large astrophysical plasmas or when access to both ends of a magnetised plasma–column is possible.

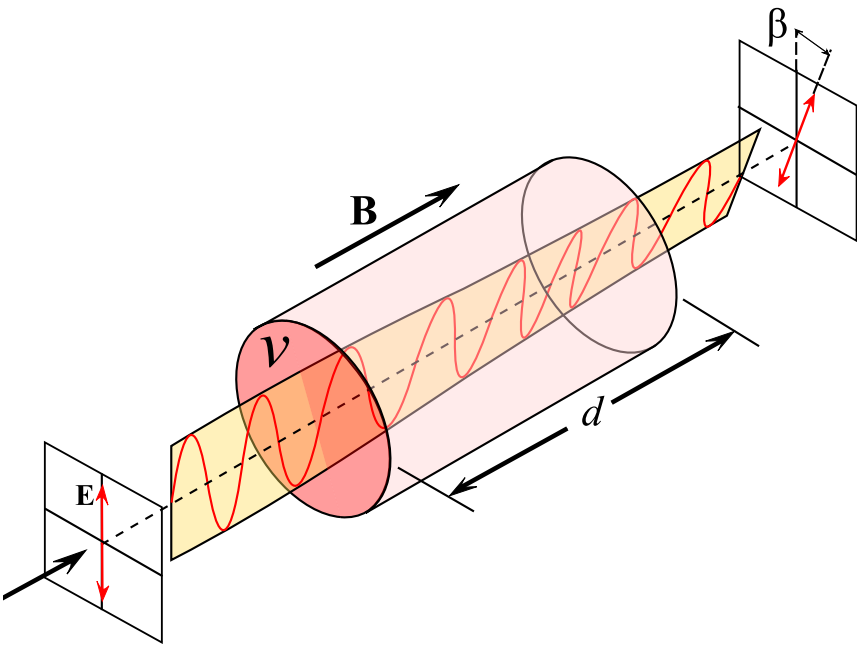

Figure 6.7: Faraday rotation of the plane of polarisation of an electromagnetic wave travelling along $\mathbf{B}_0$.http://www.wikipedia.org.

Whistler waves

For the R-wave, in the limit $\omega/k \ll c$ (and $\omega \ll \omega_{\rm p} <\mid \Omega_e \mid$), if $\Omega_i \ll \omega \ll \mid \Omega_e \mid \lesssim \omega_R$ we have

$$\frac{k^2c^2}{\omega^2} \simeq 1 - \frac{\omega_{\rm p}^2}{(\omega+\Omega_i)(\omega - \mid \Omega_e \mid)} \simeq 1 + \frac{\omega_{\rm p}^2}{\omega \mid \Omega_e \mid} \simeq \frac{\omega_{\rm p}^2}{\omega \mid \Omega_e \mid} \tag{6.121}$$

Thus

$$\frac{\omega}{k} \simeq \frac{c}{\omega_{\rm p}}\sqrt{\mid \Omega_e \mid \omega} \qquad \longrightarrow \qquad \frac{w}{k} \propto \sqrt{\omega}, \quad \frac{\partial\omega}{\partial k} \propto \sqrt{\omega} \tag{6.122}$$

The phase and group velocities increase with the frequency. Thus if we send a pulse made of different frequencies in this range, along B_0, the higher frequencies will propagate faster. "*Whistler waves*" (‡) are a manifestation of this phenomenon, see figure 6.8.

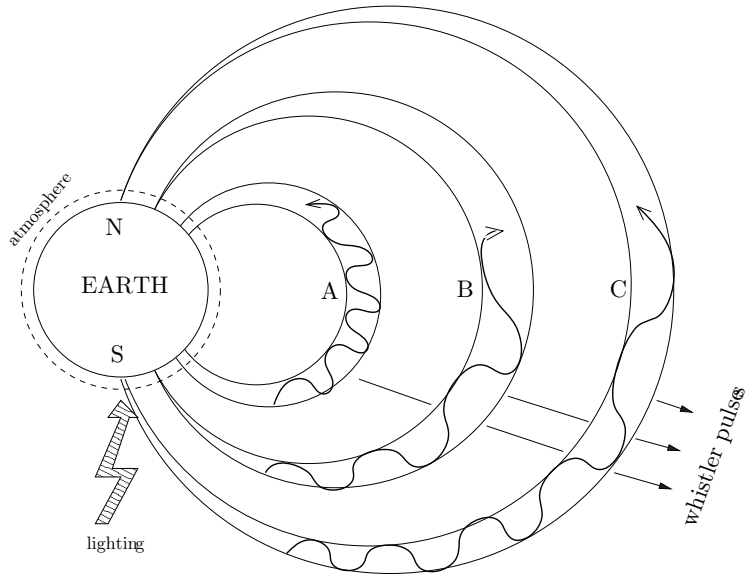

Figure 6.8: A lightning provides a broadband source of electromagnetic waves, high frequencies arrive faster, followed by lower frequencies. This leads to a falling tone in the spectrum (see figure 6.9), hence the name "whistler waves". They were discovered during radio transmissions in world–war I, where they were sometimes mistaken for bomb noise.

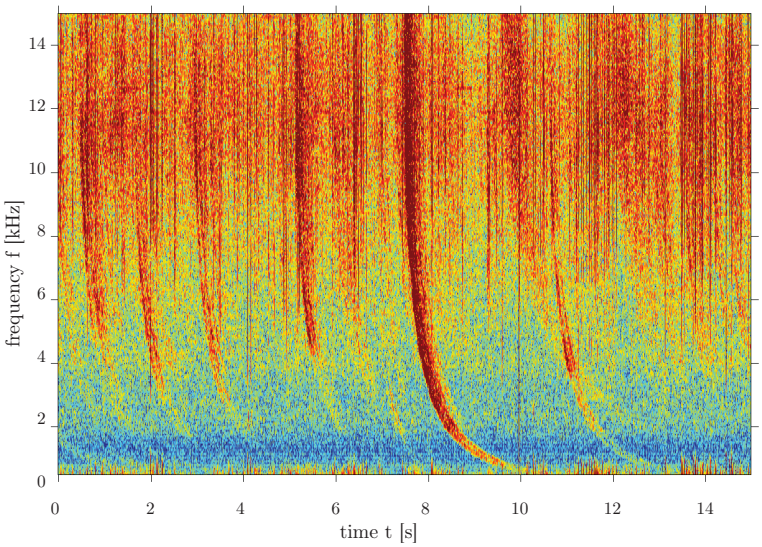

Figure 6.9: Spectrograms (frequency vs. time plot) of whistler signals, as received at Palmer Station, Antarctica on August 24, 2005 and showing the curvature caused by the low-frequency branch of the R-wave dispersion relation. At each time t, the receiver rapidly scans the frequency range between 0 and 15 kHz, tracing a vertical line. Red (blue) color corresponds to signals of strong (weak) intensity at the scanned frequency. The downward motion of the frequency with time then indicates a descending glide tone. Source: http://www.wikipedia.org.

(‡) Note that the exact slope of whistlers and the time dependence of the pulse frequency contain information on the Earth' magnetosphere plasma through which they have propagated. This is why there are several whistler recording instruments in polar regions (Antarctica).

Summary of the Dispersion Relation for Propagation Parallel to B_0, transverse waves

A summary of the dispersion relation for propagation parallel to the magnetic field is shown in figure 6.10.

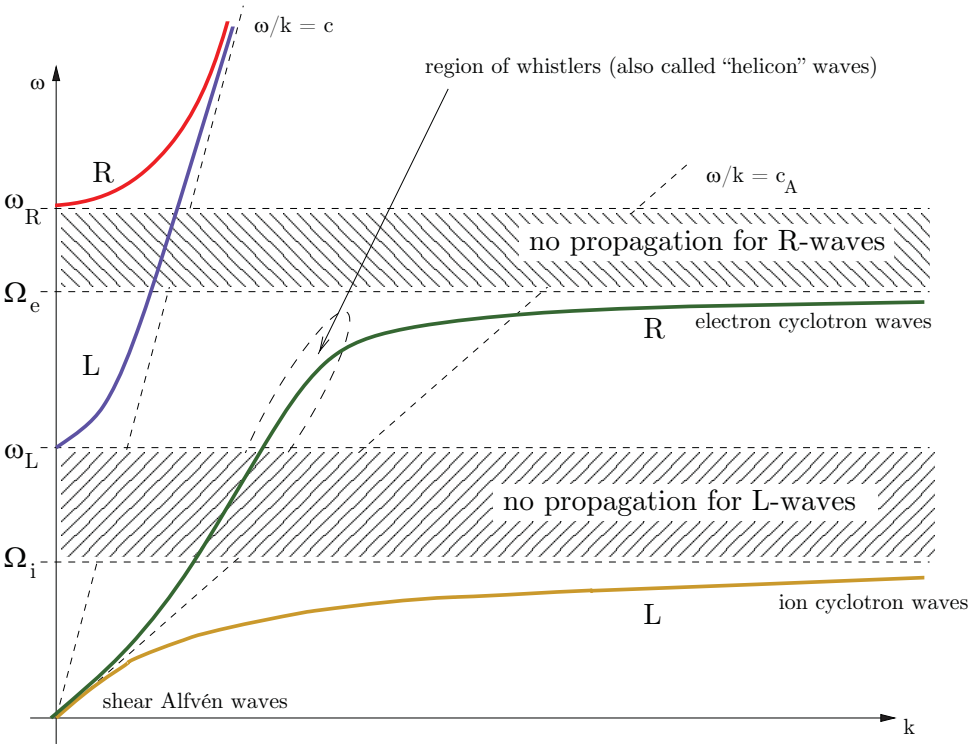

Figure 6.10: Summary of dispersion relation for parallel propagation ($\mathbf{k} \parallel \mathbf{B}_0$) and for the cold plasma model $T = 0$.

6.6.6 Propagation perpendicular to B_0: $\theta = \pi/2$

In that case, the condition for non trivial solutions – see eq.(6.34) in the previous lecture – becomes

$$\det \begin{pmatrix} -N^2+\epsilon_1 & -\mathrm{i}\epsilon_2 & 0 \\ \mathrm{i}\epsilon_2 & \epsilon_1 & 0 \\ 0 & 0 & -N^2+\epsilon_3 \end{pmatrix} = 0 \tag{6.123}$$

$$\begin{aligned} &\Rightarrow \quad \epsilon_1(-N^2+\epsilon_1)(-N^2+\epsilon_3) + \mathrm{i}\epsilon_2(\mathrm{i}\epsilon_2)(-N^2+\epsilon_3) = 0 \\ &\Rightarrow \quad \epsilon_1 N^4 + (-\epsilon_1^2 - \epsilon_1\epsilon_3 + \epsilon_2^2)N^2 + \epsilon_1^2\epsilon_3 - \epsilon_2^2\epsilon_3 = 0 \\ &\Rightarrow \quad \epsilon_1 N^4 + (\epsilon_2^2 - \epsilon_1\epsilon_3 - \epsilon_1^2)N^2 + \epsilon_3 \underbrace{(\epsilon_1+\epsilon_2)}_{\epsilon_R}\underbrace{(\epsilon_1-\epsilon_2)}_{\epsilon_L} = 0 \\ &\Rightarrow \quad AN^4 + BN^2 + C = 0 \end{aligned} \tag{6.124}$$

We already found the cut–off points where $N \to 0$ and which were independent of the angle of propagation,

$$\omega = \omega_p \qquad \omega = \omega_R \qquad \omega = \omega_L \tag{6.125}$$

Now we need to find the resonances, $N \to \infty$. As

$$N^2 = \frac{-B \pm \sqrt{B^2 - 4AC}}{2A} \tag{6.126}$$

$N \to \infty$ for $A \to 0$. Thus

$$\epsilon_1 = 1 + \sum_\alpha \frac{\omega_{\mathrm{p}\alpha}^2}{\Omega_\alpha^2 - \omega^2} = 0 \qquad \textbf{“Hybrid resonances”} \tag{6.127}$$

or explicitly

$$\omega^2 = \omega_{\mathrm{LH}}^2 = \Omega_e \Omega_i \frac{1 + \frac{m_e}{m_i}\left(\frac{\Omega_e}{\omega_{\mathrm{p}}}\right)^2}{1 + \left(\frac{\Omega_e}{\omega_{\mathrm{p}}}\right)^2} \qquad \textbf{“Lower hybrid (LH) resonance”}^{(\S)} \tag{6.128}$$

$$\omega^2 = \omega_{\mathrm{UH}}^2 \simeq \omega_{\mathrm{p}}^2 + \Omega_e^2 \qquad \textbf{“Upper hybrid (UH) resonance”} \tag{6.129}$$

We note that the lower hybrid resonance is given by a combination of ion and electron Larmor motion, whereas the upper hybrid resonance is given by a combination of space–charge and electron Larmor motion. The qualitative mechanism for the latter is given in figure 6.11.

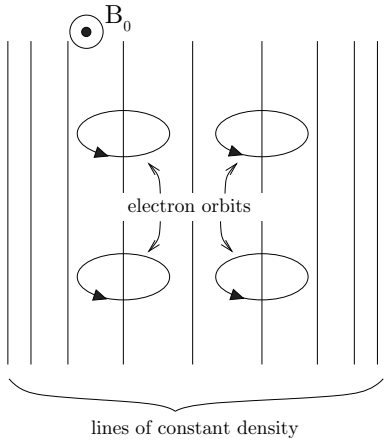

Figure 6.11: Upper hybrid (UH) oscillation. Electrons form regions of compression and rarefaction (space–charge oscillations). With $\mathbf{B}_0 \neq 0$ perpendicular to the motion, the Lorentz force constitutes an additional restoring force besides the space–charge induced electric field. The natural response frequency will be higher than in the $\mathbf{B}_0 = 0$ case.

Wave Equation and Dispersion Relation for $\theta = \pi/2$

Looking at the coefficient matrix eq.(6.123) we remark that the third component is decoupled again. Thus $E_z \neq 0$, $E_x = E_y = 0$ is a solution if $N^2 = \epsilon_3$, leading to the dispersion relation

$$\mathbf{E} \parallel \mathbf{B} \to \omega^2 = \omega_{\mathrm{p}}^2 + k^2 c^2 \qquad \text{“}\textbf{Ordinary mode}\text{”}\ (OM). \tag{6.130}$$

As expected, this is the same as for $\mathbf{B}_0 = 0$. $E_x, E_y \neq 0$, $E_z = 0$ is a solution if $(-N^2 + \epsilon_1)\epsilon_1 - \epsilon_2^2 = 0$.

$$\mathbf{E} \perp \mathbf{B} \to N^2 = \frac{(\omega^2 - \omega_R^2)(\omega^2 - \omega_L^2)}{(\omega^2 - \omega_{\mathrm{UH}}^2)(\omega^2 - \omega_{\mathrm{LH}}^2)} \qquad \text{“}\textbf{Extraordinary mode}\text{”}\ (XM). \tag{6.131}$$

(§) Lower hybrid waves are used in magnetic fusion devices to generate plasma current (localised where the wave absorption occurs) without using the ohmic transformer (“*Lower Hybrid Current Drive*”, abbreviated by “LHCD”).

where the cut–offs and resonances are as calculated above. Note that the distinction between *OM* and *XM*[(¶)] is only possible for perpendicular propagation. For $\theta \neq \pi/2$, *OM* and *XM* are coupled together. As for $\theta = 0$, we can take the limit $\omega \to 0$ and $k \to 0$. We find $\omega^2/k^2 \to c_A^2$, corresponding to *compressional* Alfvén waves already found in the MHD model.

Summary of the Dispersion Relations

The dispersion relations shown in figure 6.1 of the previous lecture and in figure 6.12 below summarise the characteristics of the waves that can propagate in a uniform, infinitely extended, magnetised "cold" plasma.[(‖)]

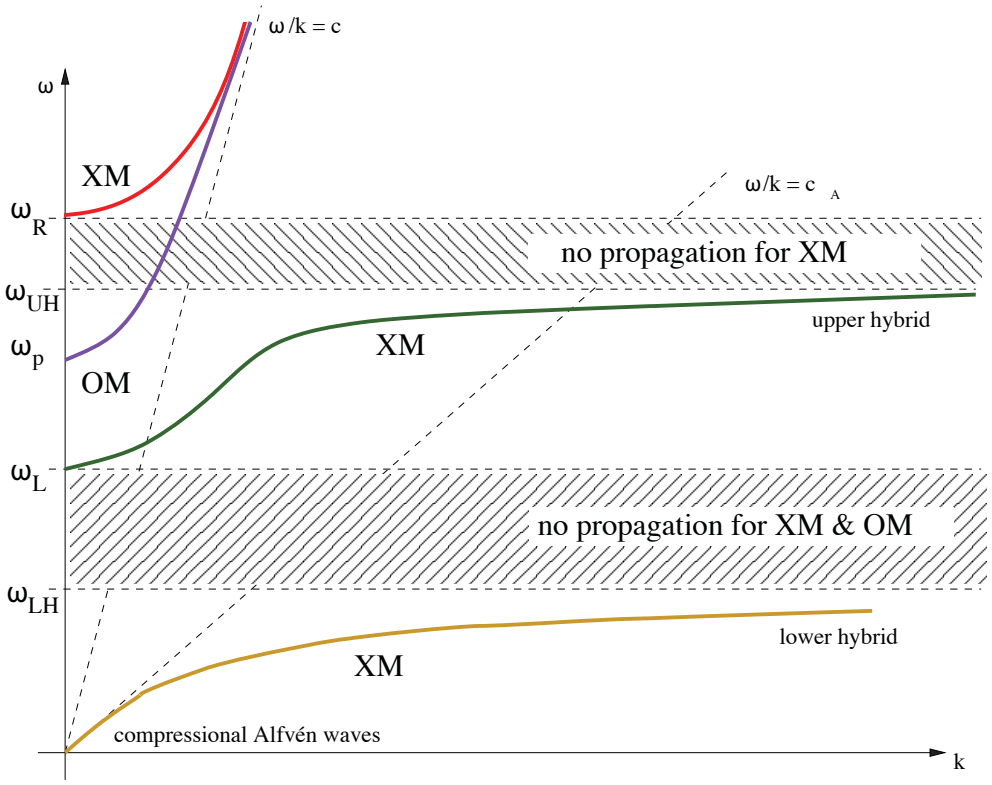

Figure 6.12: Summary of the dispersion relation for $\mathbf{B}_0 \neq 0$, $T = 0$, $\mathbf{k} \perp \mathbf{B}_0$ ($\theta = \pi/2$)

6.7 Some Comments on the Use of Wave Dispersion Relations

We will address the following issues:

- How to use the dispersion relation $D(\omega, \mathbf{k}) = 0$, $\omega(\mathbf{k})$, $\mathbf{k}(\omega)$ to calculate $\mathbf{E}$–fields?
- How good is the model used for actual plasma experiments?
  - in a bounded geometry

(¶) As $\mathbf{k} = k\mathbf{e}_y$, we can have $\mathbf{k} \parallel \mathbf{E}$, i.e. "*electrostatic*" waves, as

$$\frac{\partial \mathbf{B}_1}{\partial t} = -\nabla \times \mathbf{E} \qquad \longrightarrow \qquad \mathbf{B}_1 = \frac{\mathbf{k} \times \mathbf{E}}{\omega} = 0 \tag{6.132}$$

(‖) Examples of different kinds of waves recorded in the earth ionosphere and magnetosphere, as well as from other planets, can be found in the form of audio files at http://www.science.nasa.gov/ssl/pad/sppb/edu/lionroar/.

– with an inhomogeneous plasma (to assess the accessibility of waves)

In general, one has

$$\det(\,\cdot\,) = 0 \qquad \Longrightarrow \qquad D(\omega, \mathbf{k}) = 0 \qquad \Longrightarrow \qquad \omega(\mathbf{k}) \quad \text{or} \quad \mathbf{k}(\omega) \tag{6.133}$$

i.e. a wave exists only if $\omega = \omega(\mathbf{k})$. There are two ways to proceed, corresponding to two classes of problems.

6.7.1 Initial Condition Problem

We fix $\mathbf{E}(\mathbf{x}, t = 0)$. After applying the dispersion relation we have

$$\begin{aligned}\mathbf{E}(\mathbf{x}, t) &= \int_{\mathbb{R}^3} \mathrm{d}^3k \int_{\mathbb{C}} \mathrm{d}\omega\, \mathbf{E}_0(\mathbf{k}, \omega)\, e^{\mathrm{i}(\mathbf{k}\cdot\mathbf{x} - \omega t)} \delta\big(\omega - \omega(\mathbf{k})\big) \\ &= \int_{\mathbb{R}^3} \mathrm{d}^3k\, \underbrace{\mathbf{E}_0(\mathbf{k})\, e^{\mathrm{i}(\mathbf{k}\cdot\mathbf{x} - \omega(\mathbf{k})t)}}_{\text{normal modes}}\end{aligned} \tag{6.134}$$

where $\mathbf{E}_0(\mathbf{k})$ is to be determined. Note that $\mathbf{k} \in \mathbb{R}^3$ and $\omega \in \mathbb{C}$. This approach is usually applied to calculate instability growth rates using the imaginary part of ω, $\Im\,\omega \equiv \mathrm{Im}(\omega)$. Taking eq.(6.134) at $t = 0$ and applying the inverse Fourier transformation yields

$$\mathbf{E}_0(\mathbf{k}) = \frac{1}{(2\pi)^3} \int_{\mathbb{R}^3} \mathrm{d}^3x\, \mathbf{E}(\mathbf{x}, 0)\, e^{-\mathrm{i}\mathbf{k}\cdot\mathbf{x}} \tag{6.135}$$

Note that in general $D(\omega, \mathbf{k}) = 0$ can have more than one solution $\omega_j(\mathbf{k})$, $j = 1, 2, \ldots, N$. If this is the case we need more information than just $\mathbf{E}(\mathbf{x}, 0)$ to calculate the Fourier coefficients $\mathbf{E}_{0j}(\mathbf{k})$:

$$\mathbf{E}(\mathbf{x}, t) = \sum_{j=1}^{N} \int_{\mathbb{R}^3} \mathrm{d}^3k\, \mathbf{E}_{0j}(\mathbf{k})\, e^{\mathrm{i}\left(\mathbf{k}\cdot\mathbf{x} - \omega_j(\mathbf{k})t\right)} \tag{6.136}$$

or for $t = 0$:

$$\mathbf{E}(\mathbf{x}, 0) = \int_{\mathbb{R}^3} \mathrm{d}^3k \left\{ \sum_{j=1}^{N} \mathbf{E}_{0j}(\mathbf{k}) \right\} e^{\mathrm{i}\mathbf{k}\cdot\mathbf{x}} \tag{6.137}$$

We also need

$$\left.\frac{\partial \mathbf{E}}{\partial t}\right|_{t=0} = \int_{\mathbb{R}^3} \mathrm{d}^3k \left\{ -\mathrm{i} \sum_{j=1}^{N} \omega_j(\mathbf{k})\, \mathbf{E}_{0j}(\mathbf{k}) \right\} e^{\mathrm{i}\mathbf{k}\cdot\mathbf{x}} \tag{6.138}$$

In general we need as many derivatives (at time $t = 0$)

$$\left.\frac{\partial^{j-1} \mathbf{E}}{\partial t^{j-1}}\right|_{t=0} = \int_{\mathbb{R}^3} \mathrm{d}^3k \sum_{j=1}^{N} \big[-\mathrm{i}\omega_j(\mathbf{k}) \big]^j \mathbf{E}_{0j}(\mathbf{k})\, e^{\mathrm{i}\mathbf{k}\cdot\mathbf{x}} \qquad j = 1, \ldots, N \tag{6.139}$$

as we have roots for the dispersion relation to have a full linear system to determine all the $\mathbf{E}_{0j}(\mathbf{k})$.

6.7.2 Boundary Value Problem

Fix $\mathbf{E}(\mathbf{x}=0,t)$. Then

$$\mathbf{E}(\mathbf{x},t) = \int_{\mathbb{R}} \mathrm{d}\omega\, \mathbf{E}_0(\omega)\, e^{\mathrm{i}\left(\mathbf{k}(\omega)\cdot\mathbf{x}-\omega t\right)} \tag{6.140}$$

with $\mathbf{k}\in\mathbb{C}^3$, $\omega\in\mathbb{R}$. This implies

$$\mathbf{E}(0,t) = \int_{\mathbb{R}} \mathrm{d}\omega\, \mathbf{E}_0(\omega)\, e^{-\mathrm{i}\omega t} \tag{6.141}$$

or

$$\mathbf{E}_0(\omega) = \frac{1}{(2\pi)} \int_{\mathbb{R}} \mathrm{d}\omega\, \mathbf{E}(0,t)\, e^{\mathrm{i}\omega t} \tag{6.142}$$

For several roots $\mathbf{k}_j(\omega)$ we have analogously to eq.(6.136)

$$\mathbf{E}(\mathbf{x},t) = \sum_{j=1}^{N} \int_{\mathbb{R}} \mathrm{d}\omega\, \mathbf{E}_{0j}(\omega)\, e^{\mathrm{i}\left(\mathbf{k}_j(\omega)\cdot\mathbf{x}-\omega t\right)} \tag{6.143}$$

and we need

$$\left.\frac{\partial^\ell \mathbf{E}}{\partial \mathbf{x}^\ell}\right|_{\mathbf{x}=0} = \int_{\mathbb{R}} \mathrm{d}\omega\, \left\{\sum_{j=1}^{N} \mathbf{E}_{0j}(\omega)\left[\mathrm{i}\mathbf{k}_j(\omega)\right]^\ell\right\} e^{-\mathrm{i}\omega t}\,, \qquad \ell = 1,\ldots,N \tag{6.144}$$

to determine the $\mathbf{E}_{0j}(\omega)$.

This is the scenario used for example to heat the plasma via electromagnetic waves: an antenna is installed at the plasma edge and is fed with a given (obviously real) frequency ω.

6.8 Waves in Inhomogeneous Plasmas

6.8.1 Possible Extensions of the Model

So far we have considered uniform (unperturbed) plasmas. In general the main plasma parameters, such as the density n_0, temperature T_e, magnetic field $\mathbf{B}_0$, pressure p_0 etc. have gradients along at least one direction. Two consequences for wave propagation are:

1. One needs to check the "accessibility": the wave should be able to reach a resonance before a cut–off.

2. The solution $\mathbf{k}(\omega)$ will now depend on the spatial position $\mathbf{x}$: the plane wave formalism has a problem. One approximation around this problem is the *WKB* method: Assuming that $\mathbf{k}$ is only a slowly varying function of space (i.e. the variations occur over scales that are much longer than the wavelength), we can write

$$\mathbf{E}\exp\left\{\mathrm{i}\int_0^{\mathbf{x}} \mathbf{k}(\mathbf{x}')\cdot\mathrm{d}\mathbf{x}' - \mathrm{i}\omega t\right\} \tag{6.145}$$

instead of $\exp\left\{\mathrm{i}(\mathbf{k}\cdot\mathbf{x}-\omega t)\right\}$ along the direction of propagation of the wave ("*ray tracing*"). The method can be applied if the scale of variation is much larger than the wavelength.

6.8.2 Drift Waves

This last part has not been treated during the lecture.

In non-uniform plasmas, in addition to modifying the *local* dispersion relation (as accounted for in the *WKB* approximation), new waves are introduced, i.e. new modes of oscillation in the plasma. To illustrate this, we consider a simplified case, in which we assume

1. A plasma slab, with variations only along x.
2. Low frequency, electrostatic waves $\mathbf{E}_1 = -\nabla\phi$, $\mathbf{B}_1 = 0$, $\mathbf{B}_0 = B_0\mathbf{e}_z$.
3. Incompressible fluid $\nabla \cdot \mathbf{v} = 0$.
4. Long wavelengths $\lambda \gg \lambda_D$. Thus $n_e = n_i$ at all orders (no deviation from neutrality).
5. T_e uniform, $T_i = 0$; variations only in $n_0(x)$.
6. Adiabatic electrons, i.e. moving fast enough to *equilibrate* with potential according to Boltzmann statistics(**)

$$n_e = n_0 \exp\left\{\frac{e\phi}{T_e}\right\} \tag{6.146}$$

or at first order

$$n_{i1} = n_{e1} = n_0 \frac{e\phi}{T_e} \tag{6.147}$$

We start from the ion continuity equation

$$\frac{\partial n_i}{\partial t} + \nabla \cdot (n_i \mathbf{v}_i) = 0 \tag{6.148}$$

we linearise it using $\mathbf{v}_{i0} = 0$ and $\nabla \cdot \mathbf{v}_{i1} = 0$

$$\frac{\partial n_{i1}}{\partial t} + \mathbf{v}_{i1} \cdot \nabla n_0 = \frac{\partial n_{i1}}{\partial t} + v_{i1x}\frac{\mathrm{d}n_0}{\mathrm{d}x} = 0 \tag{6.149}$$

and do a Fourier transformation $t \to \omega$. Thus(††)

$$-\mathrm{i}\omega n_{i1} + v_{i1x}\frac{\mathrm{d}n_0}{\mathrm{d}x} = 0 \tag{6.150}$$

or with eq.(6.147)

$$-\mathrm{i}\omega e\phi = -v_{i1x}T_e\frac{1}{n_0}\frac{\mathrm{d}n_0}{\mathrm{d}x} \equiv -v_{i1x}T_e\frac{1}{L_n} \tag{6.151}$$

where L_n is the characteristic length for the density gradient. In order to obtain an expression for v_{i1x} we start from the equation of motion for ions ($Z = 1$)

$$m_i\frac{\mathrm{d}\mathbf{v}_i}{\mathrm{d}t} = e(\mathbf{E} + \mathbf{v}_i \times \mathbf{B}_0) = e(\mathbf{E} + \mathbf{v}_i \times \mathbf{B}_0) \tag{6.152}$$

(**) This corresponds to saying $m_e \to 0$.

(††) Note that we cannot do a Fourier transformation $x \to k_x$, as the medium is inhomogeneous in this direction.

where we have neglected T_i. Linearisation and Fourier transformation yields

$$-\mathrm{i}\omega m_i \mathbf{v}_{i1} = e(\mathbf{E}_1 + \mathbf{v}_{i1} \times \mathbf{B}_0) \tag{6.153}$$

Considering $\omega \ll \Omega_i$ we can neglect the left hand side and find(‡‡), for the y-component of the previous equation

$$v_{i1x} = \frac{E_{1y}}{B_0} = \frac{-\mathrm{i}k_y\phi}{B_0} \tag{6.155}$$

Using this in eq.(6.151) we finally get the dispersion relation

$$\omega = -\frac{T_e}{eB_0}\frac{1}{L_n}k_y \tag{6.156}$$

We see that the phase velocity is

$$v_{\mathrm{ph}} = \frac{\omega}{k_y} = -\frac{T_e}{eB_0}\frac{1}{L_n} \equiv v_{\mathrm{d}} \tag{6.157}$$

where v_{d} is the diamagnetic drift velocity,

$$L_n = \frac{n}{\frac{\partial n}{\partial x}}$$

is the density gradient scale length, and we have assumed uniform T_e.

Drift waves are important as they can appear in all plasmas with a pressure gradient, and can always be destabilised by the free energy associated with such a gradient. Different mechanisms for the instability can occur, including finite resistivity or effects related to the presence of different velocity classes of particles ("*kinetic effects*"). This is why drift instabilities are sometimes called *universal instabilities*.

Drift waves and instabilities are thought to be responsible for anomalous (i.e. larger than collisional) transport in magnetised plasmas. This is why they are a very important subject of theoretical and experimental investigations.

Note on the main limitations of a fluid model: The main limitation in the treatment of waves in plasmas using a fluid model is that it does not account for different responses of different plasma particles (with different velocities) to various plasma waves.

Questions

- Will we have *other* characteristic plasma oscillations and waves due to the single particle nature of the plasma, namely for short λ's and high frequency $\omega \gtrsim \Omega_i$?
- How will the *exchange of energy* between particles and waves take place (aside from slow collisional processes)?

These questions will be addressed in the next part of the course, focused on the kinetic model.

(‡‡) Another way to see this approximation is to neglect all other drift velocities against

$$\mathbf{v}_{\mathbf{E}\times\mathbf{B}} = \frac{\mathbf{E}\times\mathbf{B}}{B^2} \tag{6.154}$$

Note: The lecture has started with a short review of the previous lectures: Definition and creation of a plasma, collisions and transport, waves.

Chapter 7 The kinetic model and the Vlasov equation

7.1 Origin of the Vlasov Equation

Particles are described by means of their distribution function $f(\mathbf{x}, \mathbf{v}, t)$, with $\int_V f(\mathbf{x}, \mathbf{v}, t)\, \mathrm{d}^3x\, \mathrm{d}^3v = N_V$ (N_V being the total number of particles inside V), such that

$$f(\mathbf{x}, \mathbf{v}, t)\, \mathrm{d}^3x\, \mathrm{d}^3v \tag{7.1}$$

represents(*) the number of particles that at the time t occupy the hypervolume (in the phase space) of size $\mathrm{d}^3x\, \mathrm{d}^3v$ centred at $\mathbf{x}$, $\mathbf{v}$. The volume $\mathrm{d}^3x\, \mathrm{d}^3v$ is *macroscopically small but microscopically large*.

- *Macroscopically small*: the quantities that characterise $f(\mathbf{x}, \mathbf{v}, t)$ and determine its evolution are representative of the point $\mathbf{x}$, $\mathbf{v}$ in the phase space, and not of the entire volume.
- *Microscopically large*: there are enough particles inside the volume $\mathrm{d}^3x\, \mathrm{d}^3v$ to allow a statistical description.

We define the *position in the phase space* of the particle j by the independent variables $\mathbf{x}_j$, $\mathbf{v}_j$, with

$$\dot{\mathbf{x}}_j = \mathbf{v}_j \tag{7.2}$$

$$\dot{\mathbf{v}}_j = \frac{\mathbf{F}_j}{m_j} \qquad \text{or} \qquad \dot{\mathbf{p}}_j = \mathbf{F}_j \tag{7.3}$$

We will consider only the non-relativistic case.

The force on the particle j can be split into two contributions, $\mathbf{F}_j = \mathbf{F}_j^{\mathrm{ext}} + \mathbf{F}_j^{\mathrm{int}}$:

- The macroscopic part $\mathbf{F}_j^{\mathrm{ext}}$ (external to the volume $\mathrm{d}^3x\, \mathrm{d}^3v$) is the same for all particles in the volume.
- The microscopic part $\mathbf{F}_j^{\mathrm{int}}$ is due to collisions between particles inside $\mathrm{d}^3x\, \mathrm{d}^3v$ and may be different for different particles.
- We will assume that

$$|\mathbf{F}_j^{\mathrm{int}}| \ll |\mathbf{F}_j^{\mathrm{ext}}| \tag{7.4}$$

so we don't need to follow every particle j, but we can treat the particles in the phase space volume $\mathrm{d}^3x\ \mathrm{d}^3v$ statistically(†). The kinetic theory will therefore apply to plasmas in which collisions are relatively unimportant(‡) – as is the case for hot plasmas.

(*) Note that this interpretation depends on the normalisation we have chosen for f. If f was normalised so that $\int_{V_{\mathrm{tot}}} f(\mathbf{x}, \mathbf{v}, t)\, \mathrm{d}^3x\, \mathrm{d}^3v = 1$, instead of $\int_{V_{\mathrm{tot}}} f(\mathbf{x}, \mathbf{v}, t)\, \mathrm{d}^3x\, \mathrm{d}^3v = N_{V_{\mathrm{tot}}}$, the distribution function would have the meaning of *probability* to find a particle inside the volume $\mathrm{d}^3x\, \mathrm{d}^3v$.

(†) It is basically a transition to a *continuum* description.

(‡) Note that this is indeed the regime we are interested in: in a strongly collisional plasma, distributions become Maxwellians very quickly and fluid theory provides a very good model.

The assumption (7.4) allows us to neglect the correlations between particles[(§)]. In this approximation, Liouville's theorem applies and phase space density is conserved in phase space, i.e. the *continuity equation is valid on phase space.*

Let's apply the conservation of the number of particles:

$$N_V = \int_V f(\mathbf{x}, \mathbf{v}, t)\, \mathrm{d}^3x\, \mathrm{d}^3v \tag{7.6}$$

through their evolution in phase space (Lagrangian approach). Introducing the phase space "velocity"

$$\mathbf{U} \equiv (\dot{\mathbf{x}}, \dot{\mathbf{v}}) = \left(\mathbf{v}, \frac{\mathbf{F}}{m}\right) \tag{7.7}$$

we have

$$\underbrace{\frac{\mathrm{d}N_V}{\mathrm{d}t} = 0}_{\text{Liouville}} = \int_V \frac{\partial f}{\partial t} \mathrm{d}^3x\, \mathrm{d}^3v + \underbrace{\int_{S(V)} f\mathbf{U} \cdot d^5\mathbf{S}}_{\text{net flux in phase space into volume } V} \tag{7.8}$$

Using the divergence theorem (in the 6–dimensional phase space) we obtain

$$\frac{\mathrm{d}N_V}{\mathrm{d}t} = 0 = \int_V \left\{ \frac{\partial f}{\partial t} + \nabla_{\mathrm{ps}} \cdot (f\mathbf{U}) \right\} \mathrm{d}^3x\, \mathrm{d}^3v \qquad \forall\, V \tag{7.9}$$

where the phase space differential operator is defined as

$$\nabla_{\mathrm{ps}} \equiv (\nabla_{\mathbf{x}}, \nabla_{\mathbf{v}}) \equiv \left(\frac{\partial}{\partial \mathbf{x}}, \frac{\partial}{\partial \mathbf{v}}\right) \tag{7.10}$$

As V is an arbitrary phase space volume

$$\frac{\partial f}{\partial t} + \frac{\partial}{\partial \mathbf{x}} \cdot (f\mathbf{v}) + \frac{\partial}{\partial \mathbf{v}} \cdot \left(f \frac{\mathbf{F}}{m}\right) = 0 \tag{7.11}$$

or

$$\frac{\partial f}{\partial t} + \mathbf{v} \cdot \frac{\partial f}{\partial \mathbf{x}} + \frac{\mathbf{F}}{m} \cdot \frac{\partial f}{\partial \mathbf{v}} + f \underbrace{\left\{ \frac{\partial}{\partial \mathbf{x}} \cdot \mathbf{v} + \frac{\partial}{\partial \mathbf{v}} \cdot \frac{\mathbf{F}}{m} \right\}}_{=\,0} = 0 \tag{7.12}$$

Here $\mathbf{F} = \mathbf{F}^{\mathrm{ext}}$ (first crucial passage to get the Vlasov equation).

In the last equation $\dfrac{\partial}{\partial \mathbf{x}} \cdot \mathbf{v} = 0$, as $\mathbf{x}$ and $\mathbf{v}$ are independent phase space coordinates, and $\dfrac{\partial}{\partial \mathbf{v}} \cdot \mathbf{F}/m = 0$, as the electromagnetic fields are independent of $\mathbf{v}$ and the Lorentz force is perpendicular to $\mathbf{v}$

(§) Remember that

$$\frac{E_{\mathrm{k}}}{E_{\mathrm{p}}} = \frac{T}{e^2 n^{1/3}} \sim N_D^{2/3} \gg 1, \tag{7.5}$$

as for an ideal gas.

(second crucial passage).[¶] Thus, for each species α,

$$\frac{\partial f_\alpha}{\partial t} + \mathbf{v}\cdot\frac{\partial f_\alpha}{\partial \mathbf{x}} + \frac{q_\alpha}{m_\alpha}(\mathbf{E}+\mathbf{v}\times\mathbf{B})\cdot\frac{\partial f_\alpha}{\partial \mathbf{v}} = 0 \qquad \text{“\textbf{Vlasov equation}”} \tag{7.13}$$

Indeed $\mathbf{F}^{\text{ext}}$ is the force due to the *macroscopic* fields $\mathbf{E}$ and $\mathbf{B}$ created either by external sources or by plasma particles, via

$$\rho(\mathbf{x},t) = \sum_{\alpha=e,i} q_\alpha \int f_\alpha(\mathbf{x},\mathbf{v},t)\,\mathrm{d}^3v \tag{7.14}$$

$$\mathbf{j}(\mathbf{x},t) = \sum_{\alpha=e,i} q_\alpha \int \mathbf{v}\, f_\alpha(\mathbf{x},\mathbf{v},t)\,\mathrm{d}^3v \tag{7.15}$$

7.2 Collision Terms

Collision terms can be added to the right hand side of the Vlasov equation[‖], such as

- **Krook term:**

$$\left(\frac{\partial f}{\partial t}\right)_{\text{c}} = -\nu_{\text{p}}(f - f_{\text{Maxwell}}) \tag{7.16}$$

  where we consider that, under the effects of collisions, f relaxes towards a Maxwellian distribution at a rate given by ν_{p} (momentum transfer).

- **Fokker–Planck term:**
  Including the theory of Coulomb collisions properly one finds

$$\left(\frac{\partial f}{\partial t}\right)_{\text{c}} = \underbrace{-\frac{\partial}{\partial \mathbf{v}}\left(\frac{\mathrm{d}\langle\Delta\mathbf{v}\rangle}{\mathrm{d}t} f\right)}_{\substack{\mathbf{v}\text{–space convection}\\ \text{(‘drag’)}}} + \underbrace{\frac{1}{2}\frac{\partial^2}{\partial\mathbf{v}\partial\mathbf{v}} : \left(\frac{\mathrm{d}\langle\Delta\mathbf{v}\Delta\mathbf{v}\rangle}{\mathrm{d}t} f\right)}_{\mathbf{v}\text{–space diffusion}} \tag{7.17}$$

  where $\Delta\mathbf{v}$ is a variation in $\mathbf{v}$ due to a collision, $\langle\Delta\mathbf{v}\rangle$ is the average over possible $\mathbf{v}$–increments and

$$\frac{\mathrm{d}\langle\Delta\mathbf{v}\Delta\mathbf{v}\rangle}{\mathrm{d}t} \tag{7.18}$$

  are the $\mathbf{v}$–space diffusion coefficients due to Coulomb collisions.

[¶] Explicitly

$$\begin{aligned}\nabla_{\mathbf{v}}\cdot\frac{\mathbf{F}}{m} &= \frac{q}{m}\frac{\partial}{\partial\mathbf{v}}\Big\{\mathbf{E}(\mathbf{x},t)+\mathbf{v}\times\mathbf{B}(\mathbf{x},t)\Big\}\\ &= \frac{q}{m}\frac{\partial}{\partial v_i}\Big\{\varepsilon_{ijk}\,v_j\,B_k(\mathbf{x},t)\Big\} = \frac{q}{m}\varepsilon_{ijk}\,\delta_{ij}\,B_k(\mathbf{x},t) = \frac{q}{m}\varepsilon_{iik}\,B_k(\mathbf{x},t) = 0\end{aligned}$$

Even more general: remember that $\mathbf{q}\equiv\mathbf{x}$ and $\mathbf{p}\equiv m\mathbf{v}$ are canonical variables. Thus

$$\nabla_{\mathbf{x}}\cdot(m\mathbf{v}) + \nabla_{\mathbf{v}}\cdot\mathbf{F} = \frac{\partial}{\partial\mathbf{q}}\cdot\dot{\mathbf{q}} + \frac{\partial}{\partial\mathbf{p}}\cdot\dot{\mathbf{p}} = \frac{\partial}{\partial\mathbf{q}}\cdot\Big(\frac{\partial H}{\partial\mathbf{p}}\Big) + \frac{\partial}{\partial\mathbf{p}}\cdot\Big(-\frac{\partial H}{\partial\mathbf{q}}\Big) = 0$$

[‖] The collisional Vlasov equation is often referred to as *Boltzmann equation*.

7.3 Properties of the Phase Space Evolution of f

1. Incompressible $\nabla_{\mathbf{x}} \cdot \mathbf{v} = 0$,

2. f conserved along 'characteristics' or 'particle orbits',

$$\frac{\mathrm{d}f}{\mathrm{d}t} = \frac{\partial f}{\partial t} + \frac{\partial f}{\partial \mathbf{x}} \cdot \frac{\mathrm{d}\mathbf{x}}{\mathrm{d}t} + \frac{\partial f}{\partial \mathbf{v}} \cdot \frac{\mathrm{d}\mathbf{v}}{\mathrm{d}t} = 0 \tag{7.19}$$

3. If C_j are constants of motion ($dC_j/dt = 0$), then $f \equiv f(C_1, C_2, \ldots, C_N)$ is a solution of the Vlasov equation as

$$\frac{\mathrm{d}f}{\mathrm{d}t} = \frac{\partial f}{\partial C_1}\frac{\mathrm{d}C_1}{\mathrm{d}t} + \frac{\partial f}{\partial C_2}\frac{\mathrm{d}C_2}{\mathrm{d}t} + \ldots + \frac{\partial f}{\partial C_N}\frac{\mathrm{d}C_N}{\mathrm{d}t} = 0 \tag{7.20}$$

   Note that in the full system with self–consistent fields it is virtually impossible to find the constants of motion. However, it is possible to find them in the unperturbed equilibrium (no self–consistent fields).

   Example 1: no external fields, plasma in equilibrium:

$$\mathbf{v} \cdot \frac{\partial f}{\partial \mathbf{x}} = 0. \tag{7.21}$$

   $\mathbf{v}$ is a constant of motion and *any* $f \equiv f(\mathbf{v})$ is a solution of Vlasov equation.

   Example 2: $\mathbf{B} = \mathbf{B}_0 = B_0\mathbf{e}_z$, stationary equilibrium:

$$\mathbf{v} \cdot \frac{\partial f}{\partial \mathbf{x}} + \frac{q}{m}(\mathbf{v} \times \mathbf{B}_0) \cdot \frac{\partial f}{\partial \mathbf{v}} = 0. \tag{7.22}$$

   v_z, v^2, $x + v_y/\Omega$, $y - v_x/\Omega$ are constants of motion and any

$$f \equiv f(v_z, v^2, x + \frac{v_y}{\Omega}, y - \frac{v_x}{\Omega})$$

   is a solution.

4. Total energy and momentum in particles and fields are conserved (details follow in the lecture of next week),

5. Entropy is conserved (cf. exercise 1 of problemset 8),

6. - Vlasov (no collisions): evolution is time–reversible
   - Boltzmann (collisions): evolution is irreversible, f tends to a Maxwellian

7.4 Conserved quantities

In a *collisionless* plasma, i.e. a plasma in which the interaction within the same microscopic phase space volume $\mathrm{d}^3x\mathrm{d}^3v$ can be neglected with respect to those outside the volume $\left(|\mathbf{F}_j^{\mathrm{int}}| \ll |\mathbf{F}_j^{\mathrm{ext}}|\right)$, from the Liouville theorem one finds the Vlasov equation eq.(7.13), describing the evolution of $f_\alpha(\mathbf{x}, \mathbf{v}, t)$ for the species α:

$$\frac{\partial f_\alpha}{\partial t} + \mathbf{v} \cdot \frac{\partial f_\alpha}{\partial \mathbf{x}} + \mathbf{a} \cdot \frac{\partial f_\alpha}{\partial \mathbf{v}} = 0$$

where $\mathbf{a} = \frac{q_\alpha}{m_\alpha}(\mathbf{E} + \mathbf{v} \times \mathbf{B})$, or the equivalent form:

$$\frac{\partial f_\alpha}{\partial t} + \frac{\partial}{\partial \mathbf{x}} \cdot (\mathbf{v} f_\alpha) + \frac{\partial}{\partial \mathbf{v}} \cdot (\mathbf{a} f_\alpha) = 0$$

The Vlasov equation conserves:

- Total energy (see below):

$$E_{\mathrm{tot}} = E_{\mathrm{particles}} + E_{\mathrm{fields}} = \sum_\alpha \frac{m_\alpha}{2} \int v^2 f_\alpha \, \mathrm{d}^3x \, \mathrm{d}^3v + \frac{1}{2} \int \left(\varepsilon_0 E^2 + \frac{B^2}{\mu_0} \right) \mathrm{d}^3x \quad (7.23)$$

- Total momentum:

$$\mathbf{P}_{\mathrm{tot}} = \mathbf{P}_{\mathrm{particles}} + \mathbf{P}_{\mathrm{fields}} = \sum_\alpha m_\alpha \int \mathbf{v} \, f_\alpha \, \mathrm{d}^3x \, \mathrm{d}^3v + \varepsilon_0 \int (\mathbf{E} \times \mathbf{B}) \, \mathrm{d}^3x \quad (7.24)$$

- Entropy(*) (see exercise 1 of problemset 8):

$$\frac{\mathrm{d}S}{\mathrm{d}t} = 0, \qquad S = -\iint f \ln f \, \mathrm{d}^3x \, \mathrm{d}^3v \quad (7.25)$$

  Meaning that the evolution is reversible. Of course, if we introduce collisions, $f \to f_{\mathrm{Maxwell}}$ and we loose reversibility.

7.4.1 Conservation of energy

This part has not been treated in the lecture but in exercise 1 of problemset 9.

There are two contributions to the total energy: one – E^p – from the particles and the other – E^f – from the fields:

$$E^p(t) = \sum_\alpha \int \mathrm{d}^3x \int \mathrm{d}^3v \, \frac{1}{2} m_\alpha v^2 f_\alpha(\mathbf{x}, \mathbf{v}, t) \quad (7.26)$$

$$E^f(t) = \int \mathrm{d}^3x \left(\frac{1}{2} \varepsilon_0 E^2 + \frac{1}{2\mu_0} B^2 \right) \quad (7.27)$$

For the particles:

$$\begin{aligned} \frac{\mathrm{d}E^p}{\mathrm{d}t} &= \sum_\alpha \int \mathrm{d}^3x \int \mathrm{d}^3v \, \frac{1}{2} m_\alpha v^2 \frac{\partial f_\alpha}{\partial t} \\ &= -\sum_\alpha \int \mathrm{d}^3x \int \mathrm{d}^3v \, \frac{1}{2} m_\alpha v^2 \left[\frac{\partial}{\partial \mathbf{x}} \cdot (\mathbf{v} f_\alpha) + \frac{\partial}{\partial \mathbf{v}} \cdot (\mathbf{a} f_\alpha) \right] \quad (7.28) \\ &= -\sum_\alpha \int \mathrm{d}^3v \, \frac{1}{2} m_\alpha v^2 \underbrace{\int \mathrm{d}^3x \, \frac{\partial}{\partial \mathbf{x}} \cdot (\mathbf{v} f_\alpha)}_{(A)} - \sum_\alpha \int \mathrm{d}^3x \int \mathrm{d}^3v \, \frac{1}{2} m_\alpha \underbrace{v^2 \frac{\partial}{\partial \mathbf{v}} \cdot (\mathbf{a} f_\alpha)}_{(B)} \end{aligned}$$

(*) As usual, we have put $k_B = 1$ and f is normalised first.

further, using the Gauss theorem, the term (A) in eq.(7.29) becomes

$$\int_V \mathrm{d}^3x \, \frac{\partial}{\partial \mathbf{x}} \cdot (\mathbf{v} f_\alpha) = \int_S \mathbf{v} f \cdot \mathrm{d}\boldsymbol{\sigma} = 0$$

and this integral is zero because f rapidly tends to zero when $|\mathbf{v}| \to \infty$.

$$\frac{\partial}{\partial \mathbf{v}} \cdot (v^2 \mathbf{a} f_\alpha) = v^2 \frac{\partial}{\partial \mathbf{v}} \cdot (\mathbf{a} f_\alpha) + \mathbf{a} f_\alpha \cdot \frac{\partial}{\partial \mathbf{v}} \left(v^2\right) = v^2 \frac{\partial}{\partial \mathbf{v}} \cdot (\mathbf{a} f_\alpha) + \mathbf{a} f_\alpha \cdot 2\mathbf{v} \tag{7.29}$$

where we have used

$$\frac{\partial}{\partial \mathbf{v}} \left(v^2\right) = \begin{pmatrix} \dfrac{\partial}{\partial v_x} \\ \dfrac{\partial}{\partial v_y} \\ \dfrac{\partial}{\partial v_z} \end{pmatrix} \begin{pmatrix} v_x^2 & v_y^2 & v_z^2 \end{pmatrix} = \begin{pmatrix} 2v_x \\ 2v_y \\ 2v_z \end{pmatrix} = 2\mathbf{v} \tag{7.30}$$

Using these equations to rewrite the term (B) in eq.(7.29), we get

$$\begin{aligned} \frac{\mathrm{d}E^p}{\mathrm{d}t} &= -\sum_\alpha \int \mathrm{d}^3x \int \mathrm{d}^3v \left[\frac{1}{2} m_\alpha \underbrace{\frac{\partial}{\partial \mathbf{v}} \cdot (v^2 \mathbf{a} f_\alpha)}_{=0 \text{ from Gauss theorem}} - q_\alpha (\mathbf{E} + \mathbf{v} \times \mathbf{B}) f_\alpha \cdot \mathbf{v} \right] = \\ &= +\sum_\alpha \int \mathrm{d}^3x \int \mathrm{d}^3v \, f_\alpha q_\alpha \, \mathbf{v} \cdot \mathbf{E} = \int \mathrm{d}^3x \underbrace{\int \mathrm{d}^3v \sum_\alpha q_\alpha f_\alpha \mathbf{v}}_{\mathbf{j}} \cdot \mathbf{E} = \int \mathrm{d}^3x \, \mathbf{j} \cdot \mathbf{E} \end{aligned}$$

For the fields, eq.(7.27):

$$\frac{\mathrm{d}E^f}{\mathrm{d}t} = \varepsilon_0 \int \mathrm{d}^3x \, \mathbf{E} \cdot \frac{\partial \mathbf{E}}{\partial t} + \frac{1}{\mu_0} \int \mathrm{d}^3x \, \mathbf{B} \cdot \frac{\partial \mathbf{B}}{\partial t}$$

$$\begin{cases} \dfrac{\partial \mathbf{E}}{\partial t} = c^2 \nabla \times \mathbf{B} - c^2 \mu_0 \mathbf{j} = \dfrac{1}{\varepsilon_0 \mu_0} \displaystyle\int \mathrm{d}^3x \, \mathbf{B} \cdot \frac{\partial \mathbf{B}}{\partial t} \\ \dfrac{\partial \mathbf{B}}{\partial t} = -\nabla \times \mathbf{E} \end{cases} \tag{7.31}$$

$$\begin{aligned} \frac{\mathrm{d}E^f}{\mathrm{d}t} = \; & \varepsilon_0 \textstyle\int \mathrm{d}^3x \, \mathbf{E} \cdot \left[\frac{1}{\varepsilon_0 \mu_0} \nabla \times \mathbf{B} - \frac{1}{\varepsilon_0} \mathbf{j} \right] + \frac{1}{\mu_0} \int \mathrm{d}^3x \, \mathbf{B} \cdot (-\nabla \times \mathbf{E}) = \\ & - \textstyle\int \mathrm{d}^3x \, \mathbf{j} \cdot \mathbf{E} + \frac{1}{\mu_0} \int \mathrm{d}^3x \, \mathbf{E} \cdot (\nabla \times \mathbf{B}) - \frac{1}{\mu_0} \int \mathrm{d}^3x \, \mathbf{B} \cdot (\nabla \times \mathbf{E}) \end{aligned}$$

Using the vector identity

$$\nabla \cdot (\mathbf{E} \times \mathbf{B}) = \mathbf{B} \cdot (\nabla \times \mathbf{E}) - \mathbf{E} \cdot (\nabla \times \mathbf{B})$$

we can write:

$$\int \mathrm{d}^3x \left[\mathbf{E} \cdot (\nabla \times \mathbf{B}) - \mathbf{B} \cdot (\nabla \times \mathbf{E}) \right] = -\int \mathrm{d}^3x \, \nabla \cdot (\mathbf{E} \times \mathbf{B}) = \int_S (\mathbf{E} \times \mathbf{B}) \cdot \mathrm{d}\boldsymbol{\sigma} = 0 \tag{7.32}$$

as for $\mathbf{x} \to \infty$ the fields must go to zero, to keep energy finite.

Finally we have:

$$\begin{aligned} \frac{\mathrm{d}E^{\mathrm{tot}}}{\mathrm{d}t} &= \frac{\mathrm{d}E^p}{\mathrm{d}t} + \frac{\mathrm{d}E^f}{\mathrm{d}t} = 0 && \text{total energy is conserved} \\ \frac{\mathrm{d}E^f}{\mathrm{d}t} &= -\frac{\mathrm{d}E^p}{\mathrm{d}t} = -\int \mathrm{d}^3x \, \mathbf{j} \cdot \mathbf{E} && \text{the work done by the electric field } \mathbf{E} \end{aligned}$$

7.5 Moments of the distribution function

From the distribution function we define

- the density in the configuration space:

$$n_\alpha(\mathbf{x},t) = \int f_\alpha(\mathbf{x},\mathbf{v},t)\,\mathrm{d}^3v \tag{7.33}$$

- the total number of particles (of species α):

$$N_{\alpha,\mathrm{tot}}(t) = \iint f_\alpha(\mathbf{x},\mathbf{v},t)\,\mathrm{d}^3x\,\mathrm{d}^3v = \int n_\alpha(\mathbf{x},t)\,\mathrm{d}^3x$$

- the average "fluid" velocity:

$$\Big\langle \mathbf{v}_\alpha \Big\rangle(\mathbf{x},t) = \mathbf{u}_\alpha(\mathbf{x},t) = \frac{\displaystyle\int f_\alpha(\mathbf{x},\mathbf{v},t)\,\mathbf{v}\,\mathrm{d}^3v}{\displaystyle\int f_\alpha(\mathbf{x},\mathbf{v},t)\,\mathrm{d}^3v} \tag{7.34}$$

These are just examples of "moments" of f. Let's see the general case:

If $g(\mathbf{v})$ is a polynomial function of the components of $\mathbf{v}$, its **average** value for the species α described by the distribution function f_α is

$$\Big\langle g_\alpha(\mathbf{v}) \Big\rangle = \frac{\displaystyle\int f_\alpha(\mathbf{x},\mathbf{v},t)\,g(\mathbf{v})\,\mathrm{d}^3v}{\displaystyle\int f_\alpha(\mathbf{x},\mathbf{v},t)\,\mathrm{d}^3v} = \frac{1}{n_\alpha(\mathbf{x},t)}\int f_\alpha(\mathbf{x},\mathbf{v},t)\,g(\mathbf{v})\,\mathrm{d}^3v$$

The integral(†)

$$\text{const.}\ \int f_\alpha(\mathbf{x},\mathbf{v},t)\,g(\mathbf{v})\,\mathrm{d}^3v \tag{7.35}$$

is called a moment of f_α, of order N, where N is the highest order of the polynomials defining the function $g(\mathbf{v})$.

The moments of f_α of different order represent the physical quantities averaged over $\mathbf{v}$, i.e. characteristic of the whole species α. They correspond to quantities describing the plasma as a fluid (the distinction into velocity classes has been lost by integrating).

(†)

$$\frac{\int f_\alpha(\mathbf{x},\mathbf{v},t)\,g(\mathbf{v})\,\mathrm{d}^3v}{\int f_\alpha(\mathbf{x},\mathbf{v},t)\,\mathrm{d}^3v}$$

if the quantity is normalised.

Important moments of f (with physical interpretation) are:

- 0^{th} order moment of f_α: $g(\mathbf{v}) = 1$, *i.e.* the density:

$$n_\alpha(\mathbf{x}, t) = \int f_\alpha(\mathbf{x}, \mathbf{v}, t)\, \mathrm{d}^3 v$$

- 1^{st} order moment of f_α: $g(\mathbf{v}) = \mathbf{v}$, *i.e.* the average fluid velocity of the species α:

$$\mathbf{u}_\alpha(\mathbf{x}, t) = \frac{\int f_\alpha\, \mathbf{v}\, \mathrm{d}^3 v}{\int f_\alpha\, \mathrm{d}^3 v} = \frac{1}{n_\alpha(\mathbf{x}, t)} \int f_\alpha\, \mathbf{v}\ \mathrm{d}^3 v$$

- 2^{nd} order moment of f_α, for example the energy density:

$$\rho_{E,\alpha} \quad = \quad \frac{1}{2} m_\alpha \int v^2 f_\alpha(\mathbf{x}, \mathbf{v}, t)\, \mathrm{d}^3 v = \underbrace{\frac{1}{2} m_\alpha n_\alpha |\mathbf{u}_\alpha|^2}_{\substack{\text{macroscopic} \\ \text{kinetic energy}}} + \underbrace{\frac{1}{2} m_\alpha \int (\mathbf{v} - \mathbf{u}_\alpha)^2 f_\alpha(\mathbf{x}, \mathbf{v}, t)\, \mathrm{d}^3 v}_{\substack{\text{microscopic} \\ \text{thermal energy}}}$$

  where $v^2 = (\mathbf{v} - \mathbf{u} + \mathbf{u}) \cdot (\mathbf{v} - \mathbf{u} + \mathbf{u})$.

  Using the equipartition principle[(‡)], we can define the temperature (each particle has 3 degrees of freedom) as

$$\frac{1}{2}\, m_\alpha \int (\mathbf{v} - \mathbf{u}_\alpha)^2 f_\alpha(\mathbf{x}, \mathbf{v}, t)\, \mathrm{d}^3 v \equiv \frac{3}{2}\, n_\alpha T_\alpha \tag{7.36}$$

  In general, other moments of order two can be defined, for ex. tensor terms like

$$m_\alpha \int \mathbf{v}\mathbf{v} f_\alpha(\mathbf{x}, \mathbf{v}, t)\, \mathrm{d}^3 v \tag{7.37}$$

  of which the microscopic part is the **pressure tensor**

$$\underline{\mathbf{P}}_\alpha(\mathbf{x}, t) = m_\alpha \int f_\alpha(\mathbf{x}, \mathbf{v}, t)(\mathbf{v} - \mathbf{u}_\alpha)(\mathbf{v} - \mathbf{u}_\alpha)\, \mathrm{d}^3 v$$

  i.e.

$$\left(P_{ij}\right)_\alpha(\mathbf{x}, t) = m_\alpha \int f_\alpha(\mathbf{x}, \mathbf{v}, t) \Big[(\mathbf{v} - \mathbf{u}_\alpha)_i (\mathbf{v} - \mathbf{u}_\alpha)_j \Big]\, \mathrm{d}^3 v$$

  If the distribution function f_α is symmetric around $\mathbf{u}_\alpha$[(§)], then the off-diagonal elements are zero, the pressure becomes a **scalar** and there is a clear correspondence between the **whole**

(‡) At equilibrium, each degree of freedom gets $\frac{1}{2} k_B T_\alpha$ of thermal energy. Note that in our notation $k_B = 1$.

(§) A simple and common example of this is $\begin{cases} f_\alpha \text{ isotropic} \\ \mathbf{u}_\alpha = 0 \end{cases}$

pressure tensor and the temperature $\underline{\mathbf{P}}_\alpha \leftrightarrow T_\alpha$[(¶)]. Proof for the isotropic case (and $\mathbf{u}_\alpha = 0$ for simplicity):

$$(P_{xy})_\alpha = \int \mathrm{d}^3v\, m_\alpha v_x v_y\, f_\alpha(\mathbf{v}) = 0 \tag{7.38}$$

as v_x and v_y are odd functions and we find the same result for all cross-terms:

$$(P_{xy})_\alpha = (P_{yx})_\alpha = (P_{xz})_\alpha = (P_{zx})_\alpha = (P_{yz})_\alpha = (P_{zy})_\alpha = 0 \tag{7.39}$$

We remain with the diagonal terms

$$\underbrace{(P_{xx})_\alpha = (P_{yy})_\alpha = (P_{zz})_\alpha}_{\text{identical due to symmetry}} = \int \mathrm{d}^3v\, m_\alpha v_x^2 f_\alpha(\mathbf{v}) =$$
$$= \frac{m_\alpha}{3} \int \mathrm{d}^3\, v f_\alpha(\mathbf{v}) \left(v_x^2 + v_y^2 + v_z^2\right) = \frac{m_\alpha}{3} \int \mathrm{d}^3\, v f_\alpha(\mathbf{v}) v^2 =$$
$$= \frac{2}{3}\left[\frac{1}{2} m_\alpha \int \mathrm{d}^3\, v f_\alpha(\mathbf{v}) v^2\right] = \frac{2}{3}\left[\frac{3}{2} n_\alpha T_\alpha\right] = n_\alpha T_\alpha = p_\alpha$$

In tensor notation[(‖)]:

$$\underline{\mathbf{P}}_\alpha(\mathbf{x}, t) = m_\alpha \int f_\alpha(\mathbf{x}, \mathbf{v}, t)\, \mathbf{v}\mathbf{v}\, \mathrm{d}^3v = m_\alpha \int f_\alpha(\mathbf{x}, \mathbf{v}, t) \frac{v^2}{3} \mathbb{1}\, \mathrm{d}^3v =$$
$$\left(\frac{1}{3}\, m_\alpha \int f_\alpha(\mathbf{x}, \mathbf{v}, t) v^2\, \mathrm{d}^3v\right) \mathbb{1} = n_\alpha T_\alpha \mathbb{1} = p_\alpha \mathbb{1} \quad \blacksquare \tag{7.40}$$

- 3rd order moment: for ex. $g(\mathbf{v}) = \frac{1}{2}\, m_\alpha v^2 \mathbf{v}$, from which we obtain the heat flux

$$\underline{\mathbf{S}}_\alpha \equiv \frac{1}{2} m_\alpha \int v^2 \mathbf{v} f_\alpha(\mathbf{x}, \mathbf{v}, t)\, \mathrm{d}^3v$$

This also includes both macroscopic (ordered) and microscopic (disordered, thermal) contributions.

7.6 From the Vlasov equation to the fluid equations

If we multiply the Vlasov equation by $g(\mathbf{v})$ and integrate over velocity, from the definition of the moments we can derive the fluid equations.

$$\int \mathrm{d}^3v\, g(\mathbf{v}) \left[\frac{\partial f}{\partial t} + \mathbf{v} \cdot \frac{\partial f}{\partial \mathbf{x}} + \frac{q}{m}(\mathbf{E} + \mathbf{v} \times \mathbf{B}) \cdot \frac{\partial f}{\partial \mathbf{v}}\right] = 0$$

(¶) If f_α is not symmetric around $\mathbf{u}_\alpha$, such correspondence exists only for the diagonal terms.

(‖)
$$\mathbf{v}\mathbf{v} = \begin{pmatrix} v_x^2 & v_x v_y & \dots \\ \dots & v_y^2 & \dots \\ \dots & \dots & v_z^2 \end{pmatrix} = \frac{1}{3} \begin{pmatrix} v^2 & \dots & \dots \\ \dots & v^2 & \dots \\ \dots & \dots & v^2 \end{pmatrix}$$

- 0^{th} **order moment:** $g(\mathbf{v}) = 1$

$$\frac{\partial}{\partial t}\underbrace{\int \mathrm{d}^3v\, f}_{n} + \frac{\partial}{\partial \mathbf{x}}\cdot\underbrace{\int \mathrm{d}^3v\, \mathbf{v} f}_{n\mathbf{u}} + \underbrace{\int \mathrm{d}^3v\, \frac{\partial}{\partial \mathbf{v}}\cdot\left[\frac{q}{m}\left(\mathbf{E}+\mathbf{v}\times\mathbf{B}\right) f\right]}_{\int_S \left[\frac{q}{m}(\mathbf{E}+\mathbf{v}\times\mathbf{B})f\right]\cdot \mathrm{d}\boldsymbol{\sigma} = 0^{(**)}}$$

So, we find the **continuity equation**:

$$\frac{\partial n}{\partial t} + \frac{\partial}{\partial \mathbf{x}}\cdot(n\mathbf{u}) = 0 \tag{7.41}$$

- 1^{st} **order moment:** $g(\mathbf{v}) = m\mathbf{v}$

$$\int \mathrm{d}^3v\, m\mathbf{v}\frac{\partial f}{\partial t} + \int \mathrm{d}^3v\, m\mathbf{v}\left(\mathbf{v}\cdot\frac{\partial f}{\partial \mathbf{x}}\right) + \int \mathrm{d}^3v\, m\mathbf{v}\left(\frac{\mathbf{F}}{m}\cdot\frac{\partial f}{\partial \mathbf{v}}\right) = 0$$

where $\mathbf{F} = q(\mathbf{E}+\mathbf{v}\times\mathbf{B})$

$$\Rightarrow \quad \underbrace{m\frac{\partial}{\partial t}(n\mathbf{u})}_{(1)} + \underbrace{\frac{\partial}{\partial \mathbf{x}}\cdot m\int d\mathbf{v}\,\mathbf{v}\mathbf{v} f}_{(2)} + \underbrace{\int d\mathbf{v}\,\mathbf{v}\cdot\frac{\partial(\mathbf{F}f)}{\partial \mathbf{v}}}_{(3)} = 0$$

Let's evaluate the three contributions separately:

$$\begin{aligned}
(1) &= m\mathbf{u}\frac{\partial n}{\partial t} + mn\frac{\partial \mathbf{u}}{\partial t} \overset{\text{eq.(7.41)}}{=} mn\frac{\partial \mathbf{u}}{\partial t} + m\mathbf{u}\left(-\frac{\partial}{\partial \mathbf{x}}\cdot(n\mathbf{u})\right)\\
(2) &= \frac{\partial}{\partial \mathbf{x}}\cdot m\int \mathrm{d}^3v\,(\mathbf{v}-\mathbf{u}+\mathbf{u})(\mathbf{v}-\mathbf{u}+\mathbf{u})f\\
&= \frac{\partial}{\partial \mathbf{x}}\cdot\int \mathrm{d}^3v\, m(\mathbf{v}-\mathbf{u})(\mathbf{v}-\mathbf{u})f + m\frac{\partial}{\partial \mathbf{x}}\cdot\underbrace{\int \mathrm{d}^3v\,(\mathbf{v}-\mathbf{u})\mathbf{u}f}_{=0 \text{ as } \int \mathbf{v}f\mathrm{d}^3v=\mathbf{u}}\\
&+ m\frac{\partial}{\partial \mathbf{x}}\cdot\underbrace{\int \mathrm{d}^3v\,\mathbf{u}(\mathbf{v}-\mathbf{u})f}_{=0 \text{ as } \int \mathbf{v}f\mathrm{d}^3v=\mathbf{u}} + m\frac{\partial}{\partial \mathbf{x}}\cdot\int \mathrm{d}^3\,v\,\mathbf{u}\mathbf{u}f\\
&= \frac{\partial}{\partial \mathbf{x}}\cdot\underline{\mathbf{P}} + m\frac{\partial}{\partial \mathbf{x}}\cdot\left[(n\mathbf{u})\mathbf{u}\right] = \frac{\partial}{\partial \mathbf{x}}\cdot\underline{\mathbf{P}} + mn\mathbf{u}\cdot\frac{\partial \mathbf{u}}{\partial \mathbf{x}} + m\mathbf{u}\frac{\partial}{\partial \mathbf{x}}\cdot(n\mathbf{u})\\
(3) &= \underbrace{\int \mathrm{d}^3v\,\frac{\partial}{\partial \mathbf{v}}\cdot(\mathbf{v}\mathbf{F}f)}_{=0 \text{ using Gauss theorem}} - \int \mathrm{d}^3v\,\mathbf{F}f\cdot\underbrace{\frac{\partial \mathbf{v}}{\partial \mathbf{v}}}_{\mathbb{1}}\\
&= -\int \mathrm{d}^3v\,\mathbf{F}f = -\mathbf{F}(\mathbf{u})n = -nq(\mathbf{E}+\mathbf{u}\times\mathbf{B})
\end{aligned}$$

Finally:

$$mn\frac{\partial \mathbf{u}}{\partial t} - m\mathbf{u}\frac{\partial}{\partial \mathbf{x}}\cdot(n\mathbf{u}) + \frac{\partial}{\partial \mathbf{x}}\cdot\underline{\mathbf{P}} + mn\mathbf{u}\cdot\frac{\partial \mathbf{u}}{\partial \mathbf{x}} + m\mathbf{u}\frac{\partial}{\partial \mathbf{x}}\cdot(n\mathbf{u}) = nq(\mathbf{E}+\mathbf{u}\times\mathbf{B}) \tag{7.42}$$

(**) The surface integral S is computed on the boundary of the phase space. Supposing that $f \to 0$ quickly when when $\mathbf{v}$ and $\mathbf{x} \to \infty$, the integral vanishes.

or

$$mn\left(\frac{\partial}{\partial t}+\mathbf{u}\cdot\nabla\right)\mathbf{u}=mn\frac{\mathrm{d}\mathbf{u}}{\mathrm{d}t}=-\nabla\cdot\underline{\mathbf{P}}+nq(\mathbf{E}+\mathbf{u}\times\mathbf{B}) \tag{7.43}$$

We have found the fluid equation of motion, without collisional dissipation.

We are now ready to look at plasma oscillations and waves in plasmas described by the Vlasov model (hot plasmas) and at the fundamental problem of wave-particle interaction.

7.7 Electrostatic Approximation ($\mathbf{B}_1 = 0$)

Electrostatic approximation (*electrostatic waves*): the magnetic field of the wave is 0. As the term $N^2(\frac{\mathbf{kk}}{k^2} - \mathbb{1}) \cdot \mathbf{E}$ in the wave equation derives from $\mathbf{k} \times (\mathbf{k} \times \mathbf{E})$, then from $\nabla \times (\nabla \times \mathbf{E})$, that is from $\nabla \times (-\frac{\partial \mathbf{B}}{\partial t})$, we see that

$$N^2 \left(\frac{\mathbf{kk}}{k^2} - \mathbb{1} \right) \cdot \mathbf{E} \simeq 0 \tag{7.44}$$

in the electrostatic (e.s.) approximation. The e.s. dispersion relation associated with the wave equation

$$\underline{\boldsymbol{\epsilon}} \cdot \mathbf{E} = 0 \qquad \text{is then} \qquad \det \underline{\boldsymbol{\epsilon}} = 0 \tag{7.45}$$

where $\underline{\boldsymbol{\epsilon}} = \mathbb{1} - \underline{\boldsymbol{\sigma}}/\mathrm{i}\omega\varepsilon_0$

Note:

- As a **B**–field is needed to support waves in vacuum, e.s. waves can *only* exist in the medium (in our case, in the plasma). For example we cannot excite e.s. waves with antennas unless they are immersed in the plasma.
- As

  $$\nabla \times \mathbf{E} = -\frac{\partial \mathbf{B}}{\partial t} \quad \Longleftrightarrow \quad \mathbf{k} \times \mathbf{E} = -\omega \mathbf{B} = 0 \quad \Longrightarrow \quad \mathbf{k} \parallel \mathbf{E} \tag{7.46}$$

  for e.s. waves.
- In many cases the dependence of $\underline{\boldsymbol{\epsilon}}$ on $\mathbf{k}$ is weak: as

  $$\left\{ N^2 \left[\frac{\mathbf{kk}}{k^2} - \mathbb{1} \right] + \underline{\boldsymbol{\epsilon}} \right\} \cdot \mathbf{E} = 0, \tag{7.47}$$

  for $k \to \infty$ (i.e. small wavelengths), $N \to \infty$, and the only way to satisfy the wave eq.(7.47) is to have the term $\left[\frac{\mathbf{kk}}{k^2} - \mathbb{1}\right] \cdot \mathbf{E} \simeq 0$. For $k \to \infty$, ω/k becomes small: e.s. waves are generally characterised by relatively small phase velocities (or large $N = kc/\omega$).
- The reason why we concentrate on e.s. waves in discussing waves in the kinetic model is because a wave with very large phase velocity (an "electromagnetic wave") will not interact strongly with particles as there will not be many with $v \sim \omega/k$, see figure 7.1a. Due to the weak wave–particle interaction we do not need a kinetic model of plasma/waves. The wave is so much faster than particles that the plasma can be considered as a fluid. However, if $\omega/k \to v_{\text{particles}}$, we expect a strong interaction (figure 7.1.b). To describe this situation we need the kinetic model, accounting for particles with different velocities.

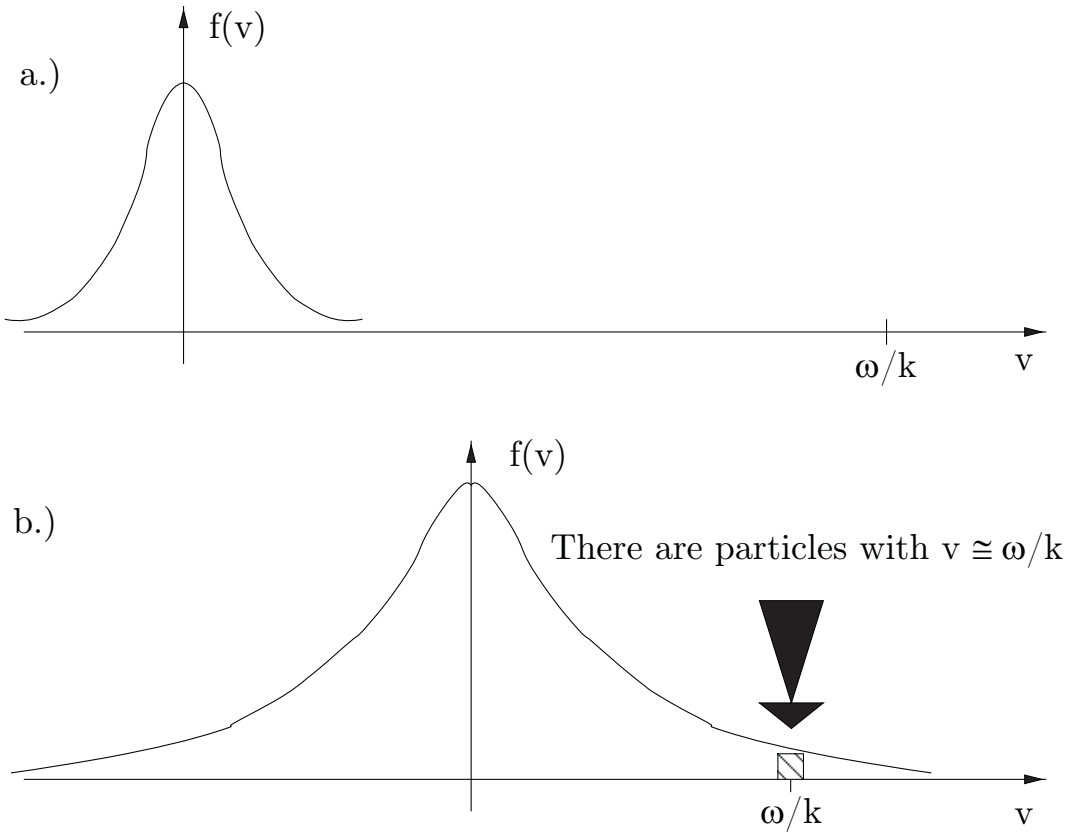

Figure 7.1: a.) Weak and b.) strong wave–particle interaction.

7.8 Vlasov–Maxwell Description of an Unmagnetised Plasma ($\mathbf{B}_0 = 0$)

The equations of the Vlasov–Maxwell system are

$$\nabla \cdot \mathbf{E} = \frac{\rho}{\varepsilon_0} + \frac{\rho_{\text{ext}}}{\varepsilon_0} \qquad \nabla \cdot \mathbf{B} = 0$$

$$\nabla \times \mathbf{E} = -\frac{\partial \mathbf{B}}{\partial t} \qquad \nabla \times \mathbf{B} = \mu_0 \mathbf{j} + \frac{1}{c^2}\frac{\partial \mathbf{E}}{\partial t}$$

but we only need Poisson's equation for e.s. waves and

$$\rho = \sum_\alpha q_\alpha \int f_\alpha \, \mathrm{d}^3 v \qquad \mathbf{j} = \sum_\alpha q_\alpha \int \mathbf{v} f_\alpha \, d^3 v$$

as well as

$$\begin{cases} \nabla \cdot \mathbf{E} = \dfrac{\rho}{\varepsilon_0} + \dfrac{\rho_{ext}}{\epsilon_0} \\ \dfrac{\partial f_\alpha}{\partial t} + \mathbf{v} \cdot \dfrac{\partial f_\alpha}{\partial \mathbf{x}} + \dfrac{q_\alpha}{m_\alpha}(\mathbf{E} + \mathbf{v} \times \mathbf{B}) \cdot \dfrac{\partial f_\alpha}{\partial \mathbf{v}} = 0 \end{cases}$$

To solve for the unknowns $\mathbf{E}$ (or ϕ) and f, we do the usual approach

1. Equilibrium: $\mathbf{E}_0 = 0$; $\mathbf{B}_0 = 0$; $f_{\alpha 0} \equiv f_{\alpha 0}(\mathbf{v})$; $\rho_{\text{ext},0} = 0$
2. Perturbation: $f_{\alpha 1}(\mathbf{x}, \mathbf{v}, t) = f_{\alpha 1}(\mathbf{v}) e^{\mathrm{i}(\mathbf{k}\cdot\mathbf{x} - \omega t)}$; $\mathbf{B}_1 = 0$ (e.s. waves)
3. Fourier: $\frac{\partial}{\partial t} \to -\mathrm{i}\omega$; $\frac{\partial}{\partial \mathbf{x}} \to \mathrm{i}\mathbf{k}$

Linearisation:

$$\begin{cases} \dfrac{\partial f_{\alpha 1}}{\partial t} + \mathbf{v} \cdot \dfrac{\partial f_{\alpha 1}}{\partial \mathbf{x}} + \dfrac{q_\alpha}{m_\alpha} \mathbf{E}_1 \cdot \dfrac{\partial f_{\alpha 0}}{\partial \mathbf{v}} = 0 \\ \nabla \cdot \mathbf{E}_1 = \dfrac{1}{\varepsilon_0} \displaystyle\sum_\alpha q_\alpha \int f_{\alpha 1} \, \mathrm{d}^3 v + \dfrac{\rho_{\text{ext}}}{\varepsilon_0} \end{cases} \tag{7.48}$$

and we do not need further equations.

Fourier:

$$\begin{cases} -\mathrm{i}(\omega - \mathbf{k} \cdot \mathbf{v}) f_{\alpha 1} + \dfrac{q_\alpha}{m_\alpha} \mathbf{E}_1 \cdot \dfrac{\partial f_{\alpha 0}}{\partial \mathbf{v}} = 0 \\ \mathrm{i}\mathbf{k} \cdot \mathbf{E}_1 = \dfrac{1}{\varepsilon_0} \displaystyle\sum_\alpha q_\alpha \int f_{\alpha 1} \, \mathrm{d}^3 v + \dfrac{\rho_{\text{ext}}}{\varepsilon_0} \end{cases} \tag{7.49}$$

Use e.s. potential: $\mathbf{E}_1 = -\nabla \phi$, i.e. in Fourier space $\mathbf{E}_1 = -\mathrm{i}\mathbf{k}\phi$ in the first equation of eq.(7.49), solve for

$$f_{\alpha 1} = -\phi \frac{q_\alpha}{m_\alpha} \frac{\mathbf{k} \cdot \frac{\partial f_{\alpha 0}}{\partial \mathbf{v}}}{\omega - \mathbf{k} \cdot \mathbf{v}} \tag{7.50}$$

and inject it in the second equation of eq.(7.49):

$$k^2 \phi = -\frac{1}{\varepsilon_0} \sum_\alpha \frac{q_\alpha^2 \phi}{m_\alpha} \int \frac{\mathbf{k} \cdot \frac{\partial f_{\alpha 0}}{\partial \mathbf{v}}}{\omega - \mathbf{k} \cdot \mathbf{v}} \, \mathrm{d}^3 v + \frac{\rho_{\text{ext}}}{\varepsilon_0} \tag{7.51}$$

Note that there is a resonance for $\omega = \mathbf{k} \cdot \mathbf{v}$, i.e. $v_{\text{part}} = \omega / k = v_{\text{ph}}$. Rewrite eq.(7.51) as

$$\underbrace{1 + \sum_\alpha \frac{q_\alpha^2}{\varepsilon_0 m_\alpha} \frac{1}{k^2} \int \frac{\mathbf{k} \cdot \frac{\partial f_{\alpha 0}}{\partial \mathbf{v}}}{\omega - \mathbf{k} \cdot \mathbf{v}} \, \mathrm{d}^3 v}_{=: \, D(\omega, \mathbf{k})} = \frac{\rho_{\text{ext}}}{\varepsilon_0 \phi k^2} \tag{7.52}$$

where $D(\omega, \mathbf{k})$ is the *dispersion function*. Note that

- If $\rho_{\text{ext}} = 0$ we have the dispersion relation for e.s. waves:

$$D(\omega, \mathbf{k}) = \det \underline{\boldsymbol{\epsilon}}(\omega, \mathbf{k}) = 0 \tag{7.53}$$

- If $\rho_{\text{ext}} \neq 0$:

$$\phi(\omega, \mathbf{k}) = \frac{1}{\varepsilon_0 k^2} \frac{\rho_{\text{ext}}(\omega, \mathbf{k})}{D(\omega, \mathbf{k})} \tag{7.54}$$

  By perturbing the plasma with $\rho_{\text{ext}}(\omega, \mathbf{k})$, we can have a large response only if we approach the zeros of $D(\omega, \mathbf{k})$, i.e. the *roots* of the dispersion relation. These are the plasma intrinsic modes of oscillation.

From such a dispersion relation we hope to calculate *which waves can exist* and *which exchange energy with particles*.

Choosing a geometry with $\mathbf{k} = k\mathbf{e}_z$ (no loss of generality) and defining $u \equiv v_z$ we get for the case $\rho_{\text{ext}} = 0$

$$0 = \epsilon = 1 + \sum_\alpha \frac{q_\alpha^2}{m_\alpha \varepsilon_0 k^2} \int \frac{k \frac{\partial f_{\alpha 0}}{\partial u}}{\omega - ku} \mathrm{d}v_x \, \mathrm{d}v_y \, \mathrm{d}u \tag{7.55}$$

or defining $F_{\alpha 0} \equiv \iint f_{\alpha 0} \, \mathrm{d}v_x \, \mathrm{d}v_y$,

$$1 + \sum_\alpha \frac{q_\alpha^2}{m_\alpha \varepsilon_0 k} \underbrace{\int_{\mathbb{R}} \frac{\frac{\mathrm{d}F_{\alpha 0}}{\mathrm{d}u}}{\omega - ku} \mathrm{d}u}_{\text{Landau integral}} = 0 \tag{7.56}$$

Landau observed that this is an ill–posed problem. $f_{\alpha 1}$ does not evolve as a plane wave: we cannot take $f_{\alpha 1} \propto \exp\{\mathrm{i}(\mathbf{k} \cdot \mathbf{x} - \omega t)\}$. The problem is that the Vlasov equation describes the *time* evolution of $f_{\alpha 1}$, therefore needs initial conditions.

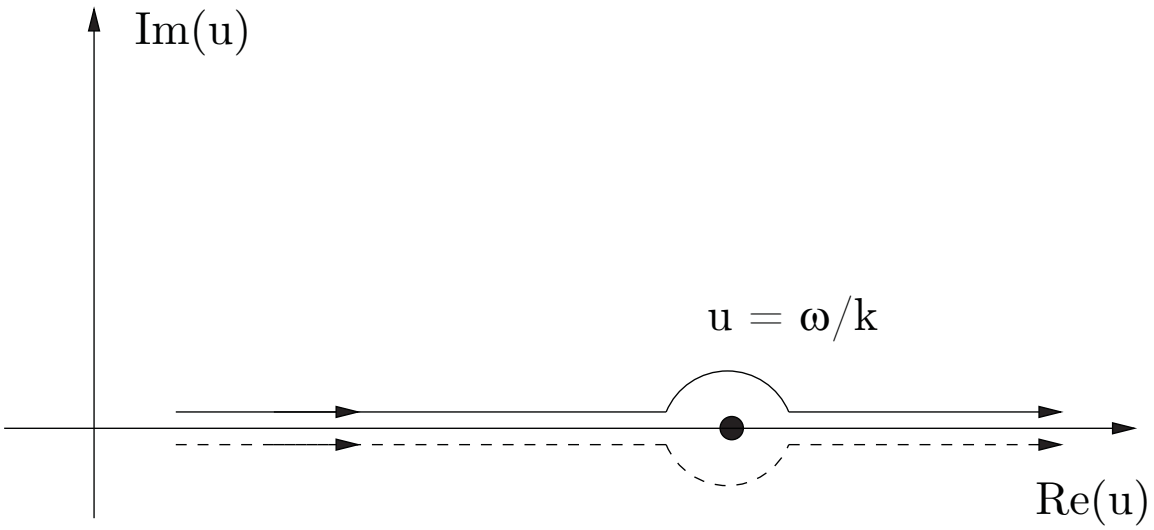

Figure 7.2: Possible integration paths around the pole.

Mathematically, the difficulty arises from the integral, since there is a pole at $u = \omega/k$. Take $\omega \in \mathbb{C}$ in general. In the complex u–plane, the path for the integral is the real axis, but how do we go around the pole?(††) The result depends on which side of the pole our path of integration passes (figure 7.2): the physics basis of the problem must be reviewed as it does not tell us how to treat the singularity.

(††) Improper integral: $\exists$ only as principal value

$$\text{P.V.} \int g(u) \, \mathrm{d}u \equiv \lim_{\varepsilon \to 0} \left\{ \int_{-\infty}^{\frac{\omega}{k} - \varepsilon} + \int_{\frac{\omega}{k} + \varepsilon}^{\infty} \right\} g(u) \, \mathrm{d}u. \tag{7.57}$$

Chapter 8 Wave–particle interactions

In the last lecture, we have reviewed the Vlasov equation

$$\frac{\partial f}{\partial t} + \mathbf{v} \cdot \frac{\partial f}{\partial \mathbf{x}} + \frac{q}{m}(\mathbf{E} + \mathbf{v} \times \mathbf{B}) \cdot \frac{\partial f}{\partial \mathbf{v}} = 0 \tag{8.1}$$

and its properties

- f is conserved along particle orbits
- All functions of constants of motion satisfy Vlasov
- Total energy, momentum and entropy are conserved

Solving the Vlasov–Maxwell system for electrostatic waves(*) we found after linearisation and Fourier transformation the *dispersion relation*

$$D(\omega, k) = 1 + \sum_{\alpha} \frac{\omega_{\mathrm{p}\alpha}^2}{n_\alpha k} \int_{\mathbb{R}} \frac{\frac{\mathrm{d}F_{0\alpha}}{\mathrm{d}u}}{\omega - ku} \mathrm{d}u = 0 \tag{8.2}$$

We have seen that in the presence of particles with $u \simeq \omega/k$, i.e. of particles that resonate with the waves, there are problems in the evaluation of the integral. Today we'll see what we can calculate by 'avoiding' the resonance:

- Streaming instability
- Dispersion relation for electron plasma waves (in order to check for consistency with the fluid model)

8.1 Streaming Instability

To enhance the energy in particle collisions (to increase the probability of producing fusion reactions) one can think of generating two *beams* colliding head–on with each other. It was immediately observed in experiments trying to produce such a situation that the two beams (or streaming plasmas) were lost immediately, due to a strong instability. The Vlasov model can be used to calculate this instability.

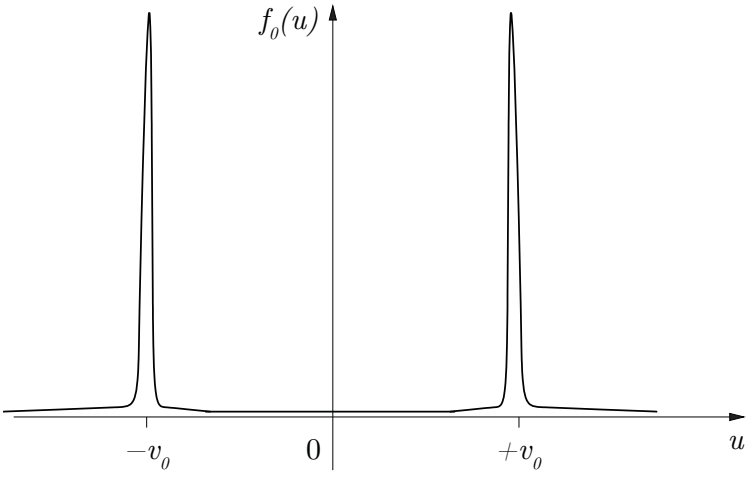

Figure 8.1: Velocity distribution for two electron streams with $T = 0$.

Consider the simplest possible one dimensional model, two beams of electrons with $T = 0$, shown in figure 8.1 and described by

$$f_0(u) = \frac{1}{2} n_e \Big[\delta(u - v_0) + \delta(u + v_0)\Big] \tag{8.3}$$

(*) In the electrostatic case the Maxwell equations reduce to the Poisson equation.

We can calculate the dispersion relation for waves in such a plasma using eq.(8.2) by integrating by parts:(†)

$$\begin{aligned}\int_{-\infty}^{\infty} \frac{\mathrm{d}f_0}{\mathrm{d}u}\frac{\mathrm{d}u}{\omega - ku} &= \frac{f_0}{\omega - ku}\Big|_{-\infty}^{+\infty} - \int_{-\infty}^{\infty} \mathrm{d}u \frac{k f_0}{(\omega - ku)^2} \\ &= -\frac{1}{2} n_e k \left\{ \frac{1}{(\omega - kv_0)^2} + \frac{1}{(\omega + kv_0)^2} \right\} \end{aligned} \tag{8.4}$$

we find with eq.(8.2)

$$D(\omega, k) = 1 - \frac{\omega_{pe}^2}{2} \left\{ \frac{1}{(\omega - kv_0)^2} + \frac{1}{(\omega + kv_0)^2} \right\} = 0 \tag{8.5}$$

Eq.(8.5) is a polynomial equation of degree 4 and thus has always 4 roots.(‡) There are two possibilities (see figure 8.2):

Case A

4 roots $\in \mathbb{R} \Rightarrow$ *no problem* $\Rightarrow$ *no instability, just oscillations.*

Case B

2 roots $\in \mathbb{R}$, 2 roots $\in \mathbb{C}$. As $D(\omega, k)$ is a polynomial with real coefficients, the two complex roots are complex conjugates, i.e. $\omega_3 = \omega_4^*$. Thus there is always one solution with $\Im\,\omega > 0$ $\Rightarrow$ *Instability.*

The condition to have case B (instability) is

$$D(\omega = 0, k) = 1 - \frac{\omega_{pe}^2}{k^2 v_0^2} < 0$$

or

$$k^2 v_0^2 < \omega_{pe}^2 \tag{8.6}$$

For sufficiently small k, i.e. sufficiently long wavelengths, the instability always occurs. The energy of the beams is then dissipated into waves in the plasma.

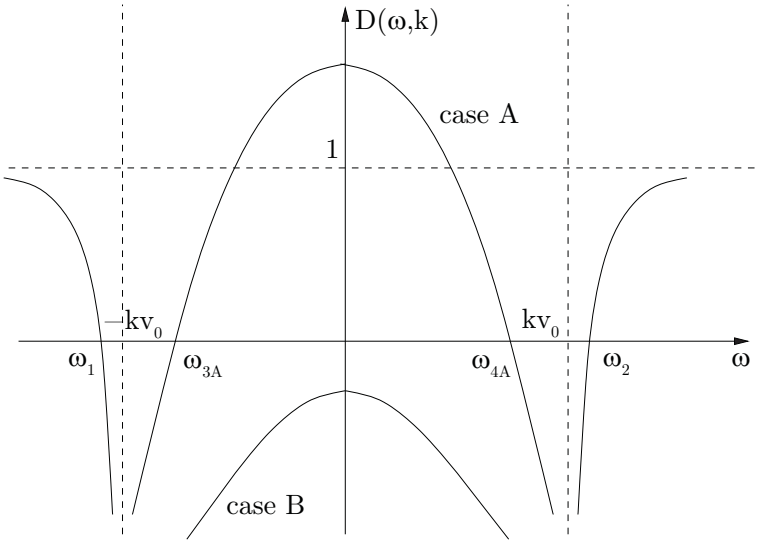

Figure 8.2: Graphical solution of eq.(8.5).

An illustration of a numerical simulation of the streaming instability can be found at
http://www.univ-orleans.fr/mapmo/membres/filbet/tsi_anim.html.

(†) Note that it *does* make sense to take the derivative of the δ–functional under the integral.

(‡) In fact, one sees easily that eq.(8.5) is degenerated to a quadratic equation for ω^2. Thus the exact solution can be written down easily,

$$\omega^2 = \frac{\omega_{pe}^2}{2} + k^2 v_0^2 \pm \frac{\omega_{pe}^2}{2} \sqrt{1 + \left(\frac{kv_0}{\omega_{pe}}\right)^2}$$

so ω is not real (i.e. we have an instability). If $\omega^2 < 0 \rightarrow k^2 v_0^2 < \omega_{pe}^2$, which is the result of eq.(8.6).

8.2 Electron Plasma Waves: Vlasov Treatment

We consider *only* electrons (Langmuir waves), with ions simply providing a neutralising background, and search for high frequency waves[§]

$$\omega \geq \omega_p \gg ku, \qquad \forall u \tag{8.7}$$

This means we assume that *no* particles can go fast enough to resonate with the wave. In this limit the resonant denominator becomes

$$\frac{1}{\omega - ku} = \frac{1}{\omega}\left\{\frac{1}{1-ku/\omega}\right\} \simeq \frac{1}{\omega}\left\{1 + \frac{ku}{\omega} + \frac{k^2u^2}{\omega^2} + \frac{k^3u^3}{\omega^3} + \cdots\right\} \tag{8.8}$$

Let's consider a 1–D maxwellian distribution

$$F_0(u) = \frac{n_e}{\sqrt{2\pi}v_{\rm th}} \exp\left\{-\frac{u^2}{2v_{\rm th}^2}\right\} \tag{8.9}$$

where $v_{\rm th} = \sqrt{T/m}$ as usual, and try the first two terms of the expansion eq.(8.8)

$$D(\omega,k) \approx 1 + \tfrac{\omega_{pe}^2}{n_e k\omega}\Big\{ \underbrace{\int_{-\infty}^{\infty} \mathrm{d}u \frac{\mathrm{d}F_0}{\mathrm{d}u}}_{0 \text{ as } F_0 \text{ is an even function}} + \int_{-\infty}^{\infty} \mathrm{d}u \frac{\mathrm{d}F_0}{\mathrm{d}u}\frac{ku}{\omega}\Big\}$$

$$= 1 + \tfrac{\omega_{pe}^2}{n_e k\omega}\left\{ F_0 \tfrac{ku}{\omega}\Big|_{-\infty}^{+\infty} - \int \mathrm{d}u\, F_0 \tfrac{k}{\omega}\right\} = 1 + \frac{\omega_{pe}^2}{n_e\omega^2}\Big\{ \underbrace{F_0 u\Big|_{-\infty}^{+\infty}}_{0} - \underbrace{\int_{-\infty}^{\infty} F_0\,\mathrm{d}u}_{n_e}\Big\} = 1 - \frac{\omega_{pe}^2}{\omega^2}$$

Thus

$$D(\omega,k) = 0 \quad \Longleftrightarrow \quad \omega^2 = \omega_{pe}^2 \qquad \text{'cold' Langmuir oscillations} \tag{8.10}$$

We need to go to higher order in ku/ω to find thermal effects.[¶] Using

$$\int_{-\infty}^{\infty} \frac{\mathrm{d}F_0}{\mathrm{d}u} u^2\,\mathrm{d}u = 0 \qquad \left[\frac{\mathrm{d}F_0}{\mathrm{d}u} \text{ is an odd function}\right] \tag{8.11}$$

$$\int_{-\infty}^{\infty} \frac{\mathrm{d}F_0}{\mathrm{d}u} u^3\,\mathrm{d}u = \underbrace{u^3 f_0\Big|_{-\infty}^{+\infty}}_{\to 0} - 3\int_{-\infty}^{\infty} u^2 F_0\,\mathrm{d}u = -3\,n_e v_{\rm th}^2 \tag{8.12}$$

we find to order 3

$$1 - \frac{\omega_{pe}^2}{\omega^2}\left\{1 + 3\frac{k^2v_{\rm th}^2}{\omega^2}\right\} = 0 \tag{8.13}$$

Assuming that $\omega^2 \gg k^2v_{\rm th}^2$ we can use the first order expression $\omega^2 \simeq \omega_{pe}^2$ in the second denominator and finally get

$$\omega^2 \simeq \omega_{pe}^2 + 3\,k^2v_{\rm th}^2. \tag{8.14}$$

This is the result found in fluid theory *with* pressure term (with an adiabatic exponent $\gamma = 3$; this corresponds to saying that the electron motion is one–dimensional along $\mathbf{E} \parallel \mathbf{k}$, and that it is adiabatic, which is a good approximation for high frequency waves).

[§] we know from fluid theory that $\omega = \omega_{\rm p}$ is a cut–off.

[¶] One shows easily that the solution to order $2j_{\max} - 1$ is

$$D(\omega,k) = 1 - \frac{\omega_{pe}^2}{\omega^2}\sum_{j=0}^{j_{\max}} (2j+1)!\Big(\frac{kv_{\rm th}}{\omega}\Big)^{2j}$$

8.3 Wave–Particle Interaction

In the following we will get to the core of the problem of *wave–particle interaction*, namely the exchange of energy between particles and waves. We will discuss:

- Experimental motivation, see for example PRL 17 (1966) 172.
- Correct treatment of the Vlasov–Maxwell system:
  - Laplace transform
  - Landau integrals
  - Calculation of wave (instability) potential
  - Analytical continuation
  - Ballistic modes and phase mixing

8.3.1 Experimental Motivation

Damping

People launch and detect waves: in the presence of resonant particles damping can be observed over time scales much shorter than the collisional ones (or distances much shorter than λ_{mfp}) $\rightarrow$ important for plasma heating (fusion and space).

Instability

Particles with $v \sim \omega/k$ can *drive* the wave, i.e. transfer energy to the wave (over short time scales). Example: α-particles can drive Alfvén waves in a tokamak reactor.

8.3.2 Correct Treatment of the Vlasov–Maxwell System

Now we *want* to consider resonant particles: we must deal with the integral

$$\int_{\mathbb{R}} \frac{\frac{\mathrm{d}F_0}{\mathrm{d}u}}{u - \frac{\omega}{k}} \mathrm{d}u \tag{8.15}$$

properly. To treat the problem correctly we need to consider initial conditions and 'maintain' them through the linearisation and plane wave (or similar) decomposition.

The *Laplace transform* "respects" the initial condition problem and causality. It is defined as

$$\tilde{f}_{\alpha 1}(p) = \int_0^\infty f_{\alpha 1}(t) e^{-pt} \mathrm{d}t$$
where $p \in \mathbb{C}, \quad (p \leftrightarrow -\mathrm{i}\omega)$
and $\Re\{p\} > p_0 > 0$

with $p_0 \in \mathbb{R}^+$ such that the integral converges at $t \rightarrow \infty$ (figure 8.3).

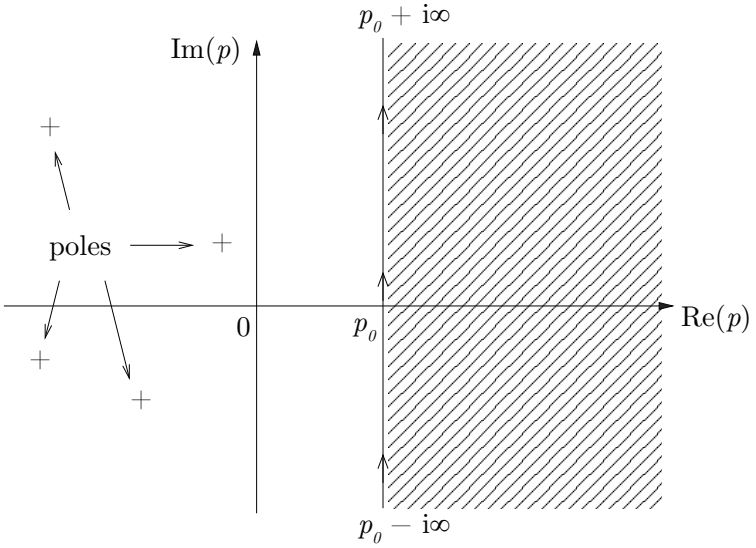

Figure 8.3: Domain of $\tilde{f}_{\alpha 1}(p)$.

The inversion formula is

$$f_{\alpha 1}(t) = \frac{1}{2\pi \mathrm{i}} \int_{p_0-\mathrm{i}\infty}^{p_0+\mathrm{i}\infty} \tilde{f}_{\alpha 1}(p) e^{+pt} \mathrm{d}p \tag{8.16}$$

where the integral is performed along the vertical line $\Re\{p\} = p_0$ situated to the right of all singularities (*poles*) of $\tilde{f}_{\alpha 1}(p)$.

The importance of the Laplace transform is that, contrarily to the Fourier transform, initial conditions are "maintained" in the problem via

$$\widetilde{\left(\frac{\partial f_{\alpha 1}}{\partial t}\right)}(p) = p\tilde{f}_{\alpha 1}(p) - f_{\alpha 1}\big|_{t=0} \tag{8.17}$$

Considering our linearised Vlasov–Poisson system[(‖)]

$$\begin{cases} \dfrac{\partial f_{\alpha 1}}{\partial t} + \mathbf{v}\cdot \mathrm{i}\mathbf{k} f_{\alpha 1} + \dfrac{q_\alpha}{m_\alpha}\mathbf{E}\cdot\dfrac{\partial f_{\alpha 0}}{\partial \mathbf{v}} = 0 \\ \mathrm{i}\mathbf{k}\cdot\mathbf{E} = \dfrac{1}{\varepsilon_0}\displaystyle\sum_\alpha q_\alpha \int f_{\alpha 1}\,\mathrm{d}^3 v \end{cases} \tag{8.18}$$

we apply the Laplace transform to the time variable t and Fourier to the spatial coordinates,

$$\begin{cases} p\tilde{f}_{\alpha 1} - g_\alpha + \mathrm{i}\mathbf{k}\cdot\mathbf{v}\tilde{f}_{\alpha 1} - \mathrm{i}\dfrac{q_\alpha}{m_\alpha}\tilde{\phi}\,\mathbf{k}\cdot\dfrac{\partial f_{\alpha 0}}{\partial \mathbf{v}} = 0 \\ k^2\tilde{\phi} = \dfrac{1}{\varepsilon_0}\displaystyle\sum_\alpha q_\alpha \int \tilde{f}_{\alpha 1}\,\mathrm{d}^3 v \end{cases} \tag{8.19}$$

where $g_\alpha \equiv g_\alpha(\mathbf{x},\mathbf{v}) := f_{\alpha 1}(\mathbf{x},\mathbf{v},t=0)$ has been defined. Inserting $\tilde{f}_{\alpha 1}$ out of the first eq.(8.19) into the second eq.(8.19) we get

$$\left[1 - \frac{\mathrm{i}}{k^2}\sum_\alpha \frac{q_\alpha^2}{\varepsilon_0 m_\alpha}\int \mathrm{d}^3 v \frac{\mathbf{k}\cdot\frac{\partial f_{\alpha 0}}{\partial \mathbf{v}}}{p + \mathrm{i}\mathbf{k}\cdot\mathbf{v}}\right]\tilde{\phi}(p) = \sum_\alpha \frac{q_\alpha}{\varepsilon_0 k^2}\int \mathrm{d}^3 v \frac{g_\alpha}{p+\mathrm{i}\mathbf{k}\cdot\mathbf{v}} \tag{8.20}$$

Choosing again $\mathbf{k} = k\mathbf{e}_z$ and introducing

$$F_{\alpha 0} := \int f_{\alpha 0}\,\mathrm{d}v_x\,\mathrm{d}v_y \qquad G_\alpha := \int g_\alpha\,\mathrm{d}v_x\,\mathrm{d}v_y \qquad u := v_z \tag{8.21}$$

we get

$$\tilde{\phi}(p) = \frac{1}{\varepsilon_0 k^2}\frac{\displaystyle\sum_\alpha q_\alpha \int \mathrm{d}u \frac{G_\alpha}{p+\mathrm{i}ku}}{1 - \dfrac{\mathrm{i}}{k}\displaystyle\sum_\alpha \frac{\omega_{\mathrm{p}\alpha}^2}{n_\alpha}\int \mathrm{d}u \frac{\mathrm{d}F_{\alpha_0}/\mathrm{d}u}{p+\mathrm{i}ku}} \tag{8.22}$$

Noting that p corresponds to $-\mathrm{i}\omega$, the potential in Laplace space can be written as

$$\tilde{\phi}(p) = \frac{-\mathrm{i}\displaystyle\sum_\alpha q_\alpha \int \mathrm{d}u \frac{G_\alpha}{u - \mathrm{i}p/k}}{\varepsilon_0 k^3\,\epsilon(\mathrm{i}p, k)} \tag{8.23}$$

(‖) Fourier transformation can be used for *space* coordinates only.

where

$$\epsilon(\mathrm{i}p,k) = D(\mathrm{i}p,k) = 1 - \frac{1}{k^2}\sum_\alpha \frac{\omega_{\mathrm{p}\alpha}^2}{n_\alpha}\int \mathrm{d}u \frac{\frac{\mathrm{d}F_{\alpha 0}}{\mathrm{d}u}}{u - \frac{\mathrm{i}p}{k}} \tag{8.24}$$

Now we can invert the Laplace transform, formally

$$\phi(t) = \frac{1}{2\pi\mathrm{i}}\int_{p_0-\mathrm{i}\infty}^{p_0+\mathrm{i}\infty} \tilde{\phi}(p)e^{+pt}\mathrm{d}p \tag{8.25}$$

with p_0 such that – for $\Re\{p\} > p_0 > 0$ – the integral $\int_0^\infty e^{-pt}\phi(t)\mathrm{d}t$ always converges. Stated otherwise, p_0 must be to the right of all poles of $\tilde{\phi}(p)$. The problem with the standard definition of the Laplace transform is the restriction $\Re\{p\} = \Re\{-\mathrm{i}\omega\} = \gamma > p_0 > 0$. The physically interesting damped waves ($\gamma < 0$) are *not included*. We therefore need to extend the definition to a domain with $\Re\{p\} < p_0$ by *analytical continuation*. This is done by moving the integration path that defines the inverse Laplace transform

$$f_{\alpha 1}(t) = \frac{1}{2\pi\mathrm{i}}\int_{p_0-\mathrm{i}\infty}^{p_0+\mathrm{i}\infty} \tilde{f}_{\alpha 1}(p)e^{pt}\mathrm{d}p \tag{8.26}$$

to the left ($p_0 \to -\infty$), but leaving all poles p_j of $\tilde{f}_{\alpha 1}$ on the same side of the contour (i.e. on the left side; see figure 8.4).

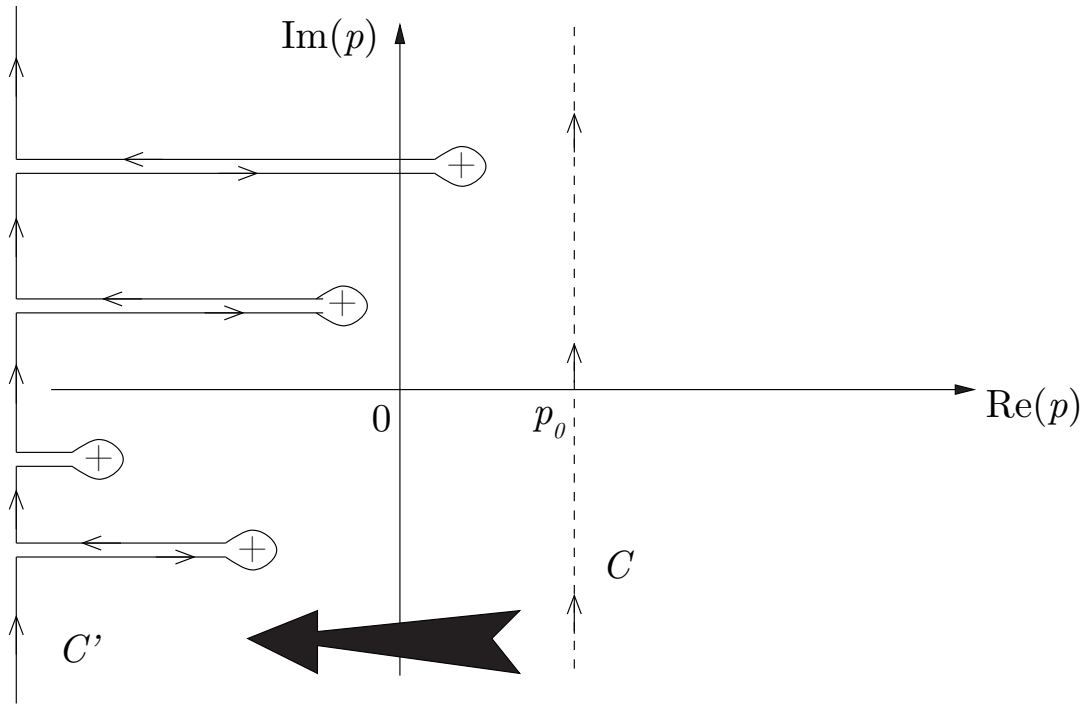

Figure 8.4: Analytical continuation of the inverse Laplace transform.

This exercise also tells us how to solve the problem of the integral over the velocity space in the presence of a resonant denominator:

$$\int \frac{h(u)}{u - \frac{\mathrm{i}p}{k}}\mathrm{d}u$$

In other words, the need to have the analytical continuation of $\tilde{\phi}(p)$ forces the contour of integration to pass *below* the pole $u = \frac{\mathrm{i}p}{k}$ if $k > 0$ (a similar result holds for $k < 0$), removing the ambiguity (*Landau's rule*). This rule is a consequence of analytical continuation (A.C.).

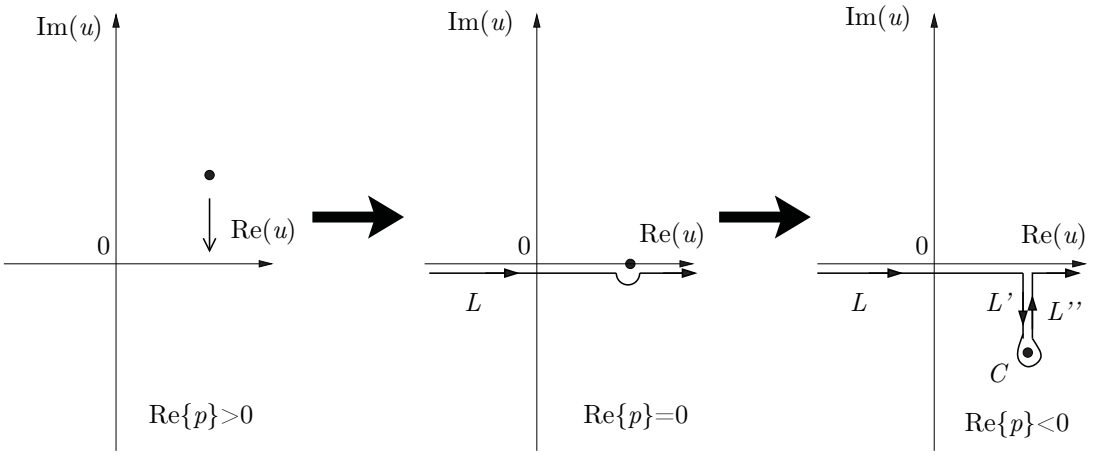

Figure 8.5: Start with $\Re\{p\} > 0$ and move the pole down until $\Re\{p\} \simeq 0$. Don't confuse u–plane and p–plane!

For $\Re\{p\} < 0$ (see figure 8.5)

$$\text{A.C.} \int_{\mathbb{R}} \mathrm{d}u \frac{h(u)}{u - \frac{\mathrm{i}p}{k}}\bigg|_{\Re\{p\}<0} = \Big\{ \int_L + \underbrace{\int_{L'} + \int_{L''}}_{=0 \text{ (equal and opposite contributions)}} + \int_C \Big\} \frac{h(u)}{u - \frac{\mathrm{i}p}{k}} \mathrm{d}u =$$

$$= \int_{-\infty}^{\infty} \frac{h(u)}{u - \frac{\mathrm{i}p}{k}} \mathrm{d}u + 2\pi\mathrm{i} \operatorname*{Res}_{u=\mathrm{i}p/k} \frac{h(u)}{u - \frac{\mathrm{i}p}{k}} = \int_{-\infty}^{\infty} \frac{h(u)}{u - \frac{\mathrm{i}p}{k}} \mathrm{d}u + 2\pi\mathrm{i}\, h\Big(\frac{\mathrm{i}p}{k}\Big)$$

For the case $\Re\{p\} = 0$, there are no paths L', L'' and the path C is only a half–circle. Moreover, the principal value (P.V.) symbol has to be kept in this case(**). Thus

$$\text{A.C.} \int_{\mathbb{R}} \mathrm{d}u \frac{h(u)}{u - \frac{\mathrm{i}p}{k}}\bigg|_{\Re\{p\}=0} = \text{P.V.} \int \frac{h(u)}{u - \frac{\mathrm{i}p}{k}} \mathrm{d}u + \mathrm{i}\pi\, h\left(\frac{\mathrm{i}p}{k}\right) \tag{8.27}$$

To perform the calculation in practice, we distinguish three cases:

$$\int_{\mathbb{R}} \frac{h(u)}{u - \frac{\mathrm{i}p}{k}} \mathrm{d}u = \begin{cases} \displaystyle\int_{-\infty}^{\infty} \frac{h(u)}{u - \mathrm{i}p/k} \mathrm{d}u & \Re\{p\} > 0 \\ \text{P.V.} \displaystyle\int \frac{h(u)}{u - \mathrm{i}p/k} \mathrm{d}u + \mathrm{i}\pi\, h(\frac{\mathrm{i}p}{k}) & \Re\{p\} = 0 \\ \displaystyle\int_{-\infty}^{\infty} \frac{h(u)}{u - \mathrm{i}p/k} \mathrm{d}u + 2\pi\mathrm{i}\, h(\frac{\mathrm{i}p}{k}) & \Re\{p\} < 0 \end{cases} \tag{8.28}$$

where $h(u)$ is a regular function. Note that there is *no discontinuity* between different cases, and that all integration contours that pass below the pole give the same result. The distinction of the three cases is simply to make calculation easy.

(**)

$$\text{P.V.} \int_{-\infty}^{+\infty} \{\cdots\}\, \mathrm{d}x \equiv \lim_{\delta \to 0} \Big\{ \int_{-\infty}^{x_0 - \delta} \{\cdots\}\, \mathrm{d}x + \int_{x_0 + \delta}^{+\infty} \{\cdots\}\, \mathrm{d}x \Big\}$$

Having solved the mathematical difficulty (at least in principle!) we can go back to the physical problem. To invert the Laplace transform we need to know the poles of the expression eq.(8.38) for $\tilde{\phi}(p)$ (in the p–plane!).
These are:

- *poles* of the numerator

$$\sum_\alpha q_\alpha \int_{\mathcal{L}} \mathrm{d}u \frac{G_\alpha(u)}{u - \frac{\mathrm{i}p}{k}}$$

  The symbol $\mathcal{L}$ means "according to Landau's rule".

- *zeros* of the denominator $\underline{\boldsymbol{\epsilon}}(\mathrm{i}p, k) = 0$

Note that this latter condition corresponds to the *dispersion relation*: each *wave* in the plasma is a root of the equation $\underline{\boldsymbol{\epsilon}}(\mathrm{i}p, k) = 0$, therefore a *pole* for $\tilde{\phi}(p)$. In general, as stated before, $p \in \mathbb{C}$, and $\Re\{p\}$ can be negative for some roots of the dispersion relation. In order to consider these physically meaningful waves, we need to *extend* the definition of the inverse Laplace transform by analytical continuation of $\tilde{\phi}(p)$ for all p down to $\Re\{p\} < 0$: this is done by moving the contour of integration towards $\Re\{p\} \to -\infty$, but leaving the poles on the same side of the contour (figure 8.4).
By definition

$$\phi(t) = \frac{1}{2\pi\mathrm{i}} \int_{p_0 - \mathrm{i}\infty}^{po + \mathrm{i}\infty} \mathrm{d}p\, \tilde{\phi}(p) e^{pt} \equiv \frac{1}{2\pi\mathrm{i}} \int_C \mathrm{d}p\, \tilde{\phi}(p) e^{pt} \tag{8.29}$$

Now

$$\phi(t) = \frac{1}{2\pi\mathrm{i}} \int_{C'} \mathrm{d}p\, \tilde{\phi}(p) e^{pt} \tag{8.30}$$

where C' is the modified integration contour.
To calculate the integral, we close the contour in the complex plane (figure 8.6), so that we can use the Cauchy formula (theorem of residues)

$$\begin{aligned} \int_C \mathrm{d}p\, \tilde{\phi}(p) e^{pt} &= \int_{C'} \mathrm{d}p\, \tilde{\phi}(p) e^{pt} \\ &= \int_{C'} \mathrm{d}p\, \tilde{\phi}(p) e^{pt} + \underbrace{\int_{C_1} \mathrm{d}p\, \tilde{\phi}(p) e^{pt}}_{=0} + \underbrace{\int_{C_2} \mathrm{d}p\, \tilde{\phi}(p) e^{pt}}_{=0} + \underbrace{\int_{\Gamma} \mathrm{d}p\, \tilde{\phi}(p) e^{pt}}_{=0} \end{aligned} \tag{8.31}$$

The integrals over C_1, C_2 and Γ are all equal to 0 because

$$\tilde{\phi}(p) \overset{|p|\to\infty}{\longrightarrow} \frac{1}{p} \longrightarrow 0 \tag{8.32}$$

For Γ, obviously $e^{pt} \to 0$ for $\Re\{p\} \to -\infty$ and $t > 0$. For C_1 and C_2, $\Re\{p\} < p_0$ and only the imaginary part of p goes to infinity. Thus e^{pt} remains finite, but $\tilde{\phi} \to 0$. Finally

$$\phi(t) = \sum_j \mathrm{Res}\left(\tilde{\phi}(p) e^{pt}, p_j\right) = \sum_j e^{p_j t} \mathrm{Res}\left(\tilde{\phi}(p), p_j\right) \tag{8.33}$$

where the p_j are the poles of $\tilde{\phi}(p)e^{pt}$.(††) If p_j is a pole of order n, the residue is given by

$$\mathrm{Res}\left(\tilde{\phi}(p), p_j\right) = \frac{1}{(n-1)!} \lim_{p \to p_j} \frac{\mathrm{d}^{n-1}}{\mathrm{d}p^{n-1}} \left[(p - p_j)^n \tilde{\phi}(p)\right] \tag{8.34}$$

(††) As e^{pt} is a regular function, the poles of $\tilde{\phi}(p)e^{pt}$ and $\tilde{\phi}(p)$ are the same.

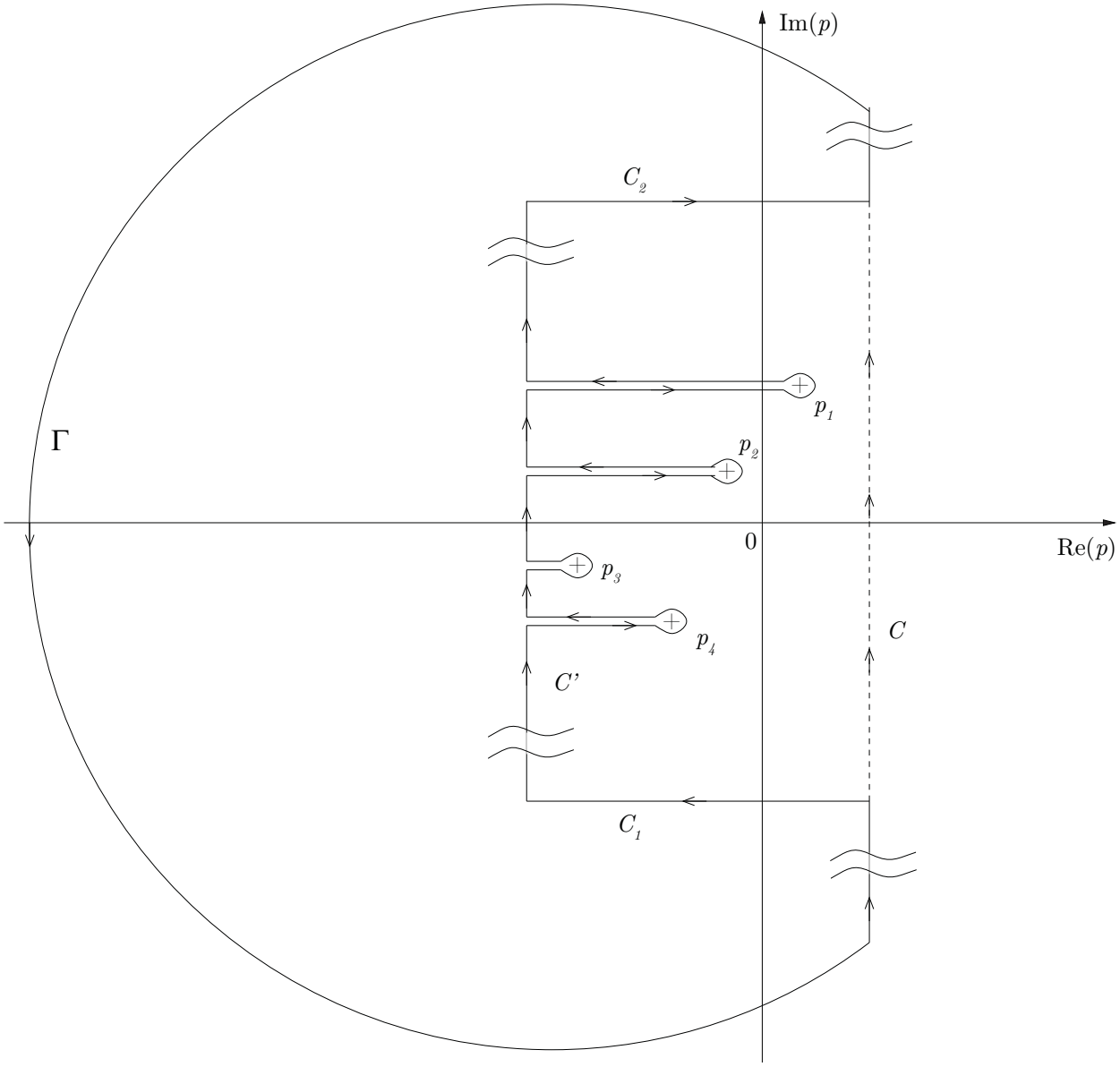

Figure 8.6: Contour for the inverse Laplace transform.

The behavior of ϕ (stable vs. unstable) depends on the sign of $\Re\{p_j\}$:

$$\phi(t) \propto \begin{cases} e^{+|\Re\{p_j\}|t}, & \Re\{p_j\} > 0 \qquad \text{unstable} \\ e^{-|\Re\{p_j\}|t}, & \Re\{p_j\} < 0 \qquad \text{stable} \end{cases} \tag{8.35}$$

Note

A *hierarchy* of poles can be established in terms of physical relevance: poles to the right (the first we meet as we move the path of integration) are the most important, as they are the most unstable (if $\Re\{p_j\} > 0$), or the least stable (if $\Re\{p_j\} < 0$). The long term response of the plasma is dominated by the first pole p_1, as $\phi(t) \propto e^{p_1 t}$.

8.4 Summary of the Landau treatment of the Vlasov–Maxwell System

- Start from the linearised, electrostatic ($\mathbf{B}_1 \equiv 0$), spatially Fourier transformed Vlasov–Poisson system, eq.(8.18)

$$\begin{cases} \dfrac{\partial f_{\alpha 1}}{\partial t} + \mathbf{v}\cdot \mathrm{i}\mathbf{k} f_{\alpha 1} + \dfrac{q_\alpha}{m_\alpha}\mathbf{E}\cdot\dfrac{\partial f_{\alpha 0}}{\partial \mathbf{v}} = 0 \\ \mathrm{i}\mathbf{k}\cdot\mathbf{E} = \dfrac{1}{\varepsilon_0}\displaystyle\sum_\alpha q_\alpha \int f_{a1}\,\mathrm{d}^3 v \end{cases} \tag{8.36}$$

- Laplace transform. In order to
  - keep the information of the initial condition $f_{\alpha 1}(t=0)$
  - conserve causality

  we apply the *Laplace transform* to the time variable $t \to p$, which is defined as

$$\tilde{f}_{\alpha 1}(p) = \int_0^\infty f_{\alpha 1}(t) e^{-pt}\mathrm{d}t, \qquad p \in \mathbb{C}, \qquad \Re\{p\} > p_0 > 0, \tag{8.37}$$

  with $p_0 \in \mathbb{R}$ such that all poles p_j of $\tilde{f}_{\alpha 1}$ have $\Re\{p_j\} < p_0$. This yields eq.(8.23)

$$\tilde{\phi}(p) = \frac{-\mathrm{i}\displaystyle\sum_\alpha q_\alpha \int \mathrm{d}u \frac{G_\alpha}{u - \mathrm{i}p/k}}{\varepsilon_0 k^3\, \epsilon(\mathrm{i}p, k)} \tag{8.38}$$

- Analytical continuation. The problem with the standard definition of the Laplace transform is the restriction $\Re\{p\} = \Re\{-\mathrm{i}\omega\} = \gamma > p_0 > 0$, i.e. the physically interesting damped waves ($\gamma < 0$) are *not included*. Thus we have to extend the definition for $\Re\{p\} < p_0$ by *analytical continuation*, which is done by moving the integration contour of the inverse Laplace transform

$$f_{\alpha 1}(t) = \frac{1}{2\pi\mathrm{i}} \int_{p_0 - \mathrm{i}\infty}^{p_0 + \mathrm{i}\infty} \tilde{f}_{\alpha 1}(p) e^{pt}\mathrm{d}p \tag{8.39}$$

  to the left ($p_0 \to -\infty$), but leaving all poles p_j of $\tilde{f}_{\alpha 1}$ on same side of the contour (i.e. on the left side; see figure 8.4).

- Calculation of the velocity integral

$$\int_{-\infty}^{\infty} \mathrm{d}u \frac{\frac{\mathrm{d}F_{\alpha 0}}{\mathrm{d}u}}{u - \frac{\mathrm{i}p}{k}} \tag{8.40}$$

  The initial definition of the Laplace transform with $\Re\{p\} > 0$ shows that the pole is (for $k > 0$) in the upper half–plane of u. Thus the integration contour is initially *below* the pole. After the analytical continuation of the p–domain, this has to stay this way (figure 8.5). *As any integration contour which passes below the pole gives the same result*, there are several possibilities to write the result. One possibility is eq.(8.28)

$$\int_{\mathbb{R}} \frac{h(u)}{u - \frac{\mathrm{i}p}{k}}\mathrm{d}u = \begin{cases} \displaystyle\int_{-\infty}^{\infty} \frac{h(u)}{u - \mathrm{i}p/k}\mathrm{d}u, & \Re\{p\} > 0 \\ \mathrm{P.V.}\displaystyle\int \frac{h(u)}{u - \mathrm{i}p/k}\mathrm{d}u + \mathrm{i}\pi\, h(\frac{\mathrm{i}p}{k}), & \Re\{p\} = 0 \\ \displaystyle\int_{-\infty}^{\infty} \frac{h(u)}{u - \mathrm{i}p/k}\mathrm{d}u + 2\pi\mathrm{i}\, h(\frac{\mathrm{i}p}{k}), & \Re\{p\} < 0 \end{cases} \tag{8.41}$$

We did note that there is *no discontinuity* between the three cases, which one can see more clearly in the compact representation

$$\int_{\mathbb{R}} \frac{h(u)}{u-\frac{\mathrm{i}p}{k}}\mathrm{d}u = \text{P.V.}\int \frac{h(u)}{u-\frac{\mathrm{i}p}{k}}\mathrm{d}u + \mathrm{i}\pi\, h\left(\frac{\mathrm{i}p}{k}\right), \qquad p\in\mathbb{C} \tag{8.42}$$

where the principal value integral is always taken on the level of the pole. However, the 'best' integration contour depends from case to case according to the particular choice of $h(u)$.

This is all we need to know to solve the dispersion relation $\epsilon(\mathrm{i}p,k)=0$.

- Inversion of the Laplace transform. Applying the residue theorem to the closed integration contour $C'\cup C_1\cup C_2\cup\Gamma$ (figure 8.6) one shows that the aid–contours C_1, C_2 and Γ are harmless and finds eq.(8.33)

$$\phi(t) = \sum_j \text{Res}\left(\tilde{\phi}(p)e^{p_j t}, p_j\right) = \sum_j e^{p_j t}\,\text{Res}\left(\tilde{\phi}(p), p_j\right) \tag{8.43}$$

where the poles p_j are either:

  - *zeros* of the denominator, i.e. solutions of the dispersion relation $\epsilon(\mathrm{i}p,k)=0$ (i.e. waves).
  - *poles* of the numerator

$$\sum_\alpha q_\alpha \int \mathrm{d}u \frac{G_\alpha(u)}{u-\frac{\mathrm{i}p}{k}}$$

    i.e. "ballistic modes"; less important, as they usually decay very quickly $\Rightarrow \Re\{p\}<0$.

  It is clear that the long term behavior will be dominated by the rightmost pole, as $\phi\propto\sum_j e^{p_j t}\approx e^{p_1 t}$, where p_1 is the pole with the maximum real part.

8.5 Ballistic Modes and Phase Mixing

The poles of the numerator of eq.(8.38) give rise to perturbations corresponding to collective motion without being solutions of the wave dispersion relation. They are called *ballistic modes* (i.e. dependent on the initial condition), and can come from

1. Singularities in $G_\alpha(u)$: This is unlikely, as $G_\alpha(u)$ is the initial perturbation of $F_\alpha(u)$ and it is hard to imagine a *physical* case with singular (i.e. infinite energy) initial distribution.

2. For regular $G_\alpha(u)$, from the term $\int \mathrm{d}u\frac{G_\alpha(u)}{u-\mathrm{i}p/k}$. It can be demonstrated that this integral can give poles only for $\Re\{p\}<0$, which are stable (for $k>0$).

A physical way of seeing this is to go back one step and look for the origin of ballistic modes in the expression for $\tilde{f}_{\alpha 1}(p)$. The expression for $\tilde{f}_{\alpha 1}(p)$ *before* integrating over velocities and *before* inverting the Laplace transform reads

$$\tilde{f}_{\alpha 1}(p,u) = \frac{G_\alpha}{p+\mathrm{i}ku} + \mathrm{i}\frac{q_\alpha}{m_\alpha}\tilde{\phi}(p)\frac{k\frac{\mathrm{d}F_{0\alpha}}{\mathrm{d}u}}{p+\mathrm{i}ku} \tag{8.44}$$

Inverting the Laplace transform we get

$$f_{\alpha 1}(t,u) = \frac{1}{2\pi \mathrm{i}} \int \frac{G_\alpha}{p + \mathrm{i}ku} e^{pt} \mathrm{d}p + \mathrm{i}\frac{q_\alpha}{m_\alpha} \int \tilde{\phi}(p) \frac{k \frac{\mathrm{d}F_{\alpha 0}}{\mathrm{d}u}}{p + \mathrm{i}ku} e^{pt} \mathrm{d}p \tag{8.45}$$

The first term, along with terms of the same kind in $\tilde{\phi}(p)$, keeps the "memory" of the initial conditions(*). As there is a pole for $p = -\mathrm{i}ku$, the integrals in eq.(8.45) will give rise to terms of the form(†)

$$f_{\alpha,1}(u) \propto e^{-\mathrm{i}(kt)u} G(u) + ... \tag{8.46}$$

which represent an oscillation in u–space with a "frequency" $\omega_u = kt$ becoming larger and larger as t increases. Thus $\int f_{\alpha 1}(u,t)\,\mathrm{d}u$, on which macroscopic quantities depend – like $n_1 = \int f_{\alpha 1}(u,t)\,\mathrm{d}u$ – will become smaller and smaller. This phenomenon is known as *phase mixing* (figure 8.8). As a result, *microscopic* perturbations remain but macroscopic effects decay exponentially (figure 8.7).

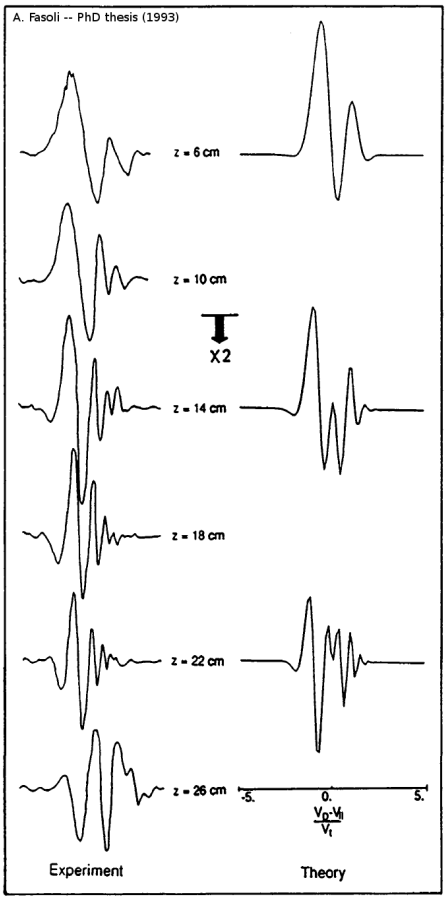

Figure 8.7: First order parallel distribution function (in phase components) at different z positions (grid at $z = 0$, $f = 43.5$ kHz, $\lambda \simeq 4.1$ cm, $\delta n/n = 5\%$). Shown on the right are the corresponding results for a linear 1-D Vlasov model: $f^1_{\omega,k}(v_\parallel, z) = f^1(v_\parallel, z=0) e^{\mathrm{i}(\omega/v_\parallel)z} + \frac{e\phi_0}{kT} \frac{\partial f_0(v_\parallel)}{\partial v_\parallel} k_\parallel \left[\frac{e^{\mathrm{i}(\omega/v_\parallel)z} - e^{\mathrm{i}k_\parallel z}}{\omega - k_\parallel v_\parallel} \right]$.

(*) Remember that the Vlasov equation conserves entropy.

(†) The second integral in eq.(8.45) will also have contributions coming from the poles of $\tilde{\phi}(p)$, i.e. the solutions of the dispersion relation.

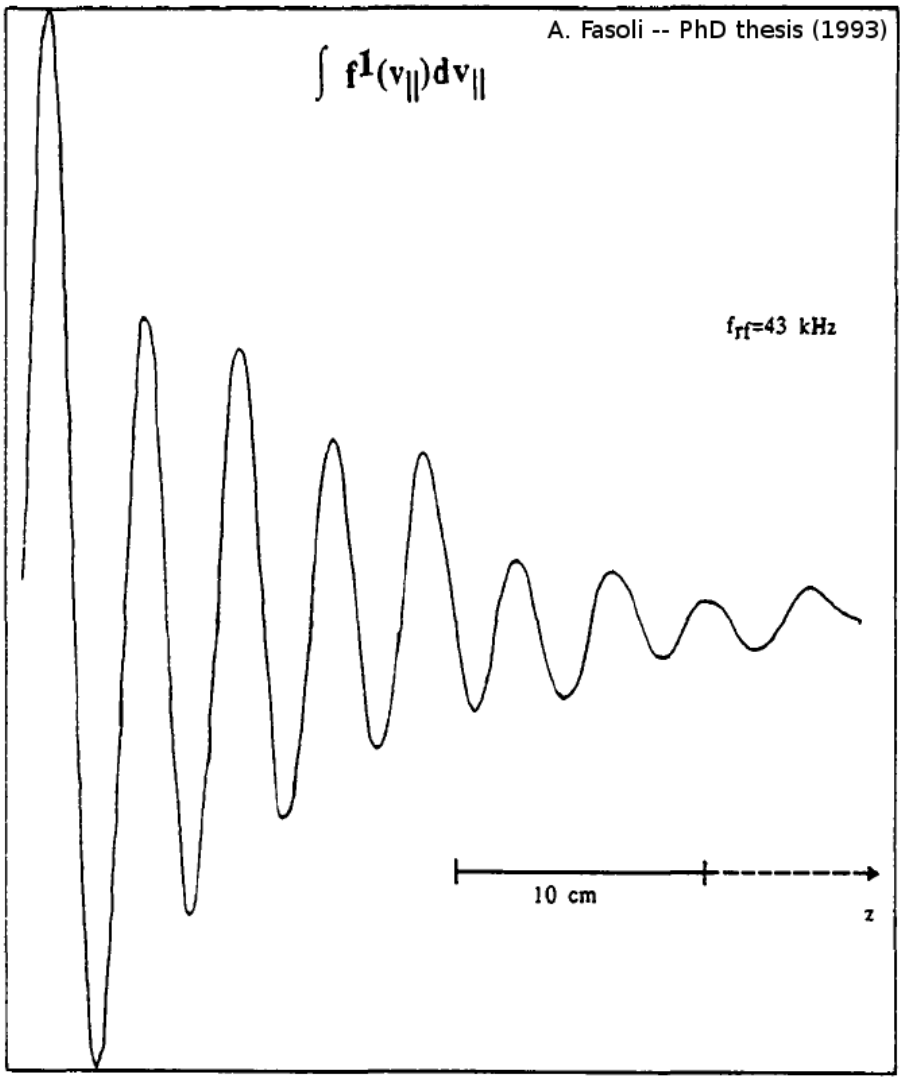

Figure 8.8: Typical LIF interferometric trace. The density pertubation $\delta n \propto \exp(ikz)$ plotted as a function of z and the exponential reduction in the wave amplitude, due to Landau damping, can be observed. See also the appendix to this chapter.

8.5.1 Phase Mixing in a Free Streaming Plasma

Let us now calculate this *phase mixing* effect explicitly, in a simple case. Consider a *free streaming* plasma, i.e. $\phi(t) = 0$ (i.e. no macroscopic fields). In this case eq.(8.45) becomes

$$f_1(t,u) = \frac{1}{2\pi \mathrm{i}} \int \frac{G(u)}{p + \mathrm{i}ku} e^{pt} \mathrm{d}p = \mathrm{Res}\left(\frac{G(u)}{p + \mathrm{i}ku} e^{pt}, p = -\mathrm{i}ku \right) = G(u) e^{-\mathrm{i}kut} \tag{8.47}$$

where we have dropped the index α.

Example 1

Let us first consider an initial perturbation of the form $G(u,k) = g(k)\,\delta(u - u_0)$ and calculate the evolution of the density

$$n_1(k,t) = \int_{-\infty}^{\infty} \mathrm{d}u\, f_1(t,u) = \int_{-\infty}^{\infty} \mathrm{d}u\, g(k)\,\delta(u-u_0)\, e^{-\mathrm{i}kut} = g(k) e^{-\mathrm{i}ku_0 t} \tag{8.48}$$

This means that if just a single velocity class carries a perturbation, there is no phase mixing effect and therefore *no decay*.

Example 2

However, if we consider a distribution with a finite width in velocity space, e.g. the gaussian form:

$$G(u,k) = \frac{g(k)}{\sqrt{2\pi}\Delta u}\exp\left\{-\frac{(u-u_0)^2}{2\Delta u^2}\right\} \tag{8.49}$$

we get

$$n_1(k,t) = \frac{g(k)}{\sqrt{2\pi}\Delta u}\int_{-\infty}^{\infty} e^{-\frac{(u-u_0)^2}{2\Delta u^2}} e^{-\mathrm{i}kut}\mathrm{d}u \tag{8.50}$$

The perform the integration, we introduce a new variable $\eta = u - u_0 \Rightarrow \mathrm{d}\eta = \mathrm{d}u$. We obtain

$$n_1(k,t) = \frac{g(k)}{\sqrt{2\pi}\Delta u} e^{-\mathrm{i}ku_0t}\int_{-\infty}^{\infty} e^{-\frac{\eta^2}{2\Delta u^2}-\mathrm{i}k\eta t}\,\mathrm{d}\eta \tag{8.51}$$

To solve this integral, let us set ("completing the square")

$$\left(\frac{\eta^2}{2\Delta u^2}+\mathrm{i}k\eta t\right) \equiv \left(\frac{\eta}{\sqrt{2}\Delta u}+\xi\right)^2 - \xi^2 \tag{8.52}$$

that gives, after explicit calculation

$$\frac{2\eta\xi}{\sqrt{2}\Delta u} = \mathrm{i}k\eta t \quad \Rightarrow \quad \xi = \frac{\mathrm{i}\sqrt{2}\,kt\Delta u}{2}$$

thus

$$\begin{aligned} -\left(\frac{\eta^2}{2\Delta u^2}+\mathrm{i}k\eta t\right) &= -\left(\frac{\eta^2}{2\Delta u^2}+\xi\right)^2 + \xi^2 = \\ &= -\left(\frac{\eta}{\sqrt{2}\Delta u}+\frac{\mathrm{i}\sqrt{2}\,kt\Delta u}{2}\right)^2 - \frac{(kt\Delta u)^2}{2} \end{aligned} \tag{8.53}$$

Now we substitute this term into the integral of eq.(8.51)

$$\begin{aligned} n_1(k,t) &= \frac{g(k)}{\sqrt{2\pi}\Delta u} e^{-\mathrm{i}ku_0t}\int_{-\infty}^{\infty}\exp\left[-\left(\frac{\eta}{\sqrt{2}\Delta u}+\frac{\mathrm{i}\sqrt{2}\,kt\Delta u}{2}\right)^2 - \frac{(kt\Delta u)^2}{2}\right]\mathrm{d}\eta \\ &= \frac{g(k)\,e^{-\frac{(kt\Delta u)^2}{2}}}{\sqrt{2\pi}\Delta u} e^{-\mathrm{i}ku_0t}\int_{-\infty}^{\infty}\exp\left[-\left(\frac{\eta}{\sqrt{2}\Delta u}+\frac{\mathrm{i}\sqrt{2}\,kt\Delta u}{2}\right)^2\right]\mathrm{d}\eta \end{aligned}$$

and, by replacing

$$x = \frac{\eta}{\sqrt{2}\Delta u}+\frac{\mathrm{i}\sqrt{2}\,kt\Delta u}{2}, \qquad \mathrm{d}\eta = \sqrt{2}\Delta u\mathrm{d}x \tag{8.54}$$

we finally obtain the solution

$$n_1(k,t) = \frac{g(k)}{\sqrt{\pi}} e^{-\mathrm{i}ku_0 t}\, e^{-\frac{(kt\Delta u)^2}{2}} \underbrace{\int_{-\infty}^{\infty} e^{-x^2}\mathrm{d}x}_{\sqrt{\pi}} = g(k) e^{-\mathrm{i}ku_0 t} e^{-\frac{(kt\Delta u)^2}{2}} \tag{8.55}$$

The decay is now exponential in t^2, and is faster for larger Δu, i.e. broader distributions in velocity space. It is the *difference in phase* of the different velocity classes that gives the decay. Again, there is no loss of information in a *microscopic* scale, but the *macroscopic* perturbation decays due to phase mixing.

8.5.2 Experimental Demonstration: Plasma Echo

This microscopic information can be recovered if we look at the *non–linear* interaction between two perturbations. Let us look at this qualitatively using an experimental demonstration.

Remember that in the experiment we can think of the initial perturbation at a given position (boundary), and the time evolution can be replaced by the evolution in space. So replacing $ut \to x$, $k \to \omega/u$ and $x \to \omega t/k$ we will have $e^{-\mathrm{i}kut} e^{-\mathrm{i}kx} \to e^{-\mathrm{i}\omega x/u} e^{-\mathrm{i}\omega t}$.

A first antenna, located at $x = 0$, excites a perturbation at ω_1. A second antenna, at $x = L$, excites a perturbation at ω_2. The perturbations produced at a generic point x will be

$$f_1^{(1)}(x,t) \propto e^{-\mathrm{i}\frac{\omega_1}{u}x} e^{-\mathrm{i}\omega_1 t} \tag{8.56}$$

$$f_1^{(2)}(x,t) \propto e^{-\mathrm{i}\frac{\omega_2}{u}(x-L)} e^{-\mathrm{i}\omega_2 t} \tag{8.57}$$

Let us *measure* the amplitude of the perturbation resulting from the *two* antennas at $\omega = \omega_2 - \omega_1$ (assume $\omega_2 > \omega_1$). The relevant *non–linear* term, the one oscillating at the difference frequency, is

$$f_1^{(1)\star} f_1^{(2)} \propto \exp\left\{ \frac{\mathrm{i}}{u} \underbrace{\Big[(\omega_1 - \omega_2)x + \omega_2 L\Big]}_{\substack{\text{this is the term} \\ \text{giving phase mixing}}} - \mathrm{i}(\omega_2 - \omega_1)t \right\} \tag{8.58}$$

So there will be no phase mixing, i.e. a *macroscopic* perturbation is possible, for

$$x = \frac{\omega_2}{\omega_2 - \omega_1} L \tag{8.59}$$

This is what we observe experimentally, see figure 8.9. This provides a good proof of reversibility in plasmas satisfying the hypothesis that lead to the Vlasov formulation of the kinetic problem.

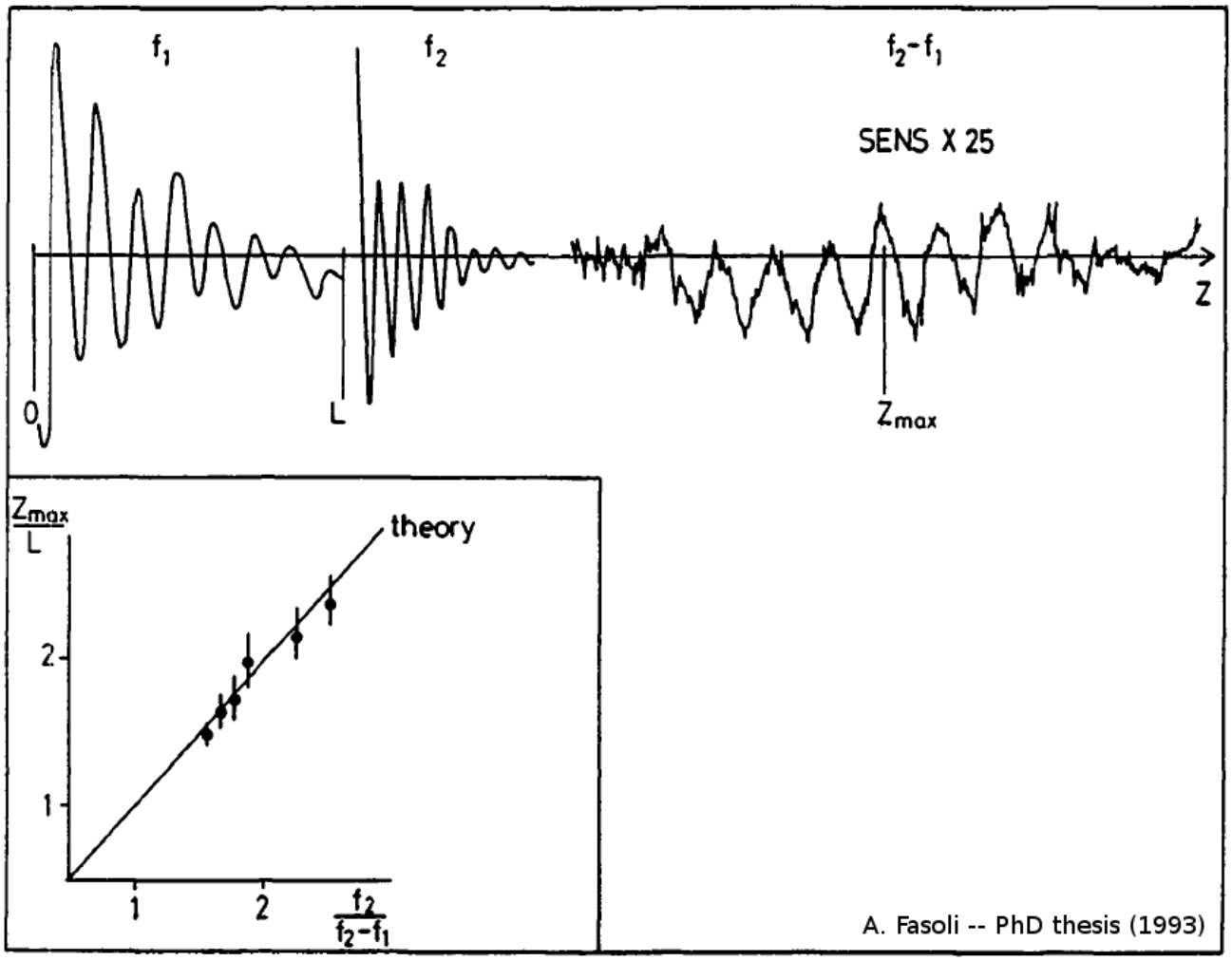

Figure 8.9: Echo measurement. The LIF signal oscillating at the difference frequency, $(\omega_2 - \omega_1)/2\pi$ is shown, along with the two first order waves ($\omega_1 < \omega_2$), which are damped before the appearance of the echo oscillations. $L = 41$ cm is the distance between the two grids. The theory line is calculated from $z_{\max}/L = \omega_2/(\omega_2 - \omega_1)$, where $z_{\max}$ is the position of the echo maximum.

8.6 Quantitative estimate of Landau damping

In practice we are interested in calculating the rate of growth or absorption of a wave that propagates in the plasma. Writing $\omega = \omega_r + \mathrm{i}\gamma$ we want to examine the case $|\gamma| \ll |\omega_r|$. In this limit we can expand the dispersion relation around $\omega = \omega_r$:

$$\begin{aligned} \epsilon(\omega, k) &= \epsilon(\omega_r + \mathrm{i}\gamma, k) \simeq \epsilon(\omega_r, k) + \mathrm{i}\gamma \frac{\partial \epsilon(\omega_r, k)}{\partial \omega_r} + \dots \\ &= \epsilon_r(\omega_r, k) + \mathrm{i}\epsilon_i(\omega_r, k) + \mathrm{i}\gamma \frac{\partial \epsilon_r(\omega_r, k)}{\partial \omega_r} + \mathrm{i}\gamma \frac{\partial [\mathrm{i}\epsilon_i(\omega_r, k)]}{\partial \omega_r} + \dots \\ &= 0 \end{aligned} \tag{8.60}$$

Separating the real and imaginary part $\epsilon = \epsilon_r + \mathrm{i}\epsilon_i$ we obtain

$$\begin{cases} \text{Real part:} & \epsilon_r(\omega_r, k) - \gamma \dfrac{\partial \epsilon_i(\omega_r, k)}{\partial \omega_r} + \mathcal{O}(\gamma^2) = 0 \\ \text{Imaginary part:} & \epsilon_i(\omega_r, k) + \gamma \dfrac{\partial \epsilon_r(\omega_r, k)}{\partial \omega_r} + \mathcal{O}(\gamma^2) = 0 \end{cases} \tag{8.61}$$

We can have three different cases, depending on the relative order of the real and imaginary parts of ϵ. For physical reasons we suppose that ϵ_r, ϵ_i are smooth functions of ω_r.

- $\epsilon_r \ll \epsilon_i$. We have

$$\begin{cases} \epsilon_r(\omega_r,k) & = \gamma \frac{\partial \epsilon_i}{\partial \omega_r} \\ \epsilon_i(\omega_r,k) = 0 & \Leftrightarrow \left.\frac{\mathrm{d}F_0}{\mathrm{d}u}\right|_{u=\frac{w}{k}} = 0 \end{cases} \qquad \Rightarrow \qquad \gamma = \frac{\epsilon_r(\omega_r,k)}{\partial \epsilon_i(\omega_r,k)/\partial \omega_r} \tag{8.62}$$

  but if $\epsilon_i = 0$ there is no exchange of energy, that is inconsistent with the finite γ given by eq.(8.62). Moreover, the dispersion relation obtained from eq.(8.62) would not be consistent with the fluid limit. We conclude that this is not a physical case.

- $\epsilon_r \sim \epsilon_i$. We obtain

$$\epsilon_r(\omega_r,k) = 0 \qquad\qquad \epsilon_i(\omega_r,k) = 0 \tag{8.63}$$

  that gives the dispersion relation, but there is no exchange of energy.

- $\epsilon_r \gg \epsilon_i$. Now ϵ_i is of the order γ, thus the term $\gamma \partial \epsilon_i/\partial \omega_r$ is of the order γ^2 and can be neglected. The equations for ω_r and γ are decoupled:

$$\epsilon_r(\omega_r,k) \simeq 0 \tag{8.64}$$

$$\gamma = -\frac{\epsilon_i(\omega_r,k)}{\partial \epsilon_r(\omega_r,k)/\partial \omega_r} \tag{8.65}$$

  and the result is consistent with both the fluid limit and the possibility that wave and particles exchange energy.

We observe that only the third case gives physical results. Eq.(8.64) gives the real frequency[‡] ω_r and eq.(8.65) the damping rate: this is the new term originating from the Laplace transform approach introduced by Landau. As

$$\epsilon(\omega,k) = 1 - \sum_\alpha \frac{\omega_{\mathrm{p}\alpha}^2}{n_\alpha k^2} \int_{\mathcal{L}} \mathrm{d}u \frac{\frac{\mathrm{d}F_{\alpha 0}}{\mathrm{d}u}}{u - \frac{\omega}{k}} \tag{8.66}$$

applying the rule we derived for the Landau integral we can write

$$\begin{aligned} \epsilon(\omega_r,k) &= 1 - \sum \frac{\omega_{\mathrm{p}\alpha}^2}{n_\alpha k^2} \int_{\mathcal{L}} \mathrm{d}u \frac{\frac{\mathrm{d}F_{\alpha 0}}{\mathrm{d}u}}{u - \frac{\omega_r}{k}} \\ &= 1 - \sum \frac{\omega_{\mathrm{p}\alpha}^2}{n_\alpha k^2} \left\{ \mathrm{P.V.} \int_{-\infty}^{\infty} \mathrm{d}u \frac{\frac{\mathrm{d}F_{\alpha 0}}{\mathrm{d}u}}{u - \frac{\omega_r}{k}} + \mathrm{i}\pi \left.\frac{\mathrm{d}F_{\alpha 0}}{\mathrm{d}u}\right|_{u=\frac{\omega_r}{k}} \right\} \end{aligned} \tag{8.67}$$

thus

$$\begin{cases} \epsilon_r(\omega_r,k) & = 1 - \sum \frac{\omega_{\mathrm{p}\alpha}^2}{n_\alpha k^2} \, \mathrm{P.V.} \int_{-\infty}^{\infty} \mathrm{d}u \frac{\frac{\mathrm{d}F_{\alpha 0}}{\mathrm{d}u}}{u - \frac{\omega_r}{k}} \\ \epsilon_i(\omega_r,k) & = -\pi \sum \frac{\omega_{\mathrm{p}\alpha}^2}{n_\alpha k^2} \left.\frac{\mathrm{d}F_{\alpha 0}}{\mathrm{d}u}\right|_{u=\frac{\omega_r}{k}} \end{cases} \tag{8.68}$$

[‡] We already calculated the dispersion relation for Langmuir waves and for ion–acoustic waves in this way.

8.6.1 Why is the damping rate proportional to the slope of F_0?

We see from eq.(8.65) to eq.(8.68) that the damping rate is proportional to the slope of the equilibrium distribution function $F_{\alpha,0}$: $\gamma \propto \mathrm{d}F_{\alpha 0}/\mathrm{d}u|_{u=\frac{\omega_r}{k}}$.

Where does it come from? Consider particles with velocities just larger than the wave phase velocity $u \gtrsim \omega/k$. They can gain or lose energy depending on the relative phase of the wave — but if they gain energy, their velocity increases and they go out of the resonance: they can not exchange energy any more. If they lose energy, they slow down and stay longer in the resonance. So, overall, they *lose energy to the wave*.
The opposite holds for particles with velocities just below the phase velocity $u \lesssim \omega/k$. Those that gain energy from the wave remain in the resonance longer, and the net effect is that they *gain energy from the wave*.

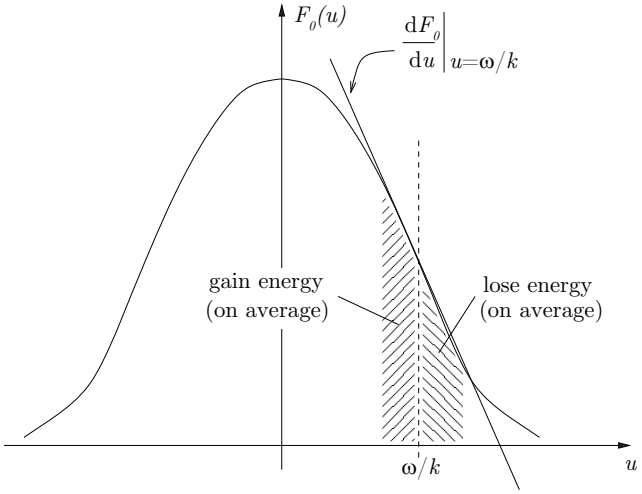

(a)

(b)

Figure 8.10: (a) Particles with $u \lesssim \omega/k$ will gain energy from the wave and particles with $u \gtrsim \omega/k$ will lose energy to the wave. As there are more particles which gain energy, the overall effect is that the wave is damped.
(b) Analogy with a surfer riding a wave.

The total energy balance is therefore given by the ratio between how many particles gain energy from the wave (with $u \lesssim \omega/k$) and how many give energy to the wave ($u \gtrsim \omega/k$). This balance can be deduced from the slope of $F_0(u)$ around the resonance $u \simeq \omega/k$ (figure 8.10).

A (very) qualitative analogy can be drawn with surfers trying to catch an ocean wave: to 'ride' the wave (i.e. to be pushed by it) the surfer must prepare himself or herself more or less at the speed of the wave ($u \simeq \omega/k$), but just a little slower.

By using the kinetic model for the plasma and the electrostatic approximation for the waves, we have demonstrated that waves can be damped even in the absence of collisions. The damping mechanism, referred to as Landau damping, resides in the interaction between waves and plasma particles. We have calculated the Landau damping rate, finding that

$$\gamma \propto \left.\frac{\mathrm{d}F_0}{\mathrm{d}u}\right|_{u=\omega/k} \tag{8.69}$$

i.e. the damping is proportional to the *slope* of the equilibrium distribution function at the wave phase velocity (the wave–particle resonance).
After the rigorous mathematical explanation, let us consider a simpler, more intuitive point of view.

8.7 An intuitive, semi-quantitative approach to Landau damping

Consider a charged particle in the field of a single e.s. wave. Its motion (in the one–dimensional case) can be described by

$$\frac{\mathrm{d}^2x}{\mathrm{d}t^2} = \frac{\mathrm{d}u}{\mathrm{d}t} = \frac{q}{m}E_0 e^{\mathrm{i}(kx-\omega t)} \tag{8.70}$$

As we are considering small amplitude waves, the perturbation to the motion due to the wave is small, and in the exponent we can set $x \simeq x_0 + u_0 t$ (unperturbed trajectory, or 'characteristic'), where u_0 is the velocity at $t = 0$. The integration yields

$$u(t) = \frac{q}{m}E_0 e^{\mathrm{i}kx_0}\frac{e^{\mathrm{i}(ku_0-\omega)t}}{\mathrm{i}(ku_0-\omega)} + C \tag{8.71}$$

and with the initial condition $u(t=0) = u_0$

$$C = u_0 - \frac{q}{m}E_0 e^{\mathrm{i}kx_0}\frac{1}{\mathrm{i}(ku_0-\omega)} \tag{8.72}$$

and then

$$u - u_0 = \frac{q}{m}E_0 e^{\mathrm{i}kx_0}\frac{e^{\mathrm{i}(ku_0-\omega)t}-1}{\mathrm{i}(ku_0-\omega)} \tag{8.73}$$

For resonant particles ($ku_0 - \omega \simeq 0$) we can expand the exponential

$$e^{\mathrm{i}(ku_0-\omega)t} \approx 1 + \mathrm{i}(ku_0-\omega)t + ... \tag{8.74}$$

and obtain

$$u - u_0 \simeq \frac{q}{m}E_0 e^{\mathrm{i}kx_0}t \tag{8.75}$$

So the deviation from the unperturbed velocity grows linearly with t (within the approximations adopted here) for the resonant particles. These are the ones that are responsible for the instability or the damping of the wave. Note that the deviation can have different sign and values depending on the phase term e^{ikx_0}.

8.8 Stability criteria

The kinetic theory allows us to gain a deeper insight into the *stability* of a plasma. We can model waves that we already found in the fluid model, characterised in general by variations of some *macroscopic* quantities like density and potential. But we can also treat more subtle problems, involving changes in phase space rather than in real space. In this case the interaction concerns the waves and a small fraction of particles, the resonant ones. The instability is then "localised" in phase space, and contrary to fluid instabilities we observe no bulk motion. We call this type of waves *micro–instabilities*. Micro-instabilities are important, for example, to understand anomalous transport, i.e. the transport that cannot be explained in terms of collisional process.
Note: we deal with waves here ($\epsilon = 0$), not ballistic modes.

8.8.1 1st Stability Criterion (Norton–Gardner Theorem)

"If the total distribution function F_0 has only one maximum then electrostatic waves are stable"(*).
To prove this statement we start from the dispersion relation

$$\begin{aligned}
\epsilon(\mathrm{i}p,k) &= 1-\sum_\alpha \frac{\omega_{\mathrm{p}\alpha}^2}{n_\alpha k^2}\int_{\mathcal{L}}\frac{\frac{\mathrm{d}F_{\alpha 0}}{\mathrm{d}u}}{u-\frac{\mathrm{i}p}{k}}\mathrm{d}u \\
&= 1-\frac{\omega_{\mathrm{pe}}^2}{n_e k^2}\int_{\mathcal{L}}\frac{\frac{\mathrm{d}F_{e0}}{\mathrm{d}u}}{u-\frac{\mathrm{i}p}{k}}\mathrm{d}u-\sum_{\alpha\neq e}\frac{\omega_{\mathrm{p}\alpha}^2}{n_\alpha k^2}\int_{\mathcal{L}}\frac{\frac{\mathrm{d}F_{\alpha 0}}{\mathrm{d}u}}{u-\frac{\mathrm{i}p}{k}}\mathrm{d}u \\
&= 1-\frac{\omega_{\mathrm{pe}}^2}{n_e k^2}\int_{\mathcal{L}}\frac{\frac{\mathrm{d}}{\mathrm{d}u}\left(F_{e0}+\sum_{\alpha\neq e}Z_\alpha^2\frac{m_e}{m_\alpha}F_{\alpha 0}\right)}{u-\frac{\mathrm{i}p}{k}}\mathrm{d}u \\
&= 1-\frac{\omega_{\mathrm{pe}}^2}{n_e k^2}\int_{\mathcal{L}}\frac{\frac{\mathrm{d}F_0}{\mathrm{d}u}}{u-\frac{\mathrm{i}p}{k}}\mathrm{d}u
\end{aligned}$$

where we have introduced the total distribution function

$$F_0 := F_{e0}+\sum_{\alpha\neq e}Z_\alpha^2\frac{m_e}{m_\alpha}F_{\alpha 0} \qquad (F_0\sim F_{e0}) \tag{8.76}$$

and the integral must be calculated according to the Landau rules. We replace $\mathrm{i}p = i(-\mathrm{i}\omega) = \omega_r + \mathrm{i}\gamma$ and show that the dispersion relation cannot be satisfied if $\gamma > 0$ (instability). In this case the Landau integral can be evaluated on the real axis

$$1-\frac{\omega_{\mathrm{pe}}^2}{k^2 n_e}\int_{-\infty}^{\infty}\mathrm{d}u\frac{\mathrm{d}F_0}{\mathrm{d}u}\frac{(u-\frac{\omega_r}{k})+\mathrm{i}\frac{\gamma}{k}}{(u-\frac{\omega_r}{k})^2+(\frac{\gamma}{k})^2}=0 \tag{8.77}$$

so the equations for real and imaginary parts can be identified:

$$\text{Real part}: \qquad 1-\frac{\omega_{\mathrm{pe}}^2}{k^2 n_e}\int_{-\infty}^{\infty}\mathrm{d}u\frac{\mathrm{d}F_0}{\mathrm{d}u}\frac{u-\frac{\omega_r}{k}}{(u-\frac{\omega_r}{k})^2+(\frac{\gamma}{k})^2}=0 \tag{8.78}$$

$$\text{Imaginary part}: \qquad \int_{-\infty}^{\infty}\mathrm{d}u\frac{\mathrm{d}F_0}{\mathrm{d}u}\frac{1}{(u-\frac{\omega_r}{k})^2+(\frac{\gamma}{k})^2}=0 \tag{8.79}$$

(*) This is also an intuitive result: if a Maxwellian for example had unstable character, plasma "thermodynamics" (based on an equilibrium state) would not make sense.

Doing a change of variable $u' = u - u_{\max}$, where $u_{\max}$ is the position of the maximum of F_0, we get

$$\text{Real part}: \quad 1 - \frac{\omega_{pe}^2}{k^2 n_e}\left(u_{\max} - \frac{\omega_r}{k}\right)\int_{-\infty}^{\infty} \mathrm{d}u' \frac{\mathrm{d}F_0}{\mathrm{d}u'} \frac{1}{(u' + u_{\max} - \frac{\omega_r}{k})^2 + (\frac{\gamma}{k})^2} - \frac{\omega_{pe}^2}{k^2 n_e}\int_{-\infty}^{\infty} \mathrm{d}u' \frac{\mathrm{d}F_0}{\mathrm{d}u'} \frac{u'}{(u' + u_{\max} - \frac{\omega_r}{k})^2 + (\frac{\gamma}{k})^2} = 0 \tag{8.80}$$

$$\text{Imaginary part}: \quad \int_{-\infty}^{\infty} \mathrm{d}u' \frac{\mathrm{d}F_0}{\mathrm{d}u'} \frac{1}{(u' + u_{\max} - \frac{\omega_r}{k})^2 + (\frac{\gamma}{k})^2} = 0 \tag{8.81}$$

Using the second equation in the first we have

$$1 - \frac{\omega_{pe}^2}{k^2 n_e}\int_{-\infty}^{\infty} \mathrm{d}u' \frac{u' \frac{\mathrm{d}F_0}{\mathrm{d}u'}}{(u' + u_{\max} - \frac{\omega_r}{k})^2 + (\frac{\gamma}{k})^2} = 0 \tag{8.82}$$

But if F_0 has only one maximum it must satisfy

$$u' \frac{\mathrm{d}F_0}{\mathrm{d}u'} = (u - u_{\max}) \frac{\mathrm{d}F_0}{\mathrm{d}(u - u_{\max})} \leq 0, \qquad \forall\, u' \in \mathbb{R} \tag{8.83}$$

Thus we can write

$$1 + \frac{\omega_{pe}^2}{k^2 n_e}\int_{-\infty}^{\infty} \mathrm{d}u' \frac{\left|u' \frac{\mathrm{d}F_0}{\mathrm{d}u'}\right|}{(u' + u_{\max} - \frac{\omega_r}{k})^2 + (\frac{\gamma}{k})^2} > 0 \tag{8.84}$$

where we see clearly that the left hand side is always positive. So the dispersion relation cannot be satisfied and the statement is proven.

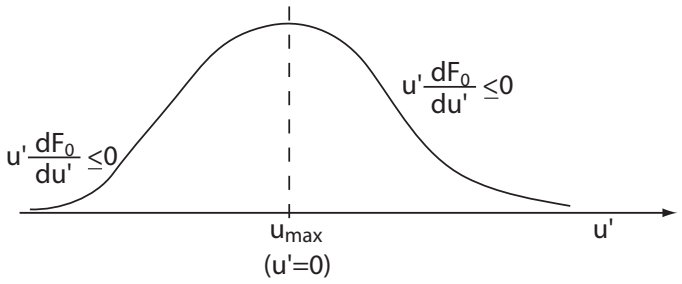

Figure 8.11: Sketch illustrating the inequality (8.83). For $u' \leq 0$, $\frac{\mathrm{d}F_0}{\mathrm{d}u'}$ is ≥ 0; for $u' \geq 0$, $\frac{\mathrm{d}F_0}{\mathrm{d}u'}$ is ≤ 0.

8.8.2 Nyquist Criterion for Instability

So far we have seen a *sufficient* condition for *stability*, i.e. a *necessary* condition for *instability*: F_0 must have at least one minimum. Now we consider a *sufficient* condition for *instability* ("Nyquist criterion"). We consider the Landau integral as a *mapping* (figure 8.12).

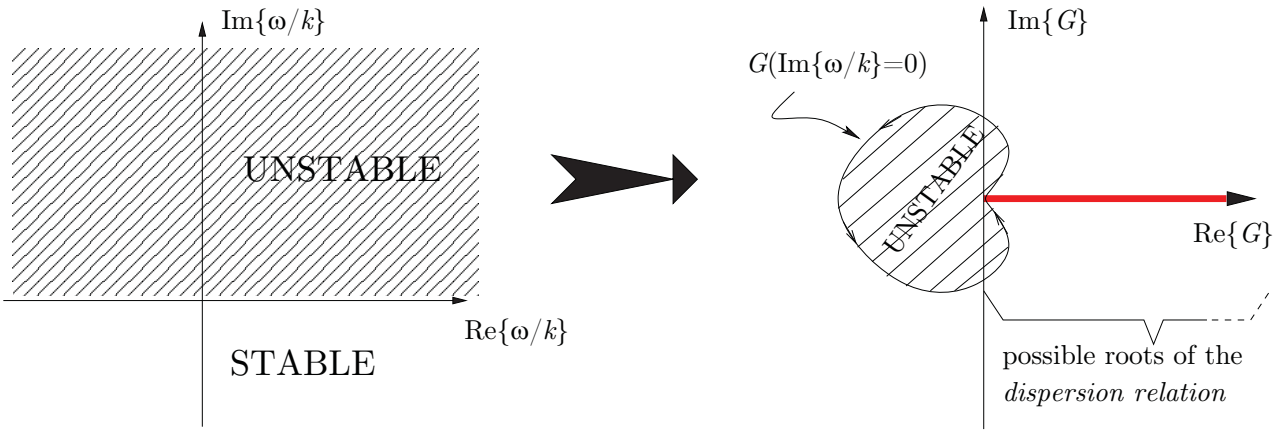

Figure 8.12: G as a mapping. In the figure on the right, the thick red line indicates possible roots of the dispersion relation. In the case shown here there are no unstable roots.

$$G : \mathbb{C} \to \mathbb{C}, \qquad \tfrac{\omega}{k} \mapsto G\left(\tfrac{\omega}{k}\right) = \int_{\mathcal{L}} \frac{\frac{\mathrm{d}F_0}{\mathrm{d}u}}{u - \frac{\omega}{k}} \mathrm{d}u, \qquad k \in \mathbb{R}^+ \tag{8.85}$$

where F_0 has been defined in (8.76). With this definition

$$\epsilon(\omega, k) = 1 - \frac{\omega_{\mathrm{pe}}^2}{n_e k^2} G\left(\tfrac{\omega}{k}\right) = 0 \tag{8.86}$$

is the dispersion relation, or

$$G\left(\tfrac{\omega}{k}\right) = \frac{n_e k^2}{\omega_{\mathrm{pe}}^2} \in \mathbb{R}^+ \tag{8.87}$$

So for roots of the dispersion relation, G must assume *positive real values*. As the limit between the stable and the unstable domain is the line

$$\Im\left\{\tfrac{\omega}{k}\right\} = 0 \tag{8.88}$$

we are interested to map it using G and see if any of the solutions of the dispersion relation $G\left(\tfrac{\omega}{k}\right) \in \mathbb{R}^+$ lies in the unstable domain $G\left(\Im\left\{\tfrac{\omega}{k}\right\} > 0\right)$. Or in other words: the question is whether the mapping of the unstable domain, $G\left(\Im\left\{\tfrac{\omega}{k}\right\} > 0\right)$ includes parts of the positive real axis of the G–plane (figure 8.13).

NOTE: for $\frac{\omega}{k} \to \quad \infty$, we have $\Re(G) \to 0^+$ and $\Im(G) \to 0^-$
for $\frac{\omega}{k} \to -\infty$, we have $\Re(G) \to 0^+$ and $\Im(G) \to 0^+$

Let us examine what happens when the mapping of the limit line $G\left(\Im\left\{\tfrac{\omega}{k}\right\} = 0\right)$ crosses the real axis $\Im\{G\} = 0$. According to Landau we have

$$G\left(\tfrac{\omega}{k}\right) = \mathrm{P.V.} \int \frac{\frac{\mathrm{d}F_0}{\mathrm{d}u}}{u - \frac{\omega}{k}} \mathrm{d}u + \mathrm{i}\pi \frac{\mathrm{d}F_0}{\mathrm{d}u}\bigg|_{u=\omega/k} \tag{8.89}$$

Since $\Im\left\{\frac{\omega}{k}\right\} = 0$, the imaginary part of G is

$$\Im(G) = \pi \frac{\mathrm{d}F_0}{\mathrm{d}u}\bigg|_{u=\omega/k} \tag{8.90}$$

thus

$$G\left(\Im\left\{\frac{\omega}{k}\right\} = 0\right) \in \mathbb{R} \quad \Longleftrightarrow \quad \frac{\mathrm{d}F_0}{\mathrm{d}u}\bigg|_{u=\omega/k} = 0 \tag{8.91}$$

i.e. crossings of the limit line with the real axis in the G–plane occur at *extrema of the equilibrium distribution function* F_0 (figure 8.13).

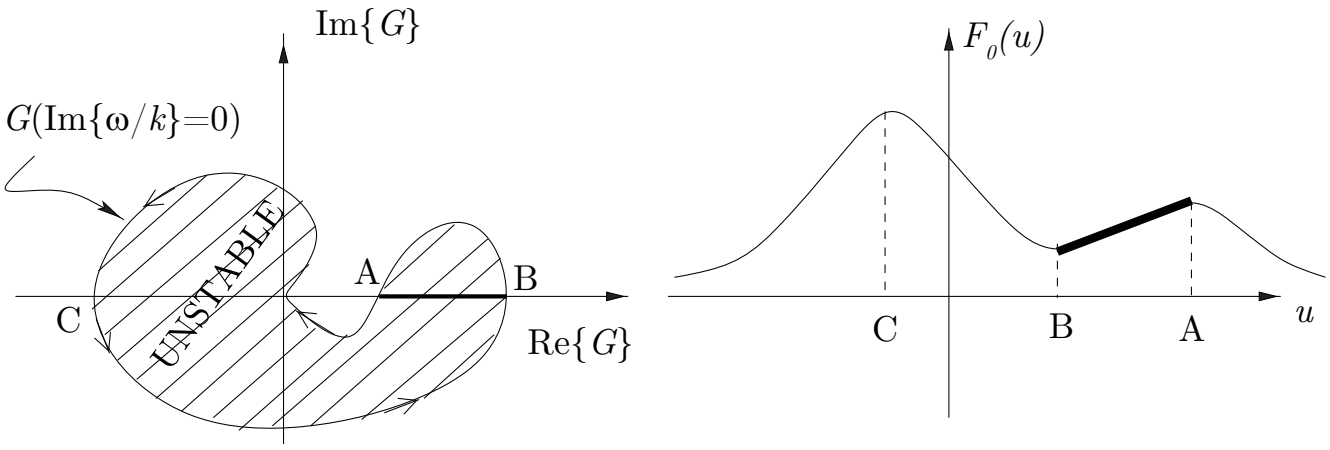

Figure 8.13: Example of instability (note that the curve can be more complex). The number of crossings of $\Im\{G\} = 0$, i.e. points A, B, C, corresponds to the number of extrema of $F_0(u)$. Here B represents a minimum, while A, C are maxima. Roots of the dispersion relation between A and B are then unstable.

The *direction* in which the limit line passes through the real axis tells us which kind we have:[(†)]

⋆ $\Im\{G\}$: from < 0 to $> 0 \Longleftrightarrow \frac{\mathrm{d}F_0}{\mathrm{d}u}$: from < 0 to $> 0 \Longrightarrow$ minimum of F_0

⋆ $\Im\{G\}$: from > 0 to $< 0 \Longleftrightarrow \frac{\mathrm{d}F_0}{\mathrm{d}u}$: from > 0 to $< 0 \Longrightarrow$ maximum of F_0

The presence of a minimum in the distribution function is necessary but not sufficient to have instability. To have a *sufficient* condition for instability we have to demand additionally that

$$\Re\left\{G\left(\tfrac{\omega}{k}\right)\right\}_{\omega/k=u_{\min}} > 0 \tag{8.92}$$

(†) A little "detail" in this argumentation is that we assume that the orientation of the limit line is always *counter–clockwise*. Let us argument in the following way: take the most simple physical case with F_0 having only one maximum. Then the argumentation of section 8.8.1 tells us that the maximum is mapped to the negative real axis of the G–plane. Furthermore we know that the points $\omega/k = \pm\infty$ are both mapped to $G = 0$, so the orientation of the limit line is in fact counter–clockwise in this case. In order to produce the other cases we change F_0 *continuously* and within the limitations of its physical sense, so we will have a *slightly* deformed limit line, which will not change its orientation for non–pathological F_0.

i.e. we cross the $\Im\{G\} = 0$ axis on the right side. Integration of eq.(8.89) yields

$$
\begin{aligned}
&\Re\big\{G(\tfrac{\omega}{k})\big\}_{\omega/k=u_{\min}} = \text{P.V.}\int_{-\infty}^{\infty} \frac{\frac{\mathrm{d}F_0}{\mathrm{d}u}}{u-u_{\min}}\mathrm{d}u \\
= &\lim_{\varepsilon\to 0}\left\{\int_{-\infty}^{u_{\min}-\varepsilon} \frac{\frac{\mathrm{d}F_0}{\mathrm{d}u}}{u-u_{\min}}\mathrm{d}u + \int_{u_{\min}+\varepsilon}^{\infty} \frac{\frac{\mathrm{d}F_0}{\mathrm{d}u}}{u-u_{\min}}\mathrm{d}u\right\} \\
= &\lim_{\varepsilon\to 0}\left\{\frac{F_0(u)}{u-u_{\min}}\bigg|_{-\infty}^{u_{\min}-\varepsilon} + \frac{F_0(u)}{u-u_{\min}}\bigg|_{u_{\min}+\varepsilon}^{\infty}\right. \\
&\qquad \left. + \int_{\infty}^{u_{\min}-\varepsilon} \frac{F_0(u)}{(u-u_{\min})^2}\mathrm{d}u + \int_{u_{\min}+\varepsilon}^{\infty} \frac{F_0(u)}{(u-u_{\min})^2}\mathrm{d}u\right\} \\
= &\lim_{\varepsilon\to 0}\left\{\frac{F_0(u_{\min}-\varepsilon)}{-\varepsilon} - \frac{F_0(u_{\min}+\varepsilon)}{\varepsilon}\right. \\
&\qquad \left. + \int_{-\infty}^{u_{\min}-\varepsilon} \frac{F_0(u)}{(u-u_{\min})^2}\mathrm{d}u + \int_{u_{\min}+\varepsilon}^{\infty} \frac{F_0(u)}{(u-u_{\min})^2}\mathrm{d}u\right\} \\
= &\lim_{\varepsilon\to 0}\left\{-2\frac{F_0(u_{\min})}{\varepsilon} + \int_{-\infty}^{u_{\min}-\varepsilon} \frac{F_0(u)}{(u-u_{\min})^2}\mathrm{d}u + \int_{u_{\min}+\varepsilon}^{\infty} \frac{F_0(u)}{(u-u_{\min})^2}\mathrm{d}u\right\} \\
= &\lim_{\varepsilon\to 0}\left\{-\int_{-\infty}^{u_{\min}-\varepsilon} \frac{F_0(u_{\min})}{(u-u_{\min})^2}\mathrm{d}u - \int_{u_{\min}+\varepsilon}^{\infty} \frac{F_0(u_{\min})}{(u-u_{\min})^2}\mathrm{d}u\right. \\
&\qquad \left. + \int_{\infty}^{u_{\min}-\varepsilon} \frac{F_0(u)}{(u-u_{\min})^2}\mathrm{d}u + \int_{u_{\min}+\varepsilon}^{\infty} \frac{F_0(u)}{(u-u_{\min})^2}\mathrm{d}u\right\} \\
= &\lim_{\varepsilon\to 0}\left\{\int_{-\infty}^{u_{\min}-\varepsilon} \frac{F_0(u)-F_0(u_{\min})}{(u-u_{\min})^2}\mathrm{d}u + \int_{u_{\min}+\varepsilon}^{\infty} \frac{F_0(u)-F_0(u_{\min})}{(u-u_{\min})^2}\mathrm{d}u\right\} \\
= &\ \text{P.V.}\int_{-\infty}^{\infty} \frac{F_0(u)-F_0(u_{\min})}{(u-u_{\min})^2}\mathrm{d}u \equiv \int_{-\infty}^{\infty} \frac{F_0(u)-F_0(u_{\min})}{(u-u_{\min})^2}\mathrm{d}u
\end{aligned}
\tag{8.93}
$$

where we have used the following approximation $F_0(u_{\min}-\varepsilon) + F_0(u_{\min}+\varepsilon) \simeq 2F_0(u_{\min})$ between the 4th and 5th line and between the 5th and 6th line we used the identity

$$
\frac{2}{\varepsilon} = \int_{-\infty}^{u_{\min}-\varepsilon} \frac{\mathrm{d}u}{(u-u_{\min})^2} + \int_{u_{\min}+\varepsilon}^{\infty} \frac{\mathrm{d}u}{(u-u_{\min})^2} \tag{8.94}
$$

Note that as $u_{\min}$ is a minimum the last integral in eq.(8.93) is not singular[‡], thus there is no need to write the principal value. Finally we have the following *sufficient condition for instability*:

- F_0 has a minimum at $u_{\min}$

and

- $\displaystyle\int_{-\infty}^{\infty} \frac{F_0(u)-F_0(u_{\min})}{(u-u_{\min})^2}\mathrm{d}u > 0$

The second point means that the minimum must be "sufficiently deep" (figure 8.14).

[‡] To be seen writing the Taylor series of $F_0(u)$ around $u_{\min}$ and using $\mathrm{d}F_0/\mathrm{d}u|_{u_{\min}} = 0$.

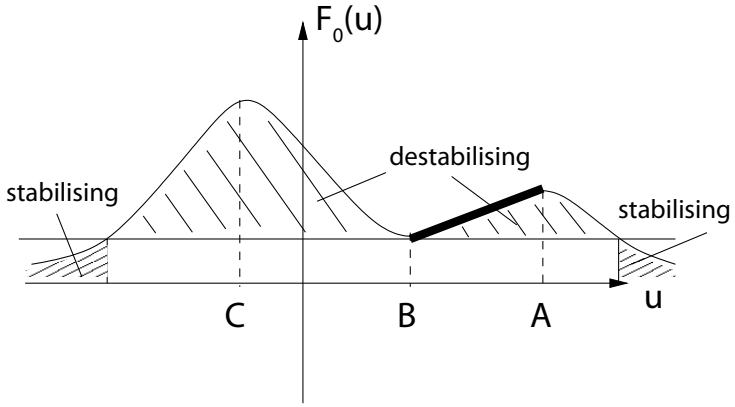

Figure 8.14: The minimum in F_0 (point B) has to be sufficiently "deep" for instability. All points for which $F_0(u) > F_0(u_{min})$ are destabilizing and all points for which $F_0(u) < F_0(u_{min})$ are stabilizing, but of course only those close to the region $u \sim u_{min}$ give a significant contribution.

Chapter 9 Waves in a hot magnetized plasma (kinetic model)

We'll look at some features of waves in a plasma described by the kinetic model in the presence of an equilibrium magnetic field, $\mathbf{B}_0$. The main concepts of wave–particle resonance, instability and (collisionless) Landau damping remain the same as in the case of $\mathbf{B}_0 = 0$, but new features appear. We'll review them considering only the main steps of the calculation.

We start from the general wave equation

$$\left\{ N^2 \left[\frac{\mathbf{kk}}{k^2} - \mathbb{1} \right] + \underline{\boldsymbol{\epsilon}} \right\} \cdot \mathbf{E} = 0 \tag{9.1}$$

where $N = kc/\omega$ and $\underline{\boldsymbol{\epsilon}} = \mathbb{1} + \frac{i}{\epsilon_0 \omega} \underline{\boldsymbol{\sigma}}$. For electrostatic waves the wave equation becomes

$$\underline{\boldsymbol{\epsilon}} \cdot \mathbf{E} = 0 \tag{9.2}$$

The problem is to find $\underline{\boldsymbol{\epsilon}}$ (or $\underline{\boldsymbol{\sigma}}$). To do it in the kinetic model, we start from the Vlasov equation, with $\mathbf{B}_0 \neq 0$, and linearise(*)

$$\frac{\partial f_1}{\partial t} + \mathbf{v} \cdot \frac{\partial f_1}{\partial \mathbf{x}} + \frac{q}{m}(\mathbf{E} + \mathbf{v} \times \mathbf{B}) \cdot \frac{\partial f_0}{\partial \mathbf{v}} + \frac{q}{m}(\mathbf{v} \times \mathbf{B}_0) \cdot \frac{\partial f_1}{\partial \mathbf{v}} = 0 \tag{9.4}$$

where we wrote $\mathbf{E} \equiv \mathbf{E}_1$ and $\mathbf{B} \equiv \mathbf{B}_1$ for simplicity, or

$$\frac{\mathrm{D} f_1}{\mathrm{D} t} = -\frac{q}{m}(\mathbf{E} + \mathbf{v} \times \mathbf{B}) \cdot \frac{\partial f_0}{\partial \mathbf{v}} \tag{9.5}$$

where

$$\frac{\mathrm{D}}{\mathrm{D} t} \equiv \frac{\partial}{\partial t} + \mathbf{v} \cdot \frac{\partial}{\partial \mathbf{x}} + \frac{q}{m}(\mathbf{E}_0 + \mathbf{v} \times \mathbf{B}_0) \cdot \frac{\partial}{\partial \mathbf{v}} = \frac{\partial}{\partial t} + \mathbf{v} \cdot \frac{\partial}{\partial \mathbf{x}} + \frac{q}{m}(\mathbf{v} \times \mathbf{B}_0) \cdot \frac{\partial}{\partial \mathbf{v}} \tag{9.6}$$

is the derivative along the unperturbed trajectories

$$\dot{\mathbf{x}} = \mathbf{v} \tag{9.7}$$

$$\dot{\mathbf{v}} = \frac{q}{m} \mathbf{v} \times \mathbf{B}_0 \tag{9.8}$$

Assuming that $f_1 \to 0$ as $t \to -\infty$, we can write

$$f_1(\mathbf{x}, \mathbf{v}, t) = -\frac{q}{m} \int_{-\infty}^{t} \mathrm{d}t' \Big[\mathbf{E}(\mathbf{x}', t') + \mathbf{v}' \times \mathbf{B}(\mathbf{x}', t') \Big] \cdot \frac{\partial f_0(\mathbf{v}')}{\partial \mathbf{v}'} \tag{9.9}$$

where $(\mathbf{x}', \mathbf{v}')$ are the unperturbed trajectories ('characteristics') that pass through $(\mathbf{x}, \mathbf{v})$ at $t' = t$. Let's express $\mathbf{B}$ as a function of $\mathbf{E}$:

$$\nabla \times \mathbf{E} = -\frac{\partial \mathbf{B}}{\partial t} \qquad \Longleftrightarrow \qquad \mathbf{B} = \frac{\mathbf{k} \times \mathbf{E}}{\omega} \tag{9.10}$$

(*) Note that

$$(\mathbf{v} \times \mathbf{B}_0) \cdot \frac{\partial f_0}{\partial \mathbf{v}} = 0 \tag{9.3}$$

in order to have an equilibrium state ($\mathrm{d} f_0 / \mathrm{d} t = 0$). Thus $f_0 \equiv f_0(v_\parallel, v_\perp)$, where $v_\parallel$ and $v_\perp$ are constants of motion.

We consider all perturbed quantities

$$\propto e^{\mathrm{i}(\mathbf{k}\cdot\mathbf{x}-\omega t)+\eta t} \tag{9.11}$$

where η is a small positive quantity which makes the perturbation vanish for $t \to -\infty$. So

$$f_1(\mathbf{v})e^{\mathrm{i}(\mathbf{k}\cdot\mathbf{x}-\omega t)+\eta t} = -\frac{q}{m}\int_{-\infty}^{t} \mathrm{d}t' \left\{ \left[1 - \frac{\mathbf{v}'\cdot\mathbf{k}}{\omega}\right]\mathbf{E} + \frac{\mathbf{v}'\cdot\mathbf{E}}{\omega}\mathbf{k} \right\} \cdot \frac{\partial f_0}{\partial \mathbf{v}'} e^{\mathrm{i}(\mathbf{k}\cdot\mathbf{x}'-\omega t')+\eta t'} \tag{9.12}$$

or

$$f_1(\mathbf{v}) = -\frac{q}{m}\int_{-\infty}^{t} \mathrm{d}t' \left\{ \left[1 - \frac{\mathbf{v}'\cdot\mathbf{k}}{\omega}\right]\mathbf{E} + \frac{\mathbf{v}'\cdot\mathbf{E}}{\omega}\mathbf{k} \right\} \cdot \frac{\partial f_0}{\partial \mathbf{v}'} e^{\mathrm{i}\mathbf{k}\cdot(\mathbf{x}'-\mathbf{x})-(i\omega-\eta)(t'-t)} \tag{9.13}$$

We now have to plug in the unperturbed trajectories, $\mathbf{B}_0 = B_0\mathbf{e}_z$, $\frac{\mathrm{d}\mathbf{v}'}{\mathrm{d}t'} = \Omega(\mathbf{v}'\times\mathbf{e}_z)$, or

$$\mathbf{v}' = \begin{pmatrix} \cos\Omega(t'-t) & \sin\Omega(t'-t) & 0 \\ -\sin\Omega(t'-t) & \cos\Omega(t'-t) & 0 \\ 0 & 0 & 1 \end{pmatrix} \cdot \mathbf{v} \tag{9.14}$$

Using cylindrical coordinates

$$v_x = v_\perp \cos\theta \tag{9.15}$$
$$v_y = v_\perp \sin\theta \tag{9.16}$$
$$v_z = v_\parallel \tag{9.17}$$

we can write this as

$$\mathbf{v}' = \begin{pmatrix} v_\perp \cos\{\theta - \Omega(t'-t)\} \\ v_\perp \sin\{\theta - \Omega(t'-t)\} \\ v_\parallel \end{pmatrix} \tag{9.18}$$

Finally we obtain for the positions

$$\mathbf{x}' - \mathbf{x} = \frac{1}{\Omega}\begin{pmatrix} -v_\perp\left[\sin\left\{\theta-\Omega(t'-t)\right\} - \sin\theta\right] \\ v_\perp\left[\cos\left\{\theta-\Omega(t'-t)\right\} - \cos\theta\right] \\ v_\parallel\Omega(t'-t) \end{pmatrix} \tag{9.19}$$

Without restriction of generality we choose $\mathbf{k} = (0, k_y, k_z)$ and define $\tau := t' - t$.

The *key point* is the exponential in the integral which becomes

$$\begin{aligned}
&\exp\Big[\mathrm{i}\mathbf{k}\cdot(\mathbf{x}'-\mathbf{x})\Big] = \exp\left\{\mathrm{i}\frac{k_y v_\perp}{\Omega}\Big[\cos(\theta-\Omega\tau)-\cos\theta\Big] + \mathrm{i}k_z v_\parallel \tau\right\} \\
= \;& \exp\left\{\mathrm{i}\frac{k_y v_\perp}{\Omega}\left[\sin\left(\theta-\Omega\tau+\frac{\pi}{2}\right)+\sin\left(-\theta-\frac{\pi}{2}\right)\right] + \mathrm{i}k_z v_\parallel\tau\right\} \\
= \;& \sum_{n=-\infty}^{\infty} J_n\left(\tfrac{k_y v_\perp}{\Omega}\right)\exp\left\{\mathrm{i}\,n\left(\theta-\Omega\tau+\frac{\pi}{2}\right)\right\} \\
&\qquad \times \sum_{m=-\infty}^{\infty} J_m\left(\tfrac{k_y v_\perp}{\Omega}\right)\exp\left\{\mathrm{i}\,m\left(-\theta-\frac{\pi}{2}\right)\right\}\exp\left\{\mathrm{i}k_z v_\parallel\tau\right\} \\
= \;& \sum_{n=-\infty}^{\infty}\sum_{m=-\infty}^{\infty} \mathrm{i}^{n-m} J_n\left(\tfrac{k_y v_\perp}{\Omega}\right) J_m\left(\tfrac{k_y v_\perp}{\Omega}\right)\exp\left\{\mathrm{i}\,n(\theta-\Omega\tau) - \mathrm{i}\,m\theta + \mathrm{i}k_z v_\parallel\tau\right\},
\end{aligned}$$

where we used the generator of Bessel functions $e^{\mathrm{i}a\sin\xi} = \sum_{n=-\infty}^{\infty} J_n(a)e^{\mathrm{i}n\xi}$. So the perturbed distribution function contains an infinite sum of *harmonics* of Ω, weighted by the Bessel functions $J_n\left(\frac{k_y v_\perp}{\Omega}\right)$. This is a *finite Larmor radius effect*, as $\frac{k_y v_\perp}{\Omega} = k_y\rho$ is the ratio between the Larmor radius and the wavelength $\lambda \propto k_y^{-1}$: the effect is due to the fact that the particles feel a different wave field during their gyro–motion. If $k_y\rho \ll 1$, then the effect tends to disappear.

The next step is to replace the $\mathbf{v}'$ in the integrand by eq.(9.18) and to calculate the current density

$$\mathbf{j} = \sum_\alpha q_\alpha n_{\alpha 0} \int \mathrm{d}^3v\, \mathbf{v}\, f_{\alpha 1}(\mathbf{v}) \tag{9.20}$$

Then the conductivity tensor $\underline{\boldsymbol{\sigma}}$ can be identified and we automatically have the dielectric tensor $\underline{\boldsymbol{\epsilon}}$. The velocity integration is done in cylindrical coordinates $\mathrm{d}^3v = v_\perp \mathrm{d}v_\perp \mathrm{d}v_\parallel \mathrm{d}\theta$, where the θ–integration

$$\int_0^{2\pi} \mathrm{d}\theta\, e^{\mathrm{i}(n-m)\theta} = 2\pi\delta_{n,m} \tag{9.21}$$

reduces the double sum to a single one. The details of the rather lengthy calculation can be found in [1](10–4). The result is

$$\underline{\boldsymbol{\epsilon}} = \left[1 - \sum_\alpha \frac{\omega_{\mathrm{p}\alpha}^2}{\omega^2}\right]\mathbb{1} - \sum_\alpha \frac{\omega_{\mathrm{p}\alpha}^2}{\omega^2 n_{\alpha 0}} \sum_n \int \mathrm{d}^3v\, \frac{\underline{\mathbf{T}}_\alpha(v_\perp, v_\parallel)}{k_z v_\parallel - \omega + n\Omega_\alpha} \left[\frac{n\Omega_\alpha}{v_\perp}\frac{\partial f_{\alpha 0}}{\partial v_\perp} + k_z \frac{\partial f_{\alpha 0}}{\partial v_\parallel}\right] \tag{9.22}$$

with

$$\underline{\mathbf{T}}_\alpha(v_\perp, v_\parallel) = \begin{pmatrix} v_\perp^2 J_n'^2 & \frac{\mathrm{i}nv_\perp^2}{a_\alpha} J_n J_n' & \mathrm{i}v_\perp v_\parallel J_n J_n' \\ -\frac{\mathrm{i}nv_\perp^2}{a_\alpha} J_n J_n' & \frac{n^2 v_\perp^2}{a_\alpha^2} J_n^2 & \frac{v_\perp v_\parallel}{a_\alpha} n J_n^2 \\ -\mathrm{i}v_\perp v_\parallel J_n J_n' & \frac{v_\perp v_\parallel}{a_\alpha} n J_n^2 & v_\parallel^2 J_n^2 \end{pmatrix} \tag{9.23}$$

where $a_\alpha \equiv \frac{k_y v_\perp}{\Omega_\alpha}$ is the argument of the Bessel functions, and J' means the derivative with respect to the argument. Here we note the resonant denominator $k_z v_\parallel - \omega + n\Omega_\alpha$, which can be interpreted as Doppler shifted cyclotron resonances

$$\omega - k_z v_\parallel = n\Omega_\alpha \tag{9.24}$$

9.0.3 Perpendicular Propagation ($k_z = 0$)

In the case of purely perpendicular propagation ($k_z = 0$), the resonances are simply $\omega = n\Omega_\alpha$. These resonances, again, are a finite Larmor radius effect. If $k_y\rho \ll 1$, only the low–order resonances are important, as the "weight" given by the Bessel functions goes down as $(k_y\rho)^{|n|}$, i.e. rapidly with n.

Note that, for $k_z \neq 0$ (k_z can be very small, but in practice it is difficult to have k_z exactly zero), the resonance $\omega = n\Omega_\alpha + k_z v_\parallel$ is satisfied for different values of $\omega - n\Omega_\alpha$. For a whole distribution characterized by a thermal velocity $v_{\mathrm{th},\parallel}$, the 'width' of the resonance, $(\omega - n\Omega_\alpha)_{\max} - (\omega - n\Omega_\alpha)_{\min}$ is of the order of $k_z v_{\mathrm{th},\parallel}$. Thus, for a toroidal plasma, where $|B| \propto R^{-1}$, the cyclotron resonance layer has a finite width, as illustrated in figure 9.1.

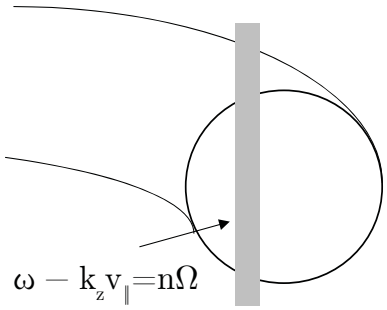

Figure 9.1: Sketch of the toroidal vessel with the width of the resonance layer.

Such a finite width layer exists also if $k_z = 0$, mainly for electrons, because of relativistic effects, which should be included as corrections to the mass ($m = \gamma m_0$) in the cyclotron frequency

$$\omega - \frac{n\Omega_\alpha}{\gamma} = 0 \qquad \gamma = \left(1 - \frac{v^2}{c^2}\right)^{-1/2} \geqslant 1$$

The resonance becomes in this case velocity dependent and it is a real wave-particle resonance. The absorption at the cyclotron wave-particle resonances can be quite efficient, and is used to heat particles (in particular electrons, if $k_z = 0$) in fusion experiments.

The resonances at $\omega = n\Omega$ were not at all present in fluid theory and represent a very useful mechanism to heat and drive current in fusion plasmas (when in practice, the wave injection can only be perpendicular to $\mathbf{B_0}$).
The absorption mechanism can be qualitatively described similarly to the Landau damping studied for $\mathbf{B_0} = 0$.

$\omega = \Omega$: At the *fundamental* frequency ($\omega = \Omega$), strong interaction from a distribution of particles is possible only for relatively large wave-lengths $k_y\rho_L \ll 1$ (or $\lambda \gg \rho_L$). If we had the opposite case, $\lambda \sim< \rho_L$, then the particle motion would not be able to stay in phase with the wave, a necessary condition for efficient energy exchange (see Fig.9.2).

$\omega = 2\Omega$: At the first harmonic, strong interaction is possible if $k_y\rho_L \sim 1$. When $\lambda \sim \rho_L$ the particle can encounter a field of the opposite sign in the second half of its Larmor cycle compared to that of the first half (see Fig.9.2), so it can be continuously accelerated (or decelerated).

If the opposite was true ($\lambda \gg \rho_L$ for ex.), there would be acceleration in one half of the Larmor orbit, deceleration in the other half, and the net effect (in the absence of the collisions) would be vanishing.

$\omega = n\Omega$: For higher harmonics (n large), to have resonance and effective exchange of energy, it should be $\omega \sim k_y v_\perp$, so $k_y\rho_L \sim \frac{\omega}{\Omega} = n$

Note: This is consistent with our Bessel-function series, as the maximum of $J_n(a)$ increases with n.

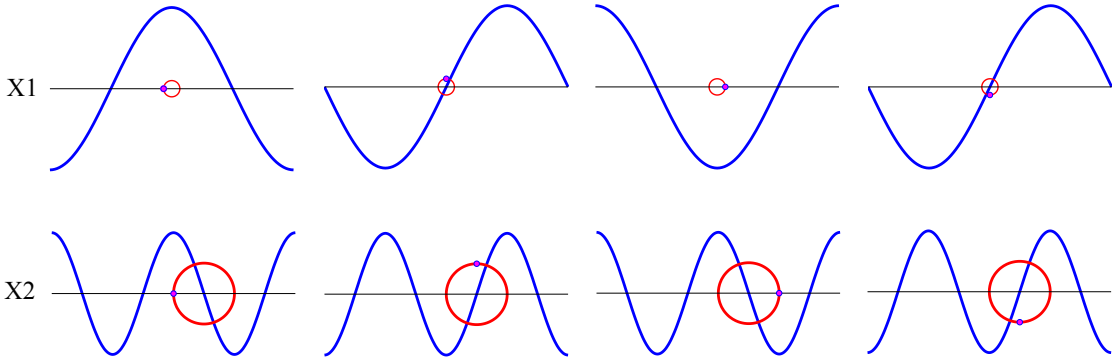

Figure 9.2: Interaction between a particle and X1/2 waves.

Naturally, we need to explore the 'accessibility' to heat the plasma. As stated above, we need to reach a resonance by avoiding cut-offs. This can be visualized in a diagram (CMA diagram), which takes into account the two main parameters varying radially, n and B (see ex.2, series XIII):

$$X = \frac{\omega_p^2}{\omega^2}(\propto n) \quad Y = \frac{\Omega_e^2}{\omega^2}(\propto B_0^2)$$

Cut-offs:

$$\begin{aligned} \mathrm{O-mode}: &\quad X = 1 \\ \mathrm{X-mode}: &\quad Y = (1-X)^2 \end{aligned}$$

Resonances:

$$\begin{aligned} \omega &= w_{UH} \quad Y = 1 - X \\ \omega &= l\Omega_e \quad Y = \tfrac{1}{l^2}(1, 0.25, ...) \end{aligned}$$

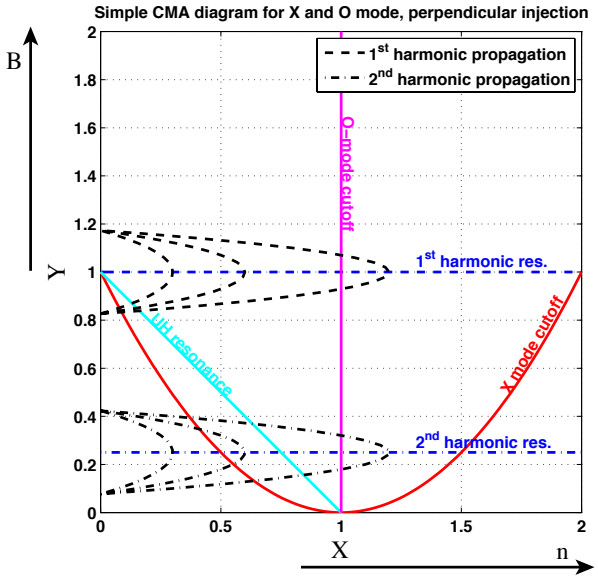

Figure 9.3: Clemmow-Mullaly-Allis diagram for X and O mode. Wave trajectories are shown for 1^{st} and 2^{nd} harmonic injection and for different core plasma densities. Note that for low field side X1 injection the wave first encounters a cutoff. X2 may encounter a cutoff or resonance, depending on the density. O mode has a higher density limit but will eventually be cut off at the plasma frequency.

The fundamental O-mode and the second harmonic of the X-mode (usually called X2) can reach the resonance from the outside, where B is lower, before they reach the cut-off. Heating using second harmonic X2, or third harmonic X3, is commonly used on the TCV tokamak (Fig. 9.4) at CRPP/EPFL, for example.

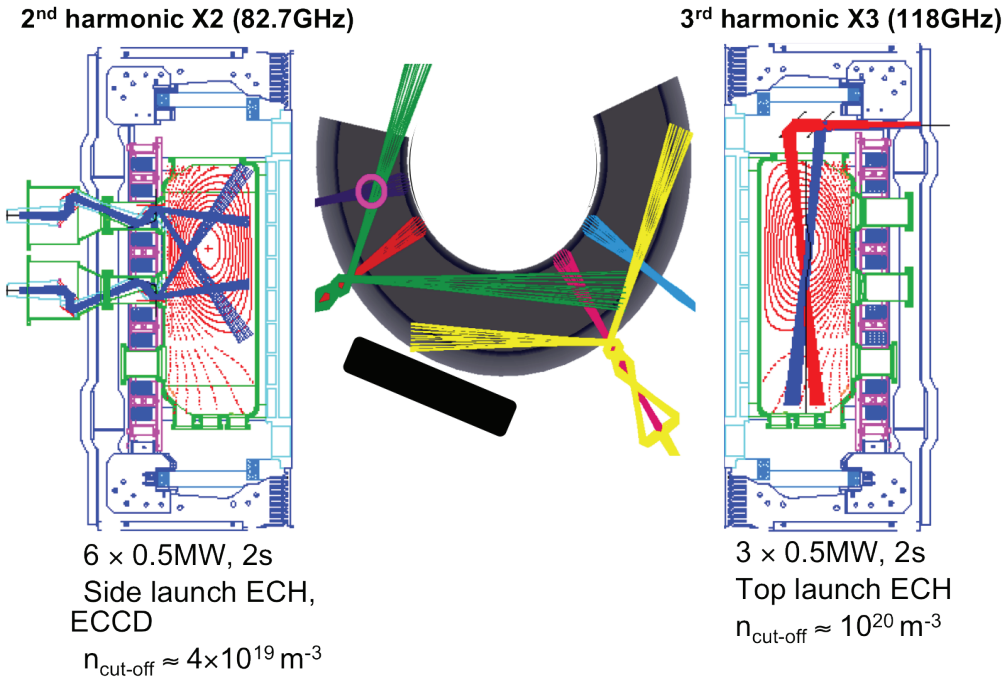

Figure 9.4: The TCV tokamak and the X2-X3 ECH system.

9.0.4 New waves introduced by the kinetic model with $B_0 \neq 0$

We have seen so far that the kinetic model introduces resonances at $n\Omega$ for perpendicular propagation, thus modifying the properties of the fluid waves. Moreover, the kinetic model revealed the existence of Bernstein waves – electrostatic waves not predicted by the fluid model. The dispersion relation is similar for ions and electrons, and an example is given in figure 9.5 for the case of ions.

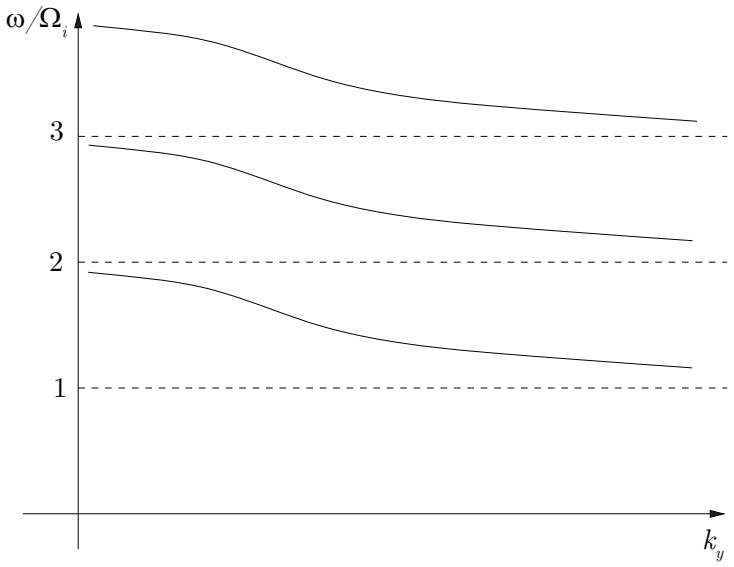

Figure 9.5: Dispersion relation for Bernstein waves. Waves with $v_g = \partial\omega/\partial k_y$ opposite to $v_{ph} = \omega/k_y$ are called *"backward waves"*.

The Bernstein waves are slowly propagating, longitudinal, electrostatic waves. They are 'backward' waves, because the phase velocity and the group velocity have opposite sign. An interesting property of electron Bernstein waves (EBW) is that they do not have a cut-off for high density, thus they can be used to heat dense plasmas. The main disadvantage is that, being electrostatic waves, they cannot propagate in vacuum and cannot be launched by an external antenna. They can nevertheless be driven via a 'mode conversion' in the plasma, from antenna driven electromagnetic waves.

9.0.5 Parallel Propagation ($k_y = 0$)

This section has not been treated in the lecture but one can refer to the first exercise of Problemset 13.

For parallel propagation ($k_y = 0$) the argument of the Bessel functions is zero and we can use

$$J_n(0) = \delta_{n,0} \tag{9.25}$$

So only the term $n = 0$ persists. However, there is also the derivative of the Bessel functions $J_n'(a)$ and the term $\frac{n}{a}J_n(a)$ which appear in the tensor $\underline{\mathbf{T}}_\alpha$. Using the formulae [2] (eq. 9.1.27):

$$\frac{n}{a}J_n(a) = \frac{1}{2}\Big[J_{n-1}(a) + J_{n+1}(a)\Big] \tag{9.26}$$

$$J_n'(a) = \frac{1}{2}\Big[J_{n-1}(a) - J_{n+1}(a)\Big] \tag{9.27}$$

we verify that

$$\underline{\mathbf{T}}_\alpha = \begin{pmatrix} \frac{v_\perp^2}{4}\big[\delta_{n,1} + \delta_{n,-1}\big] & \mathrm{i}\frac{v_\perp^2}{4}\big[\delta_{n,1} - \delta_{n,-1}\big] & 0 \\ -\mathrm{i}\frac{v_\perp^2}{4}\big[\delta_{n,1} - \delta_{n,-1}\big] & \frac{v_\perp^2}{4}\big[\delta_{n,1} + \delta_{n,-1}\big] & 0 \\ 0 & 0 & v_\parallel^2\delta_{n,0} \end{pmatrix} \tag{9.28}$$

With the notation we used in Lecture 6 we have

$$\underline{\boldsymbol{\epsilon}} = \begin{pmatrix} \epsilon_1 & -\mathrm{i}\epsilon_2 & 0 \\ \mathrm{i}\epsilon_2 & \epsilon_1 & 0 \\ 0 & 0 & \epsilon_3 \end{pmatrix} \tag{9.29}$$

where

$$\epsilon_1 = 1 - \sum_\alpha \frac{\omega_{\mathrm{p}\alpha}^2}{\omega^2}\left\{1 + \int \mathrm{d}^3v \frac{v_\perp^2}{4\,n_{\alpha 0}}\left[\frac{k_z\frac{\partial f_{\alpha 0}}{\partial v_\parallel} + \frac{\Omega_\alpha}{v_\perp}\frac{\partial f_{\alpha 0}}{\partial v_\perp}}{k_z v_\parallel - \omega + \Omega_\alpha} + \frac{k_z\frac{\partial f_{\alpha 0}}{\partial v_\parallel} - \frac{\Omega_\alpha}{v_\perp}\frac{\partial f_{\alpha 0}}{\partial v_\perp}}{k_z v_\parallel - \omega - \Omega_\alpha}\right]\right\} \tag{9.30}$$

$$\epsilon_2 = \sum_\alpha \frac{\omega_{\mathrm{p}\alpha}^2}{\omega^2}\int \mathrm{d}^3v \frac{v_\perp^2}{4\,n_{\alpha 0}}\left[\frac{k_z\frac{\partial f_{\alpha 0}}{\partial v_\parallel} + \frac{\Omega_\alpha}{v_\perp}\frac{\partial f_{\alpha 0}}{\partial v_\perp}}{k_z v_\parallel - \omega + \Omega_\alpha} - \frac{k_z\frac{\partial f_{\alpha 0}}{\partial v_\parallel} - \frac{\Omega_\alpha}{v_\perp}\frac{\partial f_{\alpha 0}}{\partial v_\perp}}{k_z v_\parallel - \omega - \Omega_\alpha}\right] \tag{9.31}$$

$$\epsilon_3 = 1 - \sum_\alpha \frac{\omega_{\mathrm{p}\alpha}^2}{\omega^2}\left\{1 + \int \mathrm{d}^3v \frac{v_\parallel^2}{n_{\alpha 0}}\frac{k_z\frac{\partial f_{\alpha 0}}{\partial v_\parallel}}{k_z v_\parallel - \omega}\right\} \tag{9.32}$$

In the limit of $T_\alpha \to 0$, i.e. when the distribution function is described by a delta function, $f(\mathbf{v}) \to \delta(\mathbf{v})$, one finds the same dispersion relation as in the fluid model (see ex.1, series 13). When $T \neq 0$, there are significant differences.

References

Waves in plasmas T.H. Stix, Springer, 1992.

Handbook of Mathematical Functions M. Abramowitz, I. Stegun, 1965

Theory of EBW T. J. M. Boyd and J. J. Sanderson, *The Physics of Plasmas*, Cambridge University Press, 2003.

ECRH J. Wesson, *Tokamaks*, Oxford University Press, 2004

Chapter 10 Examples of non–linear effects in plasmas

Our treatment of waves in plasmas and of wave–particle interaction was based upon the *linearisation* of the equations describing the plasma and the electromagnetic fields.

We have considered only the first order terms, assuming small perturbations to the equilibrium state. This allowed us to employ linear decomposition techniques (Laplace and/or Fourier transforms) to solve the problem.

However, in many real physical systems higher order terms(*) can play an important role. This may happen for

- Externally driven high amplitude waves (e.g. to heat the plasma)
- Unstable waves. As $f_1, E \propto e^{\gamma t}$, for $\gamma > 0$ the amplitude of the perturbations grows to high levels. But this exponential growth cannot go on forever(†), and the *non–linear* terms will lead to a *saturation* of the instability (see Appendix F).

In this lecture we will see some examples of non–linear phenomena in wave–particle interactions, although in principle the two aspects are coupled, namely:

- Non–linear response of particles to waves
  - Trapping of particles in wave potential
  - Modifications of $f(v)$ by large amplitude waves
  - Nonlinear Landau damping
  - Wave–induced deterministic chaos
- Modification of linear wave dynamics by strongly perturbed $f(v)$
  - Wave steepening, soliton formation

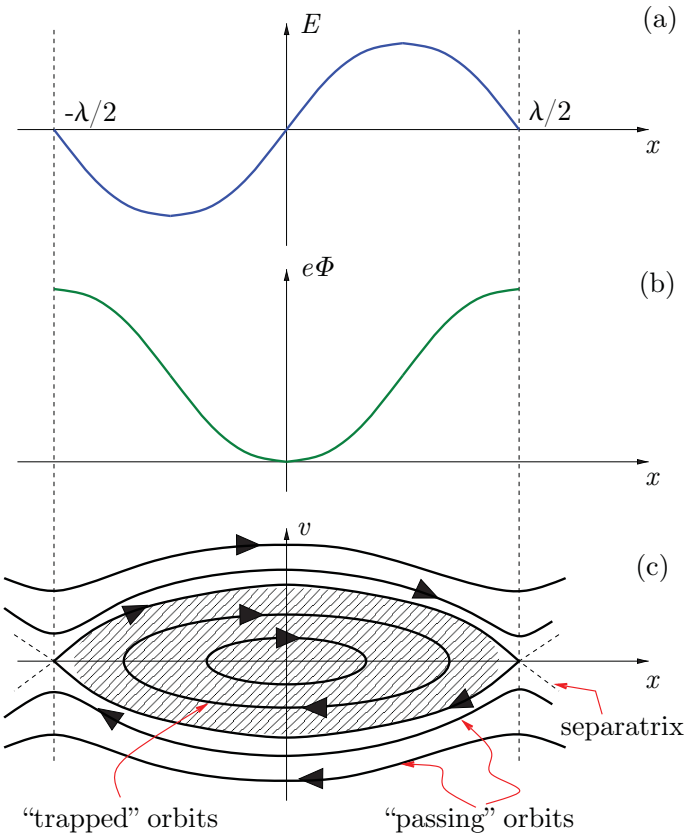

Figure 10.1: Electrons can be trapped in the potential well of a wave. (a) Electric field. (b) Potential energy. (c) Trajectories in the phase space.

10.1 Wave-particle nonlinear interactions

Wave–particle interaction involves resonant particles that will easily respond non–linearly, i.e. with strong modifications of their trajectories, reflected in substantial modifications of $f_0(v)$.

(*) Describing the fields and/or the particles, e.g. the particle distribution function $f(v)$.
(†) Otherwise it would correspond to infinite energy.

10.1.1 Particle trapping – qualitative description

Let's take a 1–D electrostatic wave and consider only the electrons. We assume weak damping, so that $E \sim$ *const* over a few wavelengths (or periods) of the wave. So

$$E(x,t) = E\sin(kx - \omega_r t) \tag{10.1}$$

In a frame moving at the same velocity as the wave phase velocity $x \to x' + v_{\rm ph}t$ the electrons see a static field $E(x') = E\sin(kx')$, to which corresponds the potential $\phi(x') = -\int E(x')\,\mathrm{d}x' = E/k\,\cos(kx')$. In the frame of the wave the electrons can therefore be 'trapped' in a potential energy well of depth $2e\phi = 2eE/k$ (figure 10.1). This happens for electrons with kinetic energy smaller than the maximum wave potential energy, so the limit velocity is determined by the condition

$$\frac{1}{2}m_e v_{\rm trapping}^2 = 2e\phi \tag{10.2}$$

that leads to

$$v_{\rm trapping} = 2\sqrt{\frac{e\phi}{m_e}} = 2\sqrt{\frac{e}{m_e}\frac{E}{k}}. \tag{10.3}$$

A measurable effect of the trapping of particles in wave potential is the creation of a 'plateau' (figure 10.2) in the (time averaged) *zero* order distribution $f_0(v)$ as trapped particles 'bounce' back and forth in the potential well with a characteristic "bounce time" τ_B.[‡]

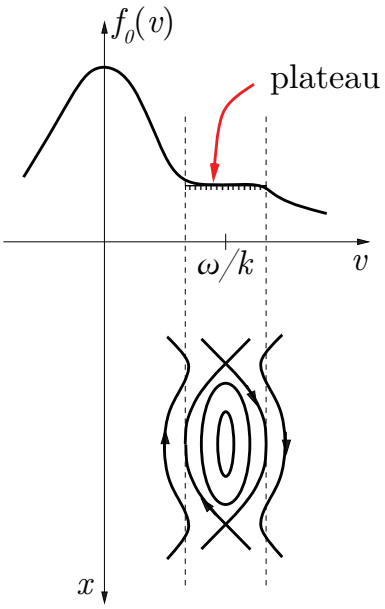

Figure 10.2: Plateau in the zero–order distribution function due to trapped particles. Note that such an 'asymmetry' in the distribution function corresponds to a *current* in the plasma. In tokamaks, a plasma current is needed to create a poloidal magnetic field which is needed to achieve magnetohydrodynamical stability. Usually, this current is induced by a transformer, with the obvious disadvantage that the tokamak cannot operate continuously. So creating a current by injection of waves into the plasma (*"current drive"*) is of great interest in order to obtain a steady–state fusion power plant.

[‡] Assuming a small width of the potential well, the bounce time for an electron with $v \sim \omega_r/k$ is calculated from

$$m_e\ddot{x} = -eE\sin(kx) \approx -eEkx. \tag{10.4}$$

So we can define a *bounce frequency* $\omega_B^2 = eEk/m_e$ or

$$\tau_B = \frac{2\pi}{\omega_B} = 2\pi\sqrt{\frac{m_e}{eEk}} = \frac{4\pi}{kv_{\rm trapping}} \tag{10.5}$$

The wave–particle resonance has therefore a finite 'width' in the velocity space, $\Delta v_{\rm res} \propto \sqrt{E}$, in the sense that particle motion in that region is strongly modified (see Appendix G for measurements of plateau formation). Trapping and plateau formation have a strong influence on:

- Wave absorption/damping (e.g. for externally launched waves). As $\gamma \propto \mathrm{d}f_0/\mathrm{d}u$, the damping rate varies due to trapping (figure 10.3)

  $\rightarrow$ *Non–linear Landau damping*[(§)]

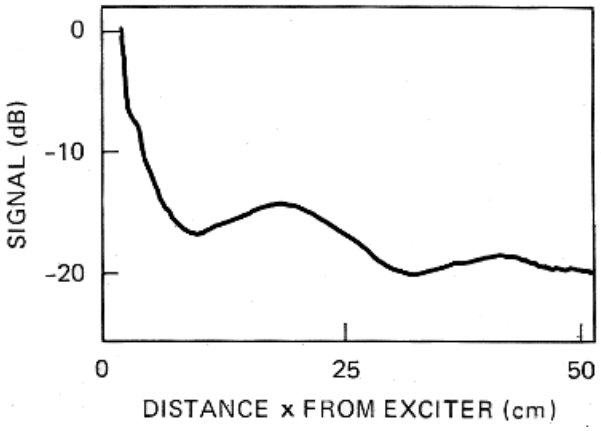

Figure 10.3: Measurement of the amplitude profile of a non–linear electron wave excited at $x = 0$, showing non–monotonic decay [S.M. Hamberger *et al*, Phys. Rev. Lett. **28** (1972) 1114].

  If the condition $\gamma > \omega_B$ is not satisfied, the trapping effect starts to play a role.

- Instability growth. Again $\mathrm{d}f_0/\mathrm{d}u$ is modified, in particular it is reduced

  $\rightarrow$ *Saturation of the linear instabilities*

Note that two characteristic time scales are in competition in the non–linear process: the collisional[(¶)] time scale $\tau_{\rm coll.}$ and the bounce time τ_B:

$\rightarrow$ If $\tau_{\rm coll.} \ll \tau_B$ particles move out from the resonance before they can create a plateau. In this case we expect instabilities to be saturated, or damped by collisions anyway.

$\rightarrow$ If $\tau_{\rm coll.} \gg \tau_B$ the formation of a plateau is robust. Steady–state is reached through saturation (see Appendix G for experimental measurements).

$\rightarrow$ If $\tau_{\rm coll.} \sim \tau_B$ we can have oscillations around a plateau ($\gamma \sim 0$), with f_0 characterised by a finite slope ($\gamma \neq 0$): *"Fishbone–like oscillations"* or *"bursts"* (see Appendix F).

10.1.2 Deterministic chaos in wave-particle interaction

The wave energy absorbed by resonant particles via Landau damping is localised in the velocity space. But we might be interested in phenomena that redistribute this energy over broader regions of $f(v)$. We have seen that collisions can do that[(‖)], but the typical time–scales are usually quite long. How can the energy be redistributed *before* collisions can play a role?
How can we modify $f_0(v)$ over an extended region of v for example to create a current, without using large wave amplitudes? And how to describe the decorrelation of the particle motion in phase space, e.g. to describe the additive action of different waves?

(§) i.e does not necessarily follow an exponential law, as would result from linearised equations.
(¶) Or equivalent mechanisms that lead to a decorrelation of the trajectories in the phase space.
(‖) The distribution function will relax to a maxwellian, and in this case we have an effective *heating*.

To answer these questions we have to introduce the concept of *chaos in particle orbits*, i.e. an exponential divergence in phase space of initially close orbits. Note that this is possible also in deterministic systems (i.e. described by deterministic equations of motion).

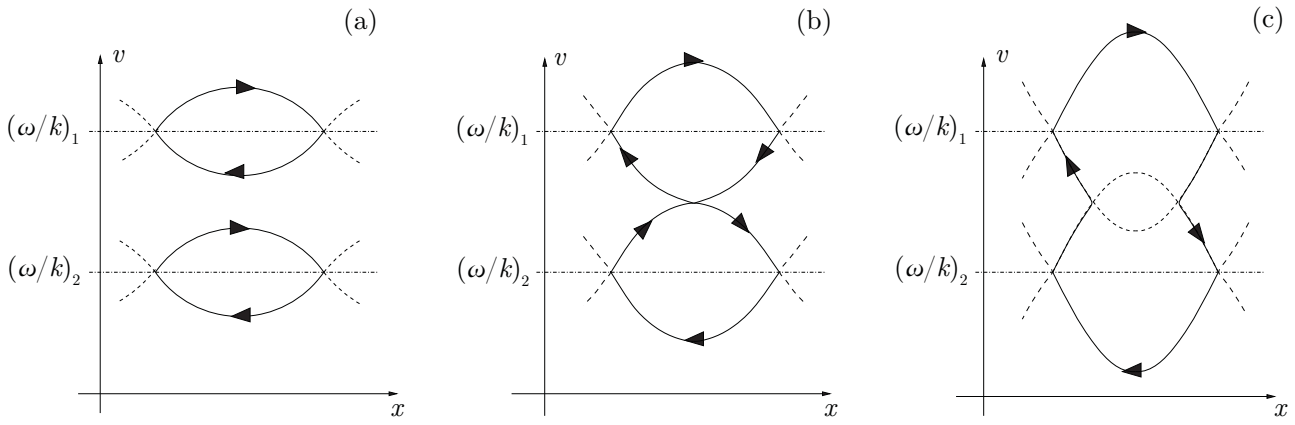

Figure 10.4: Transition to chaos with two waves. From (a) to (b) the width of the resonance $\Delta v_{\rm res} \propto \sqrt{E}$ is increased until the two separatrix touch and merge one into the other (c). This corresponds to possible "chaotic" walks in phase space (see also Appendix H).

10.1.3 Chaos in two waves

The transition to chaos occurs when the two *islands* of trapped electrons in the phase space begin to overlap ("Chirikov criterion", figures 10.4-10.5). We can define a "separation" as

$$\Delta\left(\frac{\omega}{k}\right) \equiv \left|\left(\frac{\omega}{k}\right)_1\right| - \left|\left(\frac{\omega}{k}\right)_2\right| \tag{10.6}$$

We introduce the *stochasticity parameter*

$$K := 2\left\{\sqrt{A_1} + \sqrt{A_2}\right\} \tag{10.7}$$

where

$$A_{1,2} = \frac{e\phi_{1,2}}{m}\left[\Delta\left(\frac{\omega}{k}\right)\right]^{-2} \tag{10.8}$$

For $K = 1$ the islands begin to overlap, chaos begins, and fast diffusion(**) in the velocity space occurs (see Appendix H for an experiment on two wave chaos).
Thus several resonant waves can make particles diffuse over an extended region of the velocity space even for relatively small wave amplitudes.
This process can help driving current in tokamaks, for example using several cyclotron harmonics. In some cases it can also lead to unwanted effects, like in the case of lower–hybrid (LH) current drive. Antennas exciting LH waves from the plasma edge inject a discrete spectrum of $k_\parallel$'s, containing spurious components at high $k_\parallel$ that can resonate with thermal electrons at the plasma edge(††). Due to resonance overlap, thermal electrons with energies of a few tens of eV can diffuse in velocity space up to energies of several keV (figure 10.5), forming a beam that can damage the vessel or other components installed close to the plasma edge like tiles or antennas.

(**) Much faster than collisional.
(††) As $v_{\rm res} = \omega/k$, for high k's the resonant velocity moves toward $v_{{\rm th},e}$.

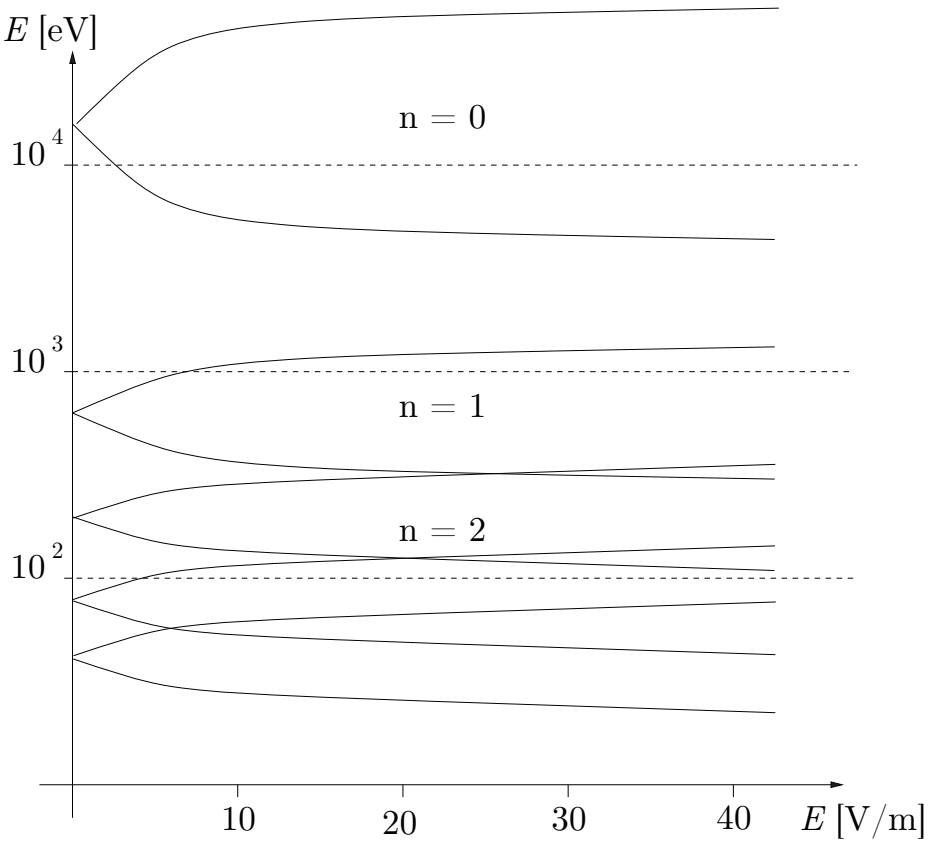

Figure 10.5: Resonance overlap diagram (Chirikov) for $n = 0, 1, ...$ components of an injected wave, as a function of the amplitude of the resulting wave (note that this is a generalisation of the effect shown in figure 10.4). At high amplitudes the overlap region spans energies from ~ 10 eV up to ~ 1 keV, i.e. thermal electrons can be accelerated to very high energies.

The use of the so–called *quasi–linear* theory is usually justified for this kind of problems. The quasi–linear theory was developed to account for the changes in $f_0(v)$ due to wave–particle interaction, yet assuming that the wave dynamics show "linear" properties (e.g. $\frac{\partial}{\partial t}|E|^2 = 2\gamma|E|^2$).

In addition to the analysis of the saturation mechanisms for instabilities, quasi–linear theory is used to calculate (non–inductive) current drive in tokamaks and seems to work fairly well.

10.2 Nonlinear wave dynamics

In the previous discussion we neglected the fact that the particles dynamics in the real space will also change, influencing the wave-particle interaction itself and the wave dynamics.
What happens if we now do consider these effects?

10.2.1 Wave steepening

Consider the example of an ion–acoustic wave, that we already characterised using both fluid and kinetic models. In one dimension (figure 10.6) we can describe it by its potential $\Phi(x,t) \propto \sin(kx - \omega t)$, with

$$T_i = 0,\ T_e \neq 0; \qquad v_\phi = \frac{\omega}{k} = c_s \Rightarrow M = \frac{v_\phi}{c_s} = 1; \qquad n_{e,i} \approx \frac{e\Phi}{T_e} \tag{10.9}$$

where M is the Mach number.

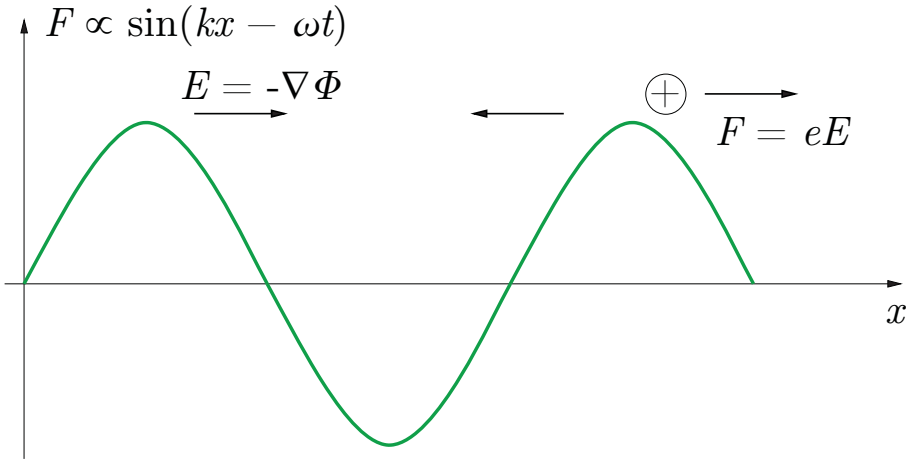

Figure 10.6: Unperturbed potential and force acting on particles (ions)

In linear Landau theory we considered the change in velocity of resonating particles, accelerated at the positive phase (for ions) and decelerated for a negative phase. We explained qualitatively the Landau damping from the argument that the particles accelerated by the wave, if they are a little slower (faster) than the wave, would stay in the resonance for a longer (shorter) time (figure 10.6). With reference to figure 10.6, the ions at the top of the potential curve have larger velocity in the direction x, i.e. the direction of v_ϕ, with respect to the ions located in the well. This is because they have been accelerated as the wave was passing by.
In a more complete (nonlinear) theory we should consider not only the change in *velocity*, but also the possible *displacement* due to large amplitude waves.
From figure 10.7 the ions at the top are accelerated to the right, those at the bottom to the left. As the density is proportional to Φ, the potential will also be distorted: the wave steepens, i.e. $E = -\nabla\Phi$ increases and there is a net flow of mass in the direction of propagation. As the wave velocity increases to $M > 1$, the wave becomes a "shock wave".

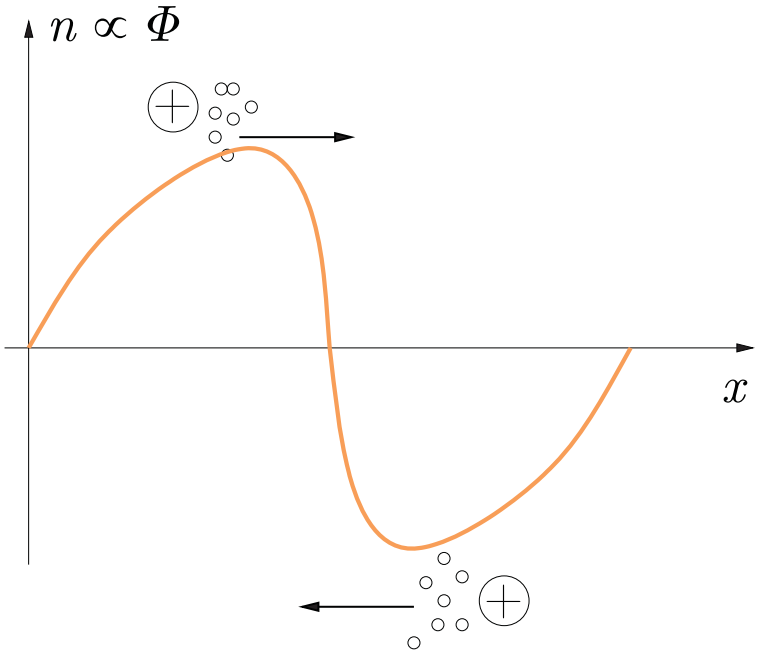

Figure 10.7: Ion density behaviour under the effects of a high amplitude ion-acoustic wave. Remember that $n_i \propto \Phi$.

10.2.2 Solitons

In the presence of dispersion, the process of steepening can be limited and a "soliton" is generated. We call soliton a pulse that propagates practically without dissipation.
A soliton is described by the Korteveg-de Vries (KdV) equation, namely

$$\frac{\partial v}{\partial t} + \alpha v \frac{\partial v}{\partial x} + \beta \frac{\partial^3 v}{\partial x^3} = 0 \tag{10.10}$$

The term $\partial^3/\partial x^3$ results from the dispersion and is the one that limits the steepening. In fact, if this term was zero, then

$$\frac{\partial v}{\partial t} + \alpha v \frac{\partial v}{\partial x} = 0 \tag{10.11}$$

and the result would be a continuous wave steepening due to convection.
For plasmas, the KdV equation can be written in the form:

$$\frac{\partial \phi}{\partial t} + \phi \frac{\partial \phi}{\partial x} + \frac{1}{2} \frac{\partial^3 \phi}{\partial x^3} = 0 \tag{10.12}$$

where ϕ is the electrostatic potential.

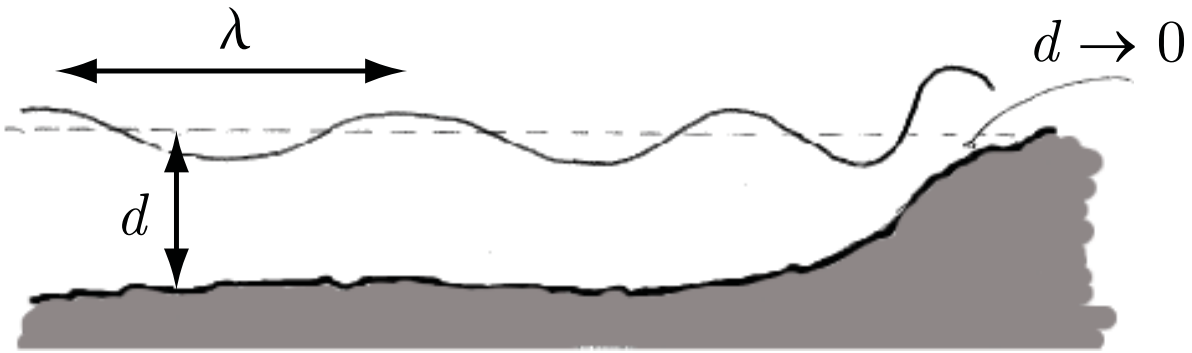

Figure 10.8: Wave propagation properties can be strongly affected by "boundary conditions", as in the case of a tsunami.

Dissipation can prevent an extreme steepening of the wave, but is not always sufficient, for example when the boundary conditions are changed.
Consider the analogy with large amplitude ocean waves (*tsunami*), described by similar equations (figure 10.8). Tsunami are characterised by very long wavelengths, $\lambda \gtrsim 100$ km, and large velocities(‡‡), $v_\phi \sim 800$ km/h. In the ocean it propagates almost as a soliton, but as it approaches the shore $d \to 0 \Rightarrow v_\phi \to 0$, the wavelength decreases and the amplitude must grow. This corresponds to a resonance, $N = \frac{kc}{\omega} \to \infty$. Thus the wave steepens as it gets closer to the shore, and eventually breaks.
Note that soliton–like waves can also have smaller amplitudes than a tsunami. They can be observed in oceans (figure 10.9) as well as in rivers.

(‡‡) Note that, as $\lambda \gg d$, where d is the depth of the ocean, even in the middle of the ocean the tsunami is a "shallow water" wave, with $v_\phi \simeq \sqrt{gd}$.
Note that a tsunami cannot be described by a linear plane wave, because no linear wave can travel for so long without dispersion (8000 km from Sumatra to the South of Africa, in the case of tsunami in December 2004).

Figure 10.9: Examples of solitons approaching the shore.

Lecture bibliography

- General, elementary level
  - F.F. Chen, Introduction to Plasma Physics, 2nd edition, Plenum Press, 1984.
- General, advanced level
  - T.J.M.Boyd and J.J.Sanderson, The physics of Plasmas, Cambridge University Press, 2003.
  - R.D. Hazeltine and F.L.Waelbroeck, The framework of plasma physics, Perseus Books, 1998.
  - R.J.Goldston and P.H.Rutherford, Introduction to Plasma Physics, IOP Publ., 1995.
  - S.Ichimaru, Principles of Plasma Physics–a Statistical Approach, W.H.Benjamin, 1973.
- Waves in plasmas
  - T.H.Stix, Waves in Plasmas, American Institute of Physics, 1992.
- Plasma diagnostics
  - I.H.Hutchinson, Principles of Plasma Diagnostics, Cambridge University Press, 1987.
- Thermonuclear fusion
  - D.J.Rose and M.Clark, Jr., Plasmas and Controlled Fusion, MIT Press and John Wiley, 1961.
- Plasma astrophysics
  - T.Tajima and K.Shibata, Plasma Astrophysics, Addison-Wesley, 1997
- The energy problem in general
  - Gordon J. Aubrecht, Energy, 2nd edition, Prentice Hall, 1995

Appendices

Appendix A Debye length - formal derivation

Here we want to derive an expression for the electrostatic potential, Φ, as a function of the other parameters. Our assumptions are:

- Cold ions: $T_i = 0 \rightarrow n_i = n_0$
- Electrons described by a Maxwell–Boltzmann distribution (i.e. the electron population is at the thermal equilibrium)

$$f(v) = A \exp\left\{-\frac{\text{energy}}{T}\right\} = A \exp\left\{-\frac{\frac{1}{2}mv^2 - e\phi}{T}\right\} \tag{A.1}$$

$$\longrightarrow n_e = n_{e0} \exp\left\{\frac{e\phi}{T}\right\} \tag{A.2}$$

- Small perturbations

$$n_e \simeq n_{e0} \qquad \text{or} \qquad \frac{e\phi}{T} \ll 1 \tag{A.3}$$

- Spherical symmetry

$$\phi \equiv \phi(r), \qquad n_e \equiv n_e(r) \tag{A.4}$$

We start from Poisson's equation for the potential:

$$\nabla^2 \Phi(r) = -\frac{\rho}{\varepsilon_0} \tag{A.5}$$

Now let's put a test particle with charge q_{test} inside the plasma, at $r = 0$. We can split the space charge ρ in two contributions. The first contribution ρ_{plasma} represents the charge due to the plasma, and the second contribution comes from the test particle:

$$\rho = \rho_{plasma} + q_{test} \equiv e(n_i - n_e) + q_{test}\delta(r) \tag{A.6}$$

Now remember the hypothesis of small perturbations: $e^{\frac{e\Phi}{T}} \approx 1 + \frac{e\Phi}{T} + ...$, then:

$$\rho \approx -en_0 \frac{e\Phi}{T} + q_{test}\delta(r) \tag{A.7}$$

Due to the hypothesis of spherical symmetry

$$\nabla^2 \Phi(r) \rightarrow \frac{1}{r}\frac{d^2[r\,\Phi(r)]}{dr^2} \tag{A.8}$$

and eq.(A.5) can be written as

$$\frac{1}{r}\frac{d^2[r\,\Phi(r)]}{dr^2} = +\frac{e^2 n_0}{\varepsilon_0}\frac{\Phi(r)}{T} - \frac{q_{test}}{\varepsilon_0}\delta(r) \tag{A.9}$$

The test charge $q_{test}\delta(r)$ represents a source term. We can solve eq.(A.9) by standard methods, looking first for a solution of the associated homogeneous equation and then taking into account the source term as a condition for a particular solution.

The homogeneous equation can be cast in the form

$$\frac{d^2[r\,\Phi(r)]}{dr^2} = +\frac{e^2 n_0}{\varepsilon_0}\,\frac{r\Phi(r)}{T} \tag{A.10}$$

and with the substitution $F(r) = r\Phi(r)$ we obtain

$$F(r) = A\exp\left(-\frac{r}{\lambda_D}\right) \quad \rightarrow \quad \Phi(r) = \frac{A}{r}\,\exp\left(-\frac{r}{\lambda_D}\right) \tag{A.11}$$

where we have introduced the *Debye length*, λ_D:

$$\lambda_D = \sqrt{\frac{\varepsilon_0 T}{n_0 e^2}} \tag{A.12}$$

Now let's go back to eq.(A.5). Consider a sphere (radius r, surface Σ, volume V) centred on our test particle. In the limit $r \to 0$ there will be no other particles inside the sphere, and we can use the Gauss Theorem to relate Φ and q_{test} and obtain the value of A:

$$\frac{q_{test}}{\varepsilon_0} = \int_V \rho dV = \int_V \nabla\cdot\mathbf{E} dV = \int_\Sigma \mathbf{E}\cdot\hat{n}\,d\Sigma \tag{A.13}$$

where $\hat{n}$ is the unitary vector normal to the surface Σ.
The electric field $\mathbf{E} = -\nabla\Phi(r)$ has only a radial component (along $\hat{n}$). In the approximation $r \to 0$ is

$$E(r) \approx \frac{A}{r^2} \tag{A.14}$$

and after a few calculations, for[§§] $r = a$:

$$\frac{q_{test}}{\varepsilon_0} = \int_\Sigma E(r) d\Sigma = 4\pi a^2\, E_a = 4\pi\, A \tag{A.15}$$

i.e. $A = \frac{q_{test}}{4\pi\varepsilon_0}$ and for $q_{test} = e$ (ion)

$$\phi(r) = \frac{e}{4\pi\varepsilon_0}\frac{1}{r}\exp\left\{-\frac{r}{\lambda_D}\right\} \tag{A.16}$$

[§§] For physical reasons r has a minimum value a, equal to the particle radius.

Appendix B Energy and momentum transfer: formal derivation

Let's see in detail the derivation of the energy and momentum transfer rate for one collision, eqs.(3.19) and (3.32), respectively.

Example: heavy ion

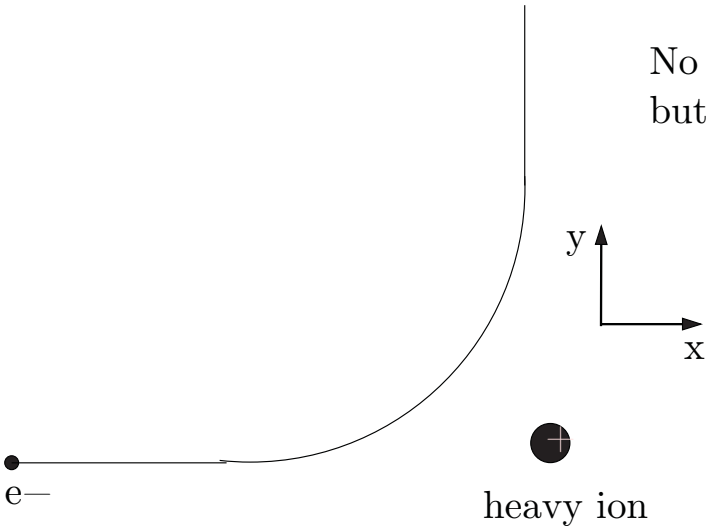

Time scales for energy or momentum exchanges can be very different!

Energy transfer rate

As $m_2 \gg m_1$, we can assume the ion at rest, $\mathbf{v}_2 = 0$. After the collision, from eq.(3.6), the velocity of the electron will have components :

$$\mathbf{v}_1' = \left(u + \frac{m_2}{m_1+m_2} v\cos\theta, \frac{m_2}{m_1+m_2} v\sin\theta \right) \tag{B.1}$$

As $\mathbf{v}_2 = 0$, the relative velocity is $\mathbf{v} = \mathbf{v}_1$ and the velocity of center of mass is $\mathbf{u} = \frac{m_1}{m_1+m_2}\mathbf{v}$, and we have:

$$\mathbf{v}_1' = \left[(m_1 + m_2\cos\theta)\frac{v}{m_1+m_2}, \frac{m_2}{m_1+m_2} v\sin\theta \right] \tag{B.2}$$

Loss in kinetic energy

$$\begin{aligned}
\Delta E_k = E_k - E_k' = \frac{1}{2} m_1 \left\{ v^2 - \left[\frac{(m_1 + m_2\cos\theta)v}{m_1+m_2} \right]^2 - \left[\frac{m_2 v\sin\theta}{m_1+m_2} \right]^2 \right\} = \\
= \frac{1}{2} m_1 v^2 \left[1 - \frac{m_1^2 + m_2^2\cos^2\theta + 2m_1 m_2\cos\theta + m_2^2\sin^2\theta}{(m_1+m_2)^2} \right] = \\
= \frac{1}{2} m_1 v^2 \left[1 - \frac{m_1^2 + m_2^2 + 2m_1 m_2\cos\theta}{(m_1+m_2)^2} \right] =
\end{aligned}$$

In the limit of small angles, we can expand $\cos\theta$ up to the second order: $\cos\theta \simeq 1 - \frac{\theta^2}{2}$,

$$= \frac{1}{2} m_1 v^2 \left[1 - \frac{m_1^2 + m_2^2 + 2m_1 m_2 - m_1 m_2 \theta^2}{(m_1 + m_2)^2} \right] =$$
$$= \frac{1}{2} m_1 v^2 \left[\frac{m_1 m_2}{(m_1 + m_2)^2} \theta^2 \right]$$

As $\tan\frac{\theta}{2} = \frac{b_{90}}{b}$, we can write $\theta \simeq 2\frac{b_{90}}{b}$ in the limit of small angles. This finally gives the energy loss for a *single collision*, in the limit of *small angles*, eq.(3.19):

$$\Delta E_k = \frac{1}{2} m_1 v^2 \frac{m_1 m_2}{(m_1 + m_2)^2} \left(2\frac{b_{90}}{b} \right)^2$$

Momentum transfer rate

Let be $\hat{x}$ the direction of the incoming particle, then the variation of momentum along $\hat{x}$ will be equal to:

$$\Delta p_x = m_1(v_1 - v'_{1x}) = m_1 v_1 \left[1 - \left(\frac{m_1}{m_1 + m_2} + \frac{m_2}{m_1 + m_2} \cos\theta \right) \right] =$$
$$= p_x \left(\frac{m_2}{m_1 + m_2} - \frac{m_2}{m_1 + m_2} \cos\theta \right) =$$
$$= p_x \frac{m_2}{m_1 + m_2} (1 - \cos\theta)$$

In the limit of small angles, $\cos\theta \simeq 1 - \frac{\theta^2}{2}$:

$$\Delta p_k \simeq \frac{m_2}{m_1 + m_2} \frac{\theta^2}{2} p_x$$

and, reminding that

$$\frac{\Delta E_k}{E_k} \simeq \frac{m_1 m_2}{(m_1 + m_2)^2} \theta^2$$

we find eq.(3.32)

$$\frac{\Delta p_k}{p_k} = \frac{1}{2} \frac{m_2}{m_1 + m_2} \theta^2 = \frac{1}{2} \frac{m_2}{m_1 + m_2} \frac{\Delta E_k}{E_k} \frac{(m_1 + m_2)^2}{m_1 m_2} =$$
$$= \frac{1}{2} \frac{m_1 + m_2}{m_1} \frac{\Delta E_k}{E_k}$$

Appendix C Examples of techniques to measure distribution functions

Electron distribution function

$f_e(v)$ can be extracted from:

- Probe measurements (Langmuir probes, see figures C.1 and C.2).
  A Langmuir probe consists of one or more electrodes, inserted into a plasma, with a constant or time-varying electric potential between the various electrodes or between them and the surrounding vessel.
  The beginning of Langmuir probe theory is the $I - V$ characteristic of the Debye sheath, that is, the current density flowing to a surface in a plasma as a function of the voltage drop across the sheath. As the potential drop in the Debye sheath is reduced, the more energetic electrons are able to overcome the potential barrier of the electrostatic sheath. By varying the potential, the electron distribution function may be reconstructed.

- Scattering of laser light from free electrons (Thomson scattering).

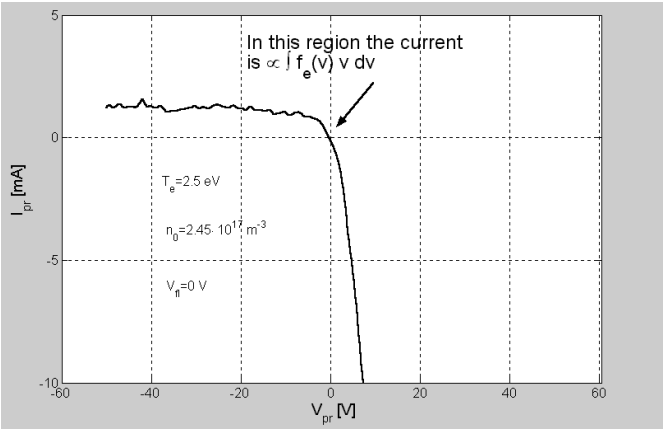

Figure C.1: Measured Current–Voltage characteristic measured by a Langmuir probe in a low-density, low-temperature plasma. The main parameters are found by fitting the data with a known function. In the region where the current changes its sign $f_e(v) \propto (dI_{pr}/dV_{pr})^{-1}$.

Ion distribution function

$f_i(v)$ can be obtained from:

- Collective Thomson scattering,

- Laser induced fluorescence (LIF) via completely ionised ions, see figure C.3.
  A tunable laser pumps a bound electron from quantum level E1 to a higher level E2. The excited electron then spontaneously decays to a lower level E3, emitting a photon. By using a very narrow band dye laser, the line width of the exciting laser line is substantially narrower than the thermal Doppler width of the plasma ions so that scanning the dye laser wavelength map out the ion velocity distribution f(x,v,t), $\omega_{\text{observed}} = \omega_{\text{laser}} - k_{\text{laser}} v_{\text{ion}}$.

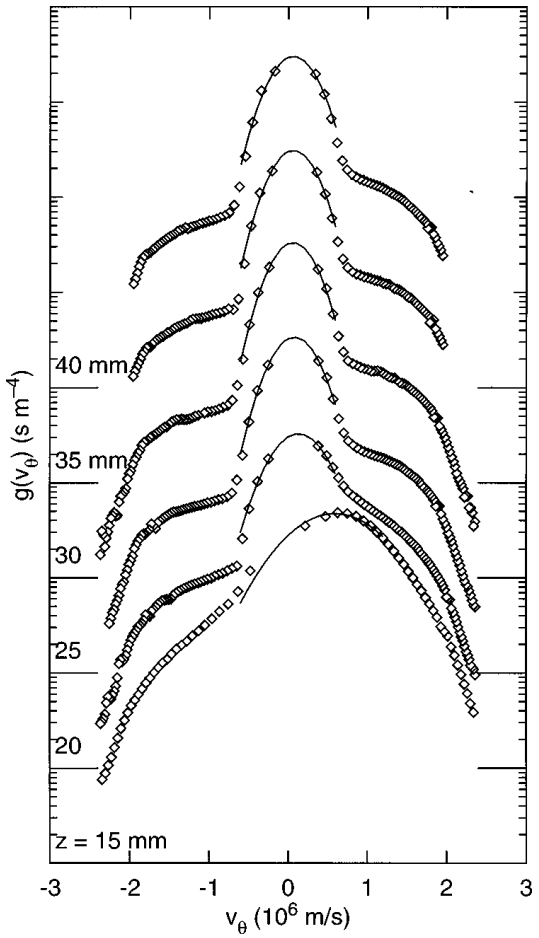

Figure C.2: Reduced electron velocity distribution functions $g(\nu_\theta)$ at $r = 17$ mm for heights $z = 15$, 20, 25, 30, 35 and 40 mm above the cathode. The abscissa is logarithmic. Each distribution function begins at 10^6 s m^{-4} at the position indicated on the g axis. An $\mathbf{E} \times \mathbf{B}$ drift is clearly seen at $z = 15$ mm. Courtesy of T. E. Sheridan et al., J. Vac. Sci. Technol. A 16(4), Jul/Aug 1998.

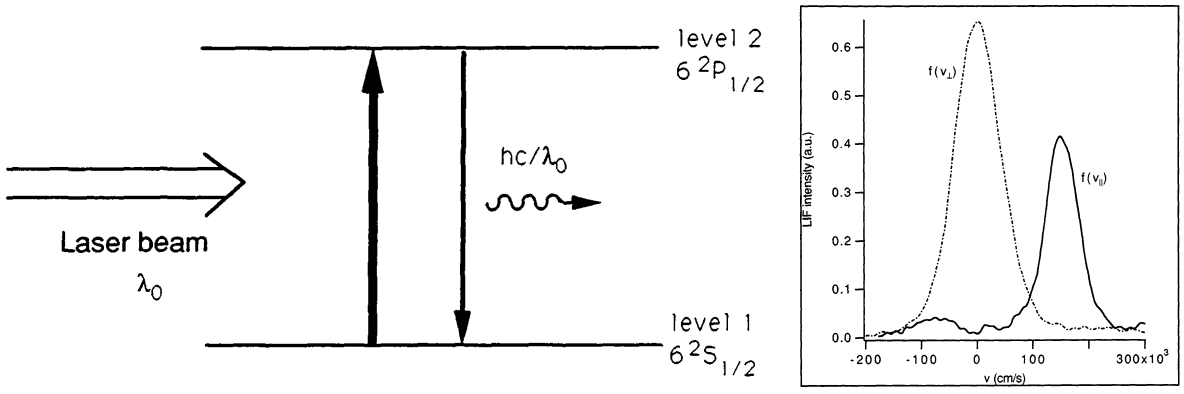

(a) (b)

Figure C.3: (a) Principle of Laser Induced Fluorescence (LIF) measurement.
(b) Example of $f(v_\perp)$, $f(v_\parallel)$ measured by LIF on a 'Q-machine'. $v_\parallel$ and $v_\perp$ are the velocity components parallel and perpendicular to the magnetic field B. Barium plasma (singly ionised). $T_{i,\perp} \simeq 2\,T_{i,\parallel} \simeq 0.23$ eV. Courtesy of A. Fasoli, PhD thesis, 1993.

Appendix D Experimental measurements of "classical" diffusion by optical tagging

We are considering a cylindrical vacuum vessel with a magnetic field along its axis. A Barium plasma is produced. Such kind of plasmas are very quiescent, i.e. without significant levels of fluctuations and turbulence.

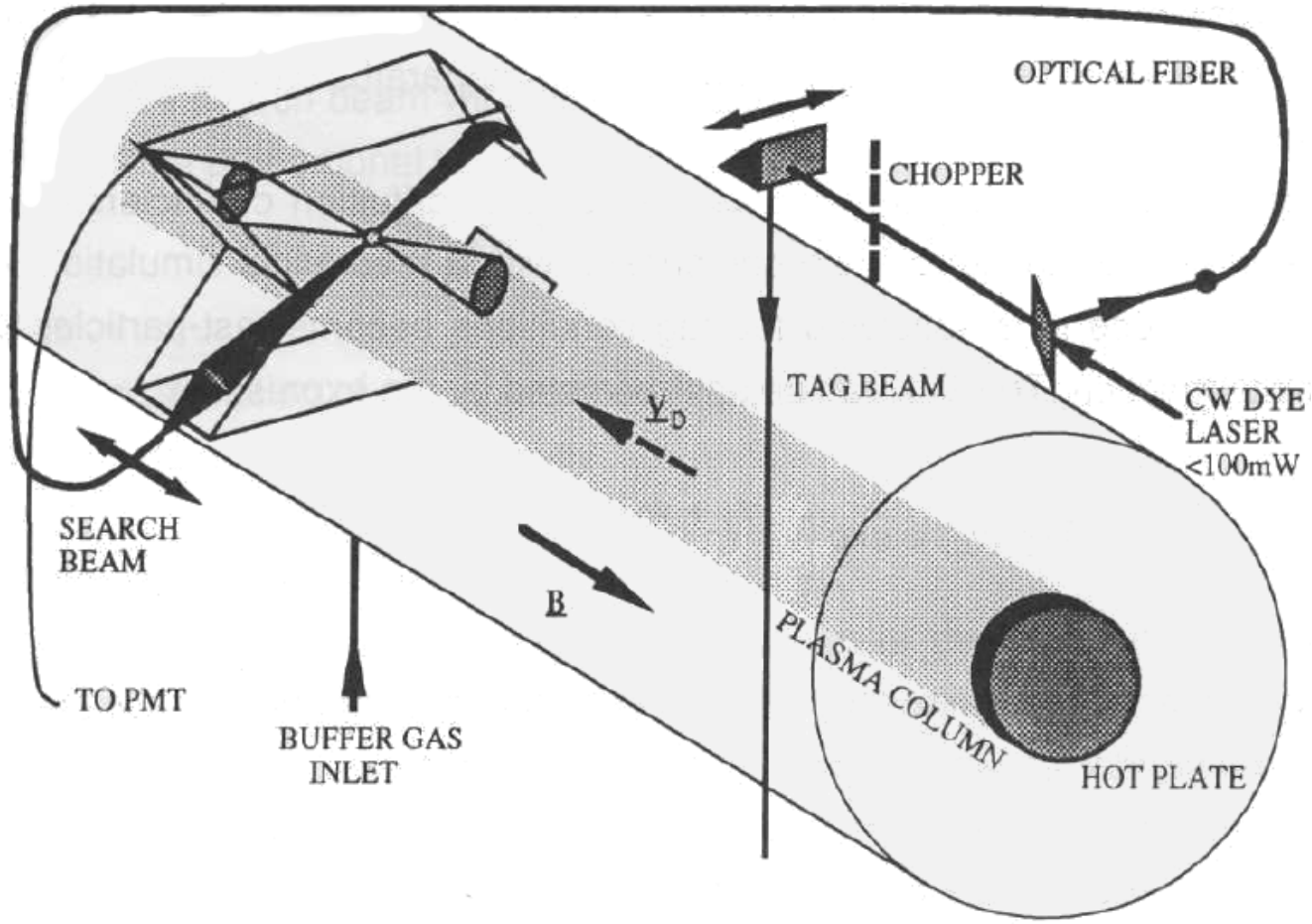

Figure D.1: Experimental set-up for cross-field transport studies

Particles in a certain region of the plasma are *tagged* by exciting them with a laser from the ground–state A to state B from where some decay to a metastable Zeeman sub-level C. i.e. for those particles, the $A \rightarrow B$ transition is no longer resonant with the laser frequency. Thus they can be identified again (perhaps in another plasma region) by a 'search' laser, to which they appear as a missing of fluorescence response.

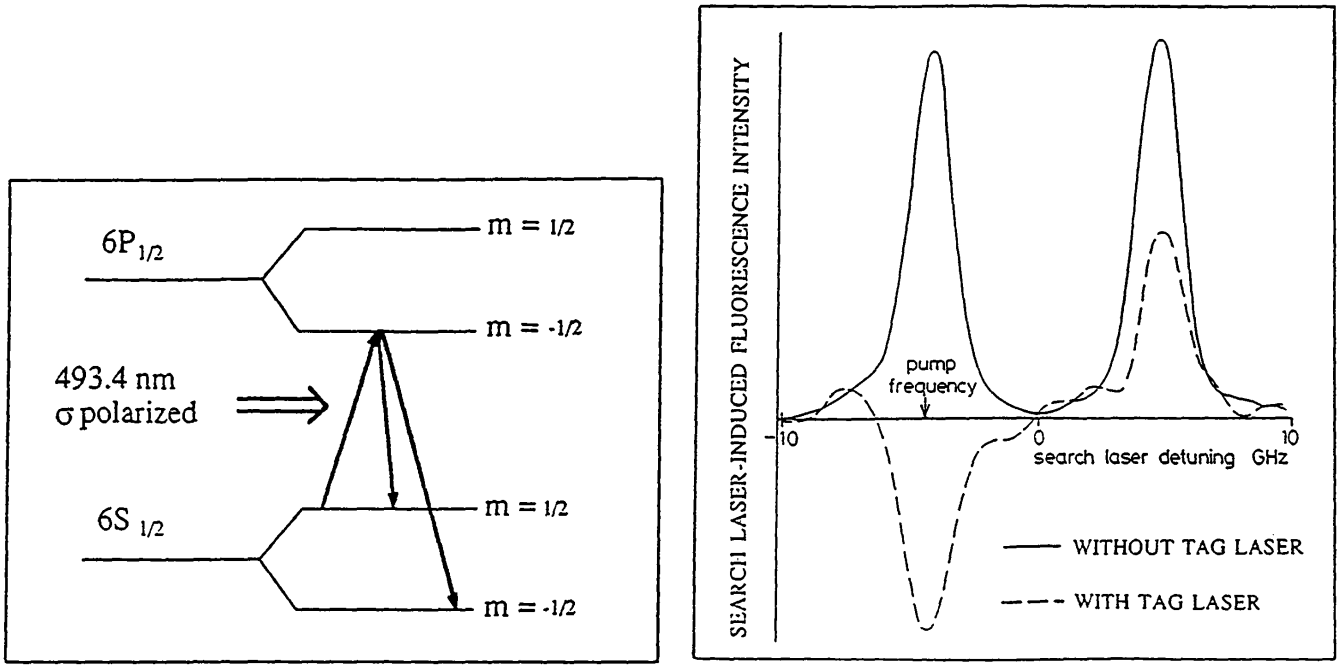

(a) (b)

Figure D.2: (a) Scheme of barium II spin state tagging.
(b) tag signal amplitude as a function of the search laser frequency, showing "dark" and "bright" characteristics. The background LIF signal from the two σ lines is also displayed (continuous line)

It can be shown (see A. Fasoli, EPFL thesis #1162, 1993) that the perpendicular diffusion coefficient is proportional to the full-width at half maximum of the tag signal:

$$D_\perp \simeq \left[\frac{\mathrm{FWHM}^2}{2.77} - a^2 - b^2\right] \frac{v_D}{4\Delta z}$$

where Δz is the distance along the magnetic field between the optical tagging position and the search one. So as Δz increases, the FWHM should increase too.

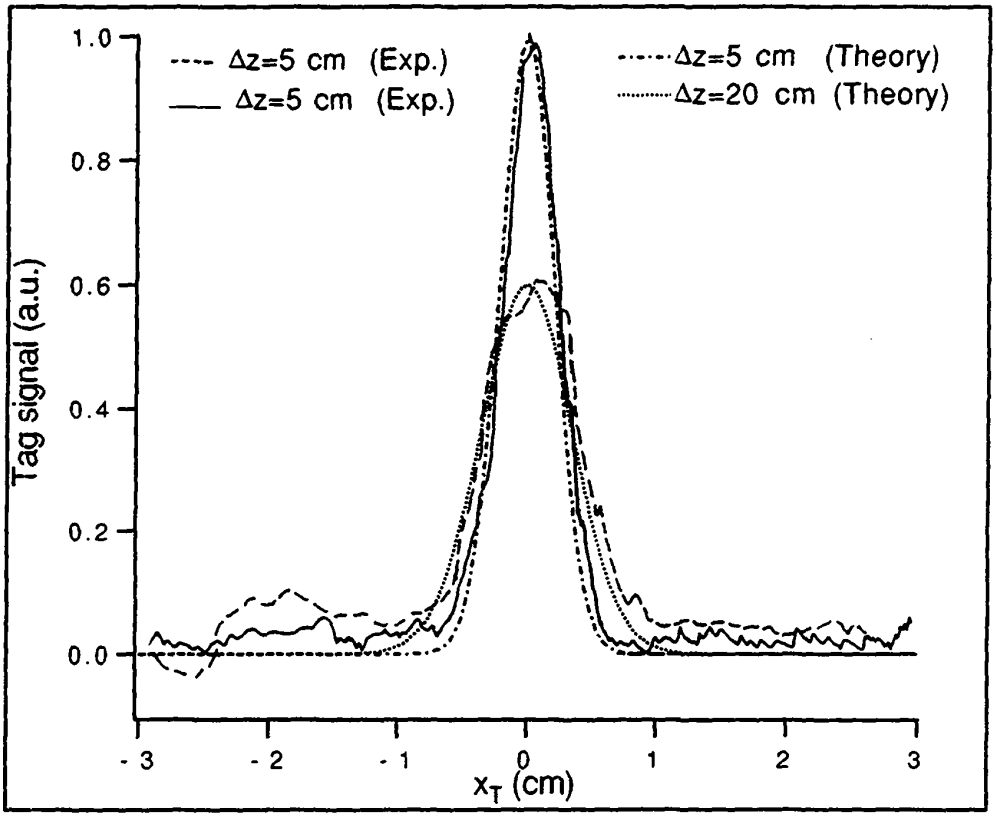

Figure D.3: Experimental verification of "classical" diffusion for a cylindrical non–turbulent plasma. *Optical tagging* was used to measure particle transport. Here, a radial scan of the tag signal expressed in arbitrary units is shown ($v_1/v_{\perp \mathrm{th}} \simeq 0$; $B \simeq 0.15$ T). Theoretical and experimental curves for two values of the tag–search distance are shown on the same scale.

The experimental results of FWHM^2 as a function of the position Δz can be fitted with a straight line. The slope is directly proportional to the perpendicular diffusion coefficient.
By changing the magnetic field, one can find if the "classical" prediction $D_\perp \propto B^{-2}$ is satisfied.

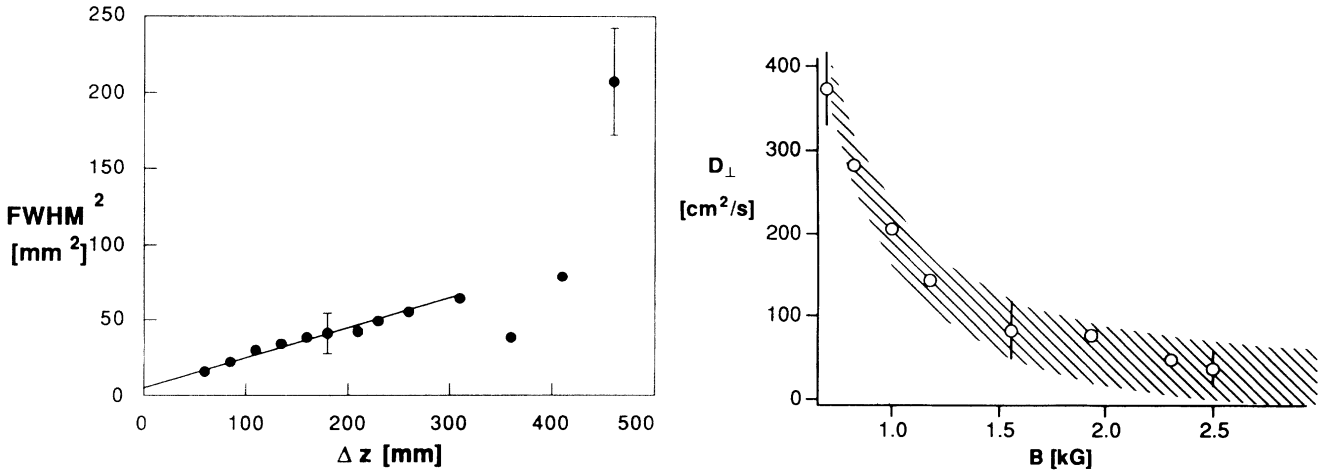

Figure D.4: Left: square of the tag radial profile FWHM as a function of the tag-search position Δz. A least square fit for $\Delta z < 30$ cm is also shown. Right: B-field scaling of the measured perpendicular diffusion coefficient. The shaded region corresponds to the values calculated from $D_\perp = 1/2\rho_i^2\nu_{ii}$.

Appendix E How is an Interferogram Measured?

In an experiment as shown in figure E.1, a wave at frequency ω is excited by an antenna, for example by applying an oscillating voltage $V_0 \cos\omega t$ to a grid immersed into the plasma. We can then measure the effects of the launched wave at the generic position x by means of a probe (electrical or optical, e.g. LIF). The measured voltage will be of the form $V_1(x)\cos(\omega t - kx + \phi_0)$. 'Mixing' the two signals we get

$$V_0 V_1(x)\cos(\omega t)\cos(\omega t - kx + \phi_0) = \frac{V_0 V_1(x)}{2}\Big[\cos(2\omega t - kx + \phi_0) + \cos(kx - \phi_0)\Big] \quad \text{(E.1)}$$

Using a low–pass filter to eliminate the component oscillating at 2ω and supposing that the wave is exponentially damped in the plasma

$$V_1(x) = V_0 e^{-k_i x} \quad \text{(E.2)}$$

the signal becomes

$$\frac{V_0^2}{2} e^{-k_i x}\cos(kx - \phi_0) = \frac{V_0^2}{2}\Re\left\{e^{\mathrm{i}(\tilde{k}x - \phi_0)}\right\} = \frac{V_0^2}{2}\Re\left\{e^{\mathrm{i}\tilde{k}x)}\right\} + \text{const.} \quad \text{(E.3)}$$

where $\tilde{k} = k_r + \mathrm{i}k_i$ is the complex wave vector. The imaginary and real parts give the damping rate and the wavelength of the wave. Varying x, both values can be measured for a fixed frequency ω imposed by the antenna.

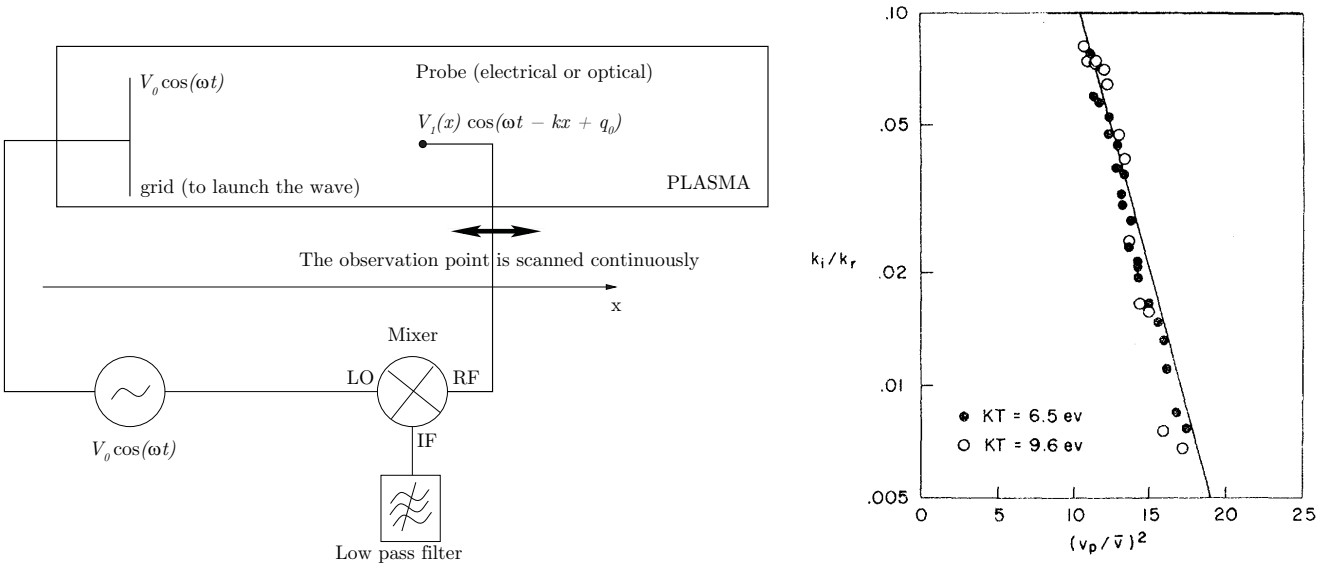

Figure E.1: (a) Interferometry experiment.
(b) Experimental evidence of Landau damping: The damping rate is in agreement with the Landau theory (solid line). J. H. Malmberg and C. B. Wharton, Phys. Rev. Lett. **17** (1966) 175.

Appendix F Example of nonlinear saturation of particle–driven instabilities

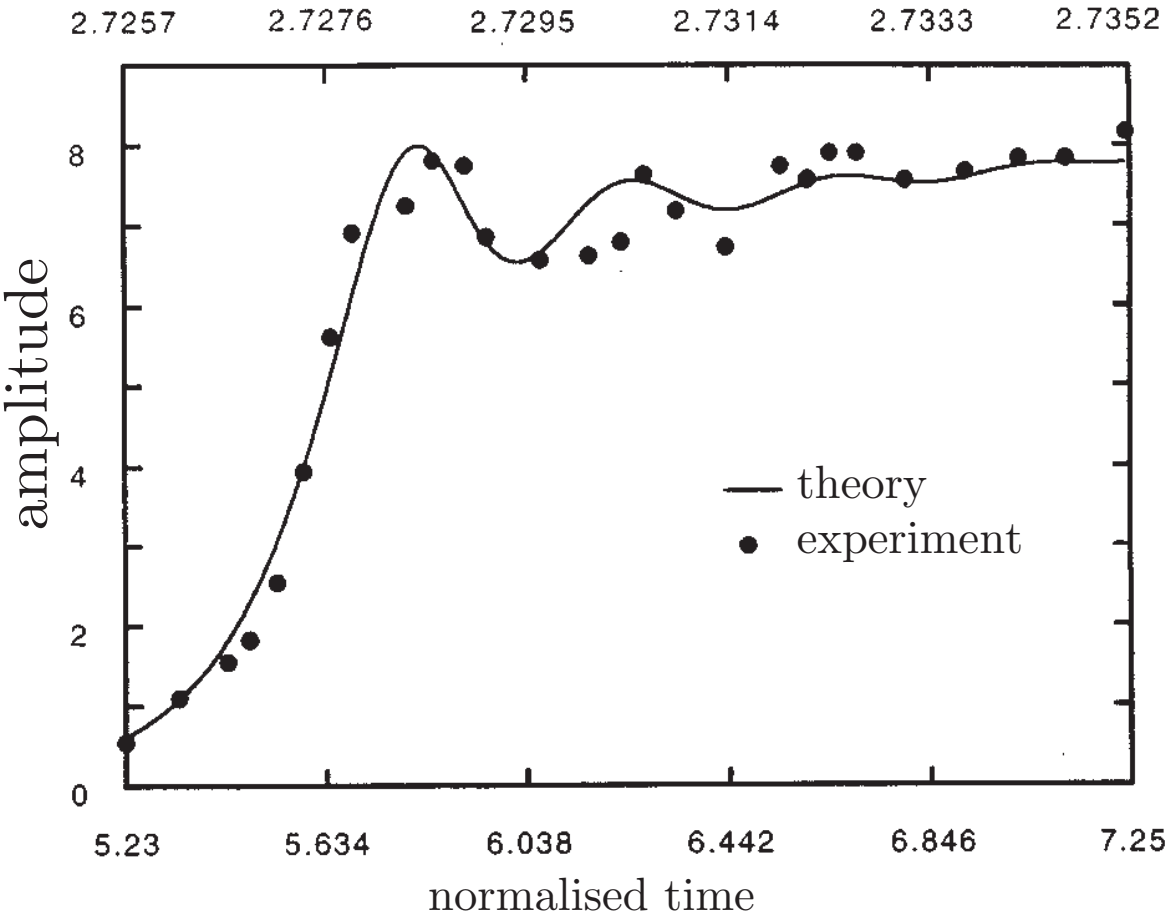

Figure F.1: Non-linear saturation of fast-particle driven Alfvén wave in a tokamak [K.L. Wong *et al.*, Phys. Plasmas **4** (1997) 393-404].

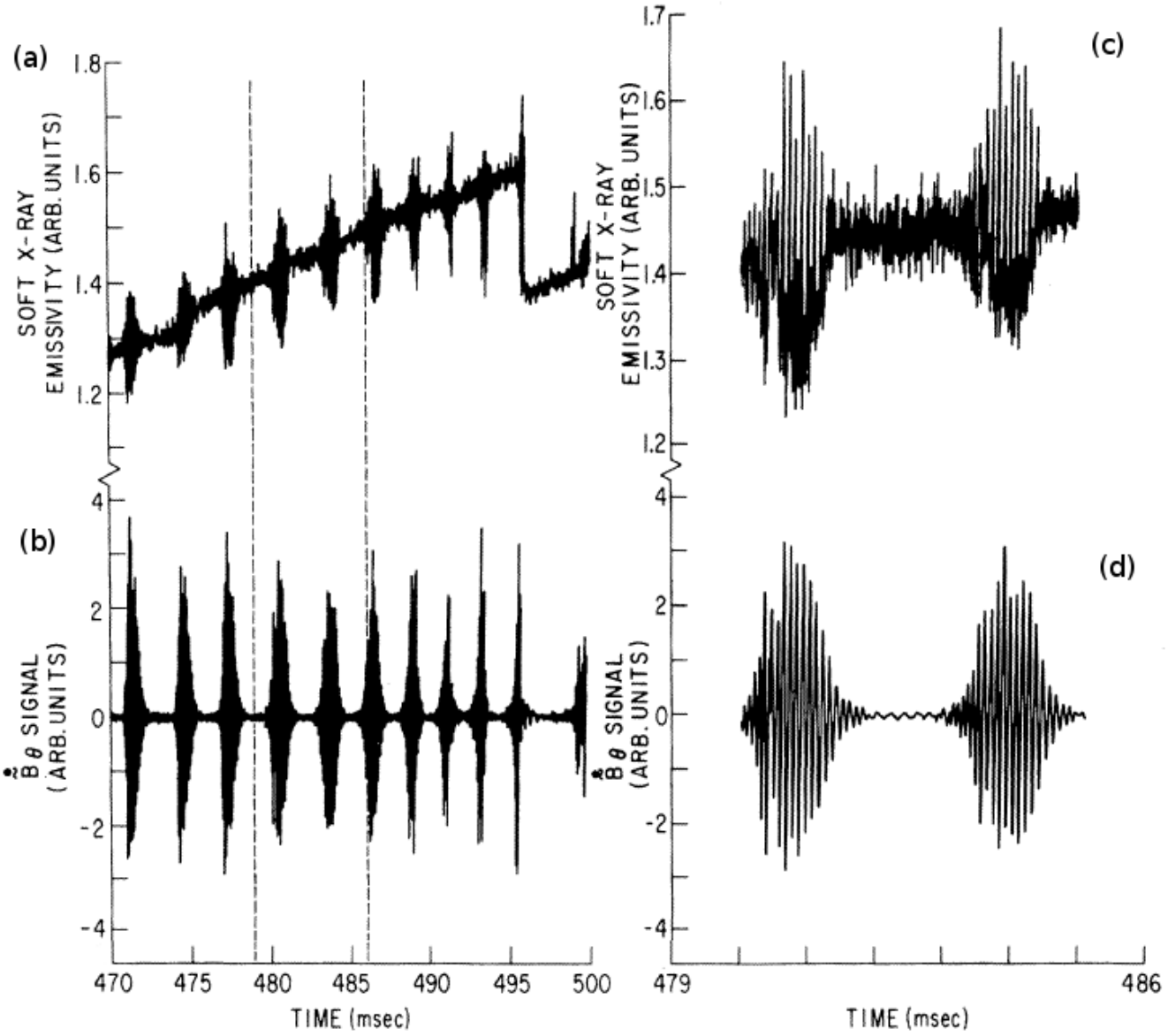

Figure F.2: "Bursting" saturation of low frequency instabilities driven by Neutral Beam Injection. Fishbone instability: (a) soft X-ray emission; (b) poloidal magnetic field fluctuations; (c-d) expanded trace of these fluctuations [K. McGuire *et al.*, Phys. Rev. Lett. **50** (1983) 891].

Appendix G Trapping effect

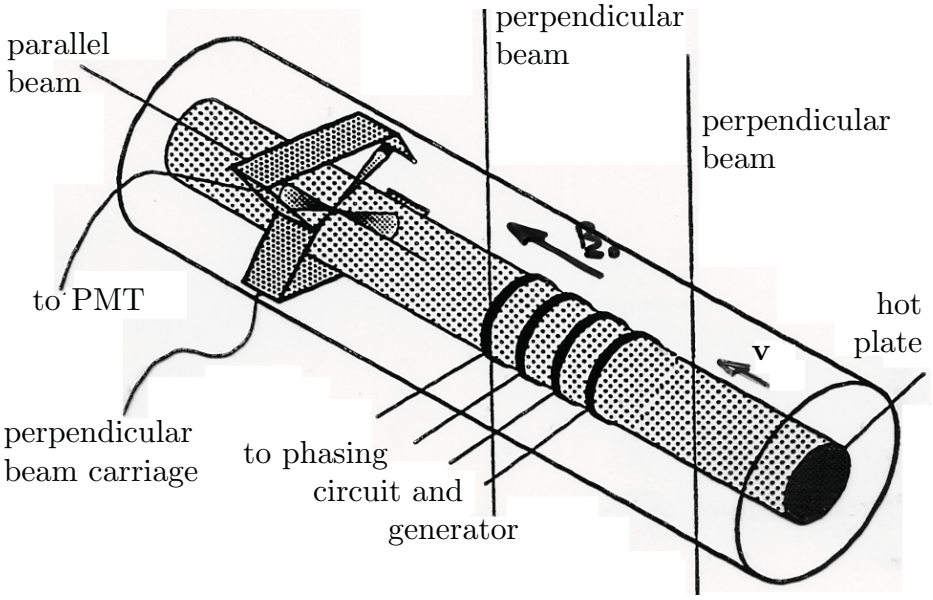

Figure G.1: Sketch of the Linear Magnetised Plasma (LMP) device at CRPP/EPFL, Lausanne. A quiescent drifting Barium plasma is created by a hot–plate continuous discharge and diagnosed with Laser Induced Fluorescence (LIF) and Optical Tagging techniques. Note the four rings surrounding the plasma column, representing an antenna for the excitation of ion–acoustic waves with tunable $k_\parallel$. $T_e \sim T_i \sim 0.2$ eV, $B_0 \sim 0.3$ T, $n_e \sim 10^{10}$ cm^{-3}.

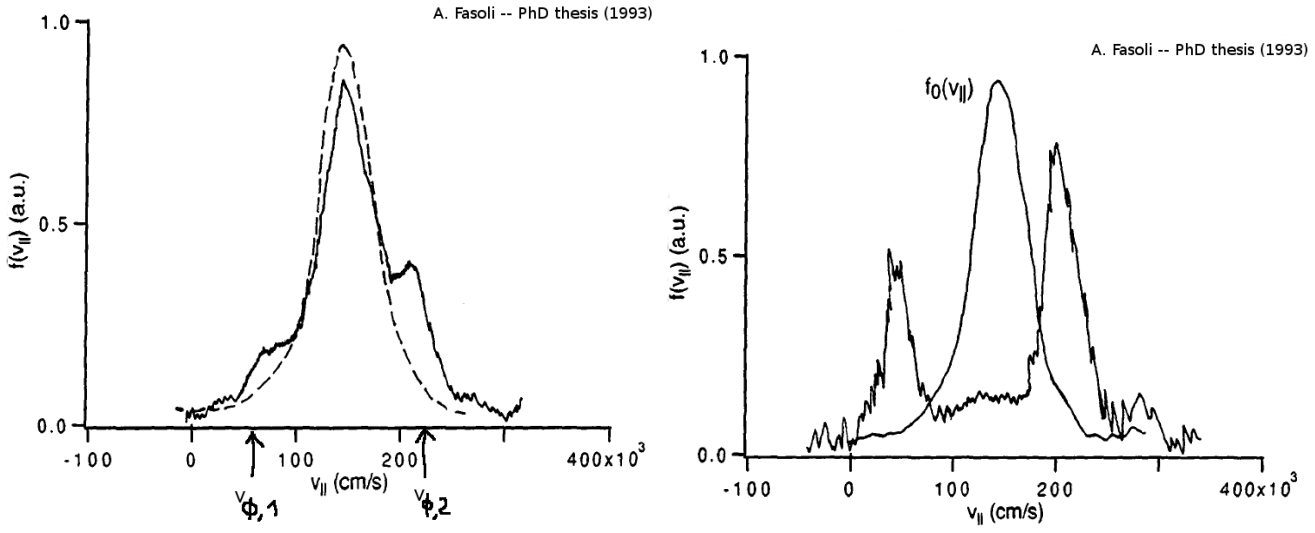

Figure G.2: Two waves trapping effect. Example of time resolved parallel ion distributions before (left) and after (right) stochastic heating. On the left the unperturbed distribution is also represented (dashed line) before the injection of two waves with phase velocities $v_{\phi,1}$ and $v_{\phi,2}$. Note the formation of a plateau around the resonant velocities.

Appendix H Stochastic heating

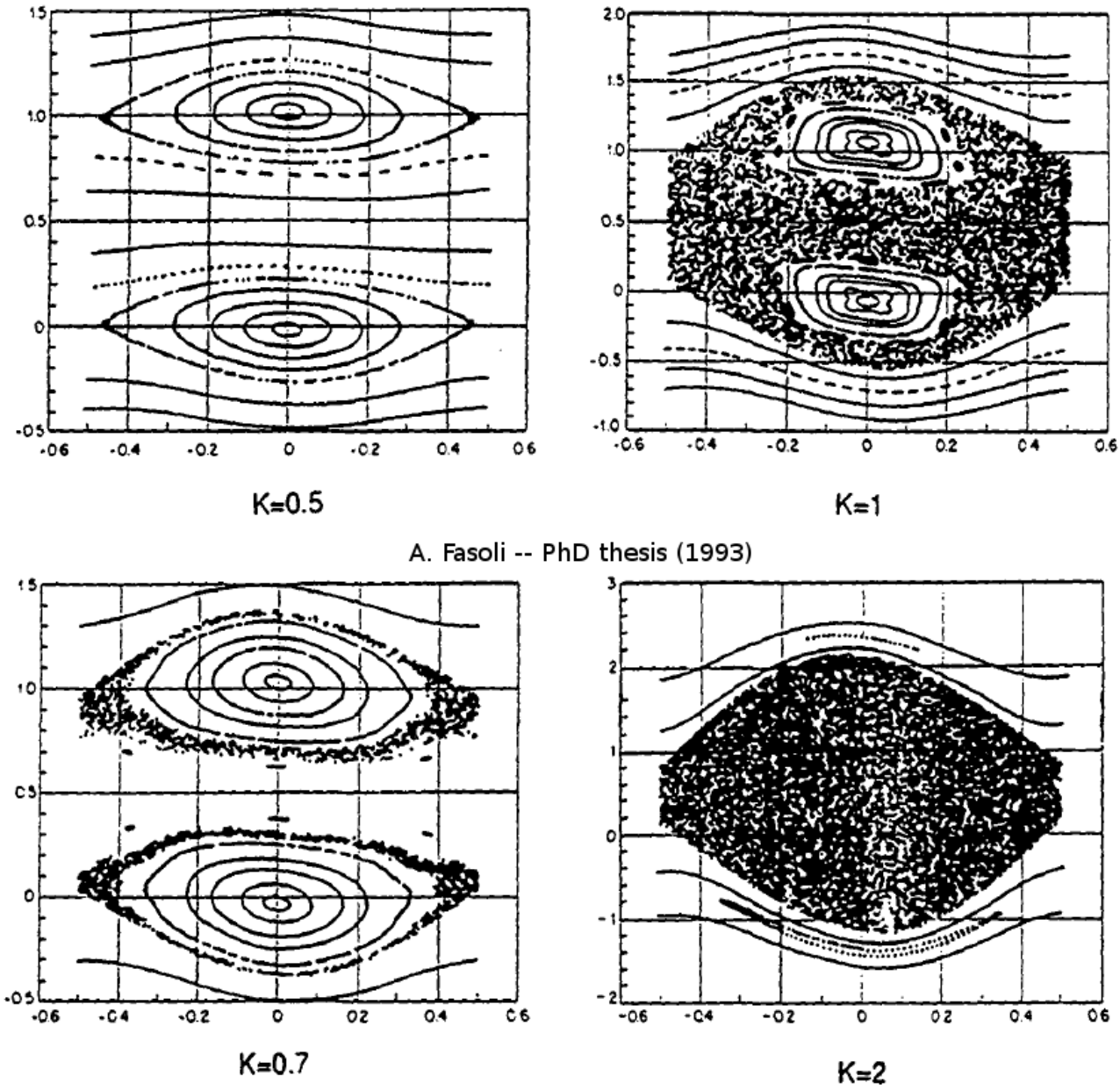

Figure H.1: Sketch of the evolution of the orbits in the phase space as a function of the stochasticity parameter K. Particles that were originally localised on the separatrix for $K < 1$ diffuse in the phase space when the two islands merge ($K > 1$).

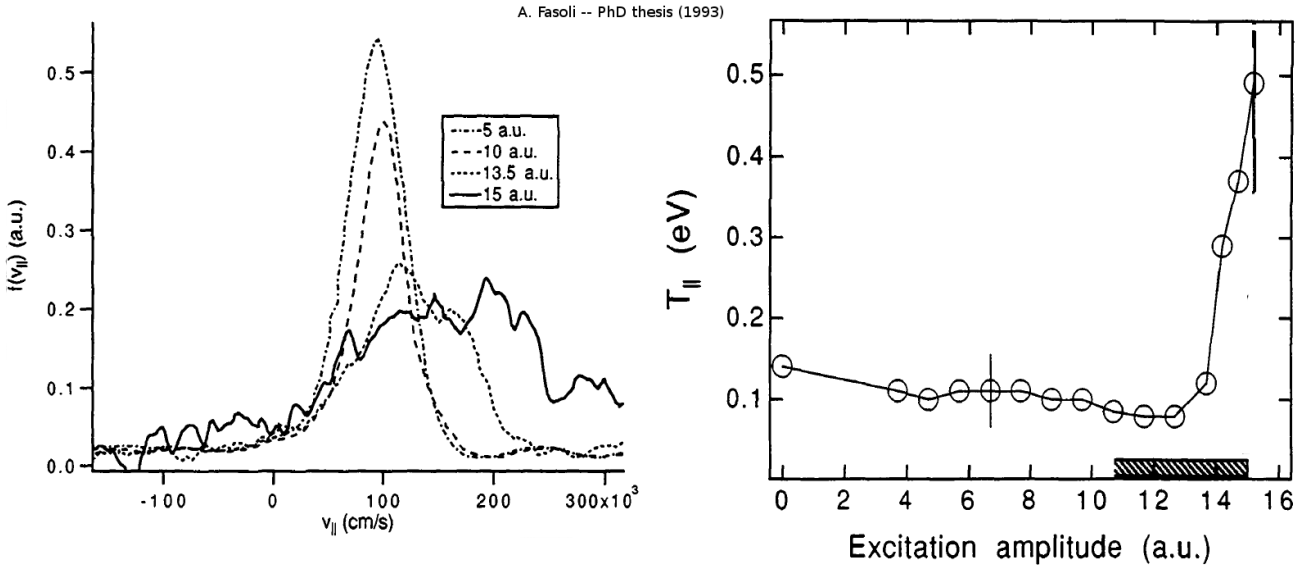

Figure H.2: Left: Parallel ion distribution function $f(v)$ for different amplitudes of the excited waves. Note the heating of the ion population for $K > 1$, evident from the broadening of $f(v)$. Right: Parallel temperature for different amplitudes. The shaded region correspond to $K \simeq 1$: two islands in the phase space can overlap, leading to a "stochastic heating" of the population.

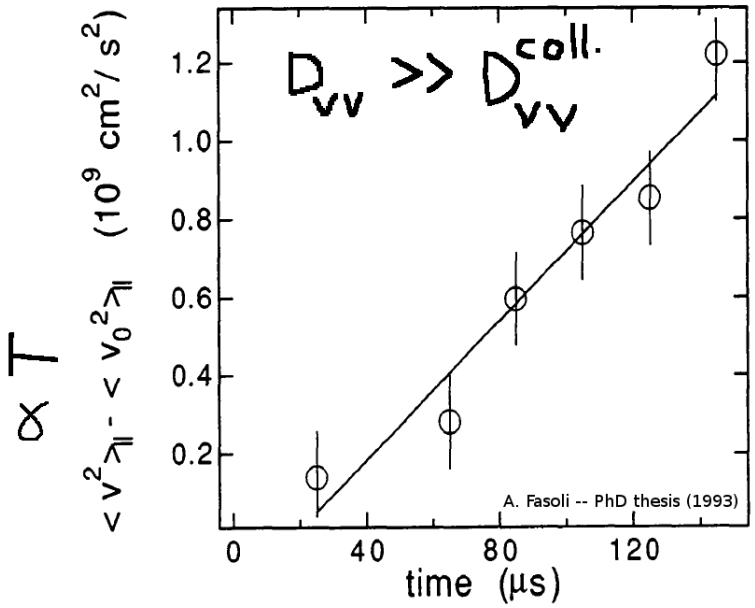

Figure H.3: For $K > 1$ non–linear heating is observed. It occurs on a time–scale ten times faster than the collisional one. The parameter D_{vv} is the diffusion coefficient in the phase space: $\frac{\partial f}{\partial t} = \frac{1}{2} \frac{\partial}{\partial v} D_{vv} \frac{\partial f}{\partial v}$.

Appendix I Test-particle transport

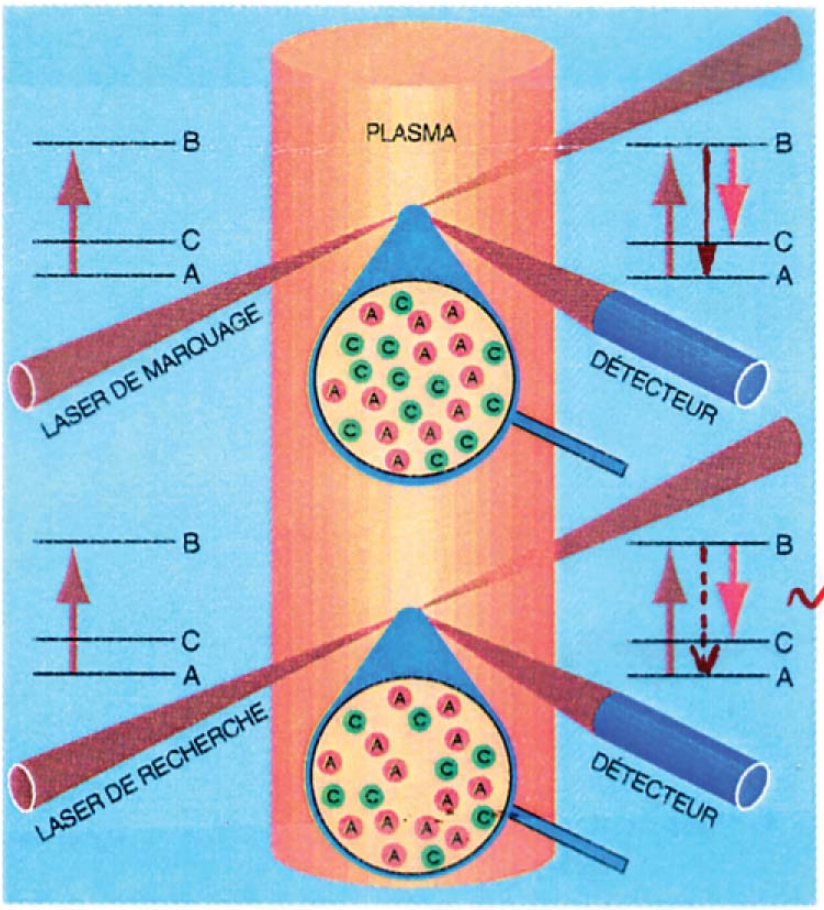

Figure I.1: Setup for the experimental characterisation of particle transport in the phase space (the measurements were made on the LMP device). A narrow–band laser injects a "tag beam" at $x \in (x_T, x_T + \Delta x)$, exciting a selected class of particles with $v \in (v_0, v_0 + \Delta v)$. This defines a volume $\Delta x \Delta v$ in the phase space with a width Γ_0. A second laser is then used as "search beam" at different positions x_S, and measures the broadening of Γ_0.

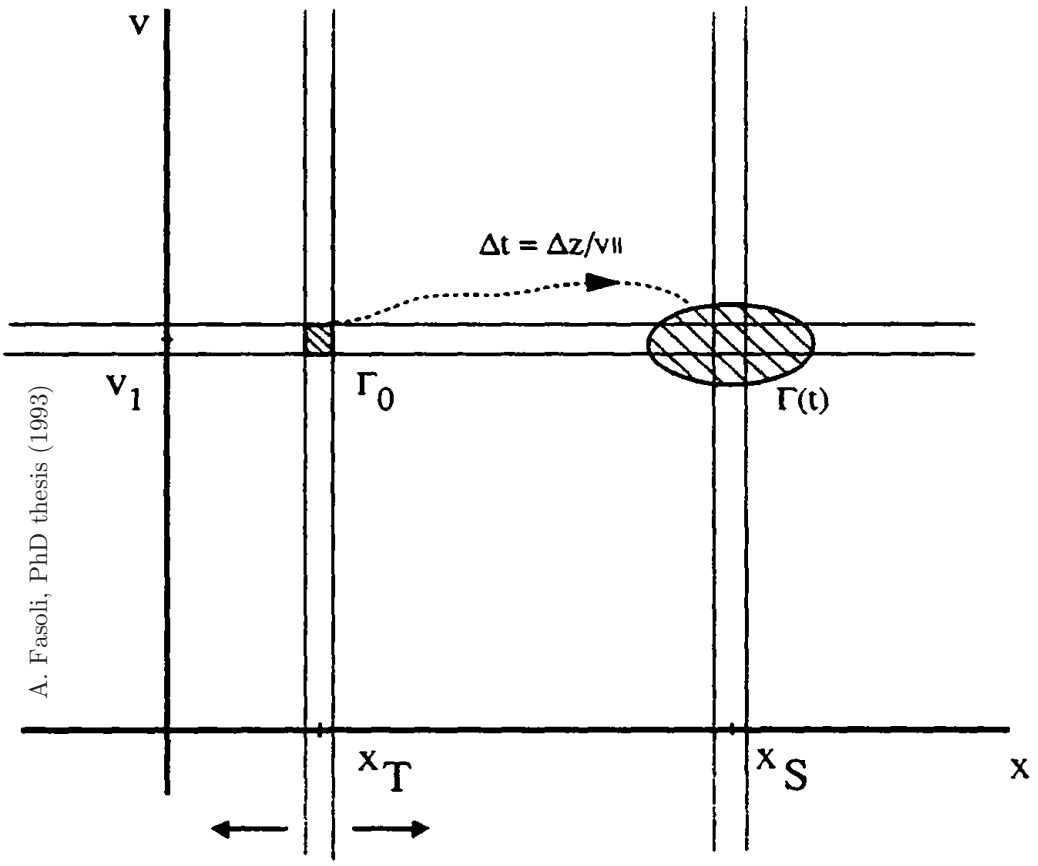

Figure I.2: A search beam at x_S measures the evolution of the width Γ_0 of the initially selected volume.

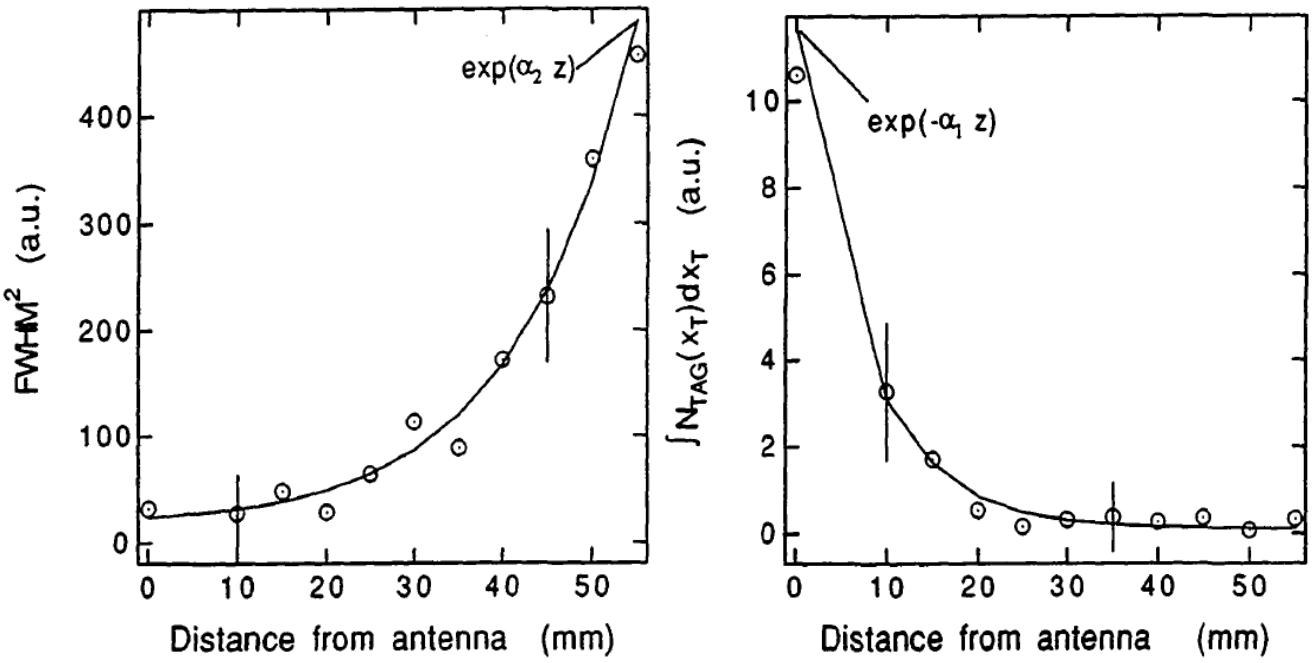

Figure I.3: Width Γ and number of particles in the observed phase space volume as a function of the distance from the exciter laser. With classical radial transport one should observe a dependence $\Gamma^2 \sim Dt$, while above the wave–particle stochastic threshold ($K > 1$) is $\Gamma^2 \sim \exp(\alpha t)$.

Index